Identification and characterization of genes controlling energy homeostasis in *Drosophila melanogaster*

Vom Fachbereich für Biowissenschaften und Psychologie
der Technischen Universität Carolo-Wilhelmina
zu Braunschweig
zur Erlangung des Grades eines
Doktors der Naturwissenschaften
(Dr. rer. nat.)
genehmigte
D i s s e r t a t i o n

von Sebastian Matthias Grönke
aus Diepholz

1. Referent:	Prof. Dr. H.-H. Arnold
2. Referent:	Prof. Dr. H. Jäckle
eingereicht am:	07.03.2005
mündliche Prüfung (Disputation) am:..	15.06.2005
	2005 (Druckjahr)

Vorveröffentlichungen der Dissertation

Teilergebnisse aus dieser Arbeit wurden mit Genehmigung der Gemeinsamen Naturwissenschaftlichen Fakultät, vertreten durch den Mentor oder den Betreuer der Arbeit, in folgenden Beiträgen vorab veröffentlicht:

Publikationen

Grönke, S., Beller, M., Fellert, S., Ramakrishnan, H., Jäckle, H., and Kühnlein, R. P. (2003). Control of fat storage by a *Drosophila* PAT domain protein. Curr Biol *13*, 603-606.

Tagungsbeiträge

Fat Flies - Control of organismal lipid storage by the *brummer* gene in *Drosophila*. (2003) Sebastian Grönke, Sonja Fellert, Herbert Jäckle and Ronald P.Kühnlein. (Vortrag) 18th European Drosophila Research Conference. Göttingen, Deutschland.

Fat Flies - Control of organismal lipid storage by the *brummer* gene in *Drosophila*. (2004) Sebastian Grönke, Sonja Fellert, Herbert Jäckle and Ronald P.Kühnlein (Vortrag) 10th Regional Drosophila Meeting. Regensburg. Deutschland.

Die vorliegende Arbeit wurde am Max-Planck-Institut für biophysikalische Chemie in Göttingen in der Abteilung Molekulare Entwicklungsbiologie unter der Leitung von Prof. Dr. Herbert Jäckle in der Arbeitsgruppe von Dr. Ronald Kühnlein durchgeführt.

Mein besonderer Dank gilt Dr. Ronald Kühnlein für seine fortwährende Betreuung, seine jederzeit vorhandene Diskussions- und Hilfsbereitschaft aber vor allem für die freundschaftliche Zusammenarbeit, die wesentlich zum Gelingen der Arbeit beigetragen hat.

Prof. Dr. Herbert Jäckle danke ich insbesonders für die Gelegenheit meine Dissertation in seiner Abteilung durchführen zu können, sowie für seine fortwährende Unterstützung und die ausgezeichneten Arbeitsbedingungen in unserer Abteilung.

Mein Dank gilt Herrn Prof. Dr. Hans-Henning Arnold für die Vertretung dieser Arbeit an der Technischen Universität Carolo-Wilhelmina zu Braunschweig.

Bei Herrn Dr. Ralph Stanewsky und den Mitarbeitern seiner Arbeitsgruppe, insbesondere Franz Glaser und Gisela Szabo, möchte ich mich für die Hilfsbereitschaft und die Unterstützung bei den Aktivitätsmessungen an Fliegen bedanken.

Herrn Dr. Norbert Tennagels, Dr. Stefan Petry and Dr. Günter Müller danke ich für die Unterstützung bei der Durchführung der Enzymaktivitätsmessungen.

Bei Dr. Kamal Chowdhury und Dr. Ho-Ryun Chung bedanke ich mich für die Hilfe bei der Durchführung und der Auswertung der GeneChip-Experimente.

Dr. Tobias Rasse und Dr. Stefan Sigrist danke ich für ihre Hilfe bei der *in vivo* Analyse der Brummer-Lokalisation.

Gordon Dowe danke ich für zahlreiche DNA-Sequenzierungen und der ständigen Diskussionsbereitschaft über den besten Fußballverein der Welt. Sonja Fellert, Iris Plischke und Ursula Jahns-Meier danke ich für ihre Hilfe bei der Generierung transgener Fliegen.

Besonders danke ich Sonja Fellert, die durch ihre jederzeit freundliche Mitarbeit einen wichtigen Beitrag zum Zustandekommen der vorliegenden Arbeit geleistet hat. Ich danke auch meinem “Banknachbarn” Patrick Steigemann, der mir mit zahlreichen angeregten Diskussion die Zeit noch kurzfristiger gestaltet hat.

Mein Dank gilt auch Alexander Mildner für seine Mitarbeit am Brummer Projekt, sowie Mathias Beller für die gute Zusammenarbeit während des Lsd-2 Projekts.

Für die gute Zusammenarbeit und eine angenehme Arbeitsatmosphäre bedanke ich mich bei allen Mitgliedern der Abteilung für Molekulare Entwicklungsbiologie. Insbesondere bei meinen Kollegen aus Labor 5, Bhavna Chanana, Sonja Fellert, Roland Graf, Jochen Hirsch, Dr. Ronald Kühnlein, Patrick Steigemann und Dr. Gerd Vorbrüggen.

Desweiteren Danke ich meinen Freunden, Andreas, Dirk, Hauke, Isabell, Lui, Martin, Michael, Mirja, Timo und allen anderen für ihre Geduld und ihr Interesse an meiner Arbeit.

Meinen Eltern und meiner Schwester danke ich für ihre fortwährende Unterstützung.

Table of Contents

Abbreviations

aa	amino acids
act-Gal4	*Actin5C*-Gal4
adp	*adipose*
AKH	Adipokinetic hormone
AKHR	AKH receptor
AMPK	AMP-activated protein kinase
BB	Brummer Box
Bmm	Brummer
bp	base pair
BSA	Bovine Serume Albumine
cAMP	cyclic Adenosine monophosphate
CCR4	Carbon Catabolite Repressor 4
cDNA	complementary DNA
CR	Conserved Region
cRNA	complementary RNA
cu	*curled*
DAG	Diacylglycerol
Dgat	Diacylglycerol transferase
dHsl	*Drosophila* Hsl
DiFMU-octanoate	6,8-difluoro-4-methylumbelliferyl octanoate
DNA	Deoxyribonucleic acid
Dob	Doppelgänger von Brummer
Dreg-2	*Drosophila* rhythmically expressed gene 2
Drosophila	*Drosophila melanogaster*
E.coli	*Escherichia coli*
EGFP	Enhanced Green Fluorescent Protein
FB	Fat body
Fig.	Figure
GST	Glutathione-S-Transferase
h	hour
hs	heat shock
Hsl	Hormone sensitive lipase
i.e.	*id est*, that is
IPTG	Isopropyl-β-D-Thiogalactopyranoside
ISH	*In situ* hybridisation
IVT	*In vitro* transcription
kb	kilo base pair
kDa	kilo Dalton
L/D	light/dark
LB	Luria-Bertani
Lsd	Lipid storage droplet
Lsd-2	Lipid storage droplet protein 2
MAG	Monoacylglycerol
µg	microgramme
µl	microliter
mg	milligramme
mRNA	messenger RNA

NBD	Nitrobenzoxadiazole
OD	Optical Density
ORF	Open Reading Frame
PCR	Polymerase Chain Reaction
pdk	Pyruvate dehydrogenase kinase
PKA	Protein kinase A
PLD	Patatin-like Domain
RNA	Ribonucleic acid
rpm	Revolutions per minute
RT-PCR	Reverse Transcriptase PCR
SDS-PAGE	Sodium Dodecyl Sulfate Polyacrylamide Gel Electrophoresis
TAG	Triacylglycerol
TTS2/ATGL	Transport secretion protein 2/Adipose triglyceride lipase
UAS	Upstream activating sequence
UTR	Untranslated Region

1 Introduction

1.1 Energy homeostasis and obesity

Animals continuously expend energy to supply their metabolic needs. Despite variability in the external environment, they maintain a relatively stable internal energy level. This fundamental property of animals is essential for their survival and requires the tight regulation of the energy balance. The regulatory processes that guarantee energy balance by regulating energy uptake, energy expenditure and energy storage have been termed energy homeostasis (outlined in Fig. 1).

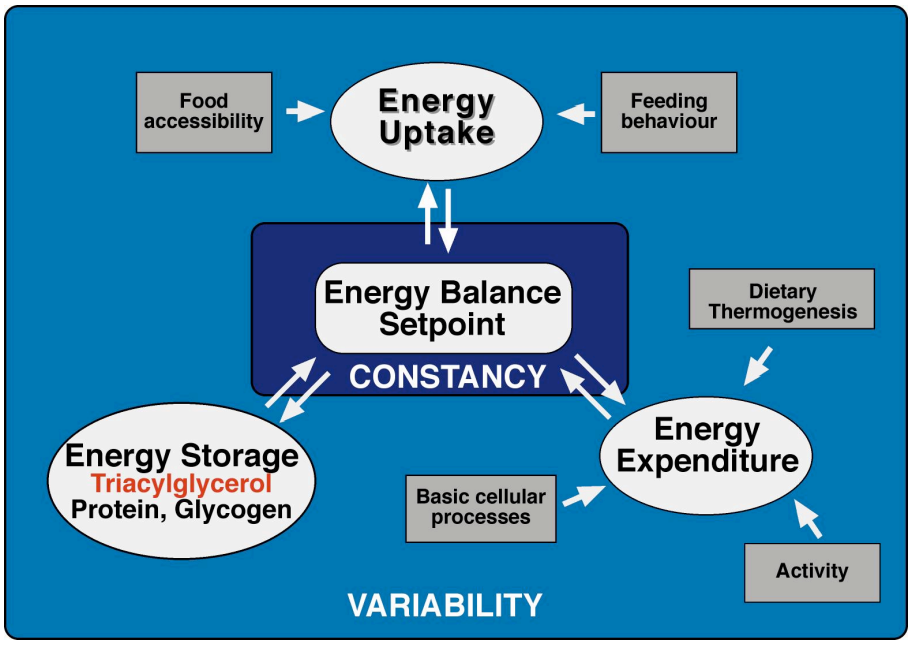

Figure 1: Organismal energy homeostasis. Energy balance is maintained by the coordinated regulation of energy uptake, energy expenditure and energy storage (for details see text).

Energy expenditure depends on metabolic rate, activity and the thermogenic effects of feeding (Fig. 1; Friedman, 2004). For example, the energy need of an adult human man is about 7,000 kJ per day under resting conditions but can increase up to 25,000 kJ per day upon hard work or sport (Stryer, 2004). To balance total energy expenditure, animals take up energy in form of food. In the short term, energy uptake and expenditure do not match closely. This is because most adult animals exhibit a discontinuous feeding behaviour, where the uptake of food is limited to certain periods of the day, whereas expenditure is a continuous process. The imbalance between food uptake and energy expenditure requires the capacity to at least temporarily store energy.

Neutral lipids, mainly Triacylglycerol (TAG), are by far the most important form of energy storage. A 70 kg human man stores about 670,000 kJ of metabolic energy, of which 84% are stored in form of TAG, 15% as protein and only 1% as carbohydrates (glycogen and glucose) (Stryer, 2004). The prominent role of TAG among the energy storage components is further emphasized by the fact that the survival time of an organism under food deprivation is mainly determined by the size of its TAG store. In humans, like in all adult mammals, most of the TAG is stored in a specialized organ termed the white adipose tissue.

Chronic imbalance in fat storage control, like increased food uptake or reduced energy expenditure, results in excessive fat accumulation and is causative for obesity in humans (reviewed in Speakman, 2004; Friedman, 2004; Flier, 2004). In recent years, obesity has become one of the mayor health problems of "westernized" societies. It is estimated that in 2004 more than 310 million people worldwide were affected by the obesity epidemic (International Obesity Task Force, 2004). Interestingly, the prevalence of obesity increased within the last 20 years in most industrialized countries (Speakman, 2004). For example, in Germany, between 1985 and 2002 the percentage of obese people increased from 17,7% to 27,7% in males and from 20,7% to 31,0% in females (Helmert and Strube, 2004). According to the current model, environmental factors, like overeating and physical inactivity, together with genetic predisposition are causative for the recent dramatic increase of obesity.
Twin studies (Allison et al., 1996, Stunkard et al., 1990, Stunkard et al., 1986) as well as genome wide linkage analyses confirmed that once certain environmental conditions are met, most of the variance in the incidence of obesity is attributable to genetic factors (Speakman, 2004; Friedman, 2004). Thus, there is a clear need to identify the genes that participate in energy balance control and to unravel the physiological and molecular mechanisms which underlie the development of obesity.

1.3 Obesity has a genetic basis

The most common forms of obesity are polygenic (reviewed in Clement et al., 2002). However, most of the genes (>95 %) responsible for the cause of obesity in humans are still unknown (Flier, 2004). In order to identify genes underlying polygenic obesity in humans, two general approaches have been used. The first approach involves genome-wide scans in different ethnic populations. Using this approach, chromosomal regions were identified which show linkage with obesity in large collections of families (Clement et al., 2002). The second approach involves the use of animal model organisms. Single-gene mutants and

genetically modified animals have been used successfully to discover genes and pathways that can regulate body fat storage (Brockmann and Bevova, 2002).

Although the cause of obesity, i.e. increased food uptake or decreased energy expenditure, is quite simple, the physiological system that regulates energy homeostasis is very complex. It involves an integrated molecular communication between different organs that includes beside the adipose tissue the central nervous system, the pancreas and the digestive tract (Fig. 2; Speakman, 2004; Friedman, 2004; Flier, 2004). These organs combine to provide the energy balance system of an organism which has a short-term and a long-term component.

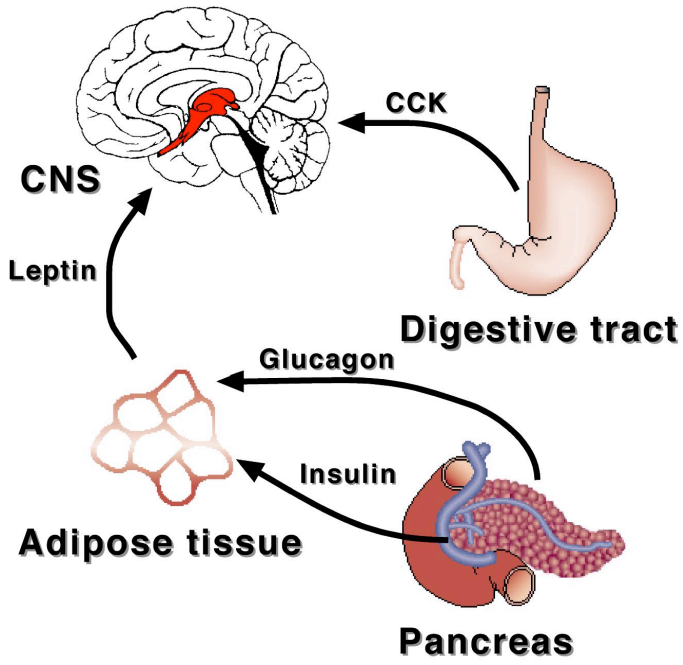

Figure 2: Control of energy homeostasis by interplay of central nervous system (CNS), digestive tract, pancreas and adipose tissue. In the short-term system, endocrine signals released by the digestive tract, like Cholecystokinin (CCK), act on CNS regions (shaded in red) involved in the control of acute feeding behaviour.
Long-term regulation of energy balance is mostly determined by interplay between adipose tissue and the CNS. The hormone leptin acts as a lipostatic signal released by the adipose tissue in proportion to the stored fat content. In the CNS, low level of leptin signal starvation. Conversely, high levels of leptin signal the fed state.
Insulin and glucagon are peptide hormones released by the pancreas. Antagonistic activities of insulin and glucagon control lipid metabolism in the adipose tissue (for details see text). (Scheme modified after Barsh and Schwartz, 2002).

In the short-term system, endocrine signals released by the digestive tract, like Cholecystokinin, influence the appetite, in particular the onset and the termination of individual meals (Moran, 2000). Digestive tract-derived short-term signals play a critical role in switching feeding behaviour on and off and regulating short-term activity patterns. In contrast, the long-term status of body energy stores is mostly determined by an interplay between the adipose tissue and the central nervous system (Flier, 2004).

According to the so-called lipostatic model (Kennedy, 1953), regulation of body fatness is controlled by a regulatory feedback loop that is generated by adipose tissue in reference to a centrally encoded so-called energy setpoint (Speakman, 2004). As a lipostatic signal, the product of the *obese* (*ob*) gene, termed Leptin, was identified (Zhang et al., 1994; Halaas et al., 1995). Leptin is a peptide hormone released by the adipose tissue which signals the fat storage status to the CNS (Halaas et al., 1995). Leptin is not the only peripheral hormone

involved in fat storage control. Two other important peptide hormones are insulin and its antagonist glucagon which are secreted by the β- and α-cells of the pancreas, respectively (Stryer, 2004; Flier, 2004). Insulin signals the fed state, whereas glucagon is a signal for starvation (Stryer, 2004). Accordingly, insulin levels fall with fasting and rise with obesity, whereas glucagon shows the opposite regulation. In the adipose tissue, insulin receptor activation stimulates the synthesis of TAG (lipogenesis) and inhibits the hydrolysis of TAG by lipases (lipolysis) (Stryer, 2004). Conversely, glucagon activates lipolysis in the adipose tissue (see 1.2 and Fig. 4). Knock-out mice lacking the activity of adipose tissue-specific insulin receptor are lean and protected from age-related and diet-related obesity (Blüher et al., 2002). These findings demonstrate that processes that control lipid metabolism in adipose cells, the adipocytes, are central to the regulation of whole body energy metabolism and thus, affect the development of obesity.

1.4 Fat storage control in mammalian adipose tissue

In the adipocytes, fat is stored in specialized organelles called lipid droplets (reviewed in Brown et al., 2001). Fully differentiated mammalian adipocytes contain only a single lipid droplet which can be as large as 100 μm (Fig. 3A) (Brasaemle et al., 2004). The lipid droplets are composed of a core of neutral lipids, mainly TAG, that is surrounded by a monolayer of phospholipids (PLP) into which numerous proteins are embedded (Fig. 3B, C) (Tauchi-Sato et al., 2002; Brown et al., 2001). Some of these proteins, like members of the PAT protein family, are involved in the regulation of TAG storage (see below).

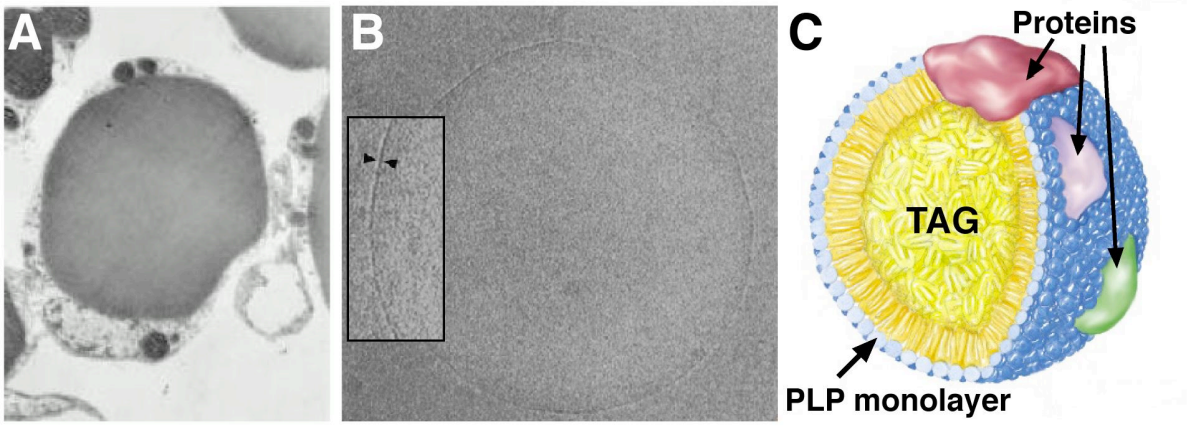

Figure 3: Fat storage in adipocytes. (**A**) Electron micrograph of an adipocyte. A small band of cytoplasm surrounds the single large lipid droplet (picture taken from Stryer, 2004). (**B**) Electron micrograph of an isolated lipid droplet. The Phospholipid (PLP) monolayer is visible in the inset as a small electron dense line (arrowheads) (picture taken from Tauchi-Sato et al., 2002). (**C**) Schematic structure of a lipid droplet. Lipid droplets are composed of a core of neutral lipids, mainly TAG, surrounded by a PLP monolayer into which numerous proteins are embedded.

In adipocytes, a regulated balance between lipogenesis and lipolysis is believed to continuously match acute energy needs of the organism by TAG mobilization and readjust organismal storage fat content during periods of excessive energy supply. Chronic imbalance between lipogenesis and lipolysis in the adipose cells affects whole body fat storage.

By now, a number of factors affecting body fat storage have been identified and characterized biochemically as well as by functional means. Overexpression of Diacylglycerol acyltransferase 1 (DGAT1), for example, which catalyzes the final step in TAG synthesis, results in increased TAG deposition (Chen et al., 2002). Conversely, mice deficient for DGAT1 are lean and resistant to diet-induced obesity (Smith et al., 2000). These findings suggest that variations in the rate of lipogenesis in the adipose tissue can result in obesity or leanness, respectively. In addition, variation in the rate of adipose tissue lipolysis does also affect whole body fat storage (see below).

Perilipin, a key regulator of TAG lipolysis in mammalian adipocytes, is a member of the PAT protein family of lipid droplet-associated proteins that includes the mammalian proteins adipose-differentiation-related protein (ADRP), TIP-47 and S3-12 (Lu et al., 2001; Wolins et al., 2003). Mice deficient for Perilipin are lean and have an increased basal lipolysis in their adipose tissue (Martinez-Botas et al., 2000; Tansey et al., 2001). Moreover, lack of Perilipin activity can revert the obesity of leptin receptor-deficient mice to near wild-type levels (Martinez-Botas et al., 2000), whereas overexpression of Perilipin in preadipocyte tissue culture cells increases TAG storage by reducing the rate of lipolysis (Brasaemle et al., 2000). These findings led to the proposal that Perilipin facilitates TAG storage by blocking the binding of TAG lipases to the lipid droplet surface and thereby provides a barrier against lipolysis (Brasaemle et al., 2000). However, under lipolysis-stimulating (lipolytic) conditions (see below), Perilipin interacts with Hormone sensitive lipase (Hsl) at the lipid droplet surface and facilitates the mobilization of TAG in adipocytes (Sztalryd et al., 2003). Hsl is a TAG lipase, which catalyzes the initial and rate limiting step in lipolysis, the hydrolysis of TAG in diacylglycerol (DAG) and a free fatty acid (FA) (Fredrikson et al., 1981).

Perilipin and Hsl activities are both regulated via phosphorylation by protein kinase A (PKA) (reviewed in Londos et al., 1999). The binding of a lipolytic hormone, such as glucagon or adrenalin, to a G-protein-coupled receptor located in the adipocyte plasma membrane activates adenylyl cyclase (AC) (Fig. 4). AC catalyzes the formation of cAMP, which in turn activates PKA (Londos et al., 1999). Mice that lack the lipolytic β-adrenergic receptors (β-

ADR) develop severe obesity when fed a high fat diet (Bachman et al., 2002). These findings establish that derogation of the lipolytic pathway can lead to obesity.

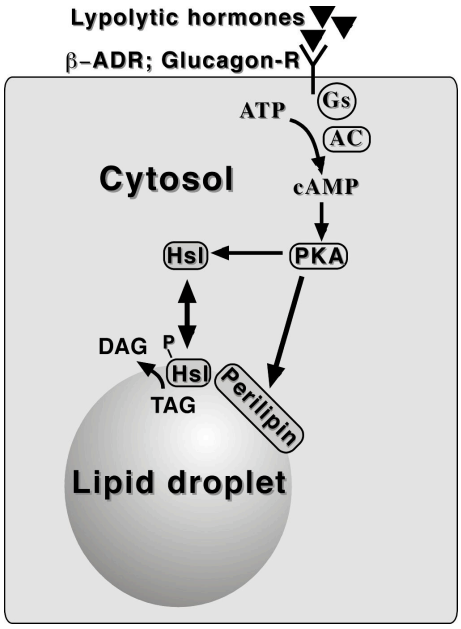

Figure 4: Control of lipolysis in mammalian adipocytes. The binding of a lipolytic hormone, such as glucagon or adrenalin, to their corresponding receptors, glucagon receptor (glucagon-R) and β-adrenergic receptor (β-ADR), respectively, activates a cAMP-signaling cascade. Via a G-protein (Gs), adenylyl cyclase (AC) is activated. AC catalyzes the formation of cAMP. Elevated cAMP level activate protein kinase A (PKA), which in turn phosphorylates Hormone sensitive lipase (Hsl) and Perilipin. Upon phosphorylation cytosolic Hsl translocates to the lipid droplet surface, where it catalyzed the hydrolysis of TAG to DAG. Under basal conditions, Perilipin blocks the binding of lipases to lipid droplets. However, under lipolytic stimulation, Perilipin is necessary for the Hsl-mediated TAG hydrolysis.

Phosphorylation of Hsl leads only to a twofold increase in hydrolytic activity *in vitro* (Fredrikson, 1981; Stralfors et al., 1983). In contrast, lipolytic stimulation of adipocytes results in an up to fiftyfold increase in TAG hydrolysis (Stralfors and Honnor, 1989). Under basal conditions, Hsl is located in the cytosol. These findings led to the conclusion that activation of Hsl relies primarily on translocation from the cytosol to the lipid droplet surface upon phosphorylation by PKA (reviewed in Holm, 2003). In addition, under prolonged starvation mouse Hsl mRNA and protein amounts are upregulated (Sztalryd and Kraemer, 1994). Concomitant with the translocation of Hsl, substantial morphological changes occur at the lipid droplet surface (Brasaemle et al., 2004). The single big lipid droplet is fragmented into numerous micro-lipid droplets, a process that vastly increases the lipid droplet surface area (Smith and Jarret, 1980; Slavin, 1972).

In conclusion, these findings led to the proposal that Hsl is the only TAG lipase that mediates lipolysis in the mammalian adipose tissue (Londos et al., 1999). Unexpectedly, however, Hsl deficient mice are not obese and exhibit substantial residual lipolytic activity in their adipose tissue (Osuga et al., 2000; Wang et al., 2001; Okazaki et al., 2002). Based on this observation, the existence of additional lipases involved in TAG storage control in the mammalian adipose tissue has been proposed (Fortier et al., 2004; Okazaki et al., 2002).

1.3 *Drosophila* as a model system for fat storage research

Like mammals, insects store fat in a specialized organ called the fat body (Arrese et al., 2001). In both cell types, mammalian adipocytes and insect fat body cells, TAG is stored in

form of lipid droplets. This observation suggests that the strategy of energy storage and possibly also the machinery and, at least in part, the control to achieve fat storage might be evolutionary conserved between mammals and insects (see below).

The fruit fly *Drosophila melanogaster*, hereafter referred to as *Drosophila*, is one of the best-established animal model organisms. *Drosophila* flies are undemanding laboratory pets that can be easily handled and bred in large numbers. This property, and a relatively small genome size distributed over only five chromosomes are mayor advantages for genetic studies. Since the discovery of the complete genome sequence of *Drosophila* (Adams et al., 2002), tools like "DNA-microarrays" and "GeneChips" have been developed that allow genome-wide examination of gene expression (reviewed in Celniker, 2000; Lipshutz et al., 1999). Sequence comparison of thousand-odd genes implicated in specific humane diseases revealed that most of them (77%) have a sequence homologue in the *Drosophila* genome (Chien et al., 2002; O´Kane, 2003). They include genes involved in glycogen or lipid storage (Chien et al., 2002; see below). These findings support the use of *Drosophila* as a model organism for energy storage research.

Another advantage of *Drosophila* is the possibility to easily generate transgenic flies (Spradling and Rubin, 1982). This method allows one the ectopic expression of genes by using the UAS/Gal4 system (Brand and Perrimon, 1993; Rorth, 1996). In addition, the integration and re-mobilization of transposable elements (P-elements) in a gene is an easy task to generate mutant flies (Spradling et al., 1999; Spradling et al., 1995). Yet another advantage of *Drosophila* is the short generation time of only 9 days at 25°C.

The life cycle of *Drosophila* is divided into four different developmental stages (embryogenesis, larval stages, pupae and adult; see Fig. 5A). The *Drosophila* embryo is a non-feeding developing organism. Thus, energy storage components, mainly TAG, necessary for the rapid proliferation and differentiation processes during embryogenesis are deposited into the egg by the mother. The loading of the egg by the mother with mRNAs, proteins and energy storage components is called maternal contribution. In the young embryo lipid droplets are distributed throughout the whole embryo (Welte et al., 1998). Later during embryonic development, the fat body differentiates from the mesoderm (Bate and Martinez Arias, 1993). In contrast to the non-feeding embryo, *Drosophila* larvae are continuous feeders (Zinke et al., 2002). Accordingly, the larvae accumulate large amounts of TAG within the fat body during development (Fig. 5B). The metamorphosis from the larvae to the adult, during the pupal stage, ends with the hatching of the immature adult fly. Most

fat body cells of the newly emerged flies descend from the larval fat body (Demerec, 1994). They represent the so-called immature fat body cells (inset in Fig. 5C) which are replaced during the first six days of adult life by the mature adipose tissue (Demerec, 1994). Correspondingly, I will hereafter refer to flies aged for 6-7 days that contain only the mature adipose cells as "mature adult flies".

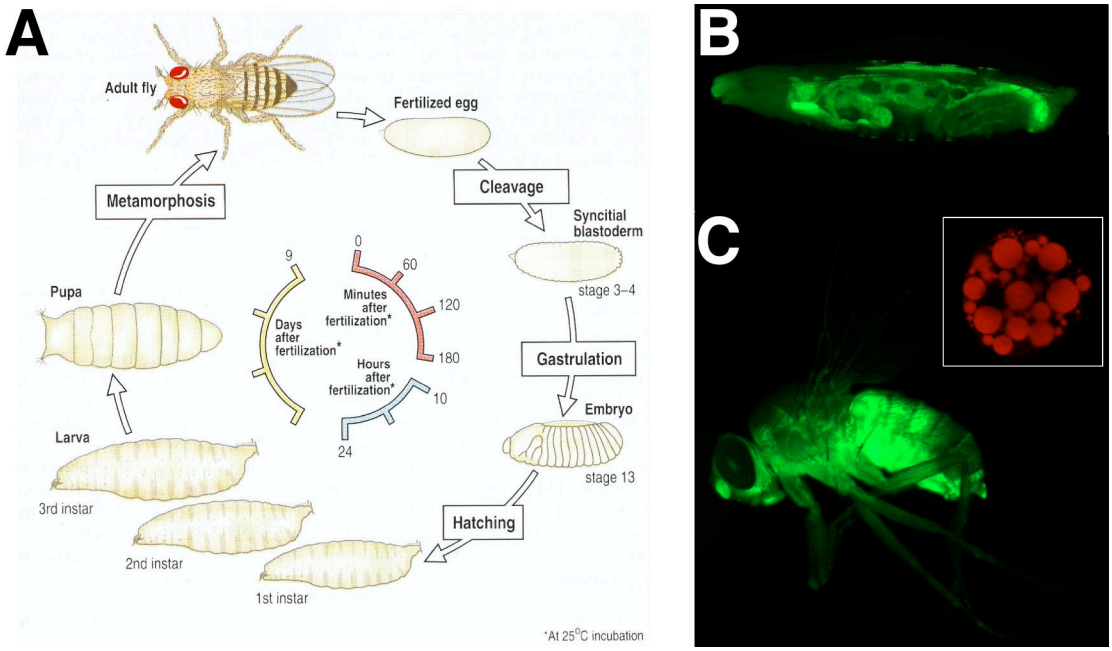

Figure 5: Life cycle and fat storage tissue of *Drosophila*. (**A**) The generation time of *Drosophila* takes 9 days at 25°C. 24 hours after fertilization of the egg embryogenesis ends with the hatching of the first instar larvae. In contrast to the non-feeding embryo, *Drosophila* larvae are continuous feeders. This supports the rapid growth from the first to the third instar larvae, a period where the larvae increase more than 200-fold in size (Lehner, 1999). The third larval stage ends with pupation. The metamorphosis to the adult fly is completed in about four days and ends with the hatching of the immature adult fly (for details see text). (**B**, **C**) Fat body of (**B**) a *Drosophila* larva and (**C**) an adult fly visualized by expression of the Enhanced Green Fluorescent Protein (EGFP). Fat body tissue is distributed throughout the animal both in larvae and adult flies. The inset in (**C**) shows an immature fat body cell (see text). The variously sized lipid droplets in the fat body cell are stained with the lipophilic dye Nile Red.

Like adult mammals, and in contrast to *Drosophila* larvae, adult *Drosophila* flies exhibit a discontinuous feeding behaviour (compare 1.1). This switch in feeding behaviour demands a homeostatic system in adult *Drosophila* which regulates energy balance in a manner similar to the system that acts in adult mammals (compare 1.2). This conclusion is supported by the observation that components of the insulin signaling cascade (compare 1.2) are conserved between *Drosophila* and mammals (reviewed in Garofalo, 2002).

The *Drosophila* genome encodes seven insulin-like peptides (dilp1-7) which are *inter alia* expressed in neurosecretory cells of the larval brain (Brogiolo et al., 2001). Ablation of insulin producing neurons results in elevated carbohydrate levels in the hemolymph (Rulifson et al., 2002). This phenotype is reminiscent of the elevated blood glucose levels in

humans that suffer from *Diabetes mellitus*, a disease that is caused by a degeneration of pancreatic islet β cells (Stryer, 2004). In addition to the essential function in carbohydrate homeostasis, insulin signaling is also implicated in the regulation of lipid metabolism in *Drosophila* (Garofalo, 2002).

Flies with mutations in the *Insulin receptor* (*InR*) gene or the gene *chico,* that encodes an insulin receptor substrate, exhibit an up to fivefold increase in stored TAG (Böhni et al., 1999; Tatar et al., 2001; Brogiolo et al., 2001). In principle, the increased lipid storage of flies devoid of insulin signaling seems to contradict the function of the mammalian insulin receptor which stimulates lipogenesis in adipose tissue upon activation (compare 1.2). However, it has been noted that the lack of insulin signaling can also result in TAG accumulation in mammals, as demonstrated by the obese phenotype of mice with a neuron-specific disruption of the *InR* gene (Brüning et al., 2000). The cause of the TAG storage phenotype in *InR* and *chico* mutant flies is still unknown (Garofalo, 2002).

In mammals, antagonistic activities of insulin and glucagon control lipid metabolism in adipocytes (compare 1.2). Insects also produce a peptide hormone called adipokinetic hormone (AKH) that acts as functional homologue of mammalian glucagon (Lee and Park, 2004; Van der Horst, 2001). Studies in various insect species, including the grasshopper *Locusta migratoria* (Gäde and Beenakkers, 1977), the tobacco hornworm *Manduca sexta* (Ziegler et al., 1990) and *Drosophila* (Lee and Park, 2004), established that AKH stimulates TAG lipolysis in the insect fat body cells. AKH is produced by the corpora cardiaca (CC) cells of the ring gland, the major endocrine organ of insects (Noyes et al., 1995). Under energy demanding situations, like flight or starvation, CC cells release AKH into the hemolymph (Gäde and Auerswald, 2003; Van der Horst et al., 2001). Like mammalian TAG mobilization, AKH-stimulated lipolysis in the insect fat body relies on signaling via a G protein-coupled receptor (AKHR) (Staubli et al., 2002), increase in intracellular cAMP and activation of PKA (Gäde and Auerswald, 2003; Van der Horst et al., 2001). In addition, AKH has been shown to induce the transcription of a cytochrome P450 gene in the fat body of cockroaches (Bradfield et al., 1991) and expression of a gene that encodes fatty acid binding protein in the flight muscle of locusts (Chen and Haunerland, 1994). These findings suggest that regulation of transcription is part of the response of insects to energy demanding situations like, for example, starvation. In fact, transcriptional regulation is also involved in the mammalian starvation response as demonstrated by the upregulation of Hsl under prolonged starvation (compare 1.2; Sztalryd and Kraemer, 1994). The mechanisms of TAG

storage control as well as the molecular identities of the effectors of lipolysis in insects, like Perilipin or Hsl in mammals, remain to be elucidated.

I initiated the functional characterization of the *Drosophila* genes *CG11055* (supplement 2) and *Lsd-2* (supplement 3), which encode putative homologues of mammalian Hsl and Perilipin, respectively. The results show that flies that lack the putative *Drosophila* Hsl homologue (dHsl) are not obese and can mobilize their TAG stores under starvation conditions. Thus, like in mammalian adipose tissue, additional TAG lipases beside dHsl must contribute to lipolysis in the fat body of insects. Furthermore, I found that Lsd-2 operates in a Perilipin-like manner and that the surface of lipid droplets represents an evolutionary conserved intracellular compartment boundary involved in the control of lipolysis. In order to further establish *Drosophila* as a model for TAG storage research, I focused my work on the identification of novel regulators of TAG storage by taking the advantages of *Drosophila* as an experimental system.

Under starvation, flies mobilize their energy storage components, most importantly TAG, to compensate for the lack of energy uptake. I reasoned that effectors of *Drosophila* lipolysis will be transcriptionally regulated under starvation conditions as shown for mammalian Hsl (Sztalryd and Kraemer, 1994). In order to identify novel effectors of lipolysis, I performed a genome-wide comparative transcriptome analysis using adult *Drosophila* that were either ad libitum fed or starved. This approach made use of "GeneChips" that allow one the simultaneous examination of the expression levels of more than 13,500 of the approximately 14,000 protein-coding genes of *Drosophila* (Misra et al., 2002; Yandell et al., 2005).

Of the in total 223 starvation-responsive genes identified (see supplemental Fig. 1), I functionally characterized the starvation upregulated genes *CG5295* and *CG5560*, a pair of genes which I called *brummer* (*bmm*) and *doppelgänger von brummer* (*dob*), respectively. *bmm* and *dob* are the only *Drosophila* members *of* an evolutionary conserved gene family, called the Bmm/Nutrin family of Patatin like domain (PLD) containing lipases. The results show that *bmm* and *dob* are new effectors of lipolysis central to organismal TAG storage control in *Drosophila*. However, flies lacking *bmm* and *dob* activities are viable, fat and starvation hyperresistant. These results show that additional lipases, beside the members of the Bmm/Nutrin family, contribute to starvation-induced TAG mobilization in *Drosophila* as has been observed with most recently identified human homologues (Zimmermann et al., 2004; Vilena et al., 2004; Jenkins et al., 2004).

In addition, I noted that about 12% of the starvation-regulated genes (supplement 4, table S4.1) exhibit a daily rhythmicity of expression, called circadian cycling (McDonald and Rosbash, 2000; Claridge-Chang et al., 2001; Lin et al., 2002; Ueda et al. 2002). In mammals, energy homeostasis and circadian rhythm processes are closely linked (for a more detailed depiction see supplement 4). I therefore tested whether this feature also exists in *Drosophila* as recently proposed for the *Drosophila* gene *takeout* (Sarov-Blat et al., 2000) by characterizing the *Drosophila* genes *nocturnin* (supplement 4) and *Drosophila rhythmically expressed gene 2* (*Dreg-2*, supplement 5).

2 Results

2.1 Starvation-response profiling by genome-wide comparative transcriptome analysis

In order to identify new genes involved in the chronic and acute control of energy homeostasis, the genome wide transcriptional response of food-deprived mature adult male wild-type flies was compared to *ad libitum* fed siblings using GeneChip technology. Under starvation conditions, wild-type (*Oregon R*) male flies have a median lifespan of 42 hours and fuel their energy demands by the continuous mobilization of TAG, glycogen and proteins (Fig. 6A and data not shown).

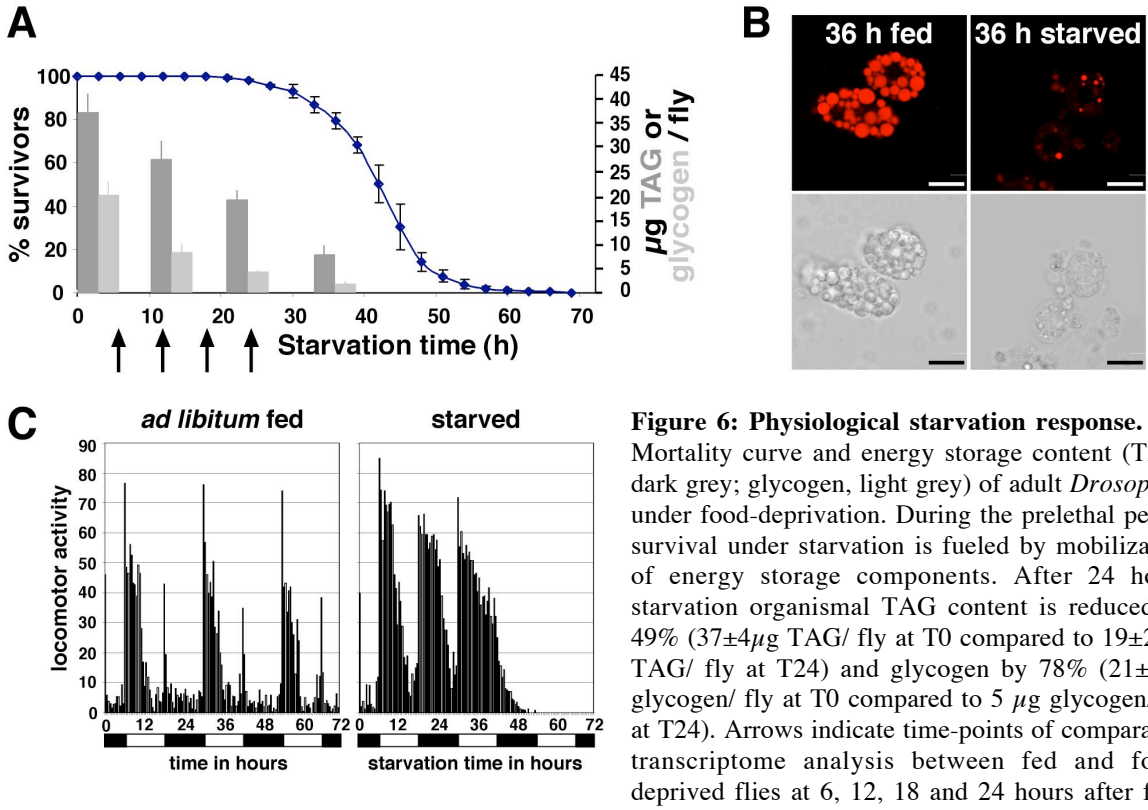

Figure 6: Physiological starvation response. (**A**) Mortality curve and energy storage content (TAG, dark grey; glycogen, light grey) of adult *Drosophila* under food-deprivation. During the prelethal period survival under starvation is fueled by mobilization of energy storage components. After 24 hours starvation organismal TAG content is reduced by 49% (37±4μg TAG/ fly at T0 compared to 19±2 μg TAG/ fly at T24) and glycogen by 78% (21±3μg glycogen/ fly at T0 compared to 5 μg glycogen/ fly at T24). Arrows indicate time-points of comparative transcriptome analysis between fed and food-deprived flies at 6, 12, 18 and 24 hours after food withdrawal. (**B**) Organismal lipid mobilization is reflected on the cellular level by the disappearance of lipid storage droplets from fat body cells isolated from starved flies. Upper panel confocal section of Nile Red stained fat body cell of *ad libitum* fed (left) or 36 h starved immature (right) adult flies. Lower panel corresponding phase contrast images. (Scale bar = 20μm). (**C**) Locomotor activity of *ad libitum* fed (left) and starved (right) male flies. Locomotor activity of *ad libitum* fed flies with two activity peaks, one early in the morning, the other one late in the evening (**C** left panel). Food deprivation induces prolonged hyperactivity prior to death (light/dark phase indicated by bar below lower panel: open bars = lights-on, filled bars = lights-off).

Fly population subjected to 24 hours starvation show no mortality and reduction in organismal TAG content by 49 % and in glycogen by 78 %. The starvation induced TAG mobilization is reflected on the cellular level by the disappearance of lipid storage droplets

from fat body cells of starved flies (Fig. 6B). In addition to the mobilization of energy reserves flies change their behaviour under starvation. Under *ad libitum* feeding flies exhibit a typical bimodal locomotor activity pattern with the mayor activity early in the morning and a smaller activity peak late in the evening. Food deprivation induces prolonged hyperactivity prior to death possibly reflecting food-seeking behaviour (Fig. 6C).

To analyze the transcriptional response associated with energy mobilization and behavioural changes under starvation a population of wild-type male flies was aged for 6-7 days and then split in subgroups. Flies from single subgroups food-deprived for 6h, 12h, 18h and 24 h (arrows in Fig. 6A) were sacrificed in parallel to age-matched *ad libitum* fed siblings and their transcriptome was compared using Affymetrix *Drosophila* GeneChips. Genes having an increased (I) or decreased (D) call at 6h and at least two more analysis time points were considered starvation-responsive. Applying this filter criterion, a total of 223 genes were identified, from which 113 are upregulated and 110 downregulated upon starvation (Supplemental Fig. 1).

Quantitative Northern blot (Fig. 7A) and RT-PCR analysis (Fig. 7B) on 9 selected genes confirm the transcriptional regulation as observed with the GeneChips (Fig. 7C, 12, S4.4, S5.3), validating the reliability of the data set. Sorting the regulated genes according to their predicted function reveals that most of the starvation-induced genes are coding for metabolic enzymes (44) (Fig. 7D). In addition, genes coding for cytochromes (10), metabolite transporters (6), kinases (5) and proteins involved in lipid metabolism (7) are among the starvation-upregulated genes (Fig. 2D). Interestingly, only few metabolic enzymes (7) are downregulated in response to starvation, where proteases and protease inhibitors form the largest group (38) (Fig. 7E). Nearly half of the starvation-induced metabolic enzymes are involved in carbohydrate catabolism, including key regulators like Hexokinase (encoded by *Hex-C*), Transketolase (*CG8036*) and Phosphoglucomutase (*Pgm*) or enzymes involved in the breakdown of oligosaccharides like an α–Amylase (*AmyD*), a α–Glucosidase (*CG11909*) and six maltases (*CG11669, CG8690, CG30359, CG30360, CG14934, CG14935*). Protein degradation is reflected by the upregulation of genes involved in amino acid catabolism, including two aminotransferases encoded by *got2* and *spat*, a phenylalanine-4-monooxygenase (*henna),* a 4-hydroxyphenylpyruvate-dioxygenase (*CG11796*) and a homogentisate-1,2-dioxygenase (*hgo*).

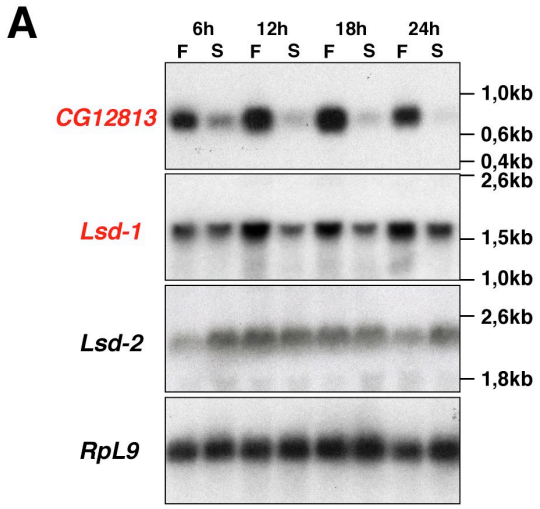

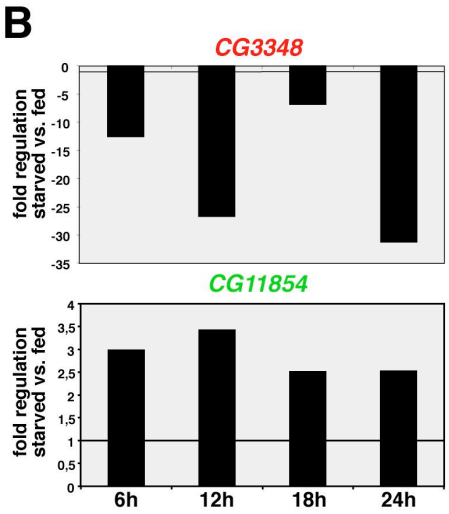

C

starvation time

	6h	12h	18h	18h	24h
CG12813	D	D	D	D	D
Lsd-1	D	D	D	D	D
Lsd-2	I	NC	NC	NC	I
RpL9	NC	NC	NC	NC	NC
CG3348	D	D	D	D	D
CG11854	I	I	I	NC	I

D=decreased, I=increased,
NC=Not changed

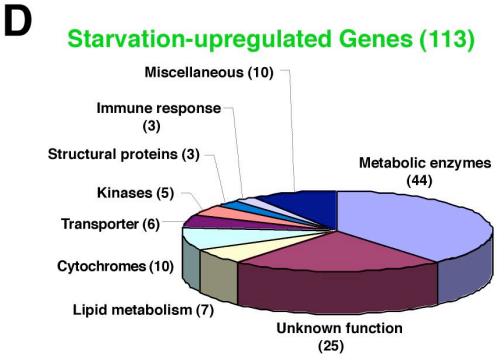

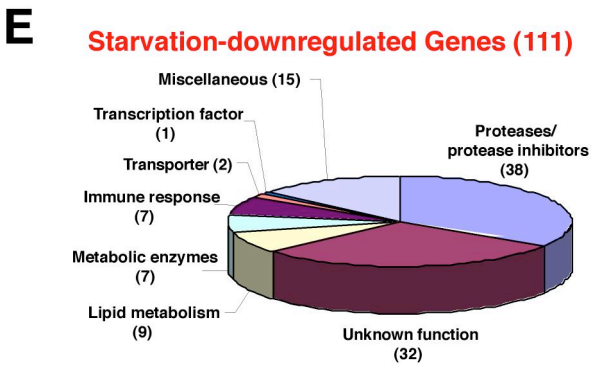

Figure 7: Validation of GeneChip data and functional classification of starvation responsive genes. To confirm GeneChip results the expression of selected genes in *ad libitum* fed (F) adult flies was compared to flies starved (S) for 6, 12, 18 and 24 hours by (**A**) Quantitative Northern blot and (**B**) RT-PCR analysis. The downregulation of CG12813 and *Lsd-1* transcripts observed on the GeneChips (**C**) was confirmed by Northern Blot analysis (**A**). Conversely, in accordance with the GeneChip results (**C**) no consistent regulation of *Lsd-2* transcript was observed under starvation conditions by the Northern blot analysis. *RpL9* expression was used as normalization control. (**B**) The gene *CG3348* was among the strongest downregulated genes in the GeneChip analysis (**C**) consistent with that, quantitative RT-PCR analysis detects a decrease in transcript amount by a factor of 12,6, 26,7, 6,9 and 31,3 at 6, 12, 18 and 24 hours respectively. The transcriptional upregulation of the *to*-like gene *CG11854* was confirmed by quantitative RT-PCR revealing a 3,0, 3,4, 2,5 and 2,5 fold increase in transcript amounts after the indicated starvation time. (**C**) Transcriptional regulation of selected genes analyzed by GeneChip analysis. D indicates downregulation, I upregulation and NC no change in response to starvation. (Note: Two 18 h data sets due to duplicate GeneChip experiments). Functional classification of 113 starvation-upregulated genes (**D**) and 110 starvation-downregulated genes (**E**) identified by comparative GeneChip analysis.

The starvation-induced metabolic activation is further reflected by the transcriptional upregulation of five regulatory kinases or kinase subunits, which all have been implicated in energy homeostasis control. While the pyruvate dehydrogenase kinase encoded by *pdk* is critical for the regulation of oxidative glucose metabolism, the β subunit of the SNF1/AMP-activated protein kinase (AMPK) acts as a cellular energy sensor (Pan and Hardie, 2002) and

the cAMP-activated protein kinase A (PKA) promotes glycogen and TAG catabolism (Londos et al., 1999). The SNF4 γ subunit *loechrig* has been implicated in cholesterol homeostasis control (Tschape et al., 2002). In addition, mutants for the Lk6 kinase have been described, which have an increased organismal TAG content, suggesting a function in the control of organismal lipid storage (Reiling et al., 2004; Arquier et al., 2004).

Among the seven upregulated genes involved in lipid metabolism are genes encoding a putative TAG-Lipase (*CG5966*), phospholipase A_2 (*CG1583*), low-density lipoprotein receptor (*LpR2*), long-chain-fatty-acid-CoA ligase (*CG9009*) and carnitine-O-palmitoyltransferase (*CPTI*). Anabolic reactions of the lipid metabolism are repressed under starvation as indicated by the transcriptional downregulation of a lipogenic 1-acylglycerol-3-P-O-acyltransferase (*CG4753*) and a long-chain-fatty-acid elongase (*CG6261*). Moreover, the PAT domain containing lipid storage droplet-associated protein *Lsd-1* (Miura et al., 2002) and three TAG lipases are among the nine genes involved in lipid metabolism which are downregulated in response to starvation. The downregulation of *Lsd-1* was confirmed by Northern blot analysis (Fig. 7A). In contrast, the second *Drosophila* PAT domain-encoding gene, *Lsd-2,* is not transcriptionally regulated according to Northern blot analysis (Fig. 7A). The transcription of the *CG12813* gene, whose mammalian homologues have been implicated in cholesterol homeostasis, is almost completely repressed under starvation (Fig. 7A). For a more detailed depiction of the transcriptional metabolic starvation response see discussion 3.1.

Taken together genome-wide transcriptome profiling of fed versus food-deprived flies displays various regulatory aspects of the metabolic starvation response in *Drosophila*, including carbohydrate, amino acid and lipid catabolism. Of the 223 starvation responsive genes, no function has been assigned to 25 of the starvation upregulated as well as 32 starvation-downregulated genes. Evolutionary conserved starvation-induced genes of unknown function are considered candidates for regulators of energy homeostasis. Four of them were subjected to further functional characterization, namely *bmm* (see below) and *dob* (supplement 1). They encode Patatin-like domains diagnostic for proteins with lipase activity and the genes *nocturnin* (supplement 4) and *Dreg-2* (supplement 5), which are candidates for linking circadian rhythm and energy homeostasis control.

2.2 Molecular characterisation of the *brummer* gene

In a genome-wide screen for starvation responsive transcripts two genes, *CG5295* and *CG5560* with unknown function were identified to be upregulated under starvation. According to the mutant phenotype (see below), *CG5295* was renamed as *brummer* (*bmm*) and *CG5560*, which is the only *bmm* paralogue, was termed *doppelgänger von brummer (dob).*

2.2.1 Genomic organization at the *brummer* gene locus

The *bmm* gene is located at the cytogenetic map position 70F5 on the left arm of the *Drosophila* 3rd chromosome (Consortium T.F., 2003). By RT-PCR, a 2375 bp *bmm* cDNA was isolated (for details see Material and Methods) corresponding to the 2402 bp cDNA LD21785 (Rubin et al., 2000). Alignment of cDNA with genomic DNA sequences (AE003533) reveals that *bmm* is encoded by 8 exons spanning about 10 kb of genomic DNA, whereby exon 1 is separated by a large intron (6897 bp) from the closely clustered exons 2-8 (Fig. 8). Exon 1 to 7 contain the 1524 bp long *bmm* ORF encoding a Brummer protein of 507 amino acids with a predicted molecular mass of 57,2 kDa.

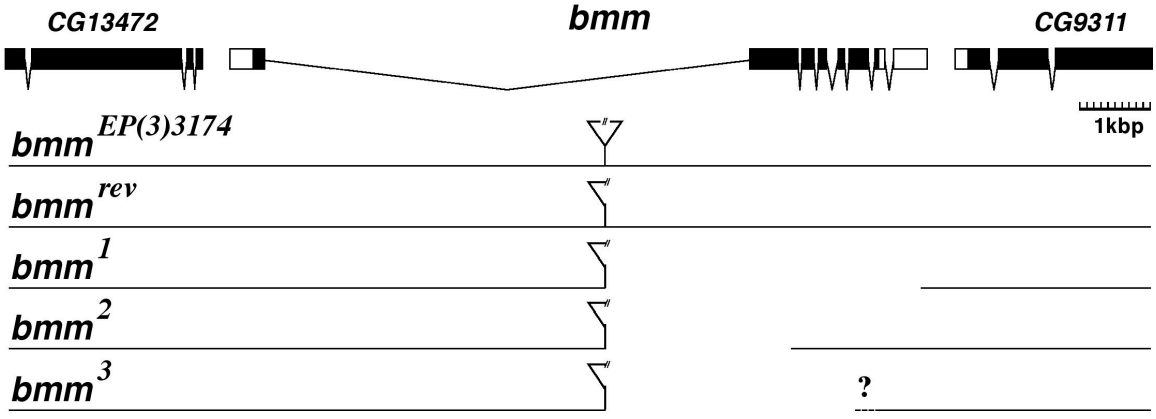

Figure 8: Molecular characterization of the *brummer* gene. (**A**) Genomic organization of the *bmm* gene locus represented by the *bmm* cDNA comprised of 8 exons (coding exons shown as black, UTRs as white boxes). Flies carrying the P-element integration EP(3)3174 (Rorth, 1996) in the first intron of the *bmm* gene were used to create *bmm* deletion mutants (bmm^1, bmm^2 and bmm^3) as well as the genetically matched control (bmm^{rev}). The bmm^3 deletion mutant is not mapped on the sequence level; therefore the putative breakpoint is indicated with a question mark.

2.2.2 Brummer is an evolutionary conserved protein

Searching protein databases (Protein-Protein Blast, NCBI) for Bmm related proteins revealed that Bmm is composed of a 243 amino acids long evolutionary conserved aminoterminal part (CR) and a non-conserved carboxyterminal variable region (VR, amino acids: 244-507) (Fig. 9A). The CR consists of a Patatin-like domain (PLD) first identified in the potato tuber

storage protein Patatin (Racusen and Foote, 1980; Andrews et al., 1988) and the so-called Brummer box (BB) of so far unknown function. Phylogenetic tree analysis based on the CR sequence of various species demonstrates that Bmm-related proteins are found from plants to humans and form the so-called Bmm/Nutrin family of PLD containing proteins (Fig. 9B).

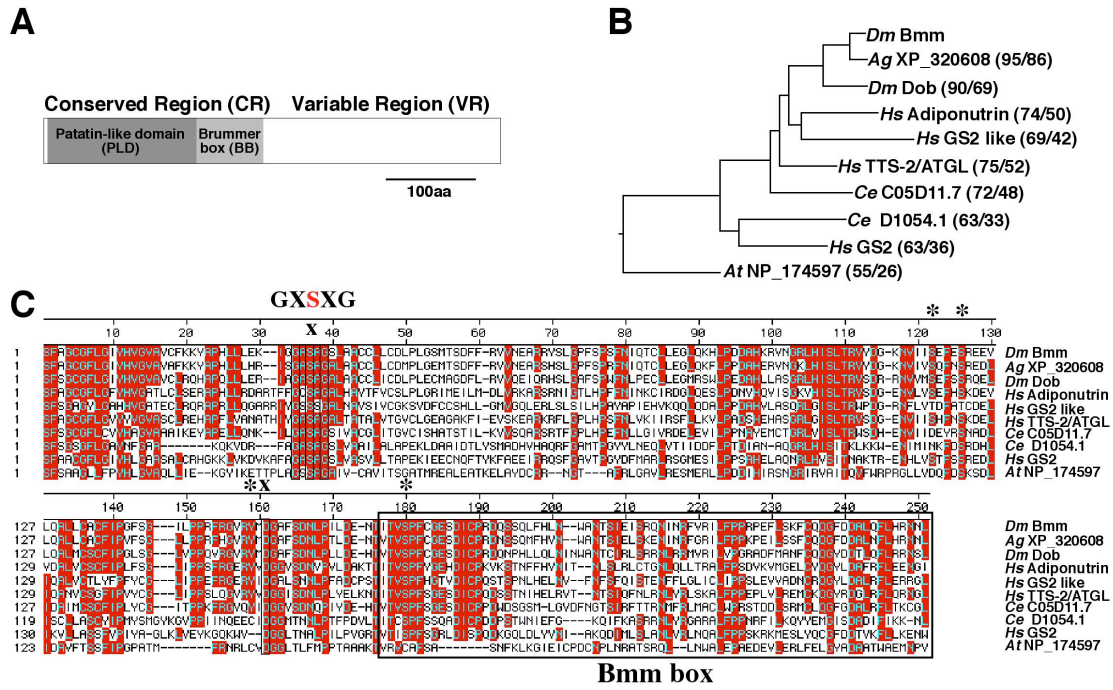

Figure 9: Protein structure of Brummer and the Brummer/Nutrin protein family. (**A**) Schematic structure of the Bmm protein, which consist of a conserved region (CR) and a variable region (VR). CR is composed of a putatively enzymatically active Patatin-like domain (PLD) and the Brummer box (BB). (**B**) Phylogenetic analysis of Bmm/Nutrin protein family members from insect, human, worm and plant based on their CR protein sequences. Besides its predicted mosquito orthologue XP-320608 and its fly paralogue Dob *Drosophila* Bmm is closely related to human Adiponutrin, TTS-2/ATGL, GS2 and GS2-like (Numbers in brackets refer to % amino acid similarity/identity; Abbreviations: *Dm: Drosophila melanogaster; Ag: Anopheles gambiae; Hs: Homo sapiens; Ce: Caenorhabditis elegans; At: Arabidopsis thaliana*). (**C**) Sequence alignment of the CR corresponding to the phylogenetic tree in (**B**). The 171 AA long Bmm PLD contains a serine hydrolase motif (GXSXG) at position 36-40. The serine residue within this motif (S38) is thought to form together with the aspartate residue in position 161 (D161) the catalytic center of the enzyme (marked by x). Evolutionary conserved putative serine (S121, S125, S175) and tyrosine phosphorylation sites are marked with an asterisk.

The closest homologue outside the *Drosophilidae* is the *bona fide Anopheles* Bmm orthologue (XP_320608), sharing 95 % similarity within the CR. *Drosophila pseudoobscura* Bmm is 97 % identical to *Drosophila melanogaster* Bmm. The closest relative of Bmm is its paralogue Dob (90 % similar in CR), which is however not conserved outside the *Drosophilidae*. In humans, four Bmm-like proteins were identified which are Transport secretion protein 2/Adipose triglyceride lipase (TTS2/ATGL), Adiponutrin, GS2 and GS2-like sharing 75%, 74%, 63% and 69 % similarity with *Drosophila* Bmm CR, respectively. Outside the vertebrate taxon, Bmm-related sequences were identified in the nematode

Caenorhabditis elegans (CE05D11.7 and CED1054) and a more distantly related protein in *Arabidopsis thaliana* (NP_174597).

Alignment of the various Bmm-related CR protein sequences identified amino acids highly conserved between the different family members (shaded in red in Fig. 9C). The presence of a PLD suggests a lipase activity of Bmm. This assumption is based on the observation that several PLD-containing proteins were shown to exhibit hydrolytic enzymatic activity on different lipid substrates. For example, the founder of the PLD gene family the mayor potato tuber storage protein Patatin has lipid acyl hydrolase activity on phospholipids, monoacylglycerol (MAG) and galactolipids, but not on di- or triacylglycerol (DAG, TAG) (Andrews et al., 1988; Hirschberg et al., 2001). Two additional plant PLD proteins, the tobacco Patatin 1 and the cucumber Patatin protein, are phospholipase A_2 enzymes (Dhondt et al., 2000; May et al., 1998). The phospholipase activity is evolutionary conserved since non-plant proteins like human Neuropathy target esterase and its orthologue the *Drosophila* Swiss Cheese protein (Glynn, 1999; van Tienhoven et al., 2002), as well as the *Pseudomonas* cytotoxin ExoU (Sato et al., 2003) are PLD-containing phospolipase A_2 enzymes.

Recently the crystal structure of the potato Patatin protein was resolved revealing that the enzymatic active site consists of a serine-aspartate catalytic dyad (Rydel et al., 2003). The active site serine is located within a serine hydrolase motif with the consensus sequence Gly-X-Ser-X-Gly (GXSXG) characteristic of esterases (Rydel et al., 2003). A serine hydrolase motif is also found in the Bmm PLD identifying serine 38 (S38) as the putative catalytic active serine residue (Fig. 9C). The serine hydrolase motif is highly conserved between all Bmm/Nutrin family members with the core residues being invariant between species underlining the essential function of this amino acids.

Site-directed mutagenesis replacing the active site serine by alanine resulted in a complete inactivation of enzyme activity (Hirschberg et al., 2001; Rydel et al., 2003). Using the same approach, the active site aspartate residue was identified (Hirschberg et al., 2001; Rydel et al., 2003). In the case of Bmm, this residue is located at amino acid position 157 and is like the serine residue present in all Bmm-like proteins (boxed in Fig. 9C).

In addition to amino acids putatively involved in enzymatic activity, other residues which possibly participate in post-transcriptional regulation of Bmm function are highly conserved as well. *In silico* predictions using the NetPhos 2.0 server (Blom et al., 1999) identified two putative serine phosphorylation sites at amino acid position 125 and 175 as well as a tyrosine residue at amino acid position 159 that are highly conserved between Bmm and the human

homologues Adiponutrin and TTS-2/ATGL (* in Fig. 9C). In summary, the Bmm protein belongs to the Bmm/Nutrin protein family of PLD containing proteins, a family of putative lipases, which is conserved from plants to humans.

2.2.3 Brummer is a novel Triacylglycerol lipase

In order to analyze the putative lipase activity of the Bmm protein, which is predicted by the presence of a PLD in the CR, recombinant Bmm protein was expressed and used for *in vitro* lipase assays on different lipid substrates (Fig. 10).

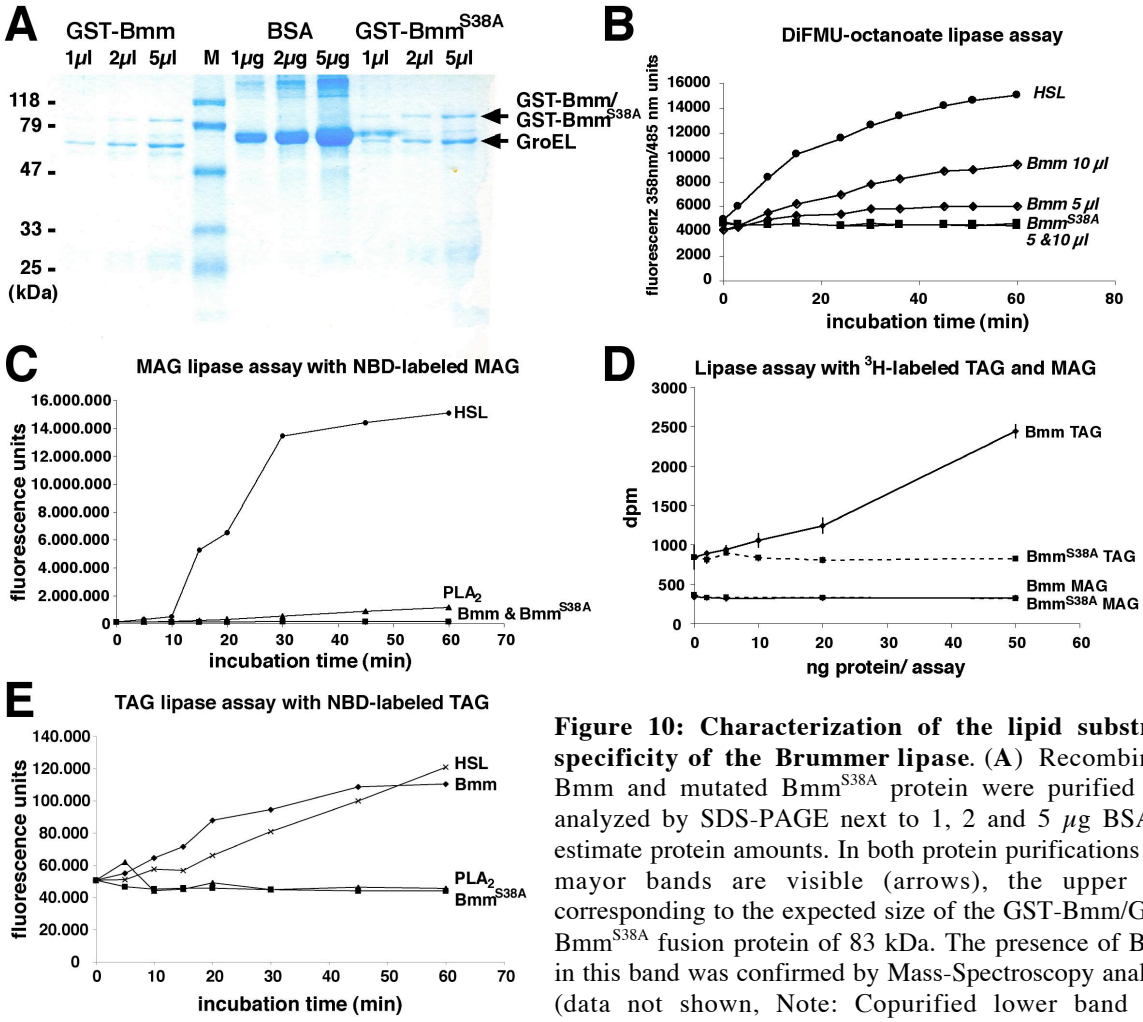

Figure 10: Characterization of the lipid substrate specificity of the Brummer lipase. (**A**) Recombinant Bmm and mutated Bmm^{S38A} protein were purified and analyzed by SDS-PAGE next to 1, 2 and 5 μg BSA to estimate protein amounts. In both protein purifications two mayor bands are visible (arrows), the upper one corresponding to the expected size of the GST-Bmm/GST-Bmm^{S38A} fusion protein of 83 kDa. The presence of Bmm in this band was confirmed by Mass-Spectroscopy analysis (data not shown, Note: Copurified lower band was identified as the bacterial contaminant protein GroEL.). (**B**) Bmm has lipase activity on a non-specific lipid substrate. Bmm but not Bmm^{S38A} protein hydrolyzes a DiFMU-octanoate substrate in a dosage dependent manner, detected by the increase in fluorescence during the incubation period. (**C-E**) *In vitro* lipase assays on fluorescent- (NBD; **C, E**) or ^{3}H-labeled (**D**) MAG and TAG substrates. Dosage-depending release of fluorescent- or radioactive-labeled fatty acid specifically from TAG but not from MAG characterizes Bmm as TAG lipase. Recombinant Hormone sensitive lipase (Hsl) was used as a positive control in (**B-D**). Phospholipase A_2 serves as a negative control for TAG lipase activity in (**C, E**). Bmm^{S38} was not active on any of the tested substrates.

As an enzymatic inactive control, the active site serine residue at amino acid position 38 was replaced by alanine thereby generating a mutated Bmm protein, referred to as Bmm^{S38A}. Both the wild-type and mutated Bmm protein versions were expressed as aminoterminal GST-fusion proteins in *E.coli* cells, purified using the GST-tag in combination with Glutathion-sepharose beads and analyzed for purity using SDS-PAGE (for details see Material and methods) (Fig. 10A). The enzymatic assays were done in collaboration with Dr. Norbert Tennagels, Dr. Stefan Petry and Dr. Günter Müller from Aventis Pharma, Deutschland.

Bmm, but not Bmm^{S38A}, exhibits a dose dependent esterase activity on an esterified fatty acid (6,8-difluoro-4-methylumbelliferyl octanoate, DiFMU-octanoate) substrate (Fig. 10B). Recombinant Hormone sensitive lipase (Hsl) was used as a positive control. In contrast to the PLD-containing proteins discussed above, Bmm did not catalyze the release of fatty acids from the A2 position of a phospholipid substrate (data not shown). In addition no MAG lipase activity was detected, neither by using a fluorescently nor a radioactively labeled MAG substrate (Fig. 10 C, E; Nitrobenzoxadiazole-(NBD)-MAG or ^{3}H-MAG respectively). Bmm hydrolyzes TAG *in vitro* in a time- and dose-dependent manner (Fig. 10 D, E), as shown by two different substrates: an NBD-labeled and a ^{3}H-labeled TAG. In contrast, Bmm^{S38A} exhibits no detectable TAG lipase activity in any of the assays, indicating the essential function of serine 38 for enzymatic activity of the Bmm protein. Recently, human Bmm/Nutrin-family members Adiponutrin, GS2 and TTS2/ATGL have been shown to exhibit *in vitro* TAG-Lipase activity (Jenkins et al., 2004, Zimmermann et al., 2004), suggesting that Bmm/Nutrin-like proteins constitute an evolutionary conserved group of novel PLD-containing TAG lipases. Since the *in vivo* function of these proteins is still unknown, I initiated the functional characterization of *bmm* gene function to reveal a possible organismic role of the *bmm* gene in TAG mobilization and energy homeostasis of *Drosophila*.

2.2.4 Expression patterns of *brummer*

Spatial and temporal expression of *bmm* transcript during embryogenesis and postembryonic stages was analyzed by developmental Northern blot analysis and RNA antisense *in situ* hybridisation (ISH) (Fig. 11).

Developmental Northern blot analysis detects a single *bmm* transcript of approximately 2,6 kb in all ontogenetic stages, corresponding well to the isolated cDNA size. While *bmm* is weakly expressed during larval and pupal development, it is strongly enriched in *ad libitum* fed adult flies of both gender, with comparable amounts in head and body. In addition strong

bmm expression is detected during embryogenesis, with an enrichment in the early embryo suggesting maternal contribution of *bmm* mRNA (Fig. 11A).

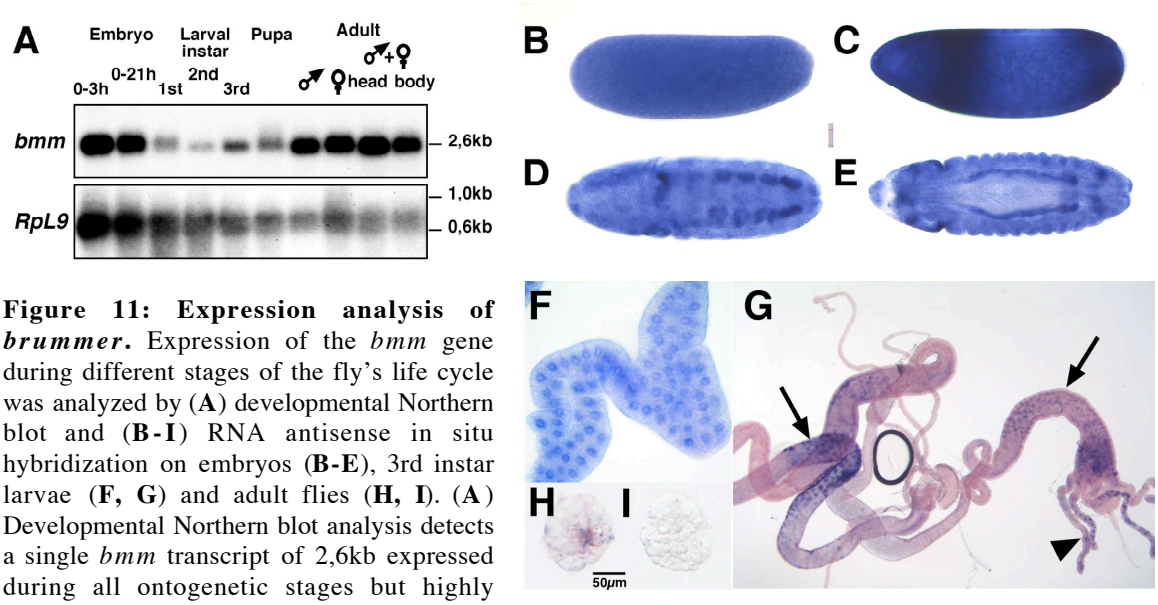

Figure 11: Expression analysis of *brummer*. Expression of the *bmm* gene during different stages of the fly's life cycle was analyzed by (**A**) developmental Northern blot and (**B-I**) RNA antisense in situ hybridization on embryos (**B-E**), 3rd instar larvae (**F, G**) and adult flies (**H, I**). (**A**) Developmental Northern blot analysis detects a single *bmm* transcript of 2,6kb expressed during all ontogenetic stages but highly abundant in early embryogenesis and adult flies of both gender. *RpL9* has been used as normalization control. In the embryo (**B-E**) ubiquitously distributed maternal *bmm* transcript is detected at the early blastoderm stage (**B**). (**C**) First zygotic *bmm* expression is visible as two broad stripes in the cellular blastoderm stage. (**D-E**) Later during development *bmm* is expressed in segmentally repeated patches of cells of the visceral mesoderm that eventually line up surrounding the digestive tract of the embryo. (**B, C**) Lateral and (**D, E**) dorsal views of embryos. (**F-I**) *bmm* is specifically expressed in the fat body and the digestive tract of postembryonic stages. Shown are fat body cells of 3rd instar larvae (**F**) and adult flies (**H**; sense control in **I**) as well as cells of the larval midgut (arrows in **G**) and gastric caeca (arrowhead in **G**).

ISH on whole mount embryos confirms the maternal contribution of *bmm* transcripts, detecting ubiquitously distributed *bmm* mRNA in early blastoderm stage embryos (Fig. 11B). First zygotic *bmm* expression is seen as two broad stripes at the beginning of the cellular blastoderm stage (Fig. 11C). Later during embryogenesis, *bmm* is expressed in visceral mesoderm cells, first seen as segmentally repeated cluster of cells at embryonic stage 11 (Fig. 11D) and in stage 13 embryos as an elongated continuous structure (Fig 11E). Besides the visceral mesoderm expression, *bmm* is also detected in other cells of unknown identity (Fig. 11D,E). In third instar larvae *bmm* is specifically expressed in the fat body (Fig. 11F) and in parts of the midgut and the gastric caeca, respectively (arrows and arrowhead in Fig. 11G). As in larvae, *bmm* is also expressed in fat body cells of adult flies (Fig. 11H). No hybridisation signal was detected in embryos, larvae or adult (data not shown and Fig 11I) using a *bmm* sense RNA probe, indicating the specificity of the ISH analysis.

Taken together, *bmm* is maternally supplied to the embryo, expressed during embryogenesis and in postembryonic stages in organs of fat storage and food resorption. These results are

consistent with the proposal that the Bmm TAG lipase is important for embryogenesis and later involved in peripheral control of energy homeostasis.

2.2.5 Nutritional regulation of *brummer*

bmm was identified in a GeneChip approach as a gene upregulated upon food-deprivation in adult wild-type male flies. To confirm the starvation induction of the gene, *bmm* mRNA amounts of starved and fed flies were compared by quantitative Northern blot analysis (Fig. 12). In accordance with the GeneChip data (supplemental Fig. 1), *bmm* transcript amounts increase after 6 hour of starvation by factor of 1.8 and stay upregulated at 12, 18 and 24 hours by 1.4, 1.8 and 3.1 fold, respectively (Fig. 12A).

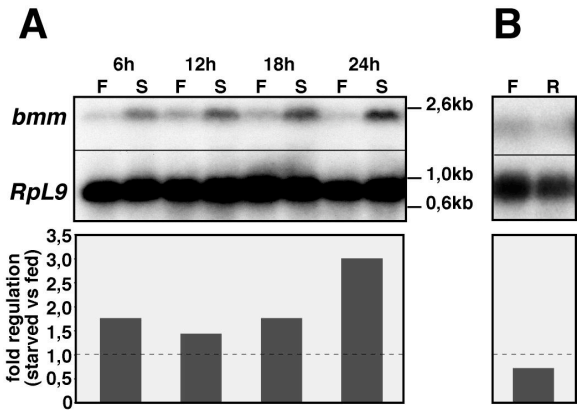

Figure 12: Nutritional regulation of *brummer*. (**A**) Quantitative Northern blot analysis detecting upregulation of *bmm* transcript abundance in flies starved (S) for 6, 12, 18 and 24 hours by factor 1,8-, 1,4-, 1,8- and 3,1 compared to *ad libitum* fed (F) controls. (B) Reversion of *bmm* transcript upregulation by poststarvation refeeding (R: 24 h starved + 24 fed) to an expression level comparable to the one of continuously fed siblings (F: 24 h fed + 24 h fed). *RpL9* gene expression was used as normalization control in **A, B**.

This upregulation is not gender-specific as female flies starved for 6 and 24 hours show *bmm* induction by factor of 1.3 and 1.5, respectively (data not shown). Upregulation of *bmm* transcript was also observed in larvae starved for 4 and 12 hours resulting in 3.0 and 5.8 fold *bmm* induction, respectively (Zinke et al., 2002). In contrast the *bmm* gene is not regulated in larvae fed with 20% sucrose, indicating a starvation-specific response (Zinke et al., 2002). The tight nutritional regulation is further supported by flies subjected to a post-starvation refeeding regimen (Fig. 12B). Within 24 hours of refeeding following an equally long starvation period, *bmm* transcript abundance is downregulated to the level of *ad libitum* fed control flies. The expression in peripheral organs of TAG storage as well as the nutritional regulation suggests that Bmm lipase is involved in TAG storage control in *Drosophila*.

2.2.6 Generation of *brummer* mutants allows *in vivo* analysis of *brummer* function

In order to examine the *in vivo* function of *bmm* in the context of energy homeostasis, *bmm* mutant flies were generated by the imprecise excision of the *P{EP}* transposable element

located in the first intron of the *bmm* gene in the fly line *P{EP}bmm*$^{EP(3)3174}$ (Fig. 8). The conventional P-element mobilization scheme used for this study is described in Ashburner (1989) and a PCR-based screening strategy (details see Material and Methods) was used to identify *bmm* deletion mutants generated by imprecise excision of the P-element.

Sequencing of the corresponding genomic fragments of mutant and wild-type DNA revealed that all three *bmm* alleles still carry residual P-element sequences, which define the 5´-breakpoint of the generated deletions (Fig. 8). In the mutant allele *bmm*^{1} a 4473 bp big deletion removes genomic sequences corresponding to Bmm amino acids 52 to 507. *bmm*^{2} lacks 2640 bp of the *bmm* genomic region corresponding to Bmm amino acids 52 to 249. The 3´ breakpoint of the *bmm*^{3} deletion is not mapped on the sequence level ("?" in Fig. 3), but PCR analysis detects a deletion of at least 3984 bp removing genomic DNA sequences corresponding to Bmm amino acids 52 to 507. In all three *bmm* mutant alleles a mayor portion of the CR coding genomic region is deleted. The deleted part includes aspartate 157, which is part of the catalytic dyad. This finding indicates that *bmm*^{1}, *bmm*^{2} and *bmm*^{3} are enzymatic lack-of-function alleles of the *bmm* gene. The excision line *bmm*^{rev} was generated as genetically matched control for phenotypic analysis. *bmm*^{rev} resembles the *bmm* deletion mutants in carrying residual P-element sequence but has an intact *bmm* coding region (Fig. 8).

2.2.7 brummer is essential for embryonic development

The strong maternal and zygotic expression of the *bmm* transcript in the embryo suggests *bmm* function to be important for embryonic development. Determination of the hatching rate of *bmm*^{1}, *bmm*^{2} and *bmm*^{3} mutant embryos lacking both maternal and zygotic *bmm* expression revealed that *bmm* is essential for embryogenesis as demonstrated by the almost complete embryonic lethality. Only 1.6 %, 2.7 % or 0.3 % of *bmm*^{1}, *bmm*^{2} and *bmm*^{3} mutant embryos hatched to first instar larvae in contrast to 87 % hatching embryos in case of the *bmm*^{rev} control (data not shown). The lethality can be paternally rescued (data not shown) indicating *bmm* function is essential in the embryo but not in the female germ line.

In order to unambiguously show, that the deletion of the *bmm* gene is responsible for the observed phenotype, the lethality was rescued by ubiquitous early zygotic expression of a *bmm* transgene using the UAS/Gal4 system (Rorth, 1996) (Fig. 13A). To this aim, the *bmm* cDNA was cloned in a pUAST vector, used to generate transgenic fly lines referred to as UAS-*bmm* and crossed in the *bmm*^{1} mutant background (for details see Material and

methods). Ubiquitous expression was induced by an *Actin5C*-Gal4 driver line (*act*-Gal4), which was also crossed in the bmm^{1} mutant background.

A

Parental genotype (males x females)	# of embryos scored	% hatched embryos
act-Gal4/CyO; bmm^{1}/bmm^{1} x *act*-Gal4/CyO; bmm^{1}/bmm^{1}	640	0.5
UAS-*bmm*/UAS-*bmm*; bmm^{1}/bmm^{1} x UAS-*bmm*/UAS-*bmm*; bmm^{1}/bmm^{1}	450	9.1
UAS-*bmm*/UAS-*bmm*; bmm^{1}/bmm^{1} x *act*-Gal4/CyO; bmm^{1}/bmm^{1}	269	45.0*
bmm^{rev}/bmm^{rev} x bmm^{rev}/bmm^{rev}	1131	93.8

B

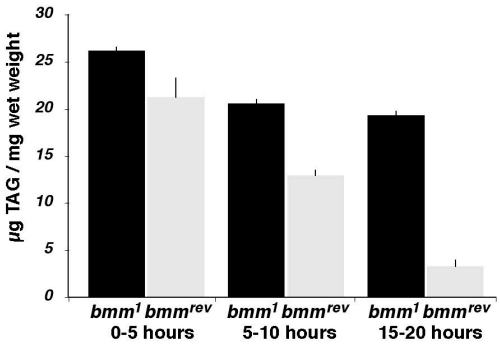

Figure 13: Embryonic phenotype of *brummer* mutants. (**A**) Hatching rate counts of maternal plus zygotic bmm^{1} mutants compared to bmm^{rev} controls reveal that loss-of *bmm* activity causes almost complete embryonic lethality. Embryonic lethality of bmm^{1} mutants is rescued to 90% by ubiquitously expressed zygotic *bmm* supplied via a *bmm* transgene under indirect control of an *Actin5C*-promotor using the UAS/Gal4 System (Rorth, 1996). * Expected hatching rate is 50%. (**B**) TAG content determination of *bmm* mutant embryos aged for ≤ 5, 5-10 and 15-20 hours reveals that bmm^{1} mutant embryos store excessive TAG and mobilize less of their TAG storage during embryogenesis. Compared to bmm^{rev} controls ≤ 5 h old bmm^{1} mutant embryos display a 19 % increase in TAG content. During embryogenesis only 26 % of this TAG is mobilized in bmm^{1} mutant embryos, while bmm^{rev} embryos metabolize 85 % of their TAG storage.

Only 0.5 % *act*-Gal4/CyO; bmm^{1}/bmm^{1} mutant embryos hatched, while 9.1 % of UAS-*bmm*/UAS-*bmm*; bmm^{1}/bmm^{1} embryos developed into first instar larvae (Fig. 13A), possibly as a result of low level constitutive expression from the UAS-*bmm* transgene. Combining the *act*-Gal4 driver, with the UAS-*bmm* transgene in the *bmm* mutant background results in an almost complete rescue (45 % hatching embryos of the expected 50 %; note that only 50% of embryos carry the balancer chromosome *CyO* and therefore do not activate the *bmm* transgene) (Fig. 13A) and proves the specificity of the bmm^{1} mutant phenotype. A closer inspection of bmm^{1} mutant embryos by ISH using a tracheal system marker (*trh*) revealed pleiotropic degeneration phenotypes (data not shown). While bmm^{1} embryos stop development at various stages, many embryos reach stage 17 of embryogenesis and die subsequently without hatching from the eggshell.

Analysing the TAG content of staged bmm^{1} embryo collections demonstrates that the mutants store excessive TAG amounts and show a defect in mobilization of these stores during embryonic development (Fig. 13B). In comparison to young bmm^{rev} (0-5 hours) embryos, bmm^{1} embryos (0-5 hours) store 19 % more TAG. While bmm^{rev} embryos use 85 % of their TAG storage to fuel developmental processes, bmm^{1} mutants mobilize only 26 % of their TAG storage during embryogenesis. These results suggest that *bmm* mutants fail to

develop into larval stages because they cannot use the energy stored in the TAG efficiently and therefore die of starvation.

2.2.8 *brummer* controls fat storage of adult *Drosophila*

While lack of maternal and zygotic *bmm* expression is lethal during embryogenesis, *bmm* zygotic mutant embryos are homozygous viable and develop into adult flies without obvious morphological abnormalities. This feature of *bmm* mutants allowed me the analysis of *bmm* function in adult energy homeostasis by applying loss-of function and gain-of function experiments (Fig. 14).

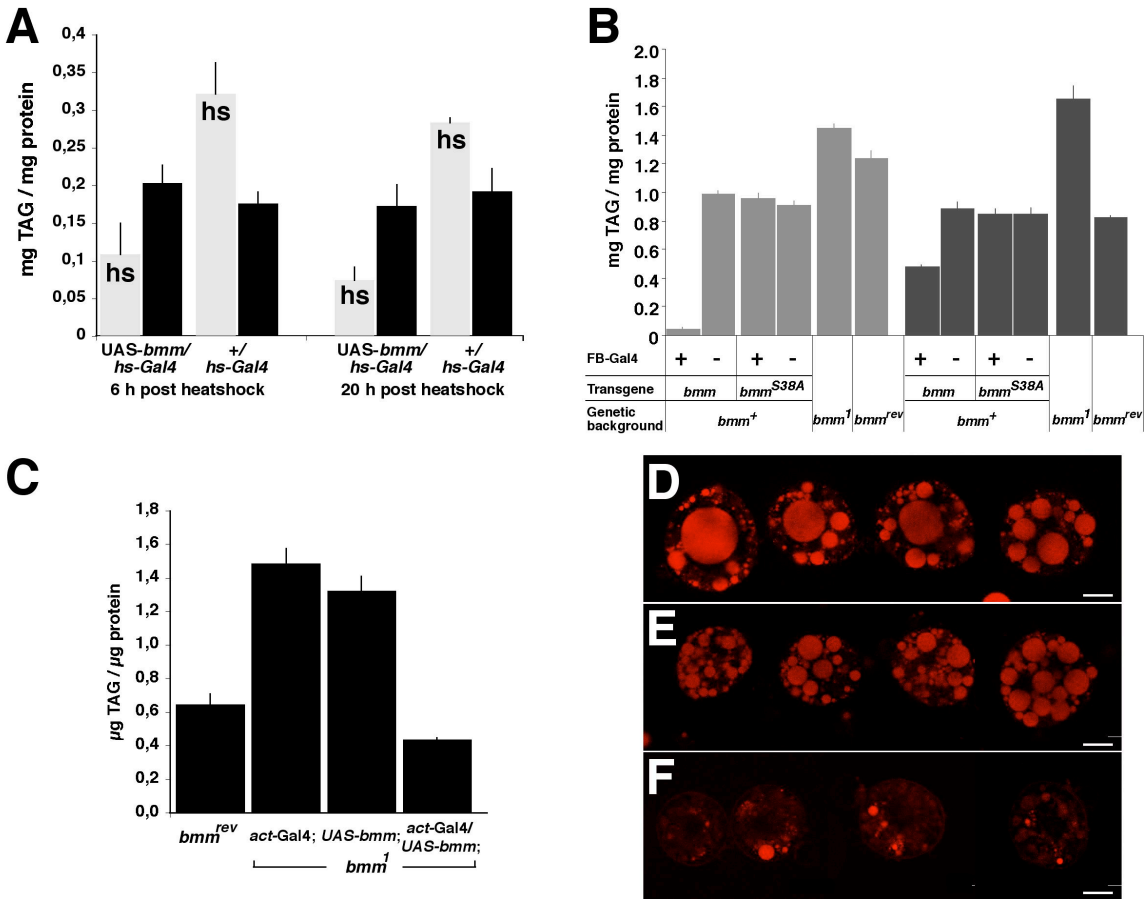

Figure 14: *brummer* is a key regulator of organismal TAG storage. (**A**) Heatshock (hs)-mediated acute induction of *bmm*-transgene expression results in rapid TAG mobilization in adult male flies. Following acute *bmm*-transgene induction for 1 h TAG content is reduced by 46 % and 57 % after 6h and 20h respectively. In contrast control flies lacking *bmm* induction gained 83% (6h) and 48 % (20h) TAG content. (**B**) Control of organismal TAG content of immature (light grey) and mature (dark grey) adult flies by *bmm* loss-of- and gain-of-function. *Ad libitum* fed bmm^{1} mutants accumulate 17% (immature adults) or 101% (mature adults) more TAG than genetically matched bmm^{rev} controls. Induction of a *bmm*-transgene but not a bmm^{S38A}-transgene in the fat body lowers the TAG content by 96% (immature adults) or 46% (mature adults). (**C**) Reversion of *bmm* obesity phenotype by ubiquitous *bmm*-transgene expression. (**D-F**) Cellular phenotype of *bmm*-dependent organismal fat storage regulation. Representative confocal sections of Nile Red stained fat body cells highlighting lipid storage droplets. Numerous, variously sized intracellular lipid droplets in bmm^{1} fat body cells (**D**) reflect the high TAG content of *bmm* loss-of-function mutants, while lipid droplets in *bmm* gain-of-function fat body cells (**F**) are reduced in size and number as compared to wild-type fat body cells (**E**) (scale bar: 20μm).

bmm expression is rapidly upregulated under starvation conditions (see 2.2.5). To mimic this acute starvation response of *bmm* under *ad libitum* fed conditions, overexpression of a UAS-*bmm* transgene was induced using a heatshock-inducible Gal4 driver line (*hs*-Gal4). At 25°C, only low level of UAS-*bmm* expression is activated by the *hs*-Gal4 driver line. To acutely induce high level of *bmm* transcription, flies were heatshocked (hs) 1 hour at 37°C and the organismal TAG content was compared between *hs* and non-*hs* flies after 6 and 20 hours recovery at 25°C, respectively (Fig. 14A). The acute induction of Bmm TAG lipase expression results in rapid TAG mobilization as seen by the decrease in TAG content by 46 % after 6 hours and 57 % after 20 hours. This TAG decrease was not induced by the heatshock treatment itself, because control flies heatshocked in parallel in contrast even gained TAG content (Fig 14A: 83 % after 6 hours and 48 % after 20 hours), probably by increased food uptake. *hs*-Gal4-mediated activation leads to ubiquitous *bmm* expression. Since *bmm* is expressed endogenously in the fat body, the tissue-specificity of *bmm* activity was analyzed. Overexpression of *bmm* exclusively in the fat body of *ad libitum* fed flies was achieved by using a fat body-Gal4 (FB-Gal4) driver in combination with the UAS-*bmm* effector. It leads to a dramatic reduction in organismal TAG content by 96 % in immature and 46 % in mature adult flies (Fig. 14B: 0.04±0.02 to 0.99±0.02 μg TAG / μg protein in immature adult males; light grey and 0.48±0.2 to 0.88±0.05 μg TAG/ μg protein in mature adult males; dark grey). This reduction is due to an overexpression-mediated increase in Bmm TAG lipase activity. Fat body-targeted overexpression of the enzymatic inactive Bmm^{S38A} mutant version, using a UAS-bmm^{S38A} construct does not change organismal TAG content in immature or mature flies (Fig. 14B).

The gain-of-function experiments, i.e. overexpression of *bmm*, demonstrate that *bmm* gene activity is sufficient to regulate organismal TAG content in *Drosophila*. To next test whether *bmm* is also necessary for this regulatory process, the TAG content of *bmm* mutant flies was examined. The lack-of zygotic *bmm* expression in bmm^{1} mutants causes an increase in organismal TAG storage of 17 % in immature (0-24 hours) and 101 % in mature (6-7 days) adult flies as compared to the genetically matched control bmm^{rev} (Fig. 14B: 1.44±0.03 to 1.23±0.06 μg TAG / μg protein in immature adult males; light grey and 1.65±0.09 to 0.82±0.02 μg TAG/μg protein in mature adult males; dark grey). In contrast to bmm^{rev} flies that mobilize 33 % of organismal TAG content during the first 6 days of their life as typically seen in wild-type flies, bmm^{1} mutants flies instead accumulate 19 % more TAG during the same period, a similar phenotype as observed in the *Drosophila* obesity model

system *adipose* (*adp*) (Häder et al., 2003; data not shown). Since bmm^2 and bmm^3 mutant flies show the same obesity phenotype as bmm^1 mutants (data not shown), only bmm^1 was subsequently used in experiments.

In order to unambiguously establish that the obesity phenotype of bmm^1 mutant flies is caused by the loss-of *bmm* function, a UAS-*bmm* transgene was ubiquitously expressed in bmm^1 mutant flies using an *act*-Gal4 driver line (Fig. 14C). The ubiquitous expression of *bmm* completely reverts the increased TAG content of bmm^1 flies, indicating that loss-of Bmm TAG Lipase activity is the cause for the obesity phenotype.

An increased organismal TAG content can be caused either by an increase in fat body cell number and/or by an increase in TAG content per fat body cell. In case of the latter, the organismal TAG content should be reflected by the cellular phenotype of the fat body cells. To address this question, bmm^1 (Fig. 14D), wild-type (Fig. 14E) and *bmm* overexpressing (Fig. 14F) fat body cells of immature adult male flies were analyzed *ex vivo* by staining the lipid droplets using the lipophilic dye Nile Red. bmm^1 mutant fat body cells accumulate variously sized lipid droplets and often very big lipid droplets with a diameter above 20 μm are found. These large lipid droplets are only rarely seen in wild-type cells. In contrast to the *bmm* mutant phenotype, fat body cells overexpressing *bmm* contain almost no or only very small lipid droplets reminiscent of fat body cells from starved flies (compare Fig. 6B). The close correlation between *bmm*-dependent organismal TAG storage and the cellular lipid droplet content suggests that *bmm* regulates the TAG content on the level of the individual fat body cell and not by controlling the number of fat body cells.

To summarize, gain-of-function and loss-of-function experiment demonstrate that the TAG lipase Bmm controls organismal fat storage *in vivo*, likely by adjusting the TAG content at the level of the individual fat body cell. All presented data were obtained using male flies. I would like to add that females show the same overexpression and mutant phenotypes (data not shown), indicating that *bmm* regulates TAG storage in both male and female *Drosophila* flies.

2.2.9 Organismal carbohydrate and protein storage is unaffected by *brummer* activity

Modulation of *bmm* gene activity results in dramatic effects on organismal and cellular TAG content. Thus, *bmm* may affect energy storage in general or is specific for fat storage. To distinguish between these possibilities I asked whether glycogen, the mayor storage form of carbohydrates in animals and like TAG predominantly stored in the fly's fat body

(Butterworth et al., 1965), is also affected in response to variable *bmm* activities. However, neither fat bmm^{1} mutants nor lean flies overexpressing *bmm* in the fat body show differences in their glycogen content when compared with each other and the genetically matched control flies (Fig. 15A). Furthermore, the protein content of *bmm* mutants and *bmm* overexpressing flies does not differ from controls (Fig. 15B). These findings indicate that *bmm* specifically controls TAG storage in *Drosophila*. In contrast to the *Drosophila* obesity model *adp* (Doane, 1960; Häder et al., 2003), there is no obvious trade-off between TAG and glycogen storage in *bmm* mutants.

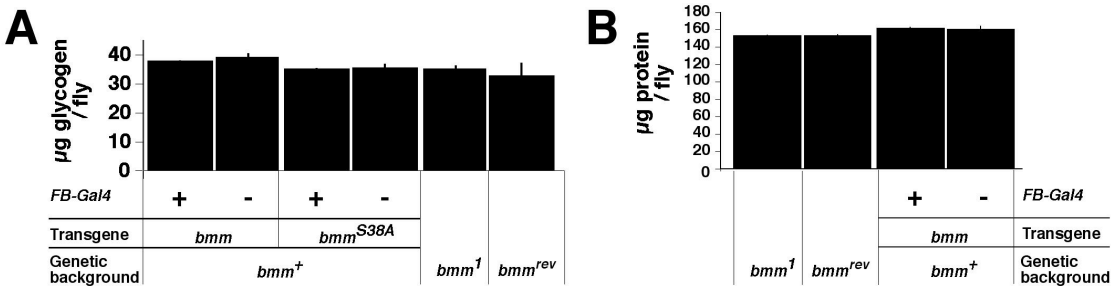

Figure 15: Organismal carbohydrate and protein content of *brummer* mutants. (**A**) Glycogen and (**B**) protein content of fat bmm^{1} mature adult mutant males equals the one of lean flies chronically overexpressing *bmm* in the fat body and is comparable to various control flies with average TAG storage (compare Fig. **14B**).

2.2.10 *brummer* controls survival time and TAG mobilization under starvation

Bmm regulates chronic TAG storage under *ad libitum* fed conditions. Starvation-induced upregulation of *bmm* transcription and TAG mobilization upon acute *bmm* overexpression suggests that *bmm* participates in the regulation of starvation-induced TAG mobilization. To address this question, the physiological starvation response of bmm^{1} mutant flies was examined.

Food-deprived bmm^{1} mutant flies outlive bmm^{rev} controls by 56 % median lifespan increase (Fig. 16A), whereas fat body-specific *bmm* overexpression results in a 17 % reduction of the median starvation lifespan (Fig. 16B). Under starvation conditions bmm^{1} mutants fuel their extended survival time by metabolizing 65 % more TAG than bmm^{rev} controls (Fig. 16C). These results demonstrate a close correlation between TAG content and starvation survival time as has been demonstrated for other fat mutants such as *adp* (Häder et al., 2003), as well as for fly strains selected for increased starvation resistance (e.g. Harshman et al., 1999; Service et al., 1987).

Although bmm^{1} mutants exhibit an increased starvation resistance, the TAG mobilization is impaired in bmm^{1} mutant flies. During the first 24 hours of starvation, TAG consumption is comparable in bmm^{1} (35μg TAG/fly) and bmm^{rev} (33μg TAG/fly) flies. However, bmm^{1}

mutants are fat mobilization defective as they retain 27 % of their stored TAG content (23±1 μg TAG/fly) *post mortem*, whereas bmm^{rev} controls deplete their fat stores almost completely before they die (2±1 μg TAG/fly) (Fig. 16C). These findings demonstrate that although Bmm TAG lipase is involved in starvation-induced TAG mobilization, the process of fat mobilization in *Drosophila* is controlled by more than one TAG lipase, as has been shown for mammals (Fortier et al., 2004; Okazaki et al., 2002; Osuga et al., 2000). Candidate genes for unidentified TAG lipases are the *bmm* paralogue *dob* (supplement 1), the genes *CG5966* and *CG11055* (supplement 2) which encode starvation-induced putative TAG lipases (supplementary Fig. 1) and the putative *Drosophila* Hsl homologue, respectively.

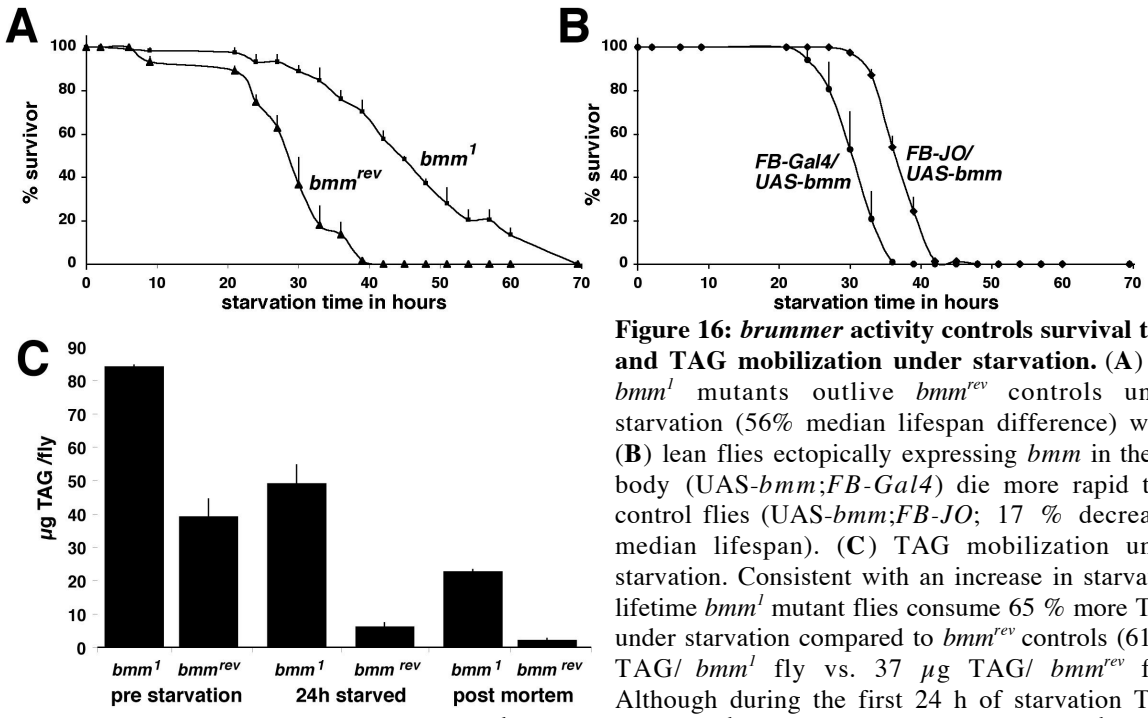

Figure 16: *brummer* activity controls survival time and TAG mobilization under starvation. (**A**) Fat bmm^{1} mutants outlive bmm^{rev} controls under starvation (56% median lifespan difference) while (**B**) lean flies ectopically expressing *bmm* in the fat body (UAS-*bmm*;*FB-Gal4*) die more rapid than control flies (UAS-*bmm*;*FB-JO*; 17 % decreased median lifespan). (**C**) TAG mobilization under starvation. Consistent with an increase in starvation lifetime bmm^{1} mutant flies consume 65 % more TAG under starvation compared to bmm^{rev} controls (61 μg TAG/ bmm^{1} fly vs. 37 μg TAG/ bmm^{rev} fly). Although during the first 24 h of starvation TAG consumption is almost identical between bmm^{1} (35 μg TAG/ bmm^{1}) and bmm^{rev} (33 μg TAG/ bmm^{1}). bmm^{1} mutants are fat mobilization-defective as they retain 27% of their stored TAG (23±1μg TAG/fly) *post mortem* while bmm^{rev} controls deplete fat stores during starvation lifetime (2±1μg TAG/fly *post mortem*). Data were obtained using mature adult male flies.

2.2.11 Bmm/Nutrin TAG lipases are sufficient but not necessary for fat mobilization

The human genome encodes four Bmm/Nutrin TAG lipases (Fig. 9B). In *Drosophila*, this family is represented by only two members: *bmm* and its paralogue *dob*. As observed with *bmm*, the transcript abundance of *dob* is upregulated in response to starvation. Ectopic expression of *dob* rescues the phenotype of bmm^{1} mutant embryos and induces a comparable gain-of-function phenotype when overexpressed in the fat body of adult flies (supplement 1). These findings indicate a Bmm-like enzymatic activity of the Dob protein and demonstrates

that *dob* activity is sufficient to control TAG storage. However, in contrast to *bmm, dob* is not essential for chronic TAG storage control. This conclusion is based on the observation that in contrast to bmm mutants, the TAG content of loss-of function mutant dob^{10} is similar to genetically matched dob^{rev} control flies (Fig. 17A and supplement 1).

Since *dob* is an obvious candidate gene for *bmm*-independent TAG mobilization under starvation, flies lacking both *bmm* and *dob* gene activity were generated and tested for their TAG content and starvation response. *Ad libitum* fed zygotic dob^{10}; bmm^{1} double individuals are homozygous viable and have a similar TAG content as the genetically matched bmm^{1} single mutants (Fig. 17, dob^{rev}; bmm^{1}). This observation supports the argument that *dob* is not involved in chronic TAG storage control. Furthermore, dob^{10}; bmm^{1} double mutants outlive control flies under starvation. This finding reflects their increased pre-starvation TAG storage (compare Fig. 17A to B) and indicates that double mutant flies are able to mobilize their additional TAG stores. Thus, in addition to members of the Bmm/Nutrin family, lipases of different kind must be involved in TAG mobilization under starvation in *Drosophila*.

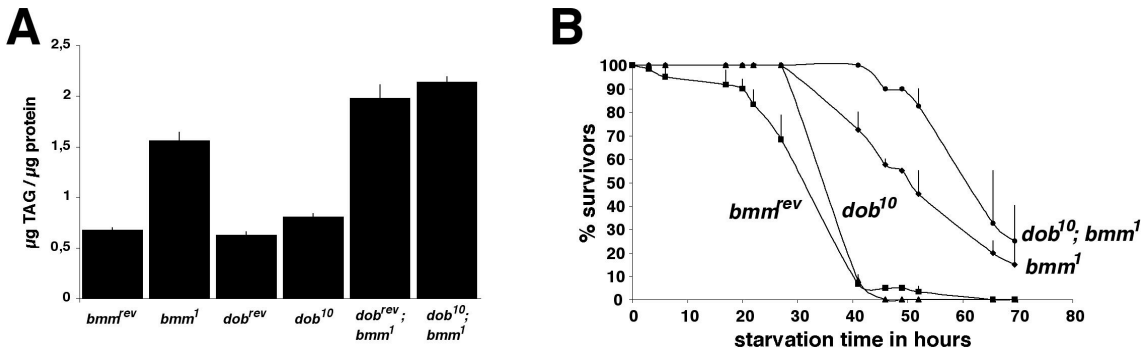

Figure 17: Physiological characterization of *dob*; *bmm* double mutants. (**A**) Organismal TAG content and (**B**) starvation survival time of dob^{10}; bmm^{1} double mutant flies compared to single mutant and revertant controls. *Ad libitum* fed zygotic dob^{10}; bmm^{1} double mutants have a similar TAG content like genetically matched bmm^{1} single mutants (dob^{rev}; bmm^{1}) (**A**) and outlive control flies under starvation to an extend reflecting their pre-starvation TAG storage (**B**).

2.2.12 brummer mutants have a decreased lifespan

Drosophila starvation-resistant flies like mutants of the insulin pathway genes insulin receptor (*InR*) and insulin receptor substrate (*chico*) have an increased TAG content and expanded lifespan under *ad libitum* fed conditions (Brogiolo et al., 2001; Tatar et al., 2001; Clancy et al., 2001; Böhni et al., 1999). In contrast, both the median and the maximum lifespan of fat bmm^{1} mutants under *ad libitum* feeding are reduced by 12 % and 11 %, respectively (Fig. 18A). These observations demonstrate that functional Bmm protein is important for flies' survival. They imply that *bmm* is not a downstream effector of insulin signalling.

Fat body-specific overexpression of *bmm* does not prolong the lifetime of flies. *FB-Gal4*;UAS-*bmm* survive as long as *FB-Gal4*;+ flies (Fig. 18B). Thus, an increased level of *bmm* expression is not detrimental for *ad libitum* fed flies.

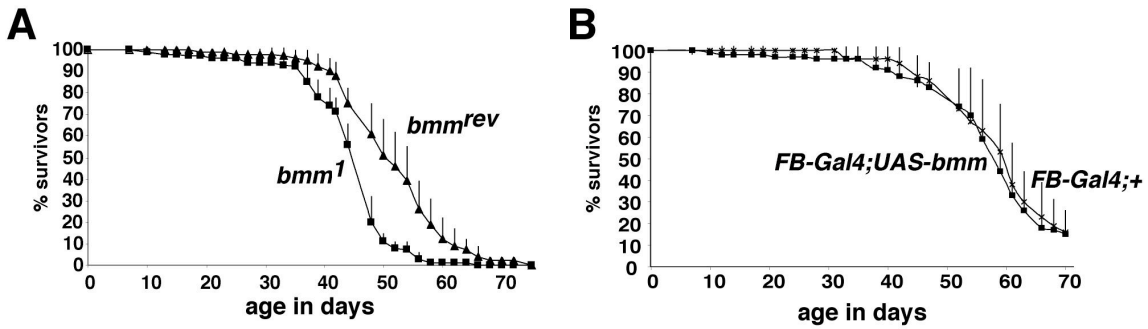

Figure 18: Lifespan analysis of *brummer* mutants. (**A**) Under *ad libitum* fed conditions the medium lifespan of bmm^{1} mutants (44 days) is reduced by 12 % compared to the genetically matched bmm^{rev} control (50 days). In addition maximum lifetime is reduced by 11 % (bmm^{1} 64 days versus. bmm^{rev} 72 days). (**B**) Ectopic expression of *bmm* in the fat body does not affect the lifespan of flies (median lifespan: *FB-Gal4*; UAS-*bmm* 56 days, *FB-Gal4*;+ 56 days).

2.2.13 Conserved region of Brummer targets the protein to lipid droplets

In mammals the intracellular compartmentalisation of TAG lipases is an important feature in the control of lipolysis and critical for proper TAG lipase function (Egan et al., 1992; Clifford et al., 2000; Brasaemle et al., 2000). In order to establish a possible correlation between localization and function of the Bmm TAG lipase in fat body cells, a series of transgenic fly lines conditionally expressing Bmm:EGFP fusion protein variants was generated and assayed for both the intracellular localization and lipolytic activity of the proteins (Fig. 19A).

Fat body-specific overexpression of a full length Bmm:EGFP fusion protein results in a reduction in organismal TAG content comparable to the decrease observed in the non-EGFP counterpart (compare Fig. 19B to 14B). Thus, the EGFP-tag, which was fused to Bmm, does not impair Bmm function. Fluorescent confocal microscopic analysis of *ex vivo* fat body cells monitoring in parallel Bmm:EGFP and lipid storage droplets counterstained with Nile Red reveals that lipolytically active Bmm:EGFP reduces size and number of lipid storage droplets. Most importantly, the Bmm:EGFP protein localizes to islands on their surface frequently representing inter droplet contact sites (Fig. 19C).

The association of Bmm:EGFP with lipid droplets is strong, since Bmm:EGFP remains attached to lipid droplets after isolation from fat body cells (Fig. 19G, H). Furthermore, the localization of Bmm is not an artefact induced by the isolation procedure, since *in vivo* imaging of Bmm:EGFP in fat body cells of anesthetized third instar larvae reveals the same

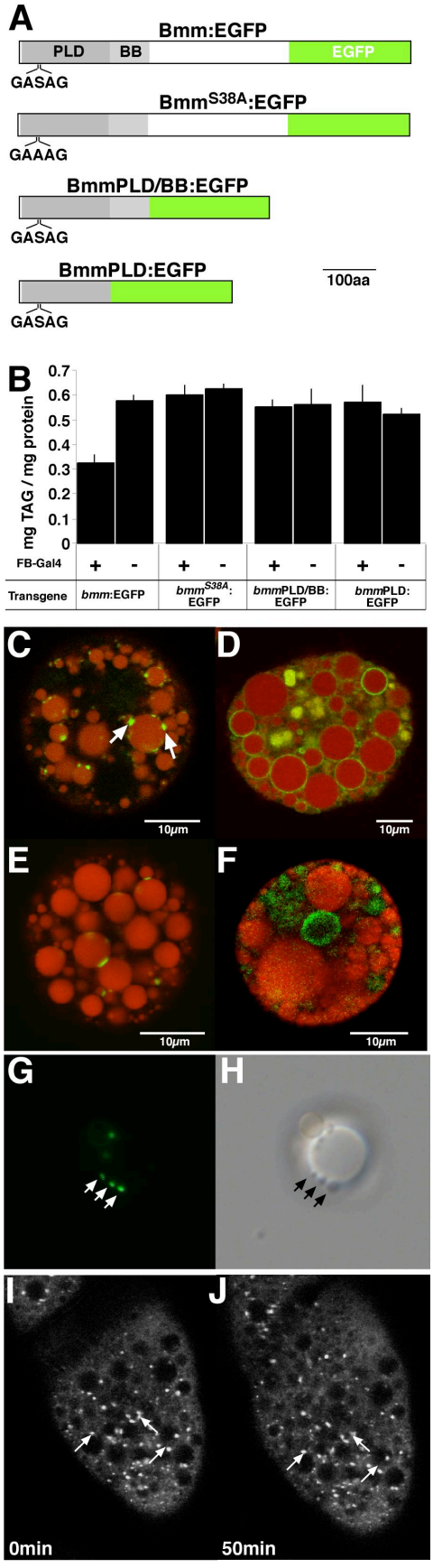

Figure 19: Localization of Bmm:EGFP fusion proteins on fat cell lipid droplets. (**A**) Schematic representation of EGFP fusion protein variants encoded by transgenes used in (**B**) and (**C**): Bmm:EGFP (C-terminal EGFP fusion to Bmm), BMM^{S38A}:EGFP (S38A exchange inactivating the serine hydrolase motif), Bmm-PLD/BB:EGFP (Bmm variable region deletion) and Bmm-PLD:EGFP (Bmm variable region and BB deletion). Abbreviations: PLD (dark grey boxes) = Patatin-like domain, BB (light grey boxes) = Brummer box, GASAG (intact) and GAAAG (mutated) serine hydrolase motif. (**B**) Total TAG content of immature male flies conditionally expressing Bmm:EGFP chimeric proteins in the fat body. Induction of Bmm:EGFP but none of the other variants shown in (**A**) decreases organismal TAG content. (**C-F**) Confocal optical sections of dual-channel fluorescence images showing localization of Bmm:EGFP chimeric protein variants (green) and Nile Red stained intracellular lipid droplets (red) in single *ex vivo* fat body cells of young adult flies. (**C**) Bmm:EGFP chimeric protein localizes to islands on the lipid droplet surface, frequently at interdroplet contact sites (arrows). (**D**) Catalytic center mutant Bmm^{S38A}:EGFP protein distributes homogenously over the lipid droplet surface (Note: Granular yellow signal between lipid droplets represents autofluorescence sporadically observed in fat body cells.). (**E**) Bmm-PLD/BB:EGFP, comprising the conserved region only, localizes similar to Bmm:EGFP. (**F**) Bmm-PLD:EGFP, lacking the BB in addition to the variable region is not associated with lipid droplets (Note: Coarse imaging in (**F**) due to high signal amplification necessary to visualize diffuse distribution of Bmm-PLD:EGFP). (**G, H**) Bmm:EGFP is closely associated with isolated lipid droplets. (**G**) Bmm:EGFP fluorescence and (**H**) phase contrast image of an isolated lipid droplet showing typical Bmm:EGFP localization at interdroplet contact sites (arrows in **G, H**). (**I, J**) *In vivo* imaging of Bmm:EGFP localization in the fat body of anesthetized third instar larvae. Bmm:EGFP localization did not change during the observation period (compare arrows in **I, J**). (**I**) 0 min: start of observation, (**J**) 50 min later.

localization pattern as observed with isolated fat body cells of immature adults (Fig. 19I). The global distribution of Bmm:EGFP protein in larval fat body cells did not change significantly during the monitoring time of 50 min. This observation indicates Bmm:EGFP protein localisation is a rather static feature in third instar larval fat body (compare arrows in Fig. 19 I to J).

In accordance with results obtained with Bmm^{S38A} (see 2.2.8), fat body overexpression of Bmm^{S38A}-EGFP fusion protein does not result in a decrease in organismal TAG content (Fig. 19B). However, the inactivation of the catalytic centre results not only in a loss of enzymatic

activity (see 2.2.3), but also causes an improper targeting of Bmm^{S38A}-EGFP protein. It is evenly distributed over the complete lipid droplet surface and appears in ring-like structures of the confocal images (Fig. 19D). The correlation between localization and enzymatic activity of Bmm:EGFP proteins suggests the Bmm:EGFP localization represent sites of active lipolysis on the lipid droplet surface and that the catalytic center is also responsible for proper localization of the protein.

In order to establish the region of the Bmm protein which is responsible for the specific localization observed with full length Bmm:EGFP, two deletion constructs were generated which either lack the VR (Fig 19A: BmmPLD/BB:EGFP) or the BB and the VR (Fig 19A: BmmPLD:EGFP) (Mildner, 2003). Fat body-specific overexpression of the two constructs did not result in a decrease of organismal TAG content (Fig. 19B). The results indicate that the VR region is important for Bmm lipolytic activity *in vivo*. Bmm-PLD/BB:EGFP localizes to lipid droplet islands similar as full-length Bmm:EGFP, whereas no lipid droplet association was observed with Bmm-PLD:EGFP. This observation identifies the Brummer Box as an essential domain required for intracellular targeting.

In summary, the results show that the evolutionary conserved regions of the Bmm protein are able to target Bmm:EGFP to specific sites on the lipid droplet surface which might represent sites of active lipolysis.

2.2.14 Organismal fat storage control by an antagonistic action of *brummer* and *Lsd-2*

The surface of lipid storage droplets represents an evolutionary conserved intracellular compartment boundary involved in the control of lipolysis (supplement 3). In mammals, the PAT domain protein Perilipin is located on the surface of lipid droplets where it protects cellular TAG stores against uncontrolled hydrolysis. Under stimulated conditions, however, Perilipin facilitates TAG hydrolysis mediated by Hsl and non-Hsl TAG lipases (Sztalryd et al., 2003). Lack-of-Perilipin function results in lean mice with an increased basal lipolysis and can revert the obesity phenotype of leptin receptor-deficient mice to near wild-type (Martinez-Botas et al., 2000; Tansey et al., 2001).

In *Drosophila*, the Perilipin-like PAT domain protein Lsd-2 is located on the surface of lipid droplets (Miura et al., 2002) in fat body cells and adjusts organismal TAG content in a dose-dependent manner (supplement 3). These findings suggest that Lsd-2 functions as an evolutionary conserved mediator of TAG lipolysis. *Lsd-2* and *bmm* mutants have opposite

phenotypes. *bmm*^{1} mutants are fat, whereas *Lsd-2* mutants are lean (Fig. 20A, B, supplement 3).

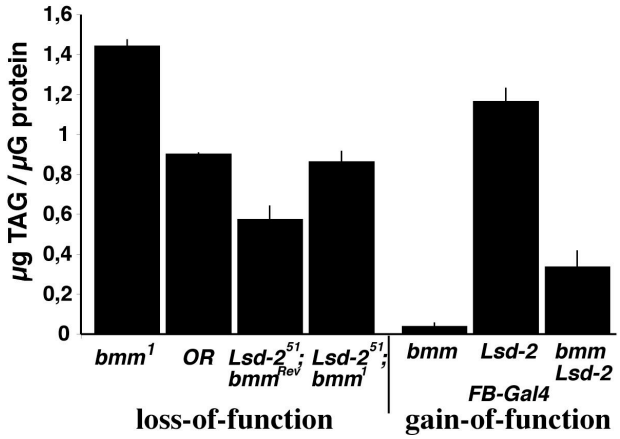

Figure 20: Antagonistic control of organismal fat storage levels by *brummer* and *Lsd-2*. Organismal TAG content of immature adult male flies with varying *bmm* and *Lsd-2* activities. Fat storage of flies having neither *bmm* nor *Lsd-2* function is comparable to *Oregon R* (*OR*) wild types. Concerted gain-of-function allows *Lsd-2* to partially compensate for *bmm*-mediated leanness (for details see text).

Flies lacking both, Bmm and Lsd-2 have wild-type-like TAG levels, demonstrating that lack of *Lsd2* reverts the fat phenotype of *bmm*^{1} mutants (Fig. 20A,B). Conversely, co-overexpression of Lsd-2 and Bmm in the fat body partially reverts the lean phenotype induced by overexpression of Bmm alone. Taken together, these data establish that the two lipid droplet-associated proteins, the TAG-lipase Bmm and the PAT domain protein Lsd-2, act in an antagonistic manner in the control of the fat storage in the adult *Drosophila* fly.

2.2.15 Regulation of *brummer* in mutants of the *adipokinetic hormone receptor* (*AKHR*)

In insects, lipolysis of the fat storage is stimulated by the adipokinetic hormone (AKH) (Gäde and Auerswald, 2003). Like mammalian TAG mobilization, AKH-stimulated lipolysis relies on signalling via a G protein-coupled receptor (AKHR) (Staubli et al., 2002), increase in intracellular cAMP and activation of protein kinase A (PKA) (Gäde and Auerswald, 2003; Van der Horst et al., 2001). However, a TAG lipase mediating the AKH-induced lipolysis is currently unknown.

Flies lacking *AKHR* function resemble *bmm* mutant flies in that they have an increased TAG content, are starvation hyperresistant and show a TAG mobilization phenotype under starvation (R. Kühnlein, personal communication). These observations suggest that AKHR is a likely candidate to function as an upstream regulator of Bmm. To genetically test whether Bmm TAG lipase activity is indeed dependent on posttranscriptional activation by PKA in response to AKH signalling, *bmm* was overexpressed in the fat body of *AKHR* mutant flies and TAG mobilization was assayed (Fig. 21A). The result showed that organismal TAG decrease induced by overexpression of *bmm* in fat body does not depend on *AKHR* function

since no difference between TAG content of *AKHR* mutants and controls was observed (Fig. 21A).

In addition to the direct activation of TAG lipases via PKA, AKH has been shown to induce the transcription of target genes via a still unknown mechanism (Bradfield et al., 1991, Haunerland 1994). In order to test whether the transcriptional induction of *bmm* under starvation is dependent on the AKH pathway, *bmm* expression was assayed by quantitative Northern blot analysis using the RNA of starved and *ad libitum* fed *AKHR* mutants, respectively and of genetically matched control $AKHR^{rev}$ flies (Fig. 21B). Contrary to the expectation, *bmm* transcription is more strongly upregulated in starved *AKHR* mutants (Fig. 21B: 6.3 fold versus 2.3 fold after 12 hours of starvation and 5.3 fold versus 4.7 fold after 24 hours of starvation) and, additionally, *AKHR* mutants appear to have a higher baseline of *bmm* expression. This effect is not due to a general effect on transcription under starvation in *AKHR* mutants, since the starvation induced downregulation of *Lsd-1* transcription is comparable in *AKHR* mutant and $AKHR^{rev}$ flies (Fig. 21B: 1.4 fold versus 1.6 fold after 12 hours of starvation and 2.3 fold versus 2.0 fold after 24 hours of starvation). These data suggest the existence of a regulatory mechanism to compensate for the lack of AKHR-transmitted lipolysis by upregulation of Bmm TAG lipase activity.

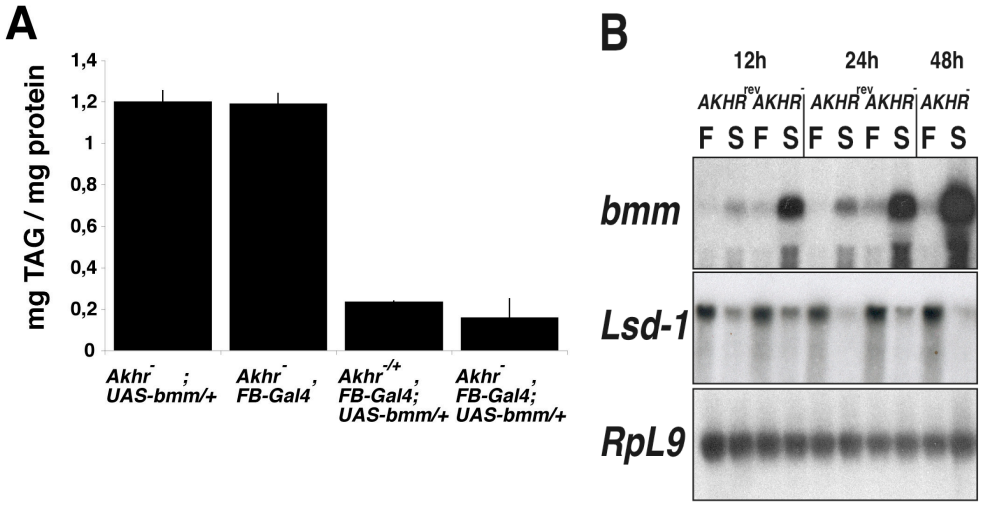

Figure 21: Regulation of *brummer* in mutants of the *adipokinetic hormone receptor* (AKHR). (**A**) *AKHR* function is not essential for ectopic-induced *bmm*-dependent TAG mobilization. Overexpression of *bmm* in *AKHR* mutant flies ($AKHR^{77/91}$) reduces organismal TAG content similar as in heterozygous control flies ($AKHR^{77}/AKHR^{+}$). (**B**) Quantitative Northern blot of *bmm* mRNA levels in starved (S) versus *ad libitum* fed (F) *AKHR* mutant flies reveals that *bmm* transcription is more strongly upregulated in response to starvation in $AKHR^{77/91}$ lack-of function mutants ($AKHR^{-}$) compared to genetically matched $AKHR^{rev}$ control flies (for details see text). *Lsd-1* starvation-downregulation is similar in mutants versus controls (details see text).

In summary, genome-wide transcriptome profiling of the starvation response identified the *bmm* gene. *bmm* encodes a *Drosophila* member of the recently identified Bmm/Nutrin gene family of Patatin-like domain-containing novel TAG lipases. The activity of *bmm* is essential for fat mobilization fueling *Drosophila* embryogenesis and functions as a nutritionally controled key regulator of chronic lipid storage in adult flies. Transcriptional control of *bmm* is also an indispensable part of the acute starvation response that allows full metabolic access to storage fat during periods of extended food deprivation. Bmm localizes to the surface of lipid droplets of fat body cells, a phenomenon that involves its evolutionary conserved sequences. Bmm acts in an antagonistical manner to Perilipin-like Lsd-2 and, thereby, can adjust the fat storage content of the adult fly.

3 Discussion

3.1 Transcriptome profiling of the *Drosophila* starvation response

A genome-wide comparative transcriptome analysis between fed and acutely food-deprived mature adult male wild-type flies was performed. In total 223 genes were considered starvation-responsive, from which 113 are transcriptionally upregulated and 110 downregulated under starvation conditions. It is likely that the actual number of transcriptionally regulated genes in starved *Drosophila* flies exceeds 223: On the one hand the entire flies were used for the analysis. Thus, genes that are only regulated in a few cells may fall below the detection sensitivity of the GeneChip technology. On the other hand, stringent filter criteria were employed (compare results). These may have excluded genes, that are only regulated at one or two analysis time-points. One example is the *dob* gene (supplement 1). *dob* was excluded among the regulated genes because according to the GeneChip results it is only regulated at two analysis time-points. However quantitative Northern blot analysis clearly demonstrated that *dob* is in fact a starvation induced gene (supplement 1). Nevertheless, applying the stringent filter criteria results in a very reliable data set which could be confirmed by quantitative Northern blot and RT-PCR analysis for a number of candidate genes. In addition, sorting the regulated genes according to their predicted function reveals that many of them can be related to processes involved in energy homeostasis. They include factors known to participate in the metabolism of lipids, carbohydrates and amino acids.

3.1.1 Dynamic transcriptome change reflects metabolic starvation response

Survival time of flies under starvation is closely correlated with the organismal TAG content (Häder et al., 2003; Harshman et al., 1999; Service et al., 1987). This correlation indicates that lipids are the most important energy storage form mobilized for energy production. Increased lipid mobilization under starvation is reflected by the transcriptional upregulation of genes involved in lipid metabolism (for an overview see Stryer, 2004), including a low-density lipoprotein receptor (*LpR2*) mediating the endocytotic uptake of low-density lipoproteins, a long-chain-fatty-acid-CoA ligase (*CG9009*) and a carnitine-O-palmitoyltransferase (*CPTI*) involved in fatty acid activation and transport prior to β−oxidation, respectively. In addition, a putative TAG-Lipase (*CG5966*) and a phospholipase A_2 (*CG1583*) were identified, showing increased mRNA amounts in response to starvation. Upregulation of Acetyl-CoA carboxylase (*DmACC, CG11198*) is particularly

interesting, since the mammalian counterparts, ACC1 and ACC2, are key enzymes involved in the regulation of fatty acid synthesis and oxidation (Hardie and Pan, 2002). Conversely, anabolic reactions of the lipid metabolism are repressed upon food-deprivation as indicated by the transcriptional downregulation of a lipogenic 1-acylglycerol-3-P-O-acyltransferase *(CG4753*) and a long-chain-fatty-acid elongase (CG6261).

Repression of phospholipid biosynthesis is reflected by the downregulation of a phosphatidylserine-decarboxylase (*CG5991*). Moreover three TAG-lipases (*CG6295, CG17192, CG5932*), a retinoic and fatty acid binding protein (*RfaBp*), a phospholipase (*CG14034*) and an unspecified lipase (*CG18301*) are downregulated in response to starvation. Of particular interest is the transcriptional downregulation of the lipid storage droplet-associated protein Lsd-1, a member of the PAT domain protein family (Miura et al., 2002). Perilipin, a mammalian member of this family has been implicated in the control of TAG storage in adipocytes (Martinez-Botas et al., 2000; Tansey et al., 2001). Lsd-2, the only other PAT domain protein encoded by the *Drosophila* genome shows no transcription response to starvation, but is involved in TAG storage control (supplement 3). The expression of *CG12813* is almost completely repressed under starvation. The gene encodes a protein with sequence homology to mammalian Niemann-Pick-Type C2 protein (NPC2), a soluble lysosomal protein binding to cholesterol (Liscum, 2000). In human, loss-of NPC gene function results in the Niemann-Pick-Type disease, an intracellular accumulation of glycosphingolipids and cholesterol, manifesting in hepatic and pulmonary failures as well as progressive neuropsychiatric phenotypes (Naureckiene et al., 2000). This analogy suggests a role for the *Drosophila* CG12813 protein in cholesterol homeostasis.

Nearly half of the transcriptionally upregulated metabolic enzymes are involved in carbohydrate catabolism (for an overview see Stryer, 2004), most of which contribute to the generation of glucose-6-P to fuel glucose oxidation via glycolysis (Fig. 22A). This includes an α−Amylase, encoded by *Amy-D,* catalyzing the endohydrolysis of glycogen into oligosaccharides, and six maltases which subsequently hydrolyze the oligosaccharides to glucose. Interestingly, the co-regulated maltase genes are organized in two clusters on the genome, one at cytogenetic position 44D1 including *CG11669, CG8690, CG30359* and *CG30360* (Fig. 22D) and the other at 33A3-4 composed of *CG14934* and *CG14935.* The genomic clustering of co-regulated genes is also observed for serine protease genes (see below) as well as for three uncharacterized genes *CG10513, CG10514, CG11892*, (Fig. 22E). This observation suggests that these genes are regulated via the same cis-regulatory

elements and transcription factors. Consistent with the resulting glucose production, I identified six starvation-induced sugar transporters, which are involved in the cellular glucose import or export. They include the $NaPO_4$ symporter *CG3036*, a member of the evolutionary conserved solute carrier 17 family (Shibui et al., 1994).

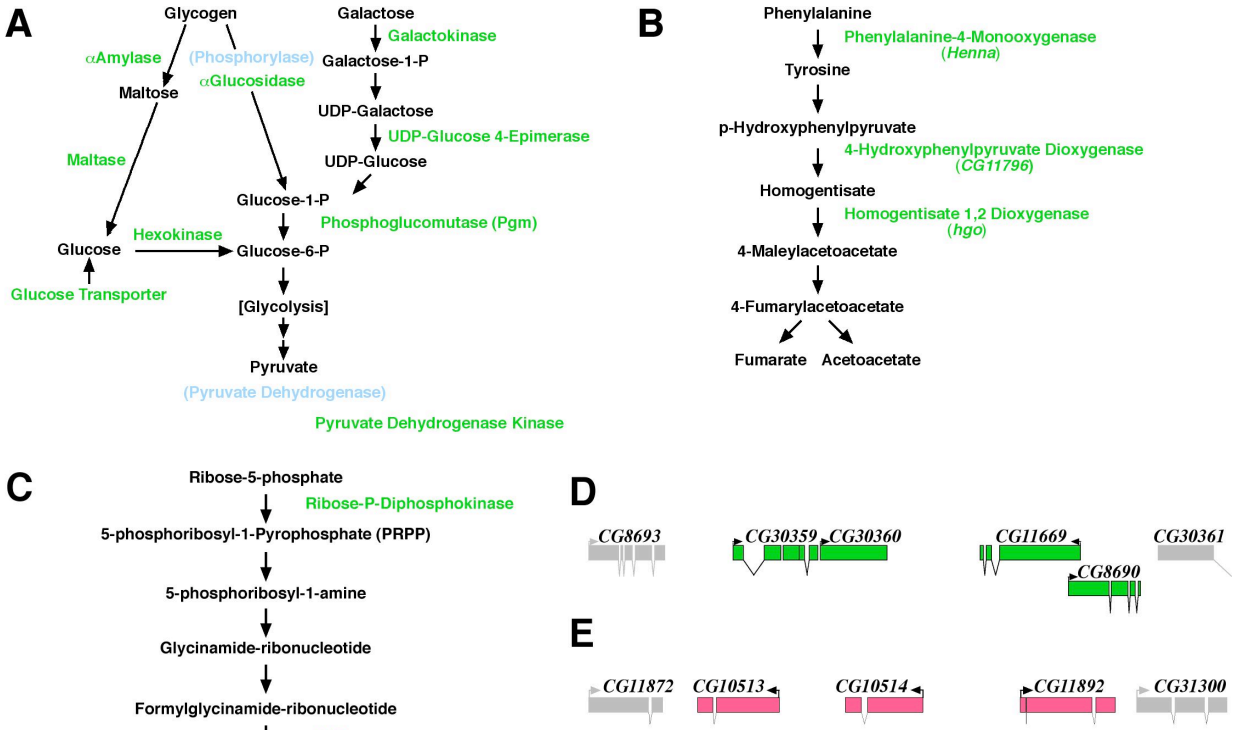

Figure 22: Starvation induced genes involved in metabolic pathways. Proteins encoded by starvation-upregulated genes (green) are involved in (**A**) carbohydrate and (**B**) amino acid catabolism, as well as (**C**) *de novo* IMP synthesis (not regulated enzymes in blue). (**D - E**) Coordinately regulated gene clusters. (**D**) Four starvation-induced maltase genes (*CG30359, CG30360, CG11669* and *CG8690*) at cytogenetic position 44D1 and (**E**) three uncharacterized genes (*CG10513, CG10514, CG11892*) downregulated under starvation at cytogenetic position 96 C8-9 (downregulated genes are indicated in red, for details see text).

Two other key enzymes of carbohydrate catabolism, Hexokinase (*Hex-C*) and Phosphoglucomutase (*Pgm*) are upregulated in starved *Drosophila* flies. Both proteins are directly involved in the generation of glucose-6-P the initial step of glycolysis. Hex-C phosphorylates glucose, whereas Pgm catalyzes the conversion of glucose-1-P to glucose-6-P. Glucose-1-P is generated by the hydrolysis of glycogen by α–Glucosidases as well as by the conversion of galactose to glucose. In both pathways, starvation-induced genes were identified. They include a α–Glucosidase (*CG11909*) and a galactokinase (*CG5288*) as well as an UDP-Glucose-4-epimerase (*CG12030*) (Fig. 22A). In summary, under starvation

condition the level of enzymes involved in the production of glucose-6-P are upregulated, reflecting an increased energy production via the glycolytic pathway.

Pyruvate, the final product of glycolysis enters the citric acid cycle as acetyl-CoA generated by oxidative decarboxylation. This reaction is catalyzed by the mitochondrial enzymatic complex pyruvate dehydrogenase and is the first irreversible step in glucose oxidation. Therefore, it is critical in the regulation of oxidative glucose metabolism (Stryer, 2004). The activity of the pyruvate dehydrogenase complex is regulated via phosphorylation by pyruvate dehydrogenase kinase encoded by *pdk* (Holness and Sugden, 2003), which is upregulated under starvation in adult *Drosophila* flies (Fig. 22A). The starvation induction of *pdk* is evolutionary conserved. The mammalian homologue *Pdk4* is upregulated under starvation in various tissues including adipose tissue, liver, kidney and skeletal muscles (Furuyama et al., 2003; Wu et al., 2000). *Pdk4* is a critical for maintaining the level of blood glucose during starvation. Furthermore, increased Pdk activity has been implicated in the pathogenesis of insulin resistance and non-insulin-dependent *Diabetes mellitus* (Bajotto et al., 2004). The conserved response in the fly, i.e. the transcriptional upregulation upon starvation, suggests that *pdk* also functions in *Drosophila* energy homeostasis.

Sorbitol dehydrogenase, an enzyme of the polyol pathway, is another example of an evolutionary conserved gene that is upregulated under starvation conditions. Its activity is implicated in the development of diabetic complications in mammals, contributing to diabetes-induced oxidative stress (Chung et al., 2003). The starvation-induced transcriptional response of genes involved in carbohydrate metabolism is further supported by the upregulation of transketolase (*CG8036*), a key enzyme that provides a reversible link between glycolysis and the pentose phosphate pathway.

In addition to their sugar reserves, flies start to degrade proteins under prolonged starvation. This feature is also reflected on the transcriptional level by the upregulation of genes involved in amino acid catabolism (for an overview see Stryer, 2004). They include genes encoding a serine type peptidase (*CG3739*), two aminotransferases (Glutamate oxaloacetate transaminase 2 encoded by *got2* and Serine-pyruvate aminotransferase encoded by *spat*) that catalyze the initial deamination step in amino acid degradation. In addition, upregulation includes the gene encoding an argininosuccinate lyase (*CG9510*) that is involved in ammonium disposal. An increase in the degradation of phenylalanine and tyrosine is suggested by the co-regulated induction of expression of the gene *henna* encoding a phenylalanine-4-monooxygenase, CG11796 encoding a 4-hydroxyphenylpyruvate-

dioxygenase and *hgo* encoding a homogentisate-1, 2-dioxygenase, all enzymes which act in the same pathway (Fig. 22B). While many genes involved in amino acid catabolism are upregulated, proteases and protease inhibitors constitute the largest group of genes, which are downregulated under starvation. Most of the proteases belong to the large gene family of serine proteases, a group of secreted enzymes which is involved in protein degradation in the digestive tract related to mammalian trypsin and chymotrypsin (Ross et al., 2003). Since no food needs to be processed in the digestive tract under starvation, the downregulation of the digestion enzymes may reflect an energy-saving mechanism in the absence of food. Remarkably, many of the coordinately downregulated serine protease genes are organized in clusters along the genome, the largest one is localized at cytogenetic position 47F1 and comprises of the genes encoding λTrypsin, ζTrypsin, ιTrypsin and τTrypsin, respectively. In contrast to the upregulated protein degradation system, protein storage is repressed under starvation. This conclusion is consistent with the finding that the transcription of *larval serum protein 1β* mRNA (*Lsp1β*), a storage protein, is downregulated upon starvation (Wolfe et al., 1977).

Purine nucleotide metabolism (for an overview see Stryer, 2004), in particular the *de novo* synthesis of inosinate (IMP), appears to be increased under starvation. This conclusion is based on the observation that the gene *CG6767* encoding Ribose-phosphate diphosphokinase, which catalyzes the initial and rate limiting step in IMP synthesis, is transcriptionally upregulated. In addition, starvation-induction of the *adenosine 2* (*ade2*), *adenosine 3* (*ade3*) and *adenosin 5* (*ade5*) genes encoding a Phosphoribosyl-formylglycinamide synthase, a Phosphoribosyl-amylamine-glycineamide-cyclo-ligase and a Phosphoribosyl-aminoimidazole-carboxylase, respectively, was observed (Fig. 22C). The physiological relevance of an increased purine metabolism under starvation is not obvious and remains to be elucidated.

As discussed above, the comparison of starvation-induced transcriptome changes resulted in the identification of many enzymes that participate in carbohydrate metabolism, protein metabolism and lipid metabolism. In addition, genes with a putative regulatory function in the control of energy homeostasis were identified. They include genes encoding five protein kinases, one transcription factor and two factors involved in translation control. The five starvation-induced protein kinases are implicated in energy homeostasis and the role of Pdk was already described in the context of carbohydrate catabolism (see above). The regulatory β and γ subunits of the *Drosophila* AMP-activated protein kinase (DmAMPK) are

transcriptionally upregulated under starvation. The βsubunit acts as a sensor of cellular energy charge that regulates AMPKs activity as a metabolic master switch. Upon activation, it switches off ATP-consuming processes and activates catabolic pathways that generate ATP (Hardie and Pan, 2002). In addition, AMPK is involved in the regulation of gene expression, e.g. activated AMPK inhibits the expression of lipogenic enzymes (Leff, 2003). The phenotype of loss-of function mutation of the *Drosophila* AMPK/SNF4 γ subunit *loechrig* indicates a function for AMPK in the control of cholesterol homeostasis in the fly (Tschape et al., 2002). In mammals, cAMP-activated protein kinase A (PKA) is a key regulator of energy storage control which promotes TAG catabolism (Londos et al., 1999). The starvation-induced upregulation of the *Drosophila Pka-C3* gene suggests a similar function for this gene in the regulation of energy homeostasis in the fly. Most recently, mutants of the starvation-induced *Lk6* kinase were generated. They exhibit an increased starvation survival time and organismal lipid content (Reiling et al., 2004; Arquier et al., 2004).

sugarbabe (*sug*) is the only transcription factor which shows a transcriptional response upon starvation. In contrast to *Drosophila* larvae, where *sug* expression is strongly upregulated upon sugar feeding but unresponsive to starvation (Zinke et al., 2002), *sug* transcription of adult flies is downregulated upon starvation. *sug* is thought to repress genes involved in fat catabolism, including a set of lipases (Zinke et al., 2002). This conclusion is consistent with the downregulation of the factor in adult flies. Finally, two genes which products are involved in the control of translation initiation are upregulated in response to starvation, *eIF3-S10* (CG9805) and *thor*. This regulation suggests that control of protein translation participates in the regulation of starvation response in *Drosophila*. Thor, the *Drosophila* homologue of mammalian PHAS1/4E-BP, is particularly interesting in this context. It is a target of the PI(3)K/Akt1 (insulin) and Target of rapamycin (Tor) pathways, which integrate signals from nutrients and growth factors (Miron et al., 2003). Interestingly, mutants in the *Drosophila* Tor gene (*dTor*) show several features of normal larvae that were starved for amino acids (Oldham et al., 2000; Zhang et al., 2000).

3.1.2 Ontogenetic changes in the starvation-response transcription pattern

In contrast to adult *Drosophila* flies that exhibit a discontinous feeding behaviour, *Drosophila* larvae are continous feeders to support the rapid growth and differentiation processes. Since the different demands on the systems controlling energy homeostasis in adults and larvae are possibly reflected by differences in their transcriptome response to

starvation, the 223 starvation responsive genes identified in this work were compared to GeneChip data of transcriptional changes upon food-deprivation in larvae (Zinke et al., 2002). Interestingly, 61 % of starvation-downregulated and 31 % of starvation-upregulated genes in adults were not affected in starved larvae. Moreover, 6,3 % of starvation-downregulated and 10,3, % of starvation upregulated even show a converse regulation. This implies differences in larva and adult energy homeostasis. However, it cannot be excluded that some of the differences are attributed to different experimental conditions, for example different analysis time-points or different fly strains used. But 67 (57%) of upregulated and 36 (33%) of downregulated genes are modulated in a corresponding manner in larva and adult. These findings establish a core set of starvation-responsive genes both in larvae and adults of *Drosophila* (Supplemental Fig. 1).

3.2 The Brummer lipase: Central effector of lipid storage control in *Drosophila*

The *brummer* gene (*bmm*, *CG5295*) was identified among the candidates for novel regulators of energy homeostasis. It encodes a nutritionally regulated protein of what I refer to as the Bmm /Nutrin family of Patatin-like domain (PLD) containing lipases. Enzymatic assays establish Bmm function as a TAG lipase *in vitro*. I*n vivo*, it appears to be essential for embryogenesis. In postembryonic stages, *bmm* is expressed in the fat body. A functional Bmm:EGFP fusion protein was found to localize to islands on the surface of intracellular lipid droplets. In response to starvation, *bmm* expression is upregulated. Ectopic activation of *bmm* in the fat body dramatically reduces the amount of organismal TAG. Conversely, *bmm* loss-of function mutant flies accumulate excess TAG. In summary, these findings demonstrate that *bmm* is a key regulator of organismal TAG storage control in *Drosophila*.

3.2.1 Brummer functions during fly ontogenesis

The regulated balance between lipogenesis and lipolysis is believed to continuously match acute energy needs by TAG mobilization and readjust organismal storage fat content to a genetically determined setpoint during periods of excessive energy supply. Remarkably, the endogenous expression level of *bmm* correlates well with the rate of lipolysis in the different developmental stages. *bmm* is weakly expressed in larvae. In contrast, *bmm* is strongly expressed during embryogenesis and in adult flies. *Drosophila* larvae accumulate large amounts of TAG during their development, suggesting that lipogenesis exceeds lipolysis in larvae. Adult flies, however, exhibit a discontinous feeding behaviour. The observation that *ad libitum* fed adult wild-type flies become leaner during the first weak of their life indicates

that during this period lipolysis exceeds lipogenesis of such adult flies. The *Drosophila* embryo, on the other hand, is a non-feeding developmental stage. Thus rapid proliferation and differentiation processes during this developmental stage must be fuelled by the mobilization of energy storage components, mainly TAG, that are deposited into the egg by the mother.

3.2.1.1 *brummer* is essential for embryogenesis

Mutations affecting lipid metabolism have been shown to impair both *Drosophila* oogenesis and embryonic development (Buszczak et al., 2002; Teixeira et al., 2003). Female flies mutant for the *midway* gene, which encodes a diacylglycerol acyltransferase (Dgat) catalysing the conversion of DAG in TAG the final step in TAG synthesis, have severely reduced levels of neutral lipids in the germline. The resulting mutant egg chambers undergo premature nurse cell death and degeneration (Buszczak et al., 2002). Furthermore, eggs laid by females mutant for the maternal effect gene *Lipid storage droplet-2* (*Lsd-2*) develop into embryos which have a reduced hatching rate and in addition a lower lipid content than wild-type. Loss-of viability could be caused by the reduced lipid amount of the embryos. In some of the mutant embryos, the stored lipids would not be sufficient to fuel embryogenesis which in turn may result in developmental arrest and hatching defects (Teixeira et al., 2003).

Embryos lacking both maternal and zygotic *bmm* expression fail to develop into first instar larvae. Thus, *bmm* function is essential for embryogenesis. Embryonic death was observed in the three independently generated *bmm* deletion alleles and was not complemented by a deficiency (Df(3R)Brd6) encompassing the *bmm* genomic region (data not shown). These findings indicate that the lethal phenotype is caused by the lack of *bmm* activity. Lethality of *bmm* mutant embryos can be paternally rescued (data not shown). Thus, *bmm* activity is essential for the embryo but not for the female germ line. However, young bmm^{1} embryos (≤5 hours) have an increased TAG content. This suggests that *bmm* is involved in regulation of the TAG storage that has been supplied by the mother to the egg. In accordance with the paternal rescue, ubiquitous early zygotic expression of a *bmm* transgene rescues the embryonic lethality of bmm^{1} mutant embryos. This result unambiguously demonstrates that the deletion of the *bmm* gene is indeed responsible for the phenotype observed.

bmm^{1} mutant embryos stop development at different stages, many reach stage 17 of embryogenesis and die subsequently prior to hatching to the larva. This phenotype is reminiscent of the pleiotropic degeneration phenotype observed in *Lsd-2* mutant embryos (Teixeira et al., 2003). It suggests that embryos lacking *bmm* activity cannot mobilize

sufficient TAG to fuel embryogenesis as it has been proposed for *Lsd-2* mutants (Teixeira et al., 2003). Consistently, fat bmm^{1} mutant embryos mobilize only 26 % of their TAG storage during embryogenesis, whereas bmm^{rev} embryos, which are wild-type with respect to *bmm* function, metabolize 85 % of their TAG stores. Taken together, these results suggest that *bmm* mutant embryos fail to mobilize the energy stored in the TAG and accordingly die of starvation.

Many maternal and zygotic bmm^{1} mutant individuals develop into late stage embryos. This suggests a *bmm*-independent TAG mobilization system is additionally active in early stage embryos. This conclusion is supported by the observation that zygotic bmm^{1} mutant embryos mobilize 21 % of their TAG storage within the first 10 hours of embryogenesis, but only 6 % between 10 and 20 hours of embryonic development. The *bmm* paralogue *dob* is a likely candidate for providing this early embryonic TAG mobilization activity. This proposal is supported by the observation that *dob* is expressed only maternally and that Dob can substitute for the lack of *Bmm* function in the embryo (compare supplement 1). In conclusion, *bmm* is involved in TAG storage mobilization which is essential during embryogenesis. Accordingly, mutation of *bmm* results in embryonic lethality.

3.2.1.2 Is *brummer* involved in larval midgut lipolysis?

In addition to the expression in the fat body, *bmm* is also expressed in parts of the larval midgut. This pattern suggests a function for *bmm* in the epithelial midgut cells (enterocytes). In insects, one of the mayor functions of the midgut is to digest dietary lipids, to adsorb and process the digestion products for export in the hemolymph (Arrese et al., 2001). In the intestinal lumen, dietary TAG undergoes hydrolysis to produce fatty acids, glycerol and partial acylglycerols like MAG and DAG. A current model is that absorbed fatty acid in the midgut cells are first converted to TAG. TAG is then stored and serves as a reservoir from which DAG is released in the hemolymph (Arrese et al., 2001).

The function of the midgut as a transient TAG storage organ is supported by findings in the dragonfly *Aeshna cyanea*, for which TAG accumulation in the midgut has been demonstrated (Komnick et al., 1984). In addition, the kissing bug *Panstrongylus megistus*, a vector of the chagas disease has been shown to accumulate TAG in form of lipid droplets in enterocytes following a blood meal. Later during digestion, TAG lipase activity is upregulated in the midgut cells which in turn results in lipid droplet depletion and release of DAG into the hemolymph (Canavoso et al., 2004). However, TAG lipases responsible for the TAG to DAG conversion in the midgut of insects are not yet identified. The expression

in the midgut as well as its TAG lipase activity makes *bmm* a good candidate for contributing to the TAG mobilization in the midgut cells, although it may not be the only TAG lipase involved in this process. This conclusion is based on the fact that transport of DAG from the midgut to the fat body is not completely impaired in *bmm* mutants as indicated by the excessive TAG accumulation in fat body cells lacking *bmm* activity (see below). Further studies including an analysis of midgut cells lacking or overexpressing *bmm,* as well as an analysis of *bmm* expression in adult midgut cells upon starvation or post-starvation-refeeding, are necessary to establish a function of the Bmm TAG lipase in midgut lipolysis and DAG release.

3.2.1.3 *brummer* is a key regulator of TAG storage in adult flies

In adult flies, Bmm is both sufficient and necessary for the regulation of the chronic TAG storage level. Fat body-specific overexpression of *bmm*, but not of the enzymatically inactive bmm^{S38A} mutant, causes lean flies. Thus, the lipase activity of Bmm in the fat body is sufficient to reduce the organismal TAG storage *in vivo*. Conversely, flies lacking *bmm* activity have a dramatically increased organismal TAG content. The resulting "obesity phenotype" is observed with the three independently generated *bmm* mutants and can be reverted to wild-type in response to the ubiquitous expression of a *bmm* transgene. These findings establish that loss of Bmm TAG lipase activity, probably resulting in an overall reduction of lipolysis, causes an increased organismal TAG content. The decreased lipolysis of *bmm* mutants is consistent with the model, predicting that *bmm* catalyzes the initial and rate limiting step of the TAG hydrolysis (compare 3.4.2). The model is supported by the observation that *ad libitum* fed adult *bmm* mutants, in contrast to wild-type flies (see above), even increase their TAG storage during the first 6 days of their life. Other *Drosophila* obesity models like *adp* or *AKHR*, show a similar TAG accumulation profile (Häder et al., 2003; data not shown; R. Kühnlein, personal communication). This correlation suggests a similar mechanism in *adp* and *AKHR* mutant individuals which could be mediated via the Bmm TAG lipase activity (compare 3.5).

In response to food deprivation, *bmm* expression is rapidly upregulated in both larvae (Zinke et al., 2002) and in adult flies. Mimicking the starvation response in *ad libitum* fed flies, by an acute induction of *bmm* expression, results in a rapid decrease in organismal TAG storage. This suggests that the Bmm lipase participates in the acute TAG mobilization under starvation. Consistent with this conclusion, fat mobilization is impaired but not completely absent in flies lacking *bmm* activity. *bmm* mutants are starvation-hyperresistant and consume

more TAG than control individuals under starvation. However, in contrast to wild-type flies, they fail to completely deplete their fat stores during starvation. These results demonstrate that - like in mammals - fat mobilization in *Drosophila* does not rely on the activity of a single lipase such as Bmm (see below). In *Drosophila* the *bmm* paralogue gene *dob* like *bmm*, is transcriptionally upregulated in response to starvation. Gain-of-function experiments indicate also a Bmm-like enzymatic activity of the Dob protein and demonstrate that *dob* activity is sufficient to regulate the organismal TAG storage. However, *dob* (*i*) is not essential for organismal TAG storage control and (*ii*) *dob*; *bmm* double mutants are able to mobilize their TAG stores under starvation. These observations suggest that in addition to the two members of the Bmm/Nutrin family additional TAG lipases are involved in starvation-induced TAG mobilization in *Drosophila*. Candidate genes for these unidentified TAG lipases are the genes *CG5966* and *CG11055*. They code for a starvation-induced putative TAG lipase and the putative *Drosophila* Hsl homologue, respectively. Functional analysis of these genes, as presented here for *bmm* and *dob*, should reveal their involvement in the regulation of organismal TAG mobilization in addition to Bmm.

3.3 Storage TAG lipases in insects and mammals – a comparison

Hormone sensitive lipase (Hsl) has been previously considered to be the only enzyme which catalyzes the rate-limiting step in TAG mobilization in mammalian adipose tissue (reviewed in Haemmerle et al., 2003; Kraemer and Shen, 2002). Recently, this view has been challenged by the observation that Hsl mutant mice – like Hsl mutant *Drosophila* (supplement 2) - are not obese and exhibit residual lipolytic activity in their adipose tissue. This suggests the functional relevance of other non-Hsl TAG lipases (Fortier et al., 2004; Okazaki et al., 2002; Osuga et al., 2000, see also supplement 2). In this context it was important to identify Brummer as a novel TAG lipase that is involved in lipolysis control in the *Drosophila* fat body. Bmm-related proteins are found from plants to humans. They can be grouped as the so-called Bmm/Nutrin protein family of Patatin-like domain (PLD) containing proteins which are characterized by an evolutionary conserved aminoterminal half, including the PLD and Bmm Box, and a non-conserved carboxyterminal region. In mammals, four such Bmm-like proteins could be identified. The Transport secretion protein 2/ Adipose triglyceride lipase (TTS2/ATGL, also called Desnutrin), Adiponutrin as well as GS2 and GS2-like. Recent analyses of these mammalian Bmm homologues indicate remarkable similarities in expression, nutritional regulation, protein localization and

enzymatic activity to *Drosophila*. These findings suggest a conserved function of these proteins in the regulation of lipid storage (see below).

The fat body is the main energy-storage organ of insects (Ritzki, 1978). It has morphological, physiological and developmental similarities to mammalian adipose tissue (Tong et al., 2000). In analogy to *bmm* expression, Adiponutrin and TTS2/ATGL are expressed at high levels in white adipose tissue in mammals (Baulande et al., 2001, Villena et al., 2004). While Adiponutrin expression is restricted to adipose tissue, TTS2/ATGL is also expressed at low level in other tissues (Villena et al., 2004). In contrast, the *GS2* gene shows a broad expression in various organs, whereas its expression in adipose tissue has not been analyzed so far (Lee et al., 1994).

Like *bmm*, TTS2/ATGL is transcriptionally upregulated in response to starvation (Villena et al., 2004; Zimmermann et al., 2004). The similarity in tissue-specific expression and nutritional response of these *bmm*-like genes suggest that the factors controlling expression of *bmm*-like genes in different organisms might also be evolutionary conserved. In mammals, several transcription factors are known to control transcription of metabolic genes, including ADD1/SREBP1, PPARs, C/EBPs (Spiegelman and Flier, 1996; Flier and Hollenberg, 1999) which have homologues in *Drosophila*: Helix loop helix protein 106 (HLH106), Ecdysone-induced protein 75B (*Eip75B*) and Slow border cells (*slbo*), respectively (Rorth and Montell, 1992; Feigl et al., 1989; Theopold et al., 1996). The expression of TTS2/ATGL is induced by glucocorticoids, hormones involved in the organisms' starvation response. However, no glucocorticoid receptor binding sites (GRE) have been found in the 5´ promoter region of the TTS2/ATGL gene (Villena et al., 2004). In addition to a direct binding to a GRE, the glucocorticoid receptor can also interact with other DNA binding transcription factors, such as C/EBPβ and thereby activate the expression of target genes (Nishio et al., 1993).

In the promoter region of TTS2/ATGL several consensus-binding sites for C/EBPβ are present, suggesting that they could mediate the glucocorticoid effect (Villena et al., 2004). A C/EBP binding site is also predicted in the 5´-upstream region of the *bmm* gene (data not shown), suggesting evolutionary conserved C/EBP could control the expression of *bmm*-like genes in organisms as different as flies and humans.

Interestingly, Adiponutrin shows an opposite nutritional regulation as compared to *bmm* or TTS2/ATGL. Adiponutrin is downregulated by fasting and upregulated by feeding, arguing for a different function of this protein (Baulande et al., 2001). This conclusion is further

supported by the intracellular localization of the Adiponutrin protein, which, unlike Bmm, is not found on lipid droplets but strictly localizes to membranes (Baulande et al., 2001). In contrast to this report, more recent evidence suggests that endogenous TTS2/ATGL is also a lipid droplet associated protein (Umlauf et al., 2004; Liu et al., 2004). However, this localization of TTS2/ATGL is possibly not specific for lipid droplets, since a TTS2/ATGL-EGFP fusion protein was also found to be localized in the cytoplasm (Villena et al., 2004). Also, a TTS2/ATGL-His tag protein was found to localize to both lipid droplets and the cytoplasm of 3T3-L1 adipocytes (Zimmermann et al., 2004). In *Drosophila*, there is currently no evidence for a cytoplasmic pool of Bmm protein, and thus it is unknown whether Bmm - like Hsl in mammalian adipocytes - translocates upon lipolytic stimulation from the cytoplasm to the lipid droplets. In mammals, translocation of Hsl as well as its activity are controlled via phosphorylation, a control event catalyzed by PKA (Londos et al., 1999). Also, TTS2/ATGL can be phosphorylated, but in contrast to Hsl, this modification is not mediated by PKA (Zimmermann et al., 2004). *In silico* analysis of Bmm identified three phosphorylation sites that are conserved in TTS2/ATGL. Thus, these sites could be of functional importance, suggesting that Bmm –like its mammalian homologue- is phosphorylated. The starvation-induced AMPK and Lk6 kinases (compare 3.1.1) are good candidates to mediate a putative PKA-independent phosphorylation of Bmm, a proposal that needs to be addressed by further studies.

Hsl is a serine hydrolase (Yeaman, 2004). It is structurally related to a superfamily of esterases and lipases which include acetylcholinesterase, bile-salt stimulated lipase and several fungal lipases. They are characterized by a catalytic triad composed of serine, aspartate and histidine residues, which are arranged in an α/β hydrolase fold (Contreras et al., 1996). Hydrolysis by Bmm is completely blocked by 1 mM diisopropylphosphofluoridate (DFP) (data not shown), an esterase-inhibitor that covalently binds to active site serine residues (Atkins and Glynn, 2000). This observation suggests that Bmm – like Hsl - functions as a serine hydrolase. Consistently, replacing the putative active site serine residue located in a serine hydrolase motif (GXSXG) by alanine completely abolishe TAG lipase activity of Bmm both *in vitro* and *in vivo*. These results resembles the one obtained with plant PLD proteins (Hirschberg et al., 2001; Rydel et al., 2003) and implies both a similar reaction mechanism and structural topology of Bmm and Patatin.

Recently, the crystal structure of the potato Patatin protein was resolved. It revealed that the protein fold of Patatin is related to the catalytic domain of cytoplasmic Phospholipase A_2

(PLA_2) but distinct from the typical α/β hydrolases like, for example, Hsl (Rydel et al., 2003). Hsl contains a catalytic triad (Contreras et al., 1996), whereas Patatin contains a catalytic dyad composed of serine and aspartate residues (Rydel et al., 2003). Bmm and Hsl are not only structurally distinct lipases but also show different substrate specificities. Hsl exhibits broad substrate specificity including mono-, di- and triacylglycerol, cholesteryl esters, retinyl esters, steroid esters and p-nitrophenyl esters (Osterlund et al., 1996; Holm, 2003), whereas Bmm is a more specific lipase. Bmm does not catalyse the release of fatty acid from the glycosylphosphatidylinositol (GPI) membrane glycolipid membrane anchor of GPI-modified proteins (5'-nucleotidase, Gce1), nor from monoacylglycerol (MAG). This specificity argues that Bmm lacks the pronounced activities of A1 or A2 phospholipase, GPI-specific phospholipase C/D and Sn-1- or Sn-3-monoacylglycerol lipases, respectively. Instead, it hydrolyzes the release of fatty acids from a trioleoylglycerol-substrate, establishing Bmm function as a TAG lipase. Most recently, TTS2/ATGL, Adiponutrin and GS2 have been shown to exhibit similar TAG-lipase activity (Jenkins et al., 2004; Villena et al., 2004; Zimmermann et al., 2004). This demonstration supports further a conservation of Bmm/Nutrin protein function between mammals and insects.

In contrast to Hsl, however, TTS2/ATGL is not active on cholesteryl ester, retinyl ester and only marginally active on DAG (Zimmermann et al., 2004). Thus Bmm-like proteins are likely to be specific TAG lipases. Human Bmm homologues also catalyze the transfer of an acyl moiety from a MAG-, or DAG-donor to a DAG-acceptor to produce TAG *in vitro* (Jenkins et al., 2004). Although we have not analyzed the acylglycerol-transacetylase activity of Bmm *in vitro*, the overexpression and mutant phenotypes are more consistent with a TAG lipase activity of the Bmm protein *in vivo*. Consistently, overexpression of TTS2/ATGL in cultured cells increased basal lipolysis, whereas RNAi-mediated knock-down resulted in decreased lipolysis (Zimmermann et al., 2004). These observation suggest TAG lipase activity of TTS2/ATGL *in vivo*. The different substrate specificities imply that Bmm- and Hsl-like proteins act coordinately in the lipolytic cascade of TAG catabolism, supporting a model in which (*i*) Bmm-like proteins catalyze the initial and rate limiting step of TAG hydrolysis and (*ii*) provide the DAG substrate for the subsequent action of Hsl. This model is supported by the observation that Hsl exhibits *in vitro* higher enzymatic activity with DAG than TAG as substrate (Fredrikson et al., 1981). It is also consistent with the notion of accumulation of DAG in adipocytes of Hsl mutant mice (Haemmerle et al., 2002; Mulder et al., 2003).

Bmm and Hsl proteins are both highly conserved between *Drosophila* and mammals. This suggests that the lipolytic cascade proposed above is also evolutionary conserved between insects and mammals. However, unlike vertebrates where the fatty acids in the stored TAG are mobilized as free fatty acids, in insects most if not all fatty acids are released from the fat body as DAG (Beenakkers et al., 1985). Consistently, the transcription of the *Drosophila Hsl* gene (*dHsl*) is not upregulated under prolonged food deprivation (data not shown), a finding opposite to the results obtained with the mammalian *Hsl* gene. Thus, under starvation, *dHsl* may contribute only marginally to the DAG release of fat body TAG stores. However, it is important for DAG degradation to produce fatty acids which are subsequently oxidized in the fat body cells.

In conclusion, proteins mediating lipolysis on the lipid droplet surface are highly conserved between insects and mammals. Bmm-like proteins catalyze the initial and rate limiting step of TAG hydrolysis. Thus, they are likely to be responsible for the residual lipolytic activity observed with adipose tissue of the Hsl mutant mice. The remarkable conservation on the level of gene regulation, intracellular protein localization, *in vitro* enzymatic activity as well as the cellular phenotype between *Drosophila* and the human protein suggest that TTS2/ATGL is a functional mammalian homologue of Bmm. As such, malfunction of the TTS2/ATGL gene might contribute to the pathology of mammalian obesity as Bmm does in the fly.

3.4 Lipid droplet targeting of proteins

The intracellular compartmentalization of TAG lipases is an important feature in the regulation of lipolysis and critical for proper TAG lipase function. In mammalian adipocytes, Hsl is diffusely distributed throughout the cytosol. Upon lipolytic stimulation, Hsl translocates from the cytosol to the surface of lipid droplets, a process concomitant with the onset of lipolysis (Eagan et al., 1992; Clifford et al., 2000; Brasaemle et al., 2000). The translocation event can be directly monitored in cultured cells using a fusion-protein of Hsl and the enhanced Green fluorescent protein (EGFP) and it closely resembles the localization and translocation of the endogenous Hsl protein (Sztalryd et al., 2003). Following the same experimental strategy, I identified the Bmm TAG lipase as a lipid droplet-associated protein in fat body cells. In contrast to an inactive Bmm mutant used as a control, the lipolytically active Bmm-EGFP protein reduces size and number of lipid droplets and localizes to islands on their surface which frequently represent inter-droplet contact sites. Recently, endogenous Bmm protein was found to be associated with lipid droplets in a proteomic screen on larval

fat body cells (M. Beller, personal communication). This finding supports the view that Bmm-EGFP, like the Hsl fusion protein in mammals, reflects the proper endogenous localization.

There are no well-defined general localization sequences known to direct proteins to lipid droplets. Oleosins, one of the best-characterized family of lipid droplet-associated proteins in plants, contain a central stretch of hydrophobic amino acids flanked by amphipathic regions and a so-called "proline knot", composed of three closely spaced proline residues, which are important for lipid droplet localization (Abell et al., 1997). However, although a similar domain is found in lipid droplet-associated Hepatitis C and GB-Virus-B proteins (Hope et al., 2002), other proteins such as Bmm and PAT domain containing proteins like *Drosophila* Lsd-2 or mammalian Perilipin do not share these characteristics. However, mammalian PAT domain proteins contain non-hydrophobic redundant localization sequences, which are not necessarily conserved between all family members. These results make it difficult to define a general lipid droplet localization sequence (Nakamura and Fujimoto, 2003; Targett-Adams et al., 2003; McManaman et al., 2003).

I found that Bmm protein lacking the VR region can localize to lipid droplets as has been observed with the full-length Bmm protein. Thus, the evolutionary conserved part of Bmm that contains the PLD and Bmm Box is sufficient for targeting the lipid droplets. Consistently, the human Bmm homologue TTS2/ATGL has been recently identified as a lipid droplet-associated protein in human and chinese hamster cell lines (Umlauf et al., 2004; Liu et al., 2004).

The Bmm PLD does not localize the EGFP protein on lipid droplets. Thus, the Bmm Box is an essential domain for intracellular targeting in case of Bmm, but we don't know yet whether the Bmm Box is also sufficient for the localization. Interestingly, two PLD containing proteins, the yeast TAG lipase YMR313c/TGL3 and a Phospholipase A_2 from cucumber, which lack a Bmm Box, can be found on lipid droplets (Athenstaedt and Daum, 2003; May et al., 1998). These results, in combination with the results obtained with Bmm so far, suggest that sequences within the PLD are necessary but not sufficient to mediate the localization of lipid droplet associated proteins.

In contrast to the other lipid droplet proteins, which are equally distributed over the surface of the lipid droplet, Bmm localizes to distinct islands. The specific localization of Bmm is correlated with the enzymatic active form of the protein, since the lipolytically inactive Bmm variant (Bmm^{S38A}) is evenly distributed over the lipid droplet surface. This finding implies

that localized Bmm reflects the sites of active lipolysis. In mammals, mature adipocytes of white fat tissue contain only a single, very large lipid droplet. Under prolonged starvation, the size of the large lipid droplets decreases concomitant with an increase in small lipid droplets which appear at the periphery of the large droplet (Slavin, 1972; Smith and Jarett, 1980). Whether a similar fragmentation mechanism exists in *Drosophila* is unknown, but the strong enrichment of Bmm at inter-droplet contact sites, together with its nutritional regulation and its TAG lipase activity are consistent with the argument that Bmm could participate in lipid droplet fragmentation under starvation as has been described for mammalian adipocytes. In contrast to mature mammalian adipocytes, *Drosophila* fat body cells accumulate numerous and variously sized lipids droplets. This feature makes it difficult to monitor droplet fragmentation in these cells. Recently, flies mutant for the Lsd-1 protein were generated. Their fat body cells resemble mature mammalian adipocytes in that they contain only a single big lipid droplet (R. Kühnlein, personal communication). Monitoring lipid droplet fragmentation upon acute induction of Bmm-EGFP in these cells could now be used to test whether Bmm can induce lipid droplet fragmentation.

3.5 Lipolysis control in the insect fat body: a scenario emerges

In the *Drosophila* fat body cell, a complex regulatory network continuously matches the magnitude of lipolysis to the energy needs of the organism (Fig. 23). As a direct effector of TAG mobilization, *bmm* activity at the surface of lipid droplets should be tightly controlled. Factors that control the activity of Bmm, either by transcriptional or posttranscriptional regulation, or via a direct interaction with Bmm at the surface of lipid droplets, are still unknown. However, a few mutants are currently described which cause a *bmm*-like fat storage phenotype. They affect genes encoding for members of the adipokinetic hormone (AKH) and insulin signaling pathways, *adipose* (*adp*) (Doane, 1960) and *mir-14* (Xu et al., 2003). Formally, each one of these genes could code for a factor that acts as an upstream regulator of the Bmm TAG lipase (Fig. 23).

Adipokinetic hormones (AKH) are neuropeptides. They mediate the mobilization of TAG stores during energy requiring situations, like flight or starvation, in various insect species including the grasshopper *Locusta migratoria* (Gäde and Beenakkers, 1977), the tobacco hornworm *Manduca sexta* (Ziegler et al., 1990) or the fruitfly *Drosophila* (Lee and Park, 2004). AKH is expressed and released from neurosecretory corpora cardiaca cells of the ring gland. It is thought to stimulate lipolysis in the fat body by signalling via a G protein-coupled AKH receptor (AKHR, Staubli et al., 2002) using the adenylate cyclase second messenger

pathway. Biochemical studies indicate that AKH-induced signalling eventually activates a TAG lipase via phosphorylation of PKA, resulting in increased lipolysis in the fat body (Gäde and Auerswald, 2003; Van der Horst et al., 2001). To date a molecularly undefined TAG lipase purified from the *Manduca* fat body is the only candidate to mediate AKH-induced lipolysis (Arrese et al., 1994). It is unlikely that this TAG lipase is a *Manduca* homolog of Bmm since it is significantly larger than the *Drosophila* or *Anopheles* Bmm proteins (*Manduca* TAG lipase 76 kDa, Bmm 58 kDa). Furthermore, it catalyzes the hydrolysis of MAG (Arrese et al., 1994). However, since *in vitro* phosphorylation by a *Manduca* PKA does not activate TAG lipase activity of the *Manduca* lipase (Patel et al., 2004), the enzyme mediating AKH-dependent lipolysis still awaits its discovery.

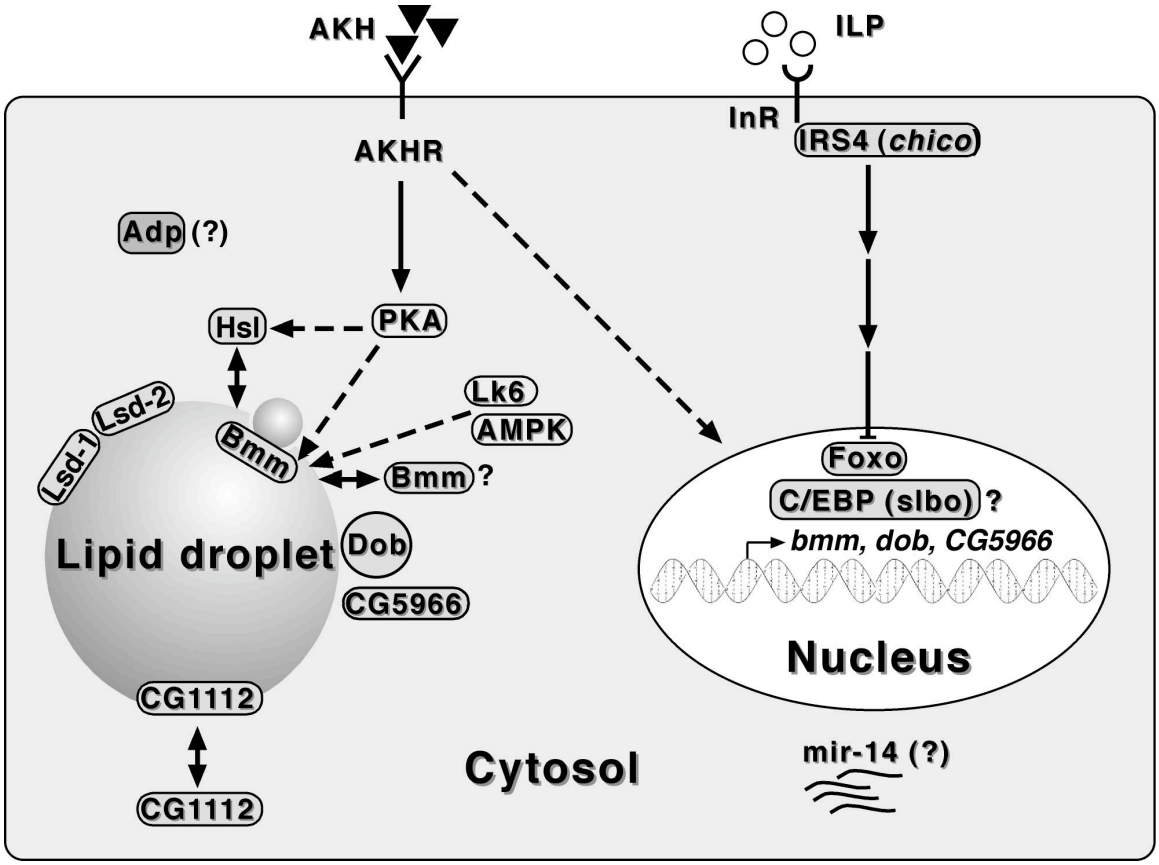

Figure 23: Hypothetical model of factors and mechanisms orchestrating lipolysis in the insect fat body. (hypothetical connections are indicated by a hatched line, double-headed arrow indicates localization to the lipid droplet surface and the cytosol, ? indicates unknown function or localization, for details see text)

In addition to the immediate early response of the adenylyl cyclase pathway, AKH has been shown to induce transcription of a cytochrome P450 in the fat body of cockroaches (Bradfield et al., 1991) and a fatty acid binding protein in the flight muscle of locusts (Haunerland, 1994). In *Drosophila*, AKHR mutants resemble flies lacking Bmm activity.

They have dramatically increased organismal TAG amounts, are starvation resistant and show a TAG mobilization defect under starvation (R. Kühnlein, personal communication). The similar phenotypes of *bmm* and AKHR mutants suggest the starvation-induced transcription and TAG lipase activity of Bmm could be regulated by the AKH pathway activity. In contrast to this proposal, *bmm* transcription is hyperactivated in starved AKHR mutants, indicating that the AKHR is not essential for transcriptional activation of *bmm*. This suggests the existence of a starvation-activated mechanism which can compensate the lack of AKHR-induced lipolysis by upregulation of *bmm* expression. However, despite the high expression level of *bmm*, starved AKHR mutants fail to completely deplete their TAG stores (R. Kühnlein, personal communication), raising the question if Bmm TAG lipase activity is dependent on AKHR signalling. The fact that overexpression of *bmm* in *ad libitum* fed AKHR mutants results in similar TAG mobilization like in the controls and the observation that the human Bmm homologue TTS2/ATGL is not phosphorylated by PKA (Zimmermann et al., 2004) argue against this hypothesis. However, it may well be that the dose of Bmm hyperactivation is not sufficient to completely compensate the lack of AKHR-induced lipolysis. In conclusion, there is currently no evidence that *bmm*-mediated lipolysis is controlled by the AKH pathway. However, recent *in vivo* studies suggest the activity of a second AKHR in *Drosophila* (R. Kühnlein, personal communication). This observation is consistent with *in vitro* data demonstrating the binding of AKH, although with a lower affinity than to AKHR, to another G protein coupled-receptor (Park et al., 2002). Further studies that include the analysis of *bmm* expression upon AKH overexpression or ablation of AKH producing neurons are needed to clarify a still possible AKH-dependent regulation of *bmm*-mediated lipolysis.

In *Drosophila*, like in mammals, the insulin-signalling pathway is involved in the regulation of metabolism, reproduction and lifespan (Garofalo, 2002). Flies with mutations in the insulin receptor (*InR*) and in the insulin receptor substrate (*chico*) exhibit an up to fivefold increase in organismal TAG content (Böhni et al., 1999; Tatar et al., 2001; Brogiolo et al., 2001). In addition, fat body-specific overexpression of the forkhead transcription factor *dfoxo*, a negatively regulated target of insulin signalling, results in lipid accumulation in the fat body (Brunet et al., 1999; Hwangbo et al., 2004). These data demonstrate the importance of insulin signalling for organismal TAG regulation and suggest that transcriptional regulation is implicated in this control. However, no difference in the expression level of *bmm* mRNA was detected in *chico* mutants as compared to wild type flies (preliminary data

not shown). This observation suggests that *bmm* is not a transcriptional target of the insulin pathway. While *bmm* mutants have a decreased lifespan, hypomorphic *InR* and *chico* mutants exhibit an extended lifespan (Tatar et al., 2001; Clancy et al., 2001). This further argues against the proposal that the fat storage phenotype of insulin pathway mutants is caused by downregulation of *bmm* activity.

A mutation in *adp* results in a *bmm*-like fat storage phenotype concomitant with an increased starvation resistant in adult flies (Doane, 1960). *adp* encodes an evolutionary conserved WD40/tetratricopeptide-repeat domain protein, which could function as an adaptor molecule for components of a signalling pathway (Häder et al., 2003). However, upstream and downstream factors of this pathway are unknown. Fat body-directed overexpression of *bmm* reverts the obesity phenotype of *adp* mutant flies (data not shown), indicating that *adp* activity is not essential for *bmm*-mediated lipolysis.

Flies that lack *mir-14* activity are obese and have a reduced lifespan. Conversely, *mir-14* overexpression leads to lean flies (Xu et al., 2003). *mir-14* encodes a microRNA. These small RNAs are known to repress gene function through interaction with their target mRNA (Xu et al., 2003). Consistent with the *mir-14* phenotype, *in silico* prediction of *mir-14* target mRNA did not result in the identification of the *bmm* mRNA (Stark and Brennecke, 2000; Enright et al., 2003), suggesting *bmm* is not a direct target of *mir-14*. However, indirect effects on *bmm*-mediated lipolysis by *mir-14* cannot be excluded.

The hydrolytic actions of TAG lipases are regulated at the lipid droplet surface by PAT domain proteins, an evolutionary conserved family of lipid droplet-associated phosphoproteins (Blanchette-Mackie et al., 1995; Greenberg et al., 1991; Miura et al., 2002). The mammalian PAT domain protein Perilipin is located on the surface of lipid droplets where it has a dual function in the control of lipolysis. Under basal conditions, Perilipin acts as a barrier to Hsl and non-Hsl TAG lipases, thereby decreasing basal lipolysis and increasing organismal TAG storage (Brasaemle et al., 2000; Souza et al., 2002; Tansey et al., 2001). Conversely, upon lipolytic stimulation Perilipin facilitates lipolysis mediated by TAG lipases and is essential for the translocation of Hsl to the lipid droplet surface (Sztalryd et al., 2003). Lack of Perilipin function results in lean mice with an increased basal lipolysis and can revert the obesity of leptin receptor-deficient mice (Martinez-Botas et al., 2000; Tansey et al., 2001). In *Drosophila*, the PAT domain protein Lsd-2 is located on the surface of lipid droplets in fat body cells (Miura et al., 2002, supplement 3) and regulates organismal TAG storage in a dose-dependent manner. *Lsd-2* overexpression results in fat flies, whereas lack

of *Lsd-2* activity leads to a lean phenotype. These results suggest that PAT domain proteins act as evolutionary conserved mediators of TAG lipolysis (supplement 3). Lsd-2 and Bmm act antagonistically in the control of organismal TAG storage as indicated by the normal TAG content of *Lsd-2*; *bmm* double mutants as well as by the partial reversion of *bmm*-induced TAG-reduction upon co-overexpression of both genes. The co-overexpression study suggests that Lsd-2 functions in a Perilipin-like manner as a barrier to the Bmm TAG lipase. However, in *Drosophila* there is currently no evidence for a cytoplasmic pool of Bmm protein and for a translocation mechanism as described for the Hsl protein (compare 3.4.2). In this context it would be interesting to see whether overexpression of Lsd-2 affects Bmm localization to the lipid droplets.

The residual lipolytic activity observed in *bmm* loss-of function mutants suggests that other lipases in addition to Bmm are involved in TAG hydrolysis at the lipid droplet surface. Candidates TAG lipases for a Bmm-independent lipolysis are the Dob protein, the *Drosophila* Hsl homologue and the starvation induced putative TAG lipase CG5966. However, the localization of these proteins to the lipid droplet surface awaits confirmation. Another candidate is the CG1112 protein, which was recently identified as a lipid droplet-associated protein in *Drosophila* (M. Beller, personal communication). The mammalian CG1112 homologue, Carboxylesterase 3 (TGH), was shown to exhibit lipase activity and localizes to lipid droplets in adipocytes (Soni et al., 2004).

In conclusion, for more than 20 years it was thought, that the mechanism of TAG hydrolysis in the mammalian storage tissue is well understood and that the enzymatic reaction is catalyzed by a single lipase, Hsl, which works at the surface of lipid droplets. The data presented in this work as well as recent results from mammalian model systems challenge this view of a single lipase and propose a more complex model of TAG hydrolysis by adding additional TAG lipases which act in a coordinated fashion in the lipolytic cascade. The functional characterization of *bmm* as a key regulator of TAG storage not only confirmed comparative transcriptome analysis as a useful approach to identify new genes involved in the control of energy homeostasis of *Drosophila* but also suggest other currently uncharacterized nutritionally responsive genes to be of functional importance for this biologically relevant regulatory system. Bmm is the first molecularly identified TAG lipase in insects and is highly conserved between flies and mammals. Thus, malfunction of human Bmm homologues may contribute to the pathology of mammalian obesity, as Bmm does in the fly.

4 Material and Methods

4.1 Molecular Biology

4.1.1 Polymerase Chain Reaction

The Polymerase Chain Reaction (PCR) allows the rapid amplification of DNA from minimal amounts of starting material (Saiki et al., 1988). In this work it was used to generate DNA fragments for cloning, to genotype alleles in mutant flies and to identify the plasmids after transformation in bacteria via colony PCR. For cloning purposes, DNA Taq polymerases with a 3´-5´ proof reading activity were used (PreciseTaq, Stratagene or Takara LA Taq, Takara). Genotyping and colony PCR experiments were done using standard DNA Taq Polymerase (Qiagen).

4.1.1.1 Colony PCR

Colony PCR was used to identify DNA constructs containing the desired DNA insert after cloning and transformation in bacteria. Primers were chosen to result only in a PCR product, when the DNA fragment was inserted in the vector. PCR was done directly on individual bacterial colonies. From these in parallel a 3 ml LB (+ antibiotics) culture was inoculated by picking a single colony with a pipette tip directly from the plate. A typical PCR reaction mix and protocol is shown below.

PCR mixture:

0,2 µl Taq DNA Polymerase (Qiagen)
2,0 µl Taq buffer (10x) (Qiagen)
4,0 µl Q-solution (Qiagen)
2,0 µl dNTPs (2 mM each)
1,0 µl Primer A (10 mM)
1,0 µl Primer B (10 mM)
9,8 µl water

PCR Protocol: 1 x 5 min 94°C, 35 x (30 sec 94°C, 50-60°C 30 sec, 1 min/kb 72°C), 1x 7 min 72°C. The annealing temperature was adjusted to the primers used in the individual experiments and was typically between 50 and 60°C. PCR was done in a GeneAmp PCR system 9700 (Applied Biosystems).

4.1.1.2 Genotyping of flies using PCR

Deletion mutants generated by imprecise mobilization of P-elements were genotyped by PCR on individual flies. DNA was prepared according to the single Fly DNA preparation protocol (4.1.9). 1 µl was used in the PCR. PCR mixture and PCR protocol were identical to the Colony PCR conditions. Large-scale analyses were done in a 96 well format.

4.1.1.3 Long Range PCR

DNA fragments with sizes larger than 4 kb were amplified with Takara LA Taq DNA polymerase (Takara) according to the protocol of the manufacturer. Genomic DNA for long range PCR was purified according to the protocol described in 4.1.10.

4.1.1.4 Quantitative Reverse Transcriptase PCR (Q-RT-PCR)

RNA preparation for Q-RT-PCR is described in chapter 4.1.15.1. For the RT reaction the Sybr® Green RT-PCR kit (Applied Biosystems) was used according to the protocol of the manufacturer. Quantitative PCR was done using the Sybr® Green PCR Master mix (Applied Biosystems) and a GeneAmp5700 light cycler (Applied Biosystems). Relative quantification of RNA amounts were done by normalization of PCR results against the RNA amounts of the starvation unresponsive Tat-binding protein-1. For the normalization the primers SGO126 and SGO127 were used (see oligonucleotide list). Relative RNA changes were calculated according to the manual of the Sybr® Green RT-PCR kit (Applied Biosystems).

4.1.2 Restriction of DNA

Restriction endonucleases (type II) were used to cut DNA fragments for cloning, to linearize plasmid DNA as templates for IVT and as analytical tool. For analytical restriction, typically 1 µg DNA was restricted for 1 h with 0,5 µl of restriction enzyme in 20 µl volume using the appropriate restriction buffer and incubation temperature as given by the manufactures. For preparative purposes, 10 µg were digested in 100 µl volume using 1,5 µl of enzyme and incubation times of 4 - 16 h.

4.1.3 DNA extraction from agarose gel

To recover DNA from agarose gels the desired DNA fragments were cut out with a scalpel. DNA extraction was done using the Qiaquick Gel Extraction kit (Qiagen) according to the protocol of the manufacturer.

4.1.4 Dephosphorylation of vector DNA

Self-ligation of vector DNA was minimized by removing the 5´-phosphate groups with alkaline phosphatase treatment. The restricted vector DNA was incubated for 30 min with 1 µl of shrimp alkaline phosphatase (SAP, USB) and the appropriate amount of dephosphorylation buffer (USB). Dephosphorylated DNA was purified using the Nucleotide removal kit (Qiagen) according to the manual.

4.1.5 DNA ligation

100 ng to 1 µg of restricted and dephosphorylated vector DNA was mixed with 5 molar excess of isolated DNA fragments, 1 µl of T4-Ligase (MBI Fermentas) and 1 µl 10 x T4-Ligase buffer in a volume of 10 µl. The ligation reaction was incubated for 12-18 h at 16°C or for 4 h at room temperature. Direct subcloning of PCR products was done using the TA-Topo cloning system (Invitrogen). Therefore, PCR fragments were gel purified and ligated directly into pCRII-Topo vector following the procedures described in the Topo cloning manual.

4.1.6 Transformation of competent E. coli:

Transformation of bacteria was done by high-voltage electroporation. Competent bacteria were prepared according to Sambrook et al. 1998. For electroporation 40 µl electrocompetent cells were thawed on ice, mixed with 1-2 µl of ligation reaction and applied to a gene pulser cuvette (Biorad). Electroporation was done in a Gene Pulser (Biorad) using following settings: 25 µFD, 1,8 kV and 200W. After the pulse, bacteria were mixed with 1 ml LB medium and incubated at 37°C for 1 h. Afterwards the cells were pelleted by centrifugation at 3500 rpm in a tabletop centrifuge, resuspended in 100 µl LB medium and plated onto LB-Agar plates supplied with the appropriate antibiotics. Plates were incubated overnight at 37°C. Bacterial colonies were analyzed by colony PCR.

4.1.7 Plasmid DNA purification

Plasmid DNA purification was done using the Quiaprep Plasmid Midi kit (Qiagen) according to the protocol of the manufacturer. Single colonies of transformed bacteriae were used to innoculate 80-100 ml of LB medium with the desired antibiotics and grown overnight at 37°C and 180 rpm. Bacteria were harvested by centrifugation at 6000 rpm in a Sorvall GS3 rotor for 15 min. The rest of the purification was done following the Plasmid Midi kit procedure.

4.1.8 DNA sequencing

DNA sequencing was done by Gordon Dowe on a ABI Prism 377 DNA sequencher (Applied Bioystems) in the MPI für biophysikalische Chemie Göttingen.

4.1.9 Single Fly DNA preparation for PCR

Single flies were placed in 1,5 ml tubes and killed by freezing. Flies were then homogenized in 50 µl squishing buffer (10 mM Tris-HCl pH 8,2; 1 mM EDTA; 25 mM NaCl; 200 µg/ml Proteinase K) using a pipette tip. The homogenate was incubated for 30 min at 37°C. Proteinase K was inactivated by incubation for 2 min. at 95°C. For PCR reactions 1 µl of the homogenate was used.

4.1.10 Genomic DNA preparation from *Drosophila*

Between 30 and 50 adult flies were homogenized in 180 µl ATL buffer (Qiagen), mixed with 20 µl Proteinase K solution and incubated for 2-3 h at 55°C. Afterwards, the homogenate was applied to DNeasy Mini Spin columns (Qiagen). Genomic DNA for long-range PCR amplification was prepared using the DNeasy tissue kit (Qiagen) according to the protocol "Isolation of total DNA from animal tissue".

4.1.11 Site-directed mutagenesis

The QuickChange Site-Directed Mutagenesis kit (Stratagene, La Jolla, USA) was used to mutate the putative enzymatic active serine in the GASAG hydrolase motif of *bmm* and *dob*. To introduce point mutations in the *bmm* cDNA primers SGO263 and SGO264 were used with the plasmid SG107 as template, while for dob primers SGO265 and SGO266 were used with plasmid SG136 following the procedures in the instruction manual (Stratagene).

4.1.12 DNA-Preparation for Embryo Injections

Plasmid DNA for P-element-mediated germline transformation of *Drosophila* was purified by Phenol-Chloroform extraction and then coprecipitated with a P-Helper plasmid which encodes the transposase source. For Phenol-Chloroform extraction, 40 µg Plasmid DNA (in 300 µl water) was mixed with 300 µl Phenol-Chloroform-Isoamylalkohol (Ambion), vortexed, transferred to a pelleted PhaseLock™ tube (Eppendorf) and centrifuged for 3 min at 14,000 rpm in a tabletop centrifuge. The aequos phase was transferred to a new tube, mixed with 30 µl 3 M NaAc (pH 5,2) and 750µl 100% ethanol and then centrifuged for 30 min at 14,000 rpm. The DNA pellet was washed twice with 70% ethanol, dried and resuspended in 20µl. DNA concentration was determined spectrophotometrically. For coprecipitation 12µg of purified plasmid DNA was mixed with 4 µg P-Helper DNA in 200µl water, 20µl 3 M NaAc (pH 5,2) and 500µl 100% ethanol. The DNA was precipitated by centrifiugation for 30 min at 14,000 rpm, washed twice with 500 µl 70% ethanol, dried and resuspended in 20 µl water by incubation at 60°C for 5 min. To remove insoluble fragments, DNA was centrifuged 5 min at 14,000 rpm. DNA concentration was determined by spectrophotometry. For injection, concentration of the Plasmid/P-Helper DNA mixture was adjusted to 400 ng/µl.

4.1.14 *In situ* hybridization (ISH)

This method is based on the *in situ* hybridization and detection of Digoxigenin (Dig)-labeled DNA-probes on mRNAs in whole mount embryo preparation according to Tautz and Pfeifle, 1989.

4.1.14.1 Preparation of RNA probes for ISH

Dig-labeled RNA probes for ISH were synthesized by *in vitro* transcription (IVT) with the RNA-labeling and detection kit (Roche). Plasmids used as templates for the IVT were linearized by restriction cleavage (4.1.2) and purified with the PCR purification kit (Qiagen).

IVT reaction:

5,0 µl linearized template (1µg)
2,0 µl Dithiotreitol (100mM)
2,0 µl DIG-RNA Labeling Mix
0,5 µl RNasin
2,0 µl Transcription buffer (10x)
7,5 µl RNase-free water
1,0 µl RNA polymerase (Sp6, T7, T3)

IVT was incubated for 2 h at 37°C. The RNA probe was purified using the RNeasy Mini kit (Qiagen) according to the "RNA clean up" protocol. An aliquot of the purified RNA probe was examined by agarose gel electrophoresis. The probe was mixed with an equal volume of Hybe-solution (4.1.14.3) and stored at -20°C. RNA probes generated during the course of this work are summarized in table 4.1.

#	Gene	Template	Restriction enzymes	RNA Polymerase	Orientation	Label
SGR66	*bmm*	SG107	XhoI	Sp6	antisense	DIG
SGR67	*bmm*	SG107	BamHI	T7	sense	DIG
	bmm	SG107	XhoI	Sp6	antisense	α^{32}P-UTP
SGR95	*bmm*	SG173	EcoRI	T3	antisense	α^{32}P-UTP
SGR88	*dob*	SG136	BamHI	T7	antisense	DIG
	dob	SG136	BamHI	T7	antisense	α^{32}P-UTP
SGR87	*Lsd2*	SG131	ClaI	T3	antisense	DIG
	Lsd2	SG131	ClaI	T3	antisense	α^{32}P-UTP
RKR103	*CG11055*	SG215	HindIII	T3	antisense	DIG
RKR104	*CG11055*	SG215	HindIII	T7	sense	DIG
SGR64	*Dreg-2*	SG106	HindIII	T7	antisense	DIG
	Dreg-2	SG106	HindIII	T7	antisense	α^{32}P-UTP
SGR65	*Dreg-2*	SG106	NotI	Sp6	sense	DIG
RKR117	*nocturnin*	SG261	NotI	Sp6	antisense	DIG
	nocturnin	SG261	NotI	Sp6	antisense	α^{32}P-UTP
RKR127	*nocturnin*	SG275	HindIII	T7	antisense	DIG
	RpL9	RK59	SacI	T3	antisense	α^{32}P-UTP

Table 4.1. RNA probes for ISH and Northern Blots.

4.1.14.2 Fixation of embryos for ISH

Appropriately staged embryos were collected from apple juice agar plates, washed briefly with water and dechorionated with 50 % Klorix (bleach). The bleach was removed by extensive washing with water and embryos were fixed for 20 min with a mixture of 8 ml heptan and 1 ml fix-solution A (100 mM Hepes pH 6,9; 2 mM $MgSO_4$; 1 mM EGTA; 37% Formaldehyd) on a rocking platform. Fix-solution was removed and the embryos were devitellineazed by adding 10 ml methanol and vortexing for 15 sec. Devitellineazed embryos sank to the bottom and were washed 3 times with methanol and afterwards stored at -20°C before the ISH.

4.1.14.3 Whole mount in situ hybridization on *Drosophila* embryos

Fixed embryos were rinsed once with 1 ml methanol, 1 ml methanol/PBT (1:1) and were then fixed for 20 min with fix-solution B (10% paraformaldehyde, 50 mM EGTA in PBS)/PBT (1:1). The fixative was washed away by rinsing 3 times and washing once for 5 min with PBT. Embryos were then treated for 5 min with Proteinase K (5 mg/ml 1:1000 in

PBT). Proteinase K was removed by rinsing three times and washing once with PBT. Embryos were fixed with fix-solution B/PBT (1:1) for 20 min and subsequently transferred to the hybridization buffer, by washing 3 times with PBT followed by one wash each with PBT/HybeB (50 % formamide, 5x SSC), HybeB- and Hybe-solution (50% Formamide, 5xSSC, 5ug/ml Heparin, 5mg/ml Torula yeast RNA, 0,1% Tween 20 pH 6,7). The embryos were prehybridized in Hybe-solution at 65°C for 30-60 min. Dig-labeled RNA probe was added (typically 1μl probe in 30μl Hybe-solution per staining) and the embryos were incubated at 65°C over night. Unspecific bound probe was removed by two washes with HybeB-solution at 65°C, followed by five washes with PBT at room temperature. To detect the Dig-labeled RNA probe, embryos were incubated for 1 h with a 1:2000 dilution of the antibody conjugate Anti-Dig-Alkaline phosphatase Fab fragments (Roche) in PBT. The antibody was preabsorbed on wild-type embryos for two hours. Unbound antibody was removed by 5 washes with PBT. For the staining reaction, embryos were equilibrated to AP-buffer (20 mM Tris/HCl pH 9,5, 100 mM NaCl, 50 mM $MgCl_2$). The staining reaction was started by the addition of 3,5 μl BCIP and 4,5 μl NBT in 1 ml AP-buffer. To stop the staining reaction, embryos were washed five times with PBT. Embryos were then dehydrated in an ethanol series and mounted in Canada balsam (Sigma) for documentation.

4.1.14.4 Whole mount in situ hybridization on *Drosophila* 3rd instar larvae

Wandering *Drosophila* 3rd instar larvae were collected, briefly washed with PBT, manually opened and fixed for 20 min in fix-solution (10% paraformaldehyde, 50 mM EGTA in PBS)/PBT (1:1). Subsequently, larvae were subjected to the same washing, hybridization and staining procedures as described in the embryo ISH protocol (4.1.14.3).

4.1.15 Comparative transcriptome analysis

A population of OregonR males aged 6-7 days was split in subgroups of 100 individuals each. Flies from single subgroups were sacrificed after 6h, 12h, 18h and 24h starvation in parallel with those from subgroups continuously supplied with food for corresponding time periods. RNA extraction from the specimens, cRNA preparation as well as hybridization and scanning of Affymetrix *Drosophila* GeneChips were done as follows:

4.1.15.1 Purification of total RNA from adult *Drosophila* flies

For each time-point between 200 and 400 flies were collected and homogenized in TriReagent (WAK Chemie Medical GmbH) using a glass potter. For 100 male flies, 2 ml of TriReagent was used for the homogenization. To get rid of the fly debris, the homogenate was transferred to a centrifugation vial (Corex), incubated for 5 min at room temperature and then centrifuged at 12,000 g for 10 min at 4°C in a Sorvall RC-5B centrifuge using a HB-6 rotor. The supernatant was transferred to a 15 ml Falcon tube, Chloroform (0,2 ml Chloroform / 1 ml TriReagent used for the homgenisation) was added and the solution was vortexed for 15 sec. It was then transferred onto a 15 ml pelleted PhaseLock™ gel (Eppendorf), incubated 10 min at room temperature and then centrifuged for 5 min at 4000 rpm in a HB-4 rotor in a Sorval RC-5B centrifuge. The aqueous phase was transferred to a 15 ml Falcon tube, mixed with 1 volume of ethanol (96-100%) and applied to an RNeasy Midi column (Qiagen). RNA was further purified following the RNA clean up protocol of the RNeasy Midi Kit (Qiagen) and eluted in RNase-free water (RNeasy Midi Kit). RNA concentration was determined spectrophotometrically.

4.1.15.2 Preparation of polyA$^+$ RNA from total RNA

Isolation of polyA$^+$-RNA from total RNA for GeneChip and developmental Northern blot analyses was done using the Oligotex Midi kit (Qiagen) according to the protocol of the manufacturer. As starting material 500-1000 μg of total RNA was used, which usually resulted in the purification of 5-15-μg polyA$^+$-RNA.

4.1.15.3 RNA precipitation

RNA was precipitated using ethanol and sodium acetate (NaAc). 100 µl total RNA was mixed with 0,1 volume of 3 M NaAc (10 µl) and 2,5 volume of 96-100 % ethanol (250 µl) and incubated over night at -20°C. The RNA was pelleted by centrifugation at 15,000 rpm and 4°C for 30 min in a tabletop centrifuge. The pellet was washed twice with 80 % ethanol, dried at room temperature and dissolved in RNase-free water. RNA concentration was determined spectrophotometrically. The integrity of the isolated RNA was controlled by gel electrophoresis on a 1,6 % agarose gel.

4.1.15.4 cDNA synthesis

cDNA from total RNA was synthesized using the SuperScript Choice System™ (Gibco BRL). 20-30µg total RNA was used for the GeneChip experiments. For other applications, 5 to 10 µg total RNA was used.

First strand cDNA synthesis:	8 µl total RNA (5-30µg)
	1 µl Oligod(T)-T7 primer (100µM)
Mix and incubate 10 min at 70°C, then transferred to ice. Add:	
	4 µl First strand buffer (5x)
	2 µl Dithiothreitol (DTT, 0,1 M)
	1 µl dNTPs (10 mM)
Mix and incubate for 2 min at 42°C in a waterbath. Add:	
	x µl SuperScript II Reverse Transcriptase (SSIIRT)

Mix and incubate 1 h at 42°C. The amount of SSIIRT is adjusted to the amount of total RNA used for the cDNA synthesis. For 5 µg RNA 1µl SSIIRT was used, whereas for 20-30 µg RNA used in the GeneChip experiments 4 µl SSIIRT were used.

Second strand cDNA synthesis:	20 µl First strand reaction mix
	91 µl water DEPC-treated
	30 µl Second strand buffer (5x)
	3 µl dNTPs (10mM)
	1 µl DNA-Ligase
	4 µl DNA-Polymerase
	1 µl RNaseH

The reaction was mixed and incubated for 2 h at 16°C. Then, 2 µl T4-DNA-polymerase were added for 5 min at 16°C. The reaction was stopped by the addition of 10 µl 0,5 M EDTA. The cDNA was purified by Phenol-Chloroform extraction.

4.1.15.5 Clean-up of double stranded cDNA

The cDNA reaction (4.1.15.4) (162 µl) was mixed with one volume (162 µl) of Phenol:Chloroform:Isoamylalkohol (24:11:1, Ambion, saturated with 10mTris-HCl, pH 8,0 and 0,1 M EDTA), vortexed for 15 sec, transferred to a pelleted 1,5 ml Phase Lock gel tube light (Eppendorf) and centrifuged 2 min at 14,000 rpm in a tabletop centrifuge. The aqueous phase was transferred to a 1,5 ml tube, mixed with 81µl 7,5M NH_4Ac, 324µl 96-100% ethanol and then centrifuged for 25 min at room temperature at 14,000 rpm. The pellet was washed twice with 500µl 80% ethanol, dried at room temperature and was subsequently resuspended in 12µl RNase-free water.

4.1.15.6 Synthesis of Biotin-labeled cRNA

Biotin-labeled cRNA was produced with the BioArray HighYield RNA transcript labeling kit (Enzo) according to the protocol of the manufacturer.

Reaction mixture:
x μl cDNA (x=volume for 1 μg cDNA)
y μl RNase-free water (y=volume for 40 μl final volume)
4 μl HY reaction buffer (10x)
4 μl Biotin labeled ribonucleotides (10x)
4 μl DTT (10x)
4 μl RNase inhibitor mix (10x)
2 μl T7 RNA polymerase

The reaction was mixed and incubated for 5 h at 37°C in a waterbath with gentle mixing every 45 min during the incubation period. The labeled cRNA was purified using the RNeasy Mini kit (Qiagen) according to the "RNA clean up" protocol. To avoid overloading of the columns, the cRNA reaction mixture was split and 20μl was used per column. cRNA was eluted in 30μl RNase-free water. The RNA concentration was measured by spectrophotometry. The amount of labeled cRNA was calculated according to the following formula: cRNA yield = RNA_m - (total RNA_i)(y)
(RNA_m = amount of cRNA measured after IVT, total RNA_i = starting amount of total RNA (μg), y = fraction of cDNA used in IVT).

4.1.15.7 Fragmentation of cRNA for GeneChip hybridisation

The cRNA is fragmented to RNA fragments in the range of 35 to 200 bases before hybridization to the GeneChip.

Fragmentation reaction:
27 μl cRNA (30 μg)
8 μl Fragmentation buffer (5x)
5 μl RNase-free water

The reaction was incubated for 35 min at 94°C and then transferred on ice. The efficiency of the fragmentation procedure was controlled by agarose gel electrophoresis. 2 μg of fragmented cRNA were loaded next to 2μg of non-fragmented cRNA on a 1,6 % agarose gel. (5xRNA fragmentation-buffer: 200mM Tris-acetate pH8,1, 500mM KOAc, 150mM MgOAc).

4.1.15.8 GeneChip hybridisation

The biotin-labeled cRNA prepared from starved and *ad libitum* fed adult *Drosophila* males was hybridized to Affymetrix *Drosophila* Genome Array 1.0 GeneChips. 12 GeneChips were hybridized. The corresponding hybridization samples (targets) are summarized in table 4.2. A hybridization mixture was prepared for each target in a 0,5 ml PCR tube:

Hybridization mixture:
37,5 μl fragmented cRNA (30 μg)
5 μl control Oligonucleotide B2 (3nM)
15 μl Eucaryotic hybridization controls (20x)
3 μl Hering sperm DNA (10 mg/ml)
3 μl Acetylated BSA (50 mg/ml)
150 μl Hybridization buffer (2x)
86,5 μl RNase-free water

20x GeneChip Eucaryotic hybridisation control (Affymetrix) was heated 5 min to 65°C before use, to allow complete resuspension of the cRNA. The hybridisation mixture was first incubated for 5 min at 99°C and then for 5 min at 45°C. Afterwards, it was centrifuged 5 min at 13,000 rpm in a 5415-D centrifuge (Eppendorf) to remove any insoluble material. Before hybridisation, GeneChips were labeled and equilibrated to room temperature. Equilibrated GeneChips were prehybridized for 10 min at 45°C with 1x hybridisation buffer (50mM MES, 0,5M [Na^+], 20mM EDTA, 0,01% Tween20) in a GeneChip hybridisation oven 640 (Affymetrix). The GeneChips were hybridised for 16 h at 45°C and 60 rpm with the hybridisation mixture.

Experiment	Hybridisation target	RNA type
RK1 F	OregonR males 24 h *ad libitum* fed	polyA
RK1 S	OregonR males 24 h starved	polyA
RK2-24F	OregonR males 24 h *ad libitum* fed	total RNA
RK2-24S	OregonR males 24 h starved	total RNA
RK2-12F	OregonR males 12 h *ad libitum* fed	total RNA
RK2-12S	OregonR males 12 h starved	total RNA
RK3-6F	OregonR males 6 h *ad libitum* fed	total RNA
RK3-6S	OregonR males 6 h starved	total RNA
RK3-18F1	OregonR males 18 h *ad libitum* fed	total RNA
RK3-18S1	OregonR males 18 h starved	total RNA
RK3-18F2	OregonR males 18 h *ad libitum* fed	total RNA
RK3-18S2	OregonR males 18 h starved	total RNA

Table 4.2: Comparative transcriptome analysis hybridisation targets.

4.1.15.9 Washing, staining and scanning of Affymetrix GeneChips

After 16 h of hybridisation, the hybridisation mixture was removed and replaced by non-stringent wash buffer A (6x SSPE; 0,01% Tween20; 0,005% Antifoam 0-30, Sigma). Washing and staining of GeneChips was done in a GeneChip Fluidics station 400 (Affymetrix). Stained GeneChips were scanned using a GeneArray scanner (Affymetrix) connected to a working station. In the single stain procedure (fluidics protocol EukGE-WS1), the hybridized biotin-labeled cRNA is bound by Streptavidin, which is linked to the flourescent dye Phycoerythrin (Streptavidin-Phycoerythrin = SAPE). To amplify the flourescent signal, one or several antibody amplification steps were used (fluidics protocol TanjaWash2). The amplification is based on the use of a biotinylated anti-streptavidin antibody, which binds to SAPE and thereby places additional biotin molecules at the binding site. These additional biotin molecules are in the next staining round recognized by the SAPE reagent.

GeneChips were washed and scanned according to the following scheme:
EukGE-WS1
First scan (no amplification)
TanjaWash 2
Second scan (1x amplification)
TanjaWash 2
Third Scan (2x amplification)
TanjaWash 2
Fourth Scan (3x amplification)
(The first and fourth scan were not included in all GeneChip experiments.)

Fluidics protocols:
EukGE-WS1(single stain):
1. Post-hybridisation wash #1: 10 cycles of 2 mixes/cycle with wash buffer A at 25 °C.
2. Post-hybridisation wash #2: 4 cycles of 15 mixes/cycle with wash buffer B at 50 °C.
3. Stain: The GeneChip was stained for 30 min in SAPE solution at 25 °C.
4. Final Wash: 10 cycles of 4 mixes/cycle with wash buffer A at 25°C.

TanjaWash 2 (antibody amplification):
1. Post-Stain Wash: 5 cycles of 4 mixes /cycle with wash buffer A at 30°C.
2. 2nd stain: The GeneChip was stained for 10 min in antibody solution at 25 °C.
3. 3rd stain: The GeneChip was stained for 10 min in SAPE solution at 25 °C.
4. Final Wash: 15 cycles of 4 mixes/cycle with wash buffer A at 30°C.

SAPE stain solution (600 µl):	300µl 2x stain buffer
	270µl RNase-free water
	24 µl Acetylated BSA (50 mg/ml)
	6 µlStreptavidin-Phycoerythrin (SAPE) (1mg/ml)
Antibody solution (600 µl):	300 µl 2x stain buffer
	266,4 µl RNase-free water
	24 µl Acetylated BSA (50 mg/ml)
	6 µl Normal goat IgG (10 mg/ml)
	3,6 µl Anti-streptavidin biotinylated antibody (0,5 mg/ml)

1x Stain buffer: 100mM MES; 1M [Na^+]; 0,05 % Tween 20; 0,005 % Antifoam 0-30 (Sigma)
Stringent wash buffer B: 100 mM MES; 0,1 M [Na^+]; 0,01 % Tween 20

4.1.15.10 Affymetrix GeneChips data processing

Data analysis was performed using Affymetrix Microarray Suite 5.0. For each analysis time-point normalized transcriptome expression values were compared between age-matched starved and fed flies. Genes that had an increased (I) or decreased (D) call at 6h and at least two more analysis time-points were considered starvation-responsive.

4.1.16 Northern blot analysis

Northern blots were done using the NorthernMax Kit (Ambion) according to the protocol of the manufacturer. 1% Formaldehyde agarose gels were prepared by melting 1 g of agarose in 90 ml of RNase-free water. The gel was cooled down to 55°C and subsequently mixed with 10 ml prewarmed 10x denaturing gel buffer (Ambion). Gels were poured to 0,6 cm thickness. For developmental Northern blots 2 -3 µg $polyA^+$ RNA was loaded per lane. For quantitative Northern blots 10 µg total RNA were used. Preparation of total RNA and $polyA^+$ RNA is described in 4.1.15.2 and 4.1.15.3, respectively. Concentration of RNA was adjusted to 2 µg/µl by RNA precipitation. RNA was mixed with 3 volumes of Formaldehyde loading dye (Ambion) and incubated at 65°C for 15 min to denature RNA secondary structures. To estimate transcript sizes, a DIG-labeled RNA molecular weigth marker (0,3-6,9 kb, Roche Diagnostics) was used. Gels were run in 1x MOPS buffer (Ambion) for 4-4,5 h at 60 V with circulation of the buffer. For the first 30 min of the gel run, voltage was reduced to 20-30 V. RNA was blotted for 90 min onto Bright Star Plus nylon membranes (Ambion) using a downward transfer method according to the NorthernMax protocol. After the transfer, RNA was crosslinked to the membrane by ultraviolet light treatment in an UV stratalinker 1800 (Stratagene). Blots were stored at -20°C until use. The lane containing the DIG-labeled marker was cut of and stained independently from the rest of the blot using the Dig Nucleic Acid Detection Kit (Roche) according to the protocol of the manufacturer.

4.1.16.1 Preparation of Northern blot probes

RNA probes were synthesized by IVT using the Strip-EZ RNA kit (Ambion). RNA probes were radioactively labeled by incorporation of αP^{32}-UTP (Hartmann). Plasmids templates for the IVT were linearized by restriction cleavage and subsequently purified with the PCR purification kit (Qiagen).

IVT reaction:	4,0 µl plasmid template (0,2 µg/µl)
	1,0 µl transcrition buffer (10x)
	0,5 µl ATP (10 mM)
	0,5 µl GTP (10 mM)
	0,5 µl UTP (0,1 mM)
	0,5 µl modified CTP (2 mM)
	2,5 µl αP^{32}-UTP
	1,0 µl RNA polymerase (Sp6, T7 or T3)

IVT reactions were incubated for 1 h at 37°C. RNA probes were subsequently purified using the RNeasy Mini kit (Qiagen) according to the "RNA clean up" protocol. Efficiency of probe labeling was estimated by measuring the dpm of the sample before and after purification in a Bioscan XCR 4000 benchcounter (Xer). RNA probes generated during the course of this work are summarized in table 4.1

4.1.16.2 Hybridisation, Washing and Exposure of Northern blots

Northern blots were hybridised in hybridisation bottles (Hybaid) at 68°C in a hybridisation oven (Hybaid) using UltraHyb (Ambion) hybridisation buffer. Northern blots were first prehybridised for 30 min with 9 ml of UltraHyb per blot. The Northern blot probe was mixed with 1 ml of UltraHyb and added to the hybridisation bottle. Northern blots were hybridised for 90 min, then washed twice for 15 min with 20 ml 2x SSC, followed by two 30 min washes with 20 ml 0,1x SSC at 68°C. The Northern blots were sealed in plastic and exposed to X-ray films (Kodak BioMax MS) at -80°C using an intensifier screen (Kodak, BioMax TranScreen-HE). Quantification of relative transcript abundance was done using a PhosphoImager (Basreader, Fuji). Signal intensity was quantified using AIDA 2.11 imaging software. For normalization, Northern blots were reprobed with an RNA probe detecting ribosomal protein *RpL9* transcripts.

4.1.16.3 Removal of hybridised probes from Northern blots

Hybridised probes were removed from Northern blots using the Strip-EZ RNA Kit (Ambion) according to the protocol of the manufacturer.

4.1.17 Recombinant expression of protein

Recombinant protein for *in vitro* substrate specificity tests was produced by cloning Bmm and Bmm^{S38A} full length ORF into vector pGEX-4T3 (Amersham Pharmacia Biotec) The corresponding proteins were expressing in E.coli BL21 cells. Large-scale cultures transformed with GST-Bmm or GST-Bmm^{S38A} were incubated at 37°C, induced with 1mM IPTG at OD 0,5 for 90 min and subsequently harvested by centrifugation. Cell pellets were extracted by lysozyme and freeze-thaw treatment in HEMG buffer (25mM Hepes KOH pH7,6, 0,5 M NaCl, 0,1% NP40, 0,1 mM EDTA, 12,5 mM $MgCl_2$, 10% glycerol, protease inhibitor (Complete EDTA-free, Roche). Cell debris was removed by centrifugation at 30,000 g for 30 min at 4°C. The supernatant was adsorbed to glutathione sepharose 4B (Amersham Biosciences) and eluted with HEMG 15 mM glutathione. Protein concentration was assessed by SDS-PAGE analysis in comparison to a BSA standard. Purified proteins were tested in MAG-, TAG-lipase and Phospholipase A2 activity assays as described (Frederikson et al., 1986; Thornqvist and Belfrage, 1981) using Monooleoyl[^{3}H]glycerol, Glycerol-tri-[9,10(n)-^{3}H]oleate and 1-Palmitoyl-2-[6-[(7-nitro-2-1,3-benodiazol-4-yl)amino]caproyl]-sn-Glycero-3-Phosphocholine (PAP) as substrates. The enzymatic assays were done in collaboration with Dr. Norbert Tennagels, Dr. Stefan Petry and Dr. Günter Müller from Aventis Pharma, Deutschland.

4.2 Physiology

4.2.1 Fly techniques

All flies were propagated on a complex cornflour-soyflour-molasse medium supplemented with dry yeast at 25ºC and 20-30% humidity with a 12h/12h light/dark cycle. TAG content and starvation response was analyzed in immature (0-24 h) and mature (6-7 days) adult male flies.

4.2.2 Starvation assay

For each genotype triplicate batches of 40 male flies each were transferred to vials providing water supply only. Mortality rates were determined by regularly counting the number of dead flies as diagnosed by the lack of sit-up response. Plotted are average survival rate values and the corresponding standard deviations of a representative experiment.

4.2.3 Longevity assay

Newly emerged bmm^{1} or bmm^{rev} adult males were collected over a 24 h period and divided into batches of 30 flies per vial. Flies were maintained at 25°C, constant humidity and a 12/12 hour light/dark cycle environment and were transferred to fresh food vials and scored for survival every 2 to 4 days. The survivorship curve of bmm^{1} mutants represents data from 180, from bmm^{rev} 450 flies, respectively.

4.2.4 Hatching rate

Drosophila eggs from each genotype were collected on apple juice agar plates supplemented with yeast over an 8-10 hour period. Eggs were aged for 48 hours at 25°C and then the number of hatched embryos determined by counting empty chorion membranes and unhatched embryos.

4.2.5 Triacylglycerol assay

For TAG content quantification, the Infinity kit (Clindia Benelux BV) was used in a microtiter format. The kit is based on enzymatic hydrolysis of the TAG in glycerol and free fatty acids followed by glycerol kinase mediated phosphorylation of the glycerol to glycerol-3-phosphate. The glycerol-3-phosphate is oxydised to dihydroxyacetonphosphate and hydrogen peroxide by glycerol phosphate oxidase. The hydrogen peroxide further reacts with 4-aminoantipyrine and 3,5,dichloro-2-hydroxybenzene sulfonate to produce a red coloured dye. The absorbance of the dye is proportional to the concentration of TAG present in the sample. Since the kit is based on measuring the glycerol release after fatty acid cleavage, it does not distinguish between MAG, DAG and TAG.
For each experiment batches of 8 males of the desired genotype were subjected to thorough homogenisation in 1ml of 0,05 % Tween 20 by using a Fast prep 120 machine (Bio101) in combination with 1/4´ ceramide cylinders (Bio101) for 20 seconds at level 4,0. To inactivate endogenous lipases, homogenates were incubated for 5 min at 70°C. Fly debris was removed by a 1 min centrifugation step (5,000 rpm in a table top centrifuge). 500μl of the supernatant was transferred to a new vial and centrifuged at 14,000 rpm for 3 min. 50 μl of the supernatant was transferred to a 96 well microtiter plate and incubated with 200 μl Infinity reagent at 37°C for 5 min. The absorbance was measured at 540 nm in a benchmark microplate reader (Biorad). Absolute TAG amounts were determined by using a TAG standard (Triglyceride calibrator, Sigma). In case of *ad libitum* fed flies, TAG amounts were scaled to the total protein content of the homogenates. TAG content of starved flies are expressed as TAG per fly. TAG assay data were processed using Microsoft Excel X (Mac) software. TAG contents of a representative experiment for each genotype are depicted as average values of triplicate measurements with corresponding standard deviations.

4.2.6 Protein assay

Protein content of adult flies was determined with the BCA protein assay Kit (Pierce). This kit allows the colorimetric detection and quantification of total protein. Fly homogenates were prepared identical as described for the Triacylglycerol assay (4.2.5). 50 μl of fly homogenate supernatant was transferred to a 96 well microtiter plate and incubated with 200

μl BCA reagent at 37°C for 30 min. The BCA reagent was freshly prepared before each experiment by mixing 50 parts of reagent A with 1 part of reagent B (BCA kit, Pierce). The absorbance was measured at 570 nm in a benchmark microplate reader (Biorad). Absolute protein amounts were determined by using the bovine serume albumine (BSA) standard supplied with the BCA kit.

4.2.7 Glycogen assay

Glycogen content of fly homogenates was determined using an enzymatic starch bioanalysis kit (R-Biopharm). The kit is based on the enzymatic hydrolysis of glycogen to D-glucose catalyzed by amyloglucosidase. The D-glucose formed by this reaction is determined with hexokinase and glucose-6-phosphate using the amount of formed NADPH as read out by means of its light absorbance at 340 nm.

For each experiment 15 males were collected. They were homogenized in 100μl dimethylsulfoxide (DMSO) and 30 μl 6,9 M hydrochloric acid (HCl) by vortexing together with a 1/4´´ceramide cylinder (Bio101). Glycogen was solubilized by incubating the homogenized samples in the DMSO/HCl solution for 1 h at 60°C with shaking at 1,000 rpm in a Thermomixer (Eppendorf). Samples were allowed to cool down to room temperature and the pH of the solution was adjusted by the addition of 30μl 6,9 M sodium hydroxide (NaOH). 250μl 1,12 M citrate buffer (pH4: citric acid (1,12 M): tri-sodium citrate (1,12M)) was added, briefly mixed and centrifuged for 5 min at 5,000 rpm in a tabletop centrifuge. 210μl of the supernatant was transferred to a new 1,5 ml vial and centrifuged for 3 min at 14,000 rpm to remove remaining fly debris. The homogenates were processed as follows:

	Sample	**Sample blank**
Sample solution	50μl	50μl
Solution #1	100μl	-

Mixed and incubated at 60°C for 15 min. Add:

Solution #2	500μl	500μl
H_2O $_{dest.}$	500μl	600μl

Transfered to plastic cuvettes and OD_{340nm} measured after 3 min (A1 value). Add:

Solution #3	10μl	10μl

Samples were thoroughly mixed. The OD_{340nm} was determined after 15 min (A2 value) with a spectrophotometer (ThermoSpectronic). Solution #1, #2 and #3 are components of the starch analysis kit (R-Biopharm). The glycogen content was calculated as follows: $DA = (A2\text{-}A1)_{sample}\text{-}(A2\text{-}A1)_{blank}$

$C_{Glycogen} = V \times MW / e / d / v / 1000 \times DA$ (g/l)

(V = final volume in ml, MW = Molecular weight glycogen (162,1 g/mol), e = extinction coefficient of NADPH at 340nm (6,31 $mmol^{-1} \times cm^{-1}$), d = lightpath in cm (1cm), v = sample volume in ml (0,05ml). For the described settings: $C_{Glycogen} = 0.596 \times DA$ g glycogen / l. Total glycogen content = 0,4ml x $C_{Glycogen}$ x 1000 / fly wet weight (μg / mg). In this work glycogen contents of a representative experiment for each genotype are depicted as average values of triplicate measurements with corresponding standard deviations.

4.2.8 Locomotor activity assay

Circadian locomotor activity of adult *Drosophila* flies was determined using Locomotor Activity Monitors of the *Drosophila* activity monitoring system (Trikinetics). In this system, flies are individually placed into glass tubes where their motion is detected and counted by an infrared light beam. Every 30 min the accumulated activity counts are uploaded to a host Macintosh computer and are stored. The Locomotor Activity Monitor measures in parallel the activity rhythms of 32 individual flies for each genotype. In order to determine locomotor

activity under *ad libitum* fed and starvation conditions, glass tubes were equipped either with 5% sucrose agarose or pure agarose, respectively. Adult *Drosophila* males 3-4 days old of the desired genotype were anaesthetized and placed individually in the glass tubes, which were inserted in the locomotor activity monitor. Recordings were done at 25°C over 9 days with a 12 h light/dark cycle during the first three days, followed by complete darkness for the rest of the experiment. Activity counts of the first 12 h hours of the experiment were not included in the data analysis, because flies first had to adapt to the experimental conditions. The locomotor activity measurements were done in collaboration with Dr. Ralph Stanewsky (University Regensburg).

4.2.9 Fluorescence microscopy

Fat body cells from immature adult flies were prepared as follows for *ex vivo* confocal laser scanning microscopy. The abdomina of male flies were manually opened and the floating fat body cells released into mounting medium (50% glycerol/PBT, Nile Red 1:55000, Molecular Probes, Nile Red stock: 10% in DMSO). Cells were analysed within 2h after mounting using a Leica TCS SP2 LSM with 543nm excitation/600-657nm emission or 488nm excitation/500-541nm emission for visualization of lipid droplets and EGFP-fusion proteins, respectively.

4.3 Genetics

4.3.1 Generation of mutant flies by imprecise mobilization of P-elements

Deletion mutants for *bmm*, *dob*, *CG11055* (*dHsl*), *nocturnin* and *Dreg-2* were generated by a conventional P-element mobilization scheme (Ashburner, 1989). Therefore, flies carrying the P-element were crossed with a "Jump starter" fly that carries a P-element transposase source. In the F1 generation, offspring's carrying both the P-element and the transposase source were crossed with flies that carries a "balancer" chromosome corresponding to the P-element insertion chromosome. P-element mobilization events were identified by the white-eye color of flies in the F2 generation. These flies were individually crossed against a corresponding balancer fly and were subsequently made homozygous for the mobilization event. Deletions in the genomic region next to the original P-element integration site were identified by large-scale PCR-based screens on flies that carried a homozygous mobilization event. Primers used for the PCR screen as well as the number of screened fly lines and the number of mutants isolated for each of the five genes are summarized in table 4.3 together with the P-element originally used to generate these stocks. The generated deletions were molecularly characterized by PCR amplification of the corresponding genomic region with primers located in the 5´and 3´flanking region. PCR products were subsequently sequenced.

Gene	P-Element	Fly stock	Primer	# Mes	# Mutants
bmm	EP(3)3174	SGF528	SGO162/140	278	3
dob	EY05880	SGF544	SGO185/200	316	14
CG11055	GE15823	SGF704	SGO430/373	200	3
nocturnin	GE22476	SGF706	SGO390/407	700	6
Dreg-2	GE23064	SGF705	SGO136/SG102	140	1

Table 4.3: Generation of mutant fly stocks by imprecise mobilization of P-elements. MES=Number of mobilization events screened.

4.3.2 Ectopic expression of genes via the UAS/GAL4 system

The UAS/Gal4 system allows the ectopic induction of genes in spatial and temporal controlled manner. This two-component system is based on the yeast transcriptional

activator protein GAL4 and its DNA target sequence the so-called UAS site (upstream activating sequence) (Brand and Perrimon, 1993). In *Drosophila,* flies of the so-called Gal4 driver line carry an enhancer sequence upstream of the GAL4 gene. Flies of the so-called effector line carry a gene of interest downstream of the UAS site. If Gal4 driver flies are crossed with UAS-effector flies the GAL4 protein binds to the UAS site and activates ectopic gene expression of the target gene in a pattern dependent on the enhancer-GAL4 construct.

4.3.2 P-Element-mediated germline transformation

Transgenic flies were generated by P-element-mediated germline transformation according to Rubin and Spradling, 1982. Plasmid DNA for injection was prepared as described in DNA-Preparation for Embryo Injections (4.1.12). Injection of the Plasmid/P-Helper DNA mixture in *Drosophila* w* embryos was done by Ursula Jahns-Meyer and Iris Plischke at the MPI für biophysikalische Chemie (Göttingen). Each hatched fly was backcrossed to w* flies. In the next generation transformed flies that carried the DNA construct were identified by their red eye color, which is due to the mini *w* marker gene within the P-element vector. The transformed chromosomes were stabilized and identified by crossing the flies with "balancer" flies using *w*;sal^{445}*/CyO for the second and *w*;$croc^{59}$ *e*/TM3 *Sb* for the third chromosome, respectively. For each experiment at least two independent transgenic fly lines were used.

list of plasmids:

bmm

#	Insert name	vector	cloning strategy
SG107	*bmm* cDNA	pCRII-Topo	PCR on cDNA with SGO139/SGO140, TA cloning
SG119	*bmm* cDNA	pUAST	SG107 cut with XhoI,SpeI; insert cloned to pUAST XhoI, XbaI
SG116	*bmm* cDNA	pUAST	SG107 cut NotI,KpnI; insert cloned to pUAST NotI,KpnI
SG141	*bmm* ORF	pGEX4T3	PCR with SGO197/SGO198 on SG107; PCR product cut with EcoRI/XhoI; cloned in pGEX-4T-3 EcoRI/XhoI
SG142	*b m m* cDNA 3´part	pGEX4T3	PCR with SGO199/SGO198 on SG107;cut PCR product with EcoRI/XhoI, clone to pGEX-4T-3 EcoRI/XhoI
SG161	*bmm*-EGFP	pEGFP-N2	PCR with SGO197/SGO226 on SG116; PCR fragment were cut with EcoRI/BamHI and ligated to pEGFP-N2 EcoRI/BamHI
SG162	*bmm*-EGFP	pUAST	SG161 cut with EcoRI/NotI, insert cloned to pUAST EcoRI/NotI
SG173	*b m m* cDNA 3´part	pBluescript II KS+	SG142 cut with EcoRI/XhoI, Insert cloned to pBST II KS+ EcoRI/XhoI
SG179	bmm^{S38A} cDNA	pCRII-Topo	see 4.1.11; bmm^{S38A} ; template SG107, primer: SGO263, SGO264
SG181	bmm^{S38A} cDNA	pUAST	SG179 cut with NotI/KpnI, cloned to pUAST NotI/KpnI
SG183	bmm^{S38A}-EGFP	pEGFP-N2	PCR on SG179 with SGO226/197, clone PCR product in pCRII-Topo, cut Insert with BamHI/EcoRI and ligate to pEGFP BamHI/EcoRI
SG186	bmm^{S38A}-EGFP	pUAST	SG183 cut with EcoRI/NotI, cloned to pUAST EcoRI/NotI
SG213	bmm^{S38A} ORF	pGEX4T3	PCR with SGO197/198 on SG179, digest PCR product with EcoRI/XhoI and clone in pGEX4T3 EcoRI/XhoI

dob

SG126	GH09195	pOT2a	BDGP
SG127	LD21294	pOT2a	BDGP
SG132	*dob* cDNA	pUAST	SG136 cut with EcoRI/XbaI; insert cloned to pUAST EcoRI/XbaI
SG136	*dob* cDNA	pCRII-Topo	PCR on SG126 with SGO178/ SGO179; TA cloning in pCRII-Topo
SG160	dob-EGFP	pEGFP-N2	PCR with SGO200/SGO228 on SG126; PCR fragment was cut with EcoRI/ApaI and cloned to pEGFP-N2 EcoRI/ApaI
SG163	dob-EGFP	pUAST	SG136 cut with EcoRI/XbaI, cloned to pUAST EcoRI/XbaI
SG178	dob^{S44A}	pCRII-Topo	see 4.1.11; dob^{S44A} ; template SG136, primer: SGO265, SGO266

SG180	dob^{S44A} cDNA	pUAST	SG178 cut with EcoRI/XbaI; insert cloned to pUAST EcoRI/XbaI
LSD2			
SG131	RE58939	pFLC-I	BDGP
SG150	LSD2 ORF	pRSetA	PCR on SG131 with SGO213/215; PCR product was cut with NheI/EcoRI and cloned in pRSetA NheI/EcoRI
SG151	LSD2 ORF	pGEX-4T-3	PCR on SG131 with SGO214/215; PCR product was cut with EcoRI and cloned in pGEX-4T-3 EcoRI
dHsl			
SG215	RE52776	pFLC-I	BDGP
Dreg-2			
SG106	*Dreg-2* cDNA	pCRII-Topo	PCR on cDNA with SGO136/SGO137; TA cloning
SG133	*Dreg-2* cDNA	pUAST	SG106 cut with EcoRI, insert cloned to pUAST EcoRI
CG31299/nocturnin			
SG258	*nocturnin* cDNA (GH03334)	pUAST	PCR on cDNA with SGO363/366, PCR product was cut with BglII/KpnI and cloned to pUAST BglII/KpnI
SG259	*nocturnin* cDNA	pUAST	PCR on cDNA with SGO364/366; PCR product cut with BglII/KpnI, cloned to pUAST BglII/KpnI
SG260	*nocturnin* cDNA (RE65127)	pUAST	PCR on cDNA with SGO365/366, PCR product was cut with BglII/KpnI and cloned to pUAST BglII/KpnI
SG261	*nocturnin* cDNA	pCRII-Topo	(GH03334) PCR on with SGO363/366, TA cloning
SG262	*nocturnin* cDNA	pCRII-Topo	PCR on cDNA with SGO364/366, TA cloning
SG263	*nocturnin* cDNA	pCRII-Topo	(RE65127) PCR on cDNA with SGO364/366, TA cloning
SG275	*nocturnin* exon2	pCRII-Topo	PCR with SGO363/391 on SG258, TA cloning
SG281	*nocturnin$^{\#368}$*	pCRII-Topo	PCR with SGO374/406 on *noctunin$^{\#368}$* cDNA, TA cloning
SG281	*nocturnin$^{\#671}$*	pCRII-Topo	PCR with SGO374/391 on *nocturnin$^{\#671}$* cDNA, TA cloning
SG283	CG6666 cDNA	pCRII-Topo	PCR with SGO418/419 on cDNA, TA cloning
SG296	nocturnin genomic rescue	pBluescript II KS+	PCR with SGO451/454 on genomic DNA, PCR product was cut with NotI/XhoI and cloned to pBS II KS+ NotI/XhoI
SG300	nocturnin genomic rescue	pBluescript II KS+	PCR on genomic DNA with SGO452/ 453, PCR product cut with KpnI/XhoI, cloned to pBS II KS+ XhoI/KpnI
SG301	nocturnin genomic rescue	pCaspeR4	SG300 cut with XhoI/KpnI, insert cloned in SG296 XhoI/KpnI. The resulting plasmid was cut was cut with NotI/KpnI and cloned in pCaspeR4 NotI/KpnI
SG302	nocturnin genomic rescue mutated version	pCaspeR4	Introduction of a stop codon in the nocturnin ORF: PCR with (a) SGO455/457 and (b) SGO456/452 on SG300. Both PCR fragments (a, b) were mixed and used as template for a PCR with SGO455/452. The resulting fragment was cut with XbaI/KpnI and cloned in SG300 XbaI/KpnI. The rest of the cloning was done according to the strategy of SG301.
SG303	*curled^{1}* cDNA	pCRII-Topo	PCR with SGO390/366 on cDNA *nocturnin$^{\#65}$/ru[1] pbl[5] h[1] th[1] st[1] cu[1] sr[1] e[s] ca[1]/;* TA cloning
SG304	*curled^{1}* cDNA	pCRII-Topo	PCR with SGO390/366 on cDNA *nocturnin$^{\#65}$*/TM6C, *cu[1] Sb[1] ca[1*]; TA cloning
SG305	*curled^{1}* cDNA	pCRII-Topo	PCR with SGO390/366 on cDNA *nocturnin$^{\#65}$*/TM6C, *cu[1] Sb[1] ca[1],* TA cloning
SG306	*curled^{2}* cDNA	pCRII-Topo	PCR with SGO390/366 on cDNA *nocturnin$^{\#65}$*/In(3L)A54, *st[1] cu[2] p[p] red[1] e[4]*; TA cloning
SG307	*curled^{2}* cDNA	pCRII-Topo	PCR with SGO390/366 on cDNA *nocturnin$^{\#65}$*/In(3L)A54, *st[1] cu[2] p[p] red[1] e[4]*; TA cloning

Oligonucleotide list.

bmm

#	Oligonucleotide name	Sequence (5´-3´)	Restriction site
SGO99	bmm QRT-PCR 5´	CTGTCTCCTCTGCGATTT	
SGO100	bmm QRT-PCR 3´	TTGAAGGAGGGACTGAAG	
SGO139	bmm cDNA 5´	ACACCGCGCCGCAATGAATG	
SGO140	bmm cDNA 3´	TAAACACAGATGGGGATTTGGATG	

SGO163	EP(3)3174 I	TGCCCTGTGAGAAGTGTAGA	
SGO186	EP(3)3174 II	GTTACGTGCTGCCCTCTTA	
SGO197	bmm ORF 5´	CGTGAATTCTATGAATCTATCATTCGCTGGC	EcoRI
SGO198	bmm ORF 3´	AGCTCGAGTTAAAAGGCTACGTCGTGTAGT	XhoI
SGO199	bmm 3´part 5´	GTGAATTCTAAGAAGCACAGAAAGGACGC	EcoRI
SGO209	EP(3)3174 III	GGGGCGTCTAATGTTATG	
SGO210	bmm QRT-PCR 5´	CAGCATGACTTCGGACTT	
SGO226	bmm ORF stop 3´	GTGGATCCATTGAAAGGCTACGTCGTGTA	BamHI
SGO263	*bmm^{S38A}* 5´	GAAGATCGGAGGCGCTGCGGCCGGTTCCC	
SGO264	*bmm^{S38A}* 3´	GGGAACCGGCCGCAGCGCCTCCGATCTTC	
dob			
SGO178	dob cDNA 5´	ATCGAATTCAAGAGCTTATTTGCCACGAC	EcoRI
SGO179	dob cDNA 3´	GGATCTAGATTTATTTTGTTCACAGCAGTC	XbaI
SGO192	dob genomic enhancer 5´	CAAAATGCTCGCTGTGCC	
SGO193	dob genomic enhancer 3´	CAGTGTGACCTTGCAAAGTAGT	
SGO200	dob ORF 5´	CAGAATTCGATGAAGATCCGAACCAGGAG	EcoRI
SGO201	dob ORF 3´	AGCTCGAGCTAATGAACACCGGATGTCC	
SGO204	LSD2 sequencing	TGCGTACTATTTCATTGAGTG	
SGO212	LSD2 genomic rescue 3´	CGTACAGTGCTGTCCCGATAAGGCCTCT	StuI
SGO228	dob ORF stop 3´	AAGGGCCCCTCATGAACACCGGATGTCC	ApaI
SGO265	*dob^{S44A}* 5´	GATTGCCGGTGCAGCCGCAGGTGCCTTG	
SGO266	*dob^{S44A}* 3´	CAAGGCACCTGCGGCTGCACCGGCAATC	
LSD2			
SGO213	LSD2 ORF 5´	TCGCTAGCATGGCCAGTGCAGAGCAGAA	NheI
SGO214	LSD2 ORF 3´	TAGAATTCGATGGCCAGTGCAGAGCAGAA	EcoRI
SGO215	LSD2 ORF 3´	TCGAATTCTACTGAGACGACACCGCCG	EcoRI
CG11055			
SGO312	*CG11055* ORF 5´	AAAGATCTGAGCCGCAATAGGTGGAC	BglII
SGO313	*CG11055* ORF stop 3´	AAGGTACCCTGATGAAGCGGCTAGACTTG	KpnI
SGO314	*CG11055* ORF 5´	CTGTCGACATGATTGACGCGGCTTCC	SalI
SGO315	*CG11055* ORF 3´	ATGCGGCCGCCTATGAAGCGGCTAGACTT	NotI
SGO316	*CG11055* sequencing I	GGGCGACACCATCAACCA	
SGO317	*CG11055* sequencing II	CAAGCCCATTCCGCCAAGT	
SGO318	*CG11055* sequencing III	GCCAGTGCCTCAGCCTCT	
SGO319	*CG11055* sequencing IV	CATGGACGCACTGATAGC	
SGO372	GE15823 insertion 5´	TGCAAGCAGTGTGACCAG	
SGO373	GE15823 insertion 3´	TCGCATTGAGACTGAAACCA	
SGO430	*CG11055* jump out screen	AGCCACTGTGCAGAAACAC	
Dreg-2			
SGO102	*Dreg-2* QRT-PCR 3´	CATTGCTGCCATTCCATCTG	
SGO136	*Dreg-2* cDNA 5´	CGAGAGTCGAAAGTCAAGAGTT	
SGO137	*Dreg-2* cDNA 3´	TGCACAATCAATCACCAGACAA	
SGO368	*Dreg-2* ORF 5´	CAGAGAATTCAGGCAAAATGCGC	EcoRI
SGO369	*Dreg-2* ORF 3´	CAGTCGACATCCCCAGACAACTGCGCCGTC	SalI
SGO376	GE23064 insertion 5´	GTTTAACACTCAGAAGCAAG	
SGO415	GE23064 insertion 5´	CCACATCCCAGCCAGACG	
SGO416	GE23064 insertion 3´	GTGCCCGAGAACCTAATGA	
CG31299/nocturnin			
SGO363	*nocturnin* cDNA 5´ (GH03334)	GGTAGATCTTAAAAGTGACAATGGATC	BglII
SGO364	*nocturnin* cDNA 5´	CCTTAGATCTTGCCGCAGACATGGAG	BglII
SGO365	*nocturnin* cDNA 5´ (RE65127)	GCACAAAAAGATCTAAATGGAGTTTC	BglII
SGO366	*nocturnin* cDNA 3´	TCGGCAAATTAGGTACCTGAAGCTTT	KpnI
SGO367	*nocturnin* ORF 3´	TGGTCGACTGTATTGAATGGATCCATGCTTG	SalI
SGO374	GE22476 insertion 5´	GTCATTGGCATTGTTATCAG	
SGO375	GE22476 insertion 3´	CCGAGGTGGCGTCTAATC	

SGO390	*nocturnin* exon 1 5´	TCAGATCTCCAGAGCATTTGAACCGC	BglII
SGO391	*nocturnin* exon 2 3´	GCGGCTCGAACTCAAACTC	
SGO392	*nocturnin*	TCACTTTTTGCAGATAGGCC	
SGO393	*nocturnin*	TAACTCGGCCCCAAAGATC	
SGO398	*nocturnin* ORF 5´	CACAAAAAGTCGACAATGGAGTTTCTA	SalI
SGO399	*nocturnin* ORF 3´	GAAACTTCTTTTGCGGCCGCTTATGAATC	NotI
SGO405	*nocturnin* 3´end 5´	TGAACTGAATCCCCCATCTAA	
SGO406	*nocturnin* 3´end 3´	GTTTGTTGTGTTACGCAATCC	
SGO418	*CG6666* cDNA 5´	CAGTCAGTGTACGGTCCCA	
SGO419	*CG6666* cDNA 3´	AATGTAATAGGTTTAGCTGGGG	
SGO420	*nocturnin* sequencing 3´	ATCACTGGCCACGCTGCG	
SGO421	*nocturnin* sequencing 3´ I	GCCTGACAATCGACTTCC	
SGO451	*nocturnin* genomic rescue 5´	GTGCGGCCGCAGCCTTACACGAATGTCG	NotI
SGO452	*nocturnin* genomic rescue 3´	ATGGTACCTGTTGCTTTGGGCGTGCTGC	KpnI
SGO453	*nocturnin* genomic rescue 5´	GGTGACTCGAGGTTTATAGG	XhoI
SGO454	*nocturnin* genomic rescue 3´	CCTATAAACCTCGAGTCACC	XhoI
SGO455	*nocturnin* genomic rescue 5´	CAGATCAAAAACTGTCTAGACT	XbaI
SGO456	*nocturnin* genomic rescue I	CCAATATCCATAGGATCACTTTTC	
SGO457	*nocturnin* genomic rescue II	GAAAAGTGATCCTATGGATATTGG	
other:			
	oligodT-T7	GGCCAGTGAATTGTAATACGACTCACTATAG GGAGGCGG-(dT)24	
SGO126	Tat binding protein 5´	AAGTCATCCGTGGATCGGGAC	
SGO127	Tat binding protein 3´	AAGCCCGTGCCCGTATTATG	

List of flies:

#	genotype	cyt	description	reference
SGF528	w^{1118} ;P{w+mC=EP}EP3174	1;3	P-insertion in *bmm* intron1	
SGF529	w^{1118} ;bmm^{1}/TM3 Sb	1;3	JO#137 rec27	this work
SGF530	w^{1118} ;bmm^{2}/TM3 Sb	1;3	JO#163 rec34	this work
SGF531	w^{1118} ;bmm^{3}/TM3 Sb	1;3	JO#169 rec14	this work
SGF532	*w**; P{w[+mC]UAST-*bmm*}#2c	1;2	UAS-*bmm*; SG119#2c	this work
SGF533	*w**; P{w[+mC]UAST-*bmm*}#2d	1;3	UAS-*bmm*; SG119#2d	this work
SGF534	*w**; P{w[+mC]UAST-*bmm*-EGFP}/CyO	1;2	UAS-*bmm*-EGFP; SG162#12	this work
SGF535	*w**; P{w[+mC]UAST-*Bmm*-EGFP}/TM3Sb	1;3	UAS-*bmm*-EGFP; SG162#30a	this work
SGF536	*w**; P{w[+mC]UAST-Bmm^{S38A}}/Cyo	1;2	UAS-bmm^{S38A}; SG181#34	this work
SGF537	*w**; P{w[+mC]UAST-Bmm^{S38A}}/TM3 Sb	1;3	UAS-bmm^{S38A}; SG181#9a	this work
SGF538	*w**; P{w[+mC]UAST-Bmm^{S38A}-EGFP}/CyO	1;2	UAS-bmm^{S38A}-EGFP; SG186#16	this work
SGF539	*w**; P{w[+mC]UAST-Bmm^{S38A}-EGFP}/TM3 *Sb*	1;3	UAS-bmm^{S38A}-EGFP; SG186#18	this work
SGF540	w^{1118} ;bmm^{Rev}/TM3 *Sb*	1;3	bmm^{Rev}; JO#17 rec25	this work
SGF541	w^{1118} ;bmm^{5}/TM3 *Sb*	1;3	bmm^{5}; JO#90	this work
SGF544	*y* * , *w* * P{w+mC y+mDint2, TrlBRcRa Scer\UAS14x.P\T(>)=EPgy2}EY05880	1	EY05880; P-insertion in *dob* 5´-UTR	
SGF546	*w**; P{w[+mC]UAST-*dob*}/CyO float	1;2	UAS-*dob*; SG132#21c	this work
SGF547	*w**; P{w[+mC]UAST-*dob*}/TM3 *Sb* float	1;3	UAS-*dob*; SG132#31a	this work
SGF548	*w**; P{w[+mC]UAST-*dob*}/CyO float	1;2	UAS-*dob*-EGFP; SG163#2a	this work
SGF550	*w**; P{w[+mC]UAST-dob^{S44A}}/CyO float	1;2	UAS-dob^{S44A}; SG180#10c	this work
SGF551	*w**; P{w[+mC]UAST-dob^{S44A}}/TM3 *Sb*	1;3	UAS-dob^{S44A}; SG180#33b	this work
SGF566	*y**, *w** dob^{2a} / FM6 float	1	*dob* deletion mutant #2a	this work
SGF567	*y**, *w** dob^{10a} / FM6 float	1	*dob* deletion mutant #10a	this work
SGF568	*y**, *w** dob^{6a} / FM6 float	1	*dob*,LSD2 mutant #6a	this work
SGF704	*w**;; P{w[+mC]=EP}GE15823	1;2	GE15823	
SGF705	*w**;; P{w[+mC]=EP}GE23064	1;3	GE23064	
SGF706	*w**;; P{w[+mC]=EP}GE22476	1;3	GE22476	
	w; sal^{445}/CyO	1;2	II chromosome balancer	
	w; croc^{59} *e*/ TM3 *Sb*	1;3	III-chromosome balancer	

RKF125	*w**; P{w[+mW.hs]=GawB}FB/SNS	1;2	FB-Gal4,	
RKF153	y[*], *w**; P{w[+mW.hs]=GawB}FB P{w[+m*]UAS-EGFP 1010T2} #2	1;2	FB-Gal4, UAS-EGFP	
RKF246	*w**; rev[P{w[+mW.hs]=GawB}FB P{w[+m*]UAS-EGFP 1010T2}]	1;2	FB-JO	
RKF182	y^1, *w**; P{w[+mC]=*Act5C*-GAL4}25FO1 / CyO, y[+]	1;2	*act*-Gal4, ubiquitous Gal4 driver line	Blo. #4414
RKF165	y^1, *w**; CyO, H{w[+mC]=PDelta2-3}HoP2.1 / Bc^1 $Egfr^{E1}$	1;2	Transposase source on CyO balancer	Blo. #2078
RKF32	*y** *w**; wg^{Sp-1} / CyO-ftz-lacZ ; Dr[*] / TM3-*ftz*-lacZ Sb^1 *ry**	1;2;3	double balancer for II & III chromosome	
GÖ832	ru^1 pbl^5 h^1 th^1 st^1 cu^1 sr^1 e^s ca^1/TM3, Sb^1	3	$curled^1$ allele	Blo. 2452
GÖ972	Df(3R)cu, Sb^1 *e**/TM6B, Tb^1	3	*curled* deficiency	Blo. 771
GÖ1152	ash^1 B^1/TM6C, cu^1 Sb^1 ca^1	3	$curled^1$ allele	Blo.5045
SGF707	*w**; *nocturnin*^{65}	1;3	deletion mutant, *nocturnin*^{65}	this work
SGF708	*w**; *nocturnin*^{368}	1;3	deletion mutant, *nocturnin*^{368}	this work
SGF709	*w**; *nocturnin*^{671}	1;3	deletion mutant, *nocturnin*^{671}	this work
SGF710	*w**; *nocturnin*^{40}	1;3	excision revertant, *nocturnin*^{40}	this work
SGF718	*w**; *dHsl*^{rev32}	1;2	excision revertant, *dHsl*^{rev32}	this work
SGF715	*w**; *dHsl*^{43}	1;2	deletion mutant, *dHsl*^{43}	this work
SGF716	*w**; *dHsl*^{63}	1;2	deletion mutant, *dHsl*^{63}	this work
SGF717	*w**; *dHsl*^{59}	1;2	deletion mutant, *dHsl*^{59}	this work
SGF711	*w**; P{w[+mC]=CaSpeR4 SG301} #43a/CyO	1;2	*nocturnin* rescue SG301	this work
SGF712	*w**; P{w[+mC]=CaSpeR4 SG302} #20a/CyO	1;2	*nocturnin* rescue SG302	this work
RKF462	*y** *Lsd-2*^{40} / Dp(1;Y) y[+] or FM6 float	1	*Lsd-2*^{40}	
RKF463	*y** *Lsd-2*^{51} / Dp(1;Y) y[+] or FM6 float	1	*Lsd-2*^{51}	
RKF456	y^1 rev[P{y[+mDint2] w[BR.E.BR]=SUPor-P}Lsd-2[KG00149]] #37 / Dp(1;Y) y[+] or hom; ry[506]	1	*Lsd-2*^{revKG00149}	
RKF444	y^1 P{y[+mDint2] w[BR.E.BR]=SUPor-P}*Lsd-2[*KG00149] / Dp(1;Y) y[+] or hom; ry^{506}	1	*Lsd-2*^{KG00149}	
RKF390	*y** float *w** ;; P{w[+mC]UAS-*Lsd-2*} **#11A**	1;3	*UAS-Lsd-2*	
SGF714	*w**; *Dreg-2*^{70}	1;3	*Dreg-2*^{70}	
SGF719	*w**; P{w[+mC]UAST-*Dreg-2*}/CyO float	1;2	UAS-*Dreg-2*, SG133#10a	

Supplements

Supplemental Figure 1

Starvation upregulated genes (113)

Comment * coregulated in larvae and adults	Calls at different starvation times										Flybase ID: gene name
	6h		12h		18h I		18h II		24h		
Metabolic enzymes (44)											
Putative Ribose-phosphate pyrophosphokinase*	P	I	P	I	P	I	P	I	P	I	FB:FBgn0036030:*CG6767*
Putative Glyoxalase I	P	I	P	I	P	I	P	I	P	I	FB:FBgn0036992:*CG11796*
Putative IMP cyclohydrolase*	P	I	P	I	P	I	P	I	P	I	FB:FBgn0039241:*CG11089*
Putative phosphoserine transaminase	P	I	P	I	P	I	P	I	P	I	FB:FBgn0039649:*CG11899*
Putative Galactokinase, Mevalonate Kinase	P	I	P	I	P	I	P	I	P	I	FB:FBgn0035950:*CG5288*
Putative Phosphoglucomutase*	P	I	P	I	P	I	P	I	P	I	FB:FBgn0036572:*CG5165*
Putative UDP-glucose 4-epimerase	P	I	P	I	P	I	P	I	P	I	FB:FBgn0035147:*CG12030*
Putative Phenylalanine 4-monooxygenase*	P	I	P	I	P	I	P	I	P	I	FB:FBgn0001208:*Henna*
Putative Phosphoribosylaminoimidazole carboxylase*	P	I	P	I	P	I	P	I	P	I	FB:FBgn0020513:*ade5*
Putative phosphoribosylformylglycinamidine synthase*	P	I	P	I	P	I	P	I	P	I	FB:FBgn0000052:*ade2*
Putative Serine pyruvate aminotransferase*	P	I	P	I	P	I	P	I	P	I	FB:FBgn0014031:*Spat*
Putative Glutathione transferase-like*	P	I	P	I	P	I	P	I	P	I	FB:FBgn0030484:*CG1681*
*	P	I	P	I	P	I	P	I	P	I	FB:FBgn0016715:*Dreg-2*
Putative NAD-dependent methylenetetrahydrofolate dehydrogenase*	P	I	P	I	P	I	P	I	P	I	FB:FBgn0010222:*Nmdmc*
Putative UDP-glucuronosyltransferase*	P	I	P	I	P	I	P	I	P	I	FB:FBgn0037861:*CG6633*
Electron-transferring-flavoprotein dehydrogenase	P	I	P	I	P	I	P	I	P	I	FB:FBgn0033465:*CG12140*
Maltase 2-like*	P	I	P	I	P	I	P	I	P	I	FB:FBgn0032382:*CG14935*
Maltase 1-like	P	I	P	I	P	I	P	I	P	I	FB:FBgn0032381:*CG14934*
Putative Glycine hydroxymethyltransferase	P	I	P	I	P	I	P	I	P	I	FB:FBgn0029823:*CG3011*
Amylase distal*	P	I	P	I	P	I	P	I	P	I	FB:FBgn0000078:*Amy-d*
Putative Phosphoribosylamine-glycine ligase*	P	I	P	I	P	I	P	I	P	I	FB:FBgn0000053:*ade3*
Argininosuccinate lyase-like	P	I	P	I	P	I	P	I	P	I	FB:FBgn0032076:*CG9510*
Sorbitol dehydrogenase 1	P	I	P	I	P	I	P	I	P	I	FB:FBgn0024289:*Sodh*
Hexokinase C	P	I	P	I	P	NC	P	I	P	I	FB:FBgn0034003:*CG8094*
Carboxylesterase-like	P	I	P	I	P	I	P	NC	P	I	FB:FBgn0037090:*CG7529*
Putative Peroxidase*	P	I	P	I	P	I	P	NC	P	I	FB:FBgn0038465:*CG8913*
Putative alpha-glucosidase	P	I	P	I	P	I	P	NC	P	I	FB:FBgn0039330:*CG11909*
nocturnin	P	I	P	I	P	I	P	NC	P	I	FB:FBgn0037872:*CG4796*
Maltase L-like	P	I	P	I	P	I	P	NC	P	I	FB:FBgn0033295:*CG8689*
*	P	I	P	I	P	NC	P	NC	P	I	FB:FBgn0039537:*CG5590*
Putative Peptidase	P	I	P	I	P	NC	P	NC	P	I	FB:FBgn0038702:*CG3739*
Maltase H-like	P	I	P	I	P	NC	P	NC	P	I	FB:FBgn0033297:*CG8690*
Alpha-amylase-like	P	I	P	I	P	NC	P	NC	P	I	FB:FBgn0033296:*CG11669*
Putative Xylulokinase	P	I	P	I	P	I	P	I	P	NC	FB:FBgn0038463:*CG3534*
Putative Aspartate aminotransferase	P	I	P	I	P	I	P	I	P	NC	FB:FBgn0031380:*CG4233*

Glycerate dehydrogenase-like	P	I	P	I	P	I	P	NC	P	NC	FB:FBgn0031428:*CG9886*
Putative Transketolase	P	I	P	NC	P	I	P	NC	P	I	FB:FBgn0037607:*CG8036*
Homogentisate 1,2-dioxygenase*	P	I	P	I	P	I	P	I	P	I	FB:FBgn0032349:*CG4779, hgo*
Gyk (Glycerol kinase)	P	I	P	I	P	I	P	NC	P	I	FB:FBgn0035108:*CG18374*
	P	I	P	I	P	I	P	NC	P	I	FB:FBgn0039493:*CG5889*
	P	I	P	I	P	NC	P	NC	P	I	BDGP:GH13437.3prime-hit
Jheh1 (Juvenile hormone epoxide hydrolase 1)	P	I	P	I	P	NC	P	NC	P	I	FB:FBgn0034404:*CG15101*
Putative Lipoyltransferase*	P	I	P	NC	P	I	P	NC	P	I	FB:FBgn0034089:*CG8446*
Hph (HIF prolyl hydroxylase)	P	I	P	NC	P	I	P	NC	P	I	FB:FBgn0037308:*CG1114*
Putative HNK-1 sulfotransferase	P	I	P	NC	P	I	P	NC	P	I	FB:FBgn0032618:*CG4826*

Lipid metabolism (7)											
Putative Phospholipase A2*	P	I	P	I	P	I	P	I	P	I	FB:FBgn0030013:*CG1583*
Putative Glycerol-3-phosphate O-acyltransferase*	P	I	P	I	P	I	P	I	P	I	FB:FBgn0027579: GH07066
Putative TAG lipase*	P	I	P	I	P	I	P	I	P	I	FB:FBgn0029831:*CG5966*
Putative Acetyl-CoA carboxylase	P	I	P	I	P	I	P	MI	P	I	FB:FBgn0033245:*CG8723*
Putative Acetyl Coenzyme A synthase	P	I	P	I	P	I	P	NC	P	I	FB:FBgn0012034:*AcCoAS*
Mitochondrial carnitine palmitoyltransferase*	P	I	P	I	P	NC	P	NC	P	I	FB:FBgn0027842:*CPTI*
Putative Long-chain-fatty-acid-CoA-ligase*	P	I	P	NC	P	I	P	NC	P	I	FB:FBgn0027601: GH02901

Unknown function (25)											
*bmm**	P	I	P	I	P	I	P	I	P	I	FB:FBgn0036449:*CG5295*
*	P	I	P	I	P	I	P	I	P	I	FB:FBgn0032699:*CG10383*
*	P	I	P	I	P	I	P	I	P	I	FB:FBgn0031971:*CG7224*
	P	I	P	I	P	I	P	I	P	I	FB:FBgn0040729:*CG15126*
*	P	I	P	I	P	I	P	I	P	I	FB:FBgn0040729:*CG15126*
*	P	I	P	I	P	I	P	I	P	I	FB:FBgn0036419:*CG13482*
*	P	I	P	I	P	I	P	I	P	I	FB:FBgn0036262:*CG6910*
*	P	I	P	I	P	I	P	I	P	I	FB:FBgn0034140:*CG8317*
	P	I	P	I	P	I	P	I	P	I	FB:FBgn0033576:*CG18240*
*	P	I	P	I	P	I	P	I	P	I	FB:FBgn0032170:*CG4658*
*	P	I	P	I	P	I	P	NC	P	I	FB:FBgn0036837:*CG18135*
	P	I	P	I	P	I	P	NC	P	I	FB:FBgn0035346:*CG1146*
*	P	I	P	I	P	I	P	NC	P	I	FB:FBgn0035228:*CG12091*
	P	I	P	I	P	I	P	NC	P	I	FB:FBgn0035176:*CG13905*
fok (fledgling of Klp38B)*	P	I	P	I	P	I	P	NC	P	I	FB:FBgn0032844:*CG10746*
New annotation CG15263	P	I	P	I	P	I	P	NC	P	I	FB:FBgn0028853:*DS07851.4*
	P	I	P	I	P	NC	P	NC	P	I	FB:FBgn0033464:*CG1441*
New annotation CG33054/CG33056*	P	I	P	I	P	NC	P	NC	P	I	FB:FBgn0037058:*CG10517*
	P	I	P	I	P	NC	P	NC	P	I	FB:FBgn0034664:*CG4377*
	P	I	P	I	P	I	M	NC	P	I	FB:FBgn0039299:*CG11854*
	P	I	P	I	P	I	P	I	P	NC	FB:FBgn0036110:*CG18348*
*	P	I	P	I	P	I	P	I	P	NC	FB:FBgn0034382:*CG18609*
*	P	I	P	NC	P	I	P	NC	P	I	FB:FBgn0033385:*CG8055*
*	P	I	P	NC	P	I	P	NC	P	I	FB:FBgn0036106:*CG6409*

	P	I	P	NC	P	I	P	NC	P	I	FB:FBgn0039398:*CG14540*
	P	I	P	NC	P	I	P	NC	P	I	FB:FBgn0035115:*CG13878*
New annotation CG32477*	P	I	P	NC	P	I	P	NC	P	I	BDGP:GH6422.3prime-hit
Kinases (5)											
	P	I	P	I	P	I	P	I	P	I	FB:FBgn0017581:*Lk6*
LK6*	P	I	P	NC	P	I	P	NC	P	I	BDGP:LD31983.3prime-hit
AMPK beta subunit*	P	I	P	I	P	I	P	NC	P	I	FB:FBgn0033383:*CG8057*
AMPK gamma subunit*	P	I	P	NC	P	I	P	NC	P	I	FB:FBgn0025803:*SNF4*
PKA-C3	P	I	P	NC	P	I	P	NC	P	I	FB:FBgn0000489:*Pka-C3 subunit*
Pdk*	P	I	P	NC	P	I	P	NC	P	I	FB:FBgn0017558:*Pdk*
Immune response (3)											
Thor*	P	I	P	I	P	I	P	I	P	I	FB:FBgn0022073:*Phas1/Thor*
IM2 (Immune induced protein 2)	P	I	P	I	P	I	P	NC	P	I	FB:FBgn0025583:*IM2*
IM1 (Immune induced protein 1)	P	I	P	I	P	I	P	NC	P	I	FB:FBgn0034329:*CG18108*
Transporter (6)											
Sugar transporter-like	P	I	P	I	P	I	P	I	P	I	FB:FBgn0037386:*CG1208*
Sugar transporter-like	P	I	P	I	P	I	P	I	P	I	FB:FBgn0034247:*CG6484*
Sugar transporter-like	P	I	P	I	P	I	P	I	P	NC	FB:FBgn0037387:*CG1213*
Glucose transporter-like	P	I	P	I	P	I	P	NC	P	I	FB:FBgn0034045:*CG8249*
	P	I	P	I	P	NC	P	NC	P	I	FB:FBgn0036068:*CG6640*
Sodium/phosphate cotransporter*	P	I	P	NC	P	I	P	NC	P	I	FB:FBgn0031645:*CG3036*
Cytochromes (10)											
Cytochrome P450*	P	I	P	I	P	I	P	I	P	I	FB:FBgn0031689:*Cyp28d1*
Cytochrome P450*	P	I	P	I	P	I	P	I	P	I	FB:FBgn0015035:*Cyp4e3*
Cytochrome P450*	P	I	P	I	P	I	P	I	P	I	FB:FBgn0000473:*Cyp6a2*
Cytochrome P450*	P	I	P	I	P	I	P	I	P	I	FB:FBgn0013772:*Cyp6a8*
Cytochrome P450*	P	I	P	I	P	I	P	NC	P	I	FB:FBgn0015714:*Cyp6a17*
Cytochrome P450*	P	I	P	I	P	I	P	NC	P	I	FB:FBgn0038194:*Cyp6d5*
Cytochrome P450*	P	I	P	I	P	NC	P	NC	P	I	FB:FBgn0033065:*Cyp6w1*
Cytochrome P450*	P	I	P	I	P	I	P	NC	P	NC	FB:FBgn0013771:*Cyp6a9*
Cytochrome P450	P	I	P	I	P	I	P	NC	P	NC	FB:FBgn0033980:*Cyp6a20*
Cytochrome P450*	P	I	P	NC	P	I	P	NC	P	I	FB:FBgn0038681:*Cyp12a4*
Structural proteins (3)											
*	P	I	P	I	P	I	P	I	P	I	FB:FBgn0028473: LD23830
Putative Actin binding protein*	P	I	P	I	P	NC	P	NC	P	I	FB:FBgn0023507:*EG:87B1*
*	P	I	P	NC	P	I	P	NC	P	I	FB:FBgn0001301: *kelch*
Miscellaneous (10)											
Translation initiation factor 3, 110 kD subunit*	P	I	P	I	P	NC	P	NC	P	I	FB:FBgn0037249:*CG9805*
Putative DEAD box helicase*	P	I	P	I	P	NC	P	NC	P	I	FB:FBgn0001565:*Hlc*
Low-density lipoprotein/calcium binding receptor-like*	P	I	P	NC	P	I	P	I	P	I	FB:FBgn0039361:*CG4823*
Putative DNA replication factor*	P	I	P	NC	P	I	P	NC	P	I	FB:FBgn0033269:*CG8709*

ATP dependent RNA helicase*	P	I	P	NC	P	I	P	NC	P	I	FB:FBgn0003261:*Rm62*
Marf (Mitochondrial assembly regulatory factor)*	P	I	P	NC	P	I	P	NC	P	I	FB:FBgn0029870:*CG3869*
JhI-26 (Juvenile hormone-inducible protein 26)*	P	I	P	I	P	NC	P	MI	P	I	FB:FBgn0034108:*CG3767*
Putative nucleic acid binding protein	P	I	P	NC	P	I	P	NC	P	I	FB:FBgn0037681:*CG16751*
RNA binding protein-like	P	I	P	NC	P	I	P	NC	P	I	FB:FBgn0035938:*CG5735*
PolyA-binding protein	P	I	P	NC	P	NC	P	I	P	I	FB:FBgn0003031:*pAbp* /

Starvation downregulated genes (110)

Comment * coregulated in larvae and adults	Calls at different starvation times										Flybase ID: gene name
	6h		12h		18h I		18h II		24h		
Proteases/protease inhibitors (38)											
Trypsin-like Serine-type endopeptidase	P	D	P	D	P	D	P	D	P	D	FB:FBgn0030688:*CG8952*
Putative Endopeptidase	P	D	P	D	P	D	P	D	P	D	FB:FBgn0039418:*CG6069*
	P	D	P	D	P	D	P	D	P	D	FB:FBgn0036969:*CG6663*
Putative Zinc carboxypeptidase*	P	D	P	D	P	D	P	D	P	D	FB:FBgn0035779:*CG8562*
Serine proteinase 2-like	P	D	P	D	P	D	P	D	P	D	FB:FBgn0035666:*CG6580*
Trypsin alpha-like	P	D	P	D	P	D	P	D	P	D	FB:FBgn0033838:*CG4812*
Putative Serine-type endopeptidase	P	D	P	D	P	D	P	D	P	D	FB:FBgn0033619:*CG12350*
Trypsin-like	P	D	P	D	P	D	P	D	P	D	FB:FBgn0032947:*CG17571*
Carboxypeptidase A	P	D	P	D	P	D	P	D	P	D	FB:FBgn0032144:*CG17633*
Spn2 (serine protease inhibitor 2)	P	D	P	D	P	D	P	D	P	D	FB:FBgn0032007:*CG8137*
Putative Serine endopeptidase*	P	D	P	D	P	D	P	D	P	D	FB:FBgn0028915:*BG:DS01068.5*
zetaTrypsin	P	D	P	D	P	D	P	D	P	D	FB:FBgn0011556:*zetaTry*
thetaTrypsin*	P	D	P	D	P	D	P	D	P	D	FB:FBgn0011555:*thetaTry*
Putative Endopeptidase	P	D	P	D	P	D	P	D	P	D	FB:FBgn0037678:*CG16749*
Putative Serine protease	P	D	P	D	P	D	P	D	P	D	FB:FBgn0031249:*CG11911*
	P	D	P	D	P	D	P	D	P	D	FB:FBgn0036024:*CG18180*
Putative Endopeptidase	P	D	P	D	M	D	P	D	P	D	FB:FBgn0035667:*CG10475*
Serine protease-like	P	D	P	D	A	D	P	D	P	D	FB:FBgn0034052:*CG8299*
Putative Glutamyl aminopeptidase	P	D	A	D	A	D	A	D	P	D	FB:FBgn0038135:*CG8773*
Signal peptidase activity	P	D	P	D	P	D	P	D	P	MD	FB:FBgn0030306:*CG1751*
iotaTrypsin	P	D	P	D	P	D	P	D	P	MD	FB:FBgn0015001:*iotaTry*
Carboxypeptidase-like	P	D	P	D	P	D	P	D	P	NC	FB:FBgn0035781:*CG8560*
*	P	D	P	D	P	D	P	D	P	NC	FB:FBgn0031929:*CG18585*
Aspartic-type endopeptidase	P	D	P	D	P	D	P	D	P	NC	FB:FBgn0032049:*CG13095*
Chymotrypsin-like serine protease	P	D	P	D	P	D	P	D	P	NC	FB:FBgn0035670:*CG10472*
Chymotrypsin-like serine protease	P	D	P	D	P	D	P	D	P	NC	FB:FBgn0035665:*CG6483*
Aminoacylase-like	P	D	P	D	P	D	P	D	P	NC	FB:FBgn0039052:*CG6733*
Aminoacylase-like	P	D	P	D	P	D	P	D	P	NC	FB:FBgn0039049:*CG6726*
Serpin	P	D	P	D	P	D	P	D	P	NC	FB:FBgn0036971:*CG6266*
Putative Endopeptidase	P	D	P	D	P	D	P	D	P	NC	FB:FBgn0032413:*CG16997*
Putative Endopeptidase	P	D	P	D	P	D	P	D	P	NC	FB:FBgn0032412:*CG16996*
Serine protease-like	P	D	P	D	P	D	P	D	P	NC	FB:FBgn0031654:*CG8869*

Serine protease-like	P	D	P	D	P	NC	P	D	P	NC	FB:FBgn0039777:*CG2229*
Serine protease 4	P	D	P	D	P	NC	P	D	P	NC	FB:FBgn0020906:*Ser4*
Trypsin-like	P	D	M	D	P	D	A	D	A	D	FB:FBgn0039778:*CG18030*
Serine protease 3*	P	D	P	NC	P	D	P	D	P	D	FB:FBgn0003358:*Ser99Dc*
Astacin-like	P	D	A	NC	P	D	P	D	P	D	FB:FBgn0028949:*BACR44L22.2*
Aminopeptidase N-like*	P	D	P	NC	P	NC	P	D	P	D	FB:FBgn0038898:*CG5839*

Unknown function (31)											
*	P	D	P	D	P	D	P	D	P	D	FB:FBgn0039311:*CG10513*
*	P	D	P	D	P	D	P	D	P	D	FB:FBgn0039313:*CG11892*
*	P	D	P	D	P	D	P	D	P	D	FB:FBgn0039312:*CG10514*
	P	D	P	D	P	D	P	D	P	D	FB:FBgn0038147:*CG14375*
*	P	D	P	D	P	D	P	D	P	D	FB:FBgn0037782:*CG12813*
	P	D	P	D	P	D	P	D	P	D	FB:FBgn0034318:*CG14500*
	P	D	P	D	P	D	P	D	P	D	FB:FBgn0034292:*CG5767*
	P	D	P	D	P	D	P	D	P	D	FB:FBgn0034153:*CG15616*
	P	D	P	D	P	D	P	D	P	D	FB:FBgn0032868:*CG17472*
	P	D	P	D	P	D	P	D	P	D	FB:FBgn0032297:*CG17124*
	P	D	P	D	P	D	P	D	P	D	FB:FBgn0030837:*CG8661*
New annotation CG7968*	P	D	P	D	P	D	P	D	P	D	FB:FBgn0028532:*DS00941.15*
	P	D	P	D	P	D	P	D	P	D	FB:FBgn0034290:*CG5773*
*	P	D	P	D	P	D	P	D	P	D	FB:FBgn0031143:*CG1532*
	P	D	P	D	P	D	P	D	P	D	FB:FBgn0030098:*CG12057*
	P	D	P	D	P	NC	P	NC	P	D	FB:FBgn0035112:*CG13877*
*	P	D	P	D	P	D	A	D	P	D	FB:FBgn0038973:*CG18594*
New annotation CG30427	P	D	P	D	P	NC	A	D	P	D	FB:FBgn0040667:*CG18680*
*	P	D	P	D	A	D	A	D	P	D	FB:FBgn0032669:*CG15155*
	P	D	P	D	P	D	P	D	P	MD	FB:FBgn0033826:*CG4734*
*	P	D	P	D	P	D	P	D	P	NC	FB:FBgn0027095:*ARP-like*
*	P	D	P	D	P	D	P	D	P	NC	FB:FBgn0032913:*CG9259*
	P	D	P	D	P	D	P	D	P	NC	FB:FBgn0032472:*CG9928*
Accessory gland peptide 62F	P	D	P	D	P	D	P	D	P	NC	FB:FBgn0020509:*Acp62F*
*	P	D	P	D	P	D	P	D	P	NC	FB:FBgn0039800:*CG11314*
	P	D	P	D	P	NC	P	D	P	NC	FB:FBgn0039483:*CG14259*
	P	D	P	D	P	NC	P	D	P	NC	FB:FBgn0033787:*CG13321*
synonyms: G9, Rtnl1	P	D	P	D	P	NC	P	D	P	NC	FB:FBgn0031666:*CG8895*
*	P	D	M	D	A	NC	A	D	P	NC	FB:FBgn0039151:*CG13607*
*	P	D	A	D	A	D	A	D	A	D	FB:FBgn0040609:*CG3348*
	P	D	P	I	P	I	P	I	P	NC	FB:FBgn0035476:*CG12766*

Miscellaneous (15)											
Lsp1β*	P	D	P	D	P	D	P	D	P	D	FB:FBgn0002563:*Lsp1beta*
Obp99b	P	D	P	D	P	D	P	D	P	D	FB:FBgn0039685:*CG7592*
Diazepam-binding inhibitor-like*	P	D	P	D	P	D	P	D	P	D	FB:FBgn0035926:*CG5804*
Pherokine 3; Protein Ser/Thr kinase	P	D	P	D	P	D	P	D	P	D	FB:FBgn0035089:*CG9358*
Antigen 5-related 2	P	D	P	D	P	D	P	D	P	D	FB:FBgn0020508:*Ag5r2*
	P	D	P	D	P	D	P	D	P	D	FB:FBgn0004414:*msopa*

Alpha-tocopherol transfer protein-like*	P	D	A	D	A	D	A	D	P	D	FB:FBgn0037323:*CG2663*
Alpha-tocopherol transfer protein-like	P	D	P	D	P	D	P	D	P	NC	FB:FBgn0032783:*CG10237*
Tapd*	P	D	P	D	P	D	P	D	P	NC	FB:FBgn0027912: GM12291
Metallothionein C	P	D	P	D	P	D	P	D	P	NC	FB:FBgn0038790:*CG5097*
Retinoid binding protein-like*	P	D	P	D	P	D	P	D	P	NC	FB:FBgn0031913:*CG5958*
Male-specific RNA 57Dc	P	D	P	D	P	NC	P	D	P	NC	FB:FBgn0011670:*Mst57Dc*
Thioredoxin-2 Trx-2*	P	D	P	D	P	NC	P	D	P	NC	FB:FBgn0032134:*CG3864*
Thioredoxin peroxidase 1; Jafrac1*	P	D	P	D	P	D	P	NC	P	NC	FB:FBgn0030472:*CG1633*
Diazepam-binding inhibitor-like*	P	D	M	NC	M	D	P	D	P	D	FB:FBgn0035744:*CG8628*
Lipid metabolism (9)											
Lsd-1*	P	D	P	D	P	D	P	D	P	D	FB:FBgn0039114:*CG10374*
RfaBp*	P	D	P	D	P	D	P	D	P	D	BDGP:GH184.3prime-hit
TAG lipase	P	D	P	D	P	D	P	D	P	D	FB:FBgn0039471:*CG6295*
New annotation CG32072; Putative long chain fatty acid elongase	P	D	P	D	P	D	P	D	P	D	FB:FBgn0036129:*CG6261*
1-Acylglycerol-3-phosphate O-acyltransferase-like*	P	D	P	D	P	D	P	D	P	D	FB:FBgn0036622:*CG4753*
Phosphatidylserine decarboxylase proenzyme	P	D	P	D	P	NC	P	D	P	D	FB:FBgn0039143:*CG5991*
TAG lipase	P	D	P	D	A	D	A	D	P	D	FB:FBgn0039472:*CG17192*
Putative phospholipase	P	D	P	D	P	D	P	D	P	NC	FB:FBgn0031691:*CG14034*
TAG lipase	P	D	P	D	A	D	A	D	M	D	FB:FBgn0036996:*CG5932*
Metabolic enzymes (7)											
Alkaline phosphatase-like*	P	D	P	D	P	D	P	D	P	D	FB:FBgn0035620:*CG5150*
GstE10	P	D	P	D	P	D	P	D	P	D	FB:FBgn0034334:*CG17522*
alpha/beta hydrolase	P	D	P	D	P	D	P	D	P	D	FB:FBgn0032265:*CG18301*
Alkaline phosphatase	P	D	P	D	P	NC	P	NC	P	D	FB:FBgn0034711:*CG3290*
Alkaline phosphatase-like	P	D	P	D	P	D	P	D	P	NC	FB:FBgn0035619:*CG10592*
	P	D	P	D	P	D	P	D	P	NC	FB:FBgn0033101:*CG9436*
Alkaline phosphatase 4	P	D	P	NC	P	D	P	D	P	D	FB:FBgn0016123:*Aph-4*
Immune response (7)											
PGRP-SC1b*	P	D	P	D	P	D	P	D	P	D	FB:FBgn0033327:*CG8577*
PGRP-SC2	P	D	P	D	P	D	P	D	P	D	FB:FBgn0033328:*CG14745*
Metchnikowin	P	D	P	D	P	D	P	D	P	D	FB:FBgn0014865:*Mtk*
DptB	P	D	P	D	P	D	P	NC	P	D	FB:FBgn0034407:*CG10794*
AttC	P	D	P	D	P	D	M	D	P	D	FB:FBgn0033833:*CG4740*
PGRP-SC1a*	P	D	P	D	P	D	M	D	A	D	FB:FBgn0033325:*CG14746*
PGRP-SB1*	P	D	P	NC	P	D	M	D	P	D	FB:FBgn0036658:*CG9681*
Transporter (2)											
Iodide symporter-like*	P	D	P	D	P	D	P	D	P	D	FB:FBgn0039391:*CG8934*
Organic cation transporter-like*	P	D	P	D	A	D	A	NC	P	D	FB:FBgn0038718:*CG17752*
Transcription factor (1)											
Sugarbabe	P	D	P	D	A	D	P	D	M	D	FB:FBgn0033782:*sug*

(P= present; A= absent; I= increase; D= decrease; MI= marginally increase; MD= marginally decrease; NC= no change)

Supplement 1: Characterization of the Drosophila gene *doppelgänger von brummer*

The gene *bmm* is a nutritionally-controlled key regulator of lipid storage in *Drosophila*. It is a member of the evolutionary conserved *bmm/nutrin* gene family which encode TAG lipases (2.2.3). In *bmm* mutants, TAG mobilization is impaired. However, residual TAG mobilizing activity in the mutants indicates that additional TAG lipases, different from *Bmm*, must be involved in organismal TAG storage mobilization under starvation. A candidate effector for *bmm*-independent inducible TAG mobilization is the *bmm* paralogue gene *CG5560*, renamed as *doppelgänger von brummer* (*dob*). I characterized the *dob* gene and examined its function by gain-of-function and loss-of-function studies in order to test whether *dob* can participate in TAG storage control and contribute to starvation induced TAG mobilization in *Drosophila*.

S1.1 Genomic organization of *the doppelgänger von brummer* gene region

The *dob* gene is located at the cytogenetic map position 13A8 on the *Drosophila* X-chromosome. It is only 2,961 kb adjacent to the *Lsd-2* gene locus (Fig. S1.1). Sequence analysis of two *dob* cDNAs (LD21294 and GH09195, Rubin et al., 2000) revealed, that *dob* is encoded by two exons (exon 1: 633 bp, exon 2: 1200 bp) spanning about 2 kb of genomic DNA. Within the 1,833 kb long *dob* cDNA, a 1,443 kb long ORF codes for a predicted protein of 480 amino acids (Dob) with a corresponding molecular mass of 54,5 kDa.

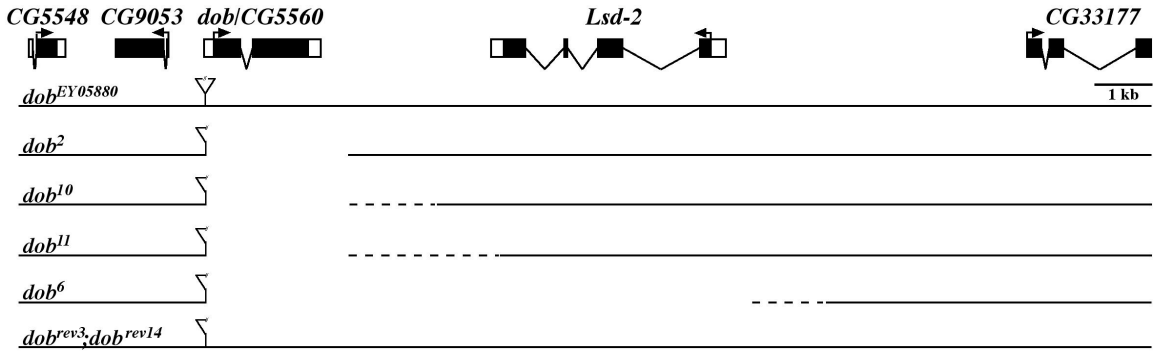

Figure S1.1: Genomic organization of the *dob* gene locus and *dob* deletion mutants. The coding exons are shown as black, UTRs as white boxes, transcription directions are indicated by arrows). Flies carrying the P-element $dob^{EY05880}$ (triangle) in the 5´ UTR of the first *dob* exon were used to generate deletion mutants dob^{2}, dob^{10}, dob^{11} and *dob, Lsd-2* double mutant dob^{6} as well as the revertant control lines dob^{rev3} and dob^{rev14}.

S1.2 The Doppelgänger von brummer protein

Like Bmm (see Fig. 9A), the Dob protein is composed of a non-conserved carboxyterminal variable region (VR, aa: 252-480) and an evolutionary conserved aminoterminal part (CR, aa: 1-251). The CR contains both the PLD (amino acids: 9-177) and the Brummer Box (BB,

amino acids: 178-251). The closest relative of Dob is the Dob orthologue of *Drosophila pseudoobscura* (GA18971-PA). However, no Dob orthologue is detected in the *Anopheles* genome (compare Fig. 9B). This suggests that in contrast to *bmm*, the *dob* gene is conserved only among *Drosophilidae* and is the result of a recent duplication of the *bmm* gene. Bmm orthologs of *D. melanogaster* and *D. pseudoobscura* are 97 % identical, whereas the Dob orthologues of these species have only 56 % of amino acids in common (PLD: 83%, BB: 76 %, VR: 21 %). This finding demonstrates a much faster rate of amino acid exchange during the evolution of Dob proteins as compared to Bmm.

S1.3 Developmental expression of *doppelgänger von brummer*

Developmental Northern blot and RNA antisense ISH analysis revealed, that *dob* expression is restricted to adult stages (Fig. S1.2A). Under *ad libitum* fed conditions, *dob* mRNA is found in heads and bodies of adult male and female flies. The stronger expression of *dob* in females as compared to males is likely to reflect the maternal *dob* transcripts which are deposited in the egg and can be later seen as maternal contribution in early embryos (0-3h). Maternal expression of *dob* was confirmed by ISH on wild-type ovaries, syncytial blastoderm stage embryos and on cellular blastoderm stage embryos (Fig. S1.2A-C). Maternal transcripts get rapidly degraded as judged by the absence of *dob* mRNA in the cellular blastoderm stage (Fig. S1.2D). No zygotic *dob* expression in later staged embryos was observed by the ISH technique (data not shown).

S1.4 Nutritional regulation of *doppelgänger von brummer*

Quantitative Northern blot analysis was used to examine the transcriptional regulation of *dob* in adult flies which were either fed or kept under starvation conditions (Fig. S1.2F). *dob* expression is increased under starvation conditions (Fig. S1.2F). However, in contrast to *bmm*, no upregulation of *dob* mRNA was detected in starved third instar larvae (Zinke et al., 2002). This difference suggests that *dob* functions specifically in the adult starvation response.

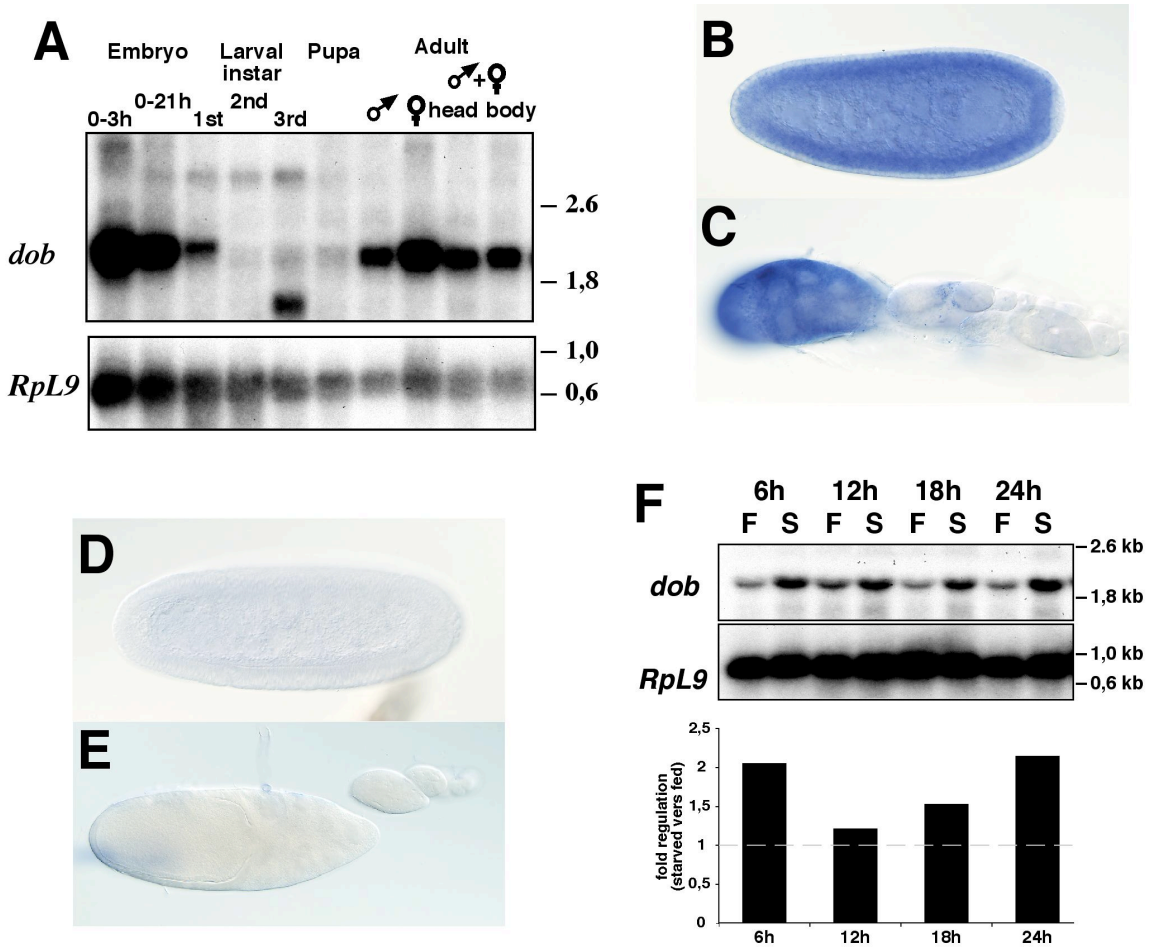

Figure S1.2: Developmental expression and nutritional regulation of *dob* (**A**) Developmental Northern blot analysis detects a single *dob* transcript of 2 kb expressed exclusively in adult males and females and during embryogenesis. Hybridisation signal in first instar larvae is likely to be derived from unfertilized eggs present in the first instar larval collection, since no expression could be detected by ISH on late stage embryos (data not shown). The origin of a smaller hybridisation signal in third instar larvae is unknown. (**B, C**) ISH hybridisation using a *dob* RNA antisense probe on wild-type syncytial blastoderm stage embryos (**B**) or adult ovaries (**C**) demonstrates maternal contribution of *dob* mRNA consistent with the developmental Northern blot analysis. (**D**) No *dob* mRNA is detectable in cellular blastoderm stage embryos, indicating the rapid degradation of maternal *dob* transcript. (**E**) The lack of hybridisation signal in dob^2 mutant ovaries documents specificity of *dob* ISH hybridisation probe and confirms dob^2 as a *dob* transcript null mutation. (**F**) Quantitative Northern blot analysis detects upregulation of *dob* transcript abundance in starved (S) flies by a factor of 2,1, 1,2, 1,5 and 2,1 after 6, 12, 18 and 24 hours, respectively, compared to *ad libitum* fed (F) controls.

S1.5 Lean flies caused by overexpression of *doppelgänger von brummer*

I examined whether *dob* activity is capable of modulating organismal TAG content. *dob* was overexpressed in the fat body of *ad libitum* fed flies using a UAS-*dob* effector line in combination with a FB-Gal4 driver line. Analogous to the inactived TAG lipase variant Bmm^{S38A}, a Dob^{S44A} protein was generated by replacing the putative active site serine at amino acid position 44 in the serine hydolase motif of the Dob PLD domain with an alanine. Fat body overexpression of *dob* but not dob^{S44A} leads to a dramatic reduction in organismal TAG content (Fig. S1.3A: 58 % in third instar larvae; undetectable TAG levels in immature adults) and survival under starvation conditions (Fig S1.3B: 40% median lifespan decrease in

immature adults). These results and the molecular similarity between Bmm and Dob suggest a Bmm-like TAG lipase activity of Dob in the fat body.

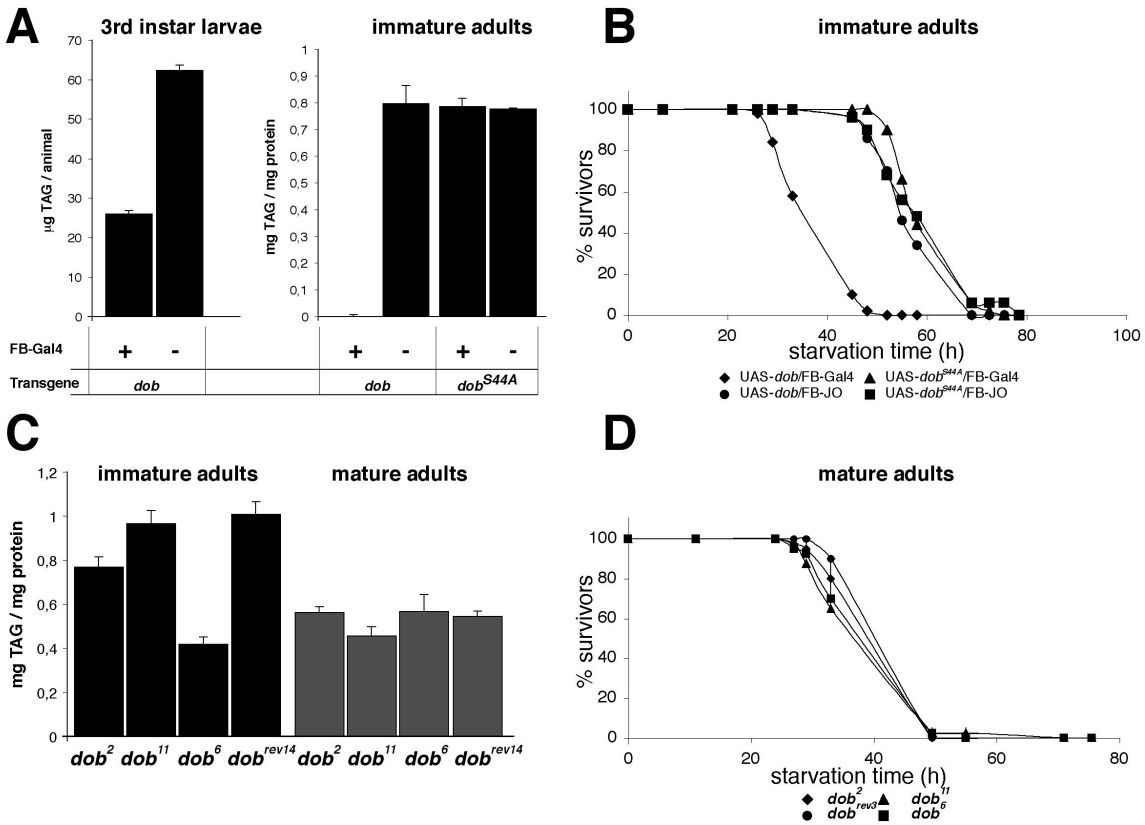

Figure S1.3: Organismal TAG content and starvation survival time of *dob* gain- and loss-of function flies. (**A-B**) Physiological consequence of *dob*-transgene induction in the fat body of *ad libitum* fed flies (catalytic center mutant dob^{S44A}). (**A**) Reduction of organismal TAG content by 58 % and 100% in third instar larvae and immature adult males, respectively. (**B**) Reduction of median starvation lifespan of immature adult male flies by 40 %. (**C-D**) *dob* loss-of function mutants have normal TAG content and median starvation lifespan. (**C**) Organismal TAG content of immature adult dob^6 (*dob,Lsd-2)* mutants is reduced by 58 % comparable with the *Lsd-2* single mutant (compare Fig. S3.4). For details see text.

S1.6 *doppelgänger von brummer* activity can substitute for the lack of *brummer* activity

In order to test whether *dob* activity can substitute for *bmm* activity, *dob* was overexpressed in bmm^1 mutant embryos and hatching rates among the corresponding individuals were determined (Table S1.1). The lack of *bmm* activity during embryogenesis results in lethality as documented by 0 % hatching rate of larvae that carry an uninduced UAS-*dob* construct in the bmm^1 mutant individuals. Ubiquitous zygotic expression of *dob* in response to an *Act5C*-Gal4 driver (*act-Gal4*) significantly rescued the *bmm* mutant embryos (Table S1.1), indicating that *dob* activity can substitute for the lack of *bmm* function *in vivo* and further supports the above conclusion that Dob has a Bmm-like TAG lipase activity. In order to

characterize the *in vivo* function of *dob* in TAG storage mobilization, flies lacking *dob* activity were generated.

Parental genotype (males x females)	# of embryos scored	% hatched embryos
act-Gal4/CyO; bmm^1/bmm^1 x *act*-Gal4/CyO; bmm^1/bmm^1	640	0.5
UAS-*bmm*/UAS-*bmm*; bmm^1/bmm^1 x *act*-Gal4/CyO; bmm^1/bmm^1	269	45.0*
UAS-*dob*/UAS-*dob*; bmm^1/bmm^1 x UAS-*dob*/UAS-*dob*; bmm^1/bmm^1	1041	0.0
UAS-*dob*/UAS-*dob*; bmm^1/bmm^1 x *act*-Gal4/CyO; bmm^1/bmm^1	911	35.1*

Table S1.1: *dob* activity can substitute *bmm* function in the embryo. Hatching rate counts of maternal zygotic bmm^1 mutant embryos ubiquitously expressing *dob*. *Bmm*-dependent embryonic lethality is partially rescued by overexpression of *dob* resulting in 35 % of hatched embryos compared to 45 % by using *bmm*. *Expected hatching rate is 50 % due to maternal *CyO* balancer chromosome.

S1.7 Generation of *doppelgänger von brummer* mutants

dob mutant alleles were generated by imprecise excision of a *P{EP}* transposable element inserted in the 5´ UTR of the *dob* first exon in the fly line $CG5560^{EY05880}$ (BDGP gene disruption project) following a conventional P-element mobilization scheme (Ashburner, 1989). Using a PCR-based screen (see Material and Methods), four different *dob* mutant alleles were identified termed dob^2, dob^{10}, dob^{11} and dob^6 (Fig. S1.1). The mutant dob^2 lacks 2385 bp of genomic sequence including the *dob* coding region. The absence of *dob* gene expression was confirmed by ISH on ovaries isolated from dob^2 mutants females (Fig. S1.2E). dob^{10} and dob^{11} mutant alleles carry bigger deletions which were not analyzed on the sequence level. However, according to PCR analysis they do not affect the coding region of the adjacent *Lsd-2* gene (Fig. S1.1). In contrast, dob^6 deletion cause double mutants that lack both the *dob* and the *Lsd-2* gene (Fig. S1.1). As "genetically matched controls", i.e. individuals with an intact *dob* genomic region, the two excision alleles dob^{rev3} and dob^{rev14} were generated (Fig. S1.1).

S1.8 doppelgänger von brummer mutants have normal organismal TAG content

Lack-of maternal and zygotic *dob* expression in dob^2, dob^{10} and dob^{11} mutants results in viable flies without any discernible morphological phenotype. Thus, Dob activity is dispensable during development. In contrast, embryos laid by homozygous dob^6 mutant females, which lack both Dob and Lsd-2 activities, have a reduced hatching rate as observed with *Lsd-2* single mutants (Teixeira et al., 2003). This observation confirmes in biological terms the lack of Lsd-2 activity in these flies (data not shown).

Immature dob^6 flies have a decreased organismal TAG content (Fig. S13C: dob^6 0,42±0,03 to dob^{14} 1,00±0,05 μg TAG/μg protein). This result indicates that Dob, in contrast to Bmm, can

not antagonize TAG mobilization induced by lack of Lsd-2 activity (compare with results shown in Fig. 16). Accordingly, *ad libitum* fed flies that lack only *dob* activity have a normal organismal TAG content (Fig. S1.3C: dob^{2} 0,76±0,05, dob^{11} 0,97±0,06 to dob^{14} 1,00±0,05 in immature adults and dob^{2} 0,56±0,03, dob^{11} 0,45±0,04 to dob^{14} 0,54±0,02 in mature adults, respectively). This observation indicates that *dob* is not essential for chronic regulation of TAG storage in *Drosophila*. Consistently, the lack-of-*dob*-function is not detrimental to *ad libitum* fed flies, as shown by the fact that *dob* mutants have the same median lifespan as dob^{rev} controls (dob^{2}: 54-56 days, dob^{10}: 54-56 days, dob^{rev3}: 54 days, data not shown). Furthermore, *dob* loss-of-function mutants survive as long as control flies under starvation (Fig. S1.3D). In summary, *dob* is not essential for chronic TAG storage control and starvation-induced TAG mobilization under acute food-deprivation.

S1.9 Discussion

The results indicate that *dob* gene activity is not essential for the control of organismal TAG storage in *Drosophila*. This finding is different from the results obtained for the gene *bmm*, since the TAG content of *dob* lack-of-activity mutants is not altered in contrast to *bmm* mutants. This finding is unexpected in the light of the fact that gain-of-function experiments (i.e. overexpression of *dob* in the fat body of larvae or adult flies) revealed that *dob* activity can affect organismal TAG storage in a *bmm*-like manner. In addition, *dob* overexpression can rescue the embryonic lethality of bmm^{1} mutants, indicating that *dob* activity can substitute for the lack of *bmm in vivo* activity. Thus, Dob exerts a Bmm-like TAG lipase activity.

In *ad libitum* fed adult flies, *dob* is expressed in heads and bodies of males and females. Aside from the expression in the ovary of females, the tissue specific distribution of *dob* mRNA in adults is unknown. It is possible, however, that endogenously *dob* is normally not expressed in the fat body and is, therefore, not involved in chronic TAG storage control. *In situ* hybridisation or RT-PCR analysis on adult fat body tissue would be necessary to answer this question. Another possibility is that other TAG lipases, such as Bmm, are sufficient to overcome the lack-of *dob* activity under the conditions applied. If this conclusion were true, flies that lack both *dob* and *bmm* activity should have an increased organismal TAG content. However, $dob^{10};bmm^{1}$ double mutants have a TAG content comparable to bmm^{1} single mutants (compare Fig. 17A, B). This finding supports the conclusion, that *dob* is not involved in control of chronic organismal TAG storage. On the other hand, it cannot be excluded that other TAG lipases in addition to *Bmm* could also compensate for *dob* function

(see below). Since the developmental Northern blot analysis does not allow reliable quantification of *dob* transcripts, it is possible that *dob* is expressed only at very low levels in *ad libitum* fed flies and thus, does not significantly contribute to organismal TAG storage control in adult wild-type flies.

The maternal contribution of *dob* mRNA points towards a function of *dob* during early embryogenesis. However maternal and zygotic *dob* mutant embryos have no obvious phenotype and they develop into viable adults. During embryogenesis, bmm^{rev} embryos mobilize most (85%) of their TAG storage to fuel developmental processes (see Fig. 13B). In contrast, bmm^{1} mutant embryos mobilize only 26 % of their TAG storage and, although many reach late embryonic stages, they fail to develop into first instar larvae, because they are likely to die of starvation (see results Fig. 13B). Remarkably, although maternal and zygotic bmm^{1} mutant embryos fail to mobilize TAG during later stages, i.e. only 6 % TAG mobilization between 10 and 20 hours of embryonic development, they can mobilize 21 % of their TAG storage within the first 10 hours of embryogenesis, a period that overlaps with the presence of maternal *dob* transcript in the embryo. Thus, during the initial phase of early embryogenesis Dob could provide the early TAG mobilizing activity which, in part, can substitute early but not late for the lack of *Bmm* activity in maternal and zygotic bmm^{1} mutant embryos. This conclusion needs to be confirmed by analysing TAG mobilization in $dob^{10};bmm^{1}$ double mutant embryos.

In contrast to *bmm*, *dob* is not an essential gene. This result correlates with a lower degree of conservation between Dob orthologs. Bmm orthologues of *D. melanogaster* and *D. pseudoobscura* are 97 % identitical, whereas only 56 % of amino acids are conserved among the corresponding Dob homologues. No Dob orthologue is detected in the *Anopheles* genome, suggesting that *dob* is the result of a recent gene duplication which happened after the divergence of *Anopheles* and the *Drosophilidae* around 250 million years ago (Celniker and Rubin, 2003). The conservation of Dob among *D. melanogaster* and *D. pseudoobscura*, which diverged around 46 million years ago (Celniker and Rubin, 2003), suggests that *dob* gene function contributes to an increased fitness of fly population in the wild, which is, however, not apparent under laboratory conditions. It could also be an adjustment to the very rapid development of *Drosophila* embryos which requires an efficient mobilization of maternally stored TAGs.

In conclusion, *dob* is the only paralogue of the *bmm* gene, a key regulator of chronic lipid storage in *Drosophila*. In contrast to *bmm*, *dob* is not essential for chronic TAG storage

control. However, the transcriptional upregulation under starvation and the Bmm-like TAG mobilization activity upon overexpression in the fat body suggests that *dob* is involved in acute TAG mobilization under starvation in adult *Drosophila* flies. *dob*; *bmm* double mutants outlive control flies under starvation in a way correlated to the pre-starvation TAG content (see results Fig. 17A to B). This finding clearly indicates that double mutant flies are able to mobilize their additional TAG stores implying sufficient TAG mobilizing activity in these flies. In contrast to mammalian genomes, which encode four Bmm/Nutrin family members, the *Drosophila* genome encodes only for two family members, Bmm and Dob. These data suggest that beside the members of the Bmm/Nutrin family other lipases are involved in TAG mobilization under starvation in *Drosophila*. One candidate for a non-Bmm/Nutrin TAG lipase is the putative *Drosophila* homologue of the mammalian hormone sensitive lipase, encoded by the gene *CG11055* (supplement 2).

Supplement 2: Characterization of the putative *Drosophila* Hormone sensitive lipase homologue *CG11055*

Bmm/Nutrin-like proteins constitute an evolutionary conserved group of TAG lipases. They mediate lipolysis on the surface of lipid droplet present in energy storage tissues of insects and mammals. Lack of Bmm/Nutrin protein activities in *Drosophila* results in viable, starvation hyperresistant flies (see 2.2.11) This finding forces the argument that lipases different from the two Bmm/Nutrin family members Bmm and Dob are involved in TAG mobilization of the fly.

Hormone sensitive lipase (Hsl) has been considered to catalyze the rate-limiting step in TAG mobilization in mammalian adipose tissue (reviewed in Haemmerle et al., 2003; Kraemer and Shen, 2002). Upon lipolytic stimulation, cytoplasmic Hsl translocates to the surface of lipid droplets concomitant with an increase in lipolysis (Egan et al., 1992; Clifford et al., 2000). Mice lacking Hsl activity are not obese and exhibit residual lipolysis in adipose tissue, consistent with the activity of Bmm/Nutrin-like proteins in adipocytes (Fortier et al., 2004; Okazaki et al., 2002; Osuga et al., 2000). In order to further establish the evolutionary conservation of factors mediating lipolysis on lipid droplet surfaces and to address Bmm/Nutrin-independent lipolysis in flies, a search for the *Drosophila* Hsl homologue was initiated.

S2.1 *CG11055* is the putative *Drosophila* Hormone sensitive lipase homologue

Searching protein sequence databases (NCBI, blastp on non-redundant GenBank entries) with a rat HSL protein sequence (CAA35777) identified a single 881 amino acid *Drosophila* protein with significant sequence similarity (e-value $3*e^{-71}$). This protein is encoded by the gene *CG11055* which I renamed as *dHsl.* Phylogenetic tree analysis with proteins present in *Caenorhabditis elegans*, *Anopheles gambiae*, *Apis mellifera*, *Tetraodon nigrorviridis, Rattus norvegicus, Mus musculus* and *Homo sapiens* revealed that, like *Drosophila*, the genome of these organisms code for a single Hsl protein only (Fig. S2.1A). The closest homologue of dHsl is the *Anopheles* protein XP_312370. It exhibits 62 % sequence similarity and 46 % identity with the *Drosophila* protein. Compared to the human or rodent Hsl proteins, dHsl exhibits 53 % similarity and 36 % identity of its amino acid sequence. The Hsl protein consist of an aminoterminal domain, putatively involved in protein-protein or protein-lipid interactions, and a carboxyterminal catalytic domain with a predicted α/β hydrolase fold frequently observed in lipases (Fig. S2.1B) (reviewed in Yeaman, 2004).

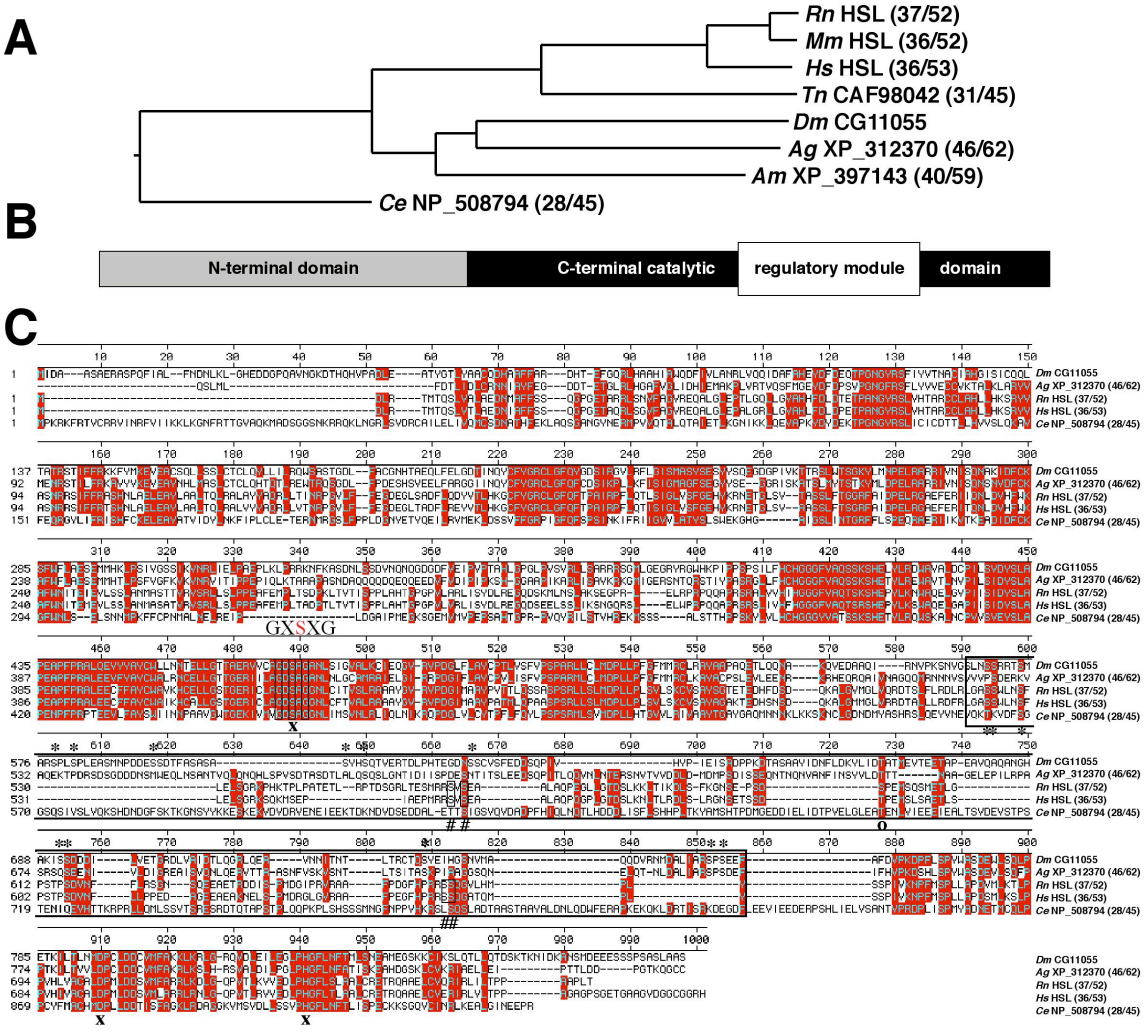

Figure S2.1: Evolutionary conservation of Hsl proteins. (**A**) Phylogenetic tree analysis of Hsl proteins from *Rattus norvegicus* (*Rn*), *Mus musculus* (*Mm*), *Homo sapiens* (*Hs*), *Tetraodon nigroviridis* (*Tn*), *Drosophila melanogaster* (*Dm*), *Anopheles gambiae* (*Ag*), *Apis mellifera* (*Am*) and *Caenorhabditis elegans* (*Ce*). Number in brackets indicate amino acid sequence identity/similarity. (**B**) Proposed Hsl domain structure consisting of an aminoterminal domain and a carboxyterminal catalytic domain containing a regulatory module. (**C**) Sequence alignment of various Hsl proteins indicating the high degree of aa conservation (shaded in red) between *Drosophila* and mammalian Hsl proteins. The catalytically active serine residue is located in a serine hydrolase motif (GXSXG) atamino acid position 473 and forms together with D794 and H834 the catalytic triad of dHSL **(x).** Phosphorylated residues within the regulatory module (box) of rat Hsl are marked with #, predicted serine phosphorylation sites in the putative dHsl regulatory module are marked by an asterisk (*). A conserved ERK phosphorylation site is indicated by **o**.

Hsl is a serine hydrolase with a catalytic triad identified by site-directed mutagenesis in the rat protein as amino acid residues S423, D703 and H723 (Holm et al., 1994). The active site serine is located in a serine hydrolase motif (GXSXG), which is conserved between *Drosophila* (S473) and mammalian Hsl proteins as are the catalytic aspartate and histidine residues (D794, H834, Fig. S2.1C). This notion suggest enzymatic TAG lipase activity which is conserved among the different insect and mammalian Hsl homologues. Enzymatic activity and translocation to lipid storage droplets of the characterized mammalian Hsl proteins are regulated by reversible phosphorylation of amino acids present within the

regulatory loop, a 150 amino acid module contained in the catalytic domain (Fig. S2.1B) (Yeaman, 2004). In the rat polypeptide, four phosphorylated serine residues were identified. One of them, S565, is phosphorylated under basal conditions (Garton et al., 1989), whereas the remaining three S563, S659 and S660 are phosphorylated under stimulated conditions by PKA (Garton et al., 1988). As compared to the catalytic residues, these regulatory amino acids are not well conserved between *Drosophila* and mammalian Hsl proteins (Fig. S2.1C). However, i*n silico* analysis of dHsl using the NetPhos 2.0 server (Blom et al., 1999) identified several putative phosphorylation sites (* in Fig S2.1C) which are positioned close to the corresponding positions of rat regulatory serine residues (# in Fig 1C). These similarities suggest that the *Drosophila* homologue is regulated by phosphorylation as well.
Phosphorylation of rat Hsl by the evolutionary conserved extracellular signal-regulated kinase (ERK) leads to an increase in enzyme activity (Greenberg et al., 2001). The ERK phosphorylation site is highly conserved between *Drosophila* (Fig. S2.1C) and mammalian Hsl (rat S600). This finding supports the proposal that dHsl is indeed regulated in a phosphorylation-dependent manner. I therefore characterized the gene with respect to a possible involvement in TAG mobilization.

S2.2 Developmental expression of *dHsl*

Developmental Northern blot analysis reveals a single *dHsl* transcript of 4 kb which is expressed during all stages of the *Drosophila* life cycle (Fig. S2.2A). Larvae express only moderate levels of *dHsl* mRNA. *dHsl* expression is upregulated during pupal development and in adult males and females with no preference for head or body. Strong *dHsl* expression is observed in embryos with an enrichment in very early stage embryos (0-3h), likely to represent a strong maternal contribution of the *dHsl* transcript. ISH on blastoderm stage embryos (Fig. S2.2B) is in accordance with the maternal expression of *dHsl* mRNA, which in later stage embryos is restricted to the embryonic digestive tract.

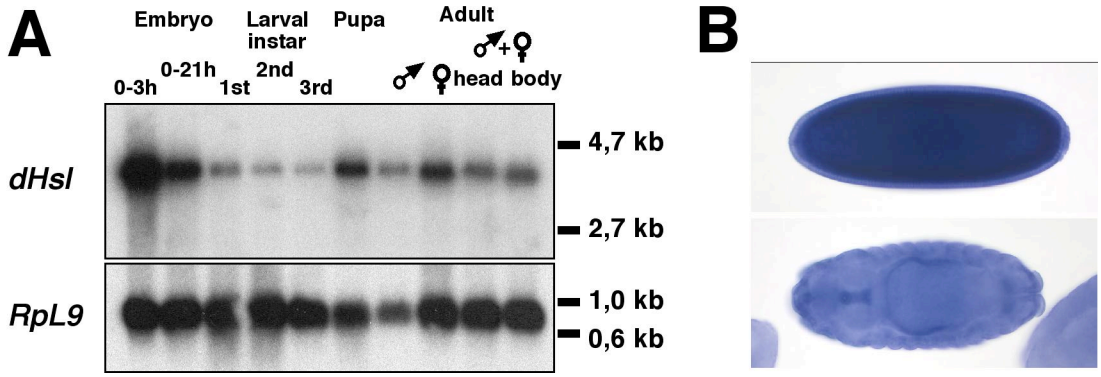

Figure S2.2: Developmental expression of *dHsl*. (**A**) Developmental Northern blot analysis reveals a single *dHsl* transcript with an estimated size of 4kb, present during all ontogenetic stages of *Drosophila*, with a strong enrichment during early embryogenesis suggesting a maternal contribution of *dHsl* mRNA. *Rpl9* expression was used as normalization control. (**B**) Ubiquitous distribution of *dHsl* transcript in blastoderm stage embryos detected by RNA antisense ISH analysis confirms the maternal contribution of *dHsl* mRNA, which in later stages is expressed in parts of the embryonic digestive tract.

S2.3 Genomic organization at the *dHsl* gene locus

The *dHsl* gene is located at the cytogenetic map position 56F11 on the right arm of the *Drosophila* second chromosome in close proximity to the *ate1* and the *mus209* genes (Fig. S2.3). Alignment between cDNA and genomic DNA sequences revealed, that the *dHsl* gene spans 4,2 kb of genomic region. The gene encodes six different exons which give rise to three transcripts (*dHsl* RA, RB and RC), differing in the 5´ UTR. However they have a common ORF of 2646 bp. The three transcripts differ only slightly in their length (RA: 3564 bp, RB 3530 bp, RC: 3623 bp, Consortium, T.F., 2003). This similar length is consistent with the single band of 4 kb that was detected in the developmental Northern blot analysis (Fig. S2.2)

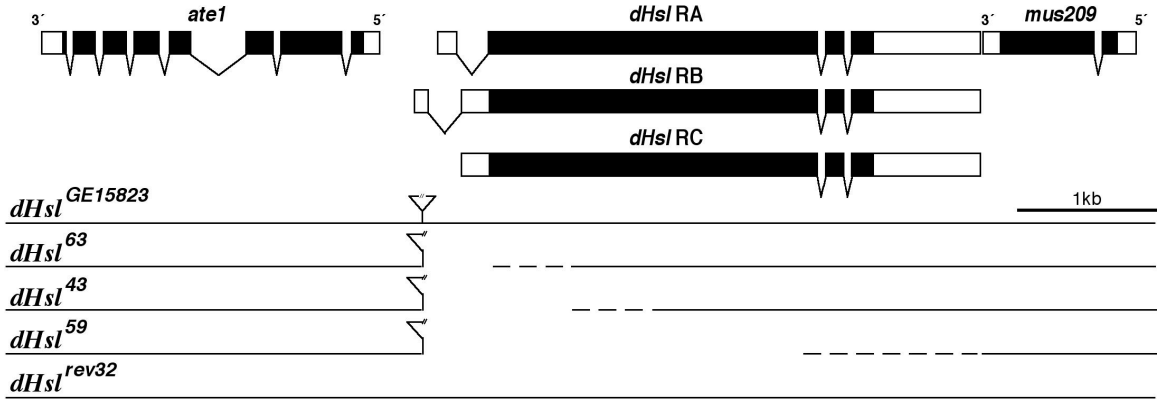

Figure S2.3: Genomic organization of the *dHsl* gene locus and *dHsl* deletion mutants. The *dHsl* gene is encoded by 6 exons that give rise to 3 different transcrips (RA, RB, RC) by differential promotor use and alternative splicing. All transcripts share the same ORF (coding regions in black, UTR in white boxes). A transposable P-element present in the 5´ UTR of the first *dHsl* exon was used to generate *dHsl* deletion mutants $dHsl^{63}$, $dHsl^{43}$, $dHsl^{59}$ as well as the precise excision control $dHsl^{rev32}$.

S2.4 Generation of *dHsl* mutants

In order to examine the *in vivo* function of *dHsl* in the context of TAG mobilization, *dHsl* mutant alleles were generated by the imprecise excision of a transposable P-element inserted in the 5´ UTR of the first *dHsl* exon ($dHsl^{GE15823}$) using a conventional P-element mobilization procedure (Ashburner, 1989). Imprecise excision events were identified using a PCR based screen and further characterized by PCR analysis (details see Material and Methods).

Three different *dHsl* mutant alleles were identified. Two small deletions ($dHsl^{63}$, $dHsl^{43}$) lack the predicted *dHsl* ATG start codon, whereas a large deletion ($dHsl^{59}$) is completely devoid of the *dHsl* coding sequence (Fig S2.3). Loss-of-function mutation of the immediate neighbour of *dHsl*, the genes *ate1* and *mus209* are lethal (Spradling et al., 1999; Henderson et al., 2000). In contrast, *dHsl* loss-of function mutants $dHsl^{63}$, $dHsl^{43}$ and $dHsl^{59}$ are homozygous viable. Thus, the deletions obtained by imprecise excision of the P-element inserted into the *dHsl* gene affect dHsl activity only. As a "genetically matched control" for physiological assays, the revertant line $dHsl^{rev32}$ was generated. It carries an intact *dHsl* genomic region. (Fig. S2.3)

S2.5 *dHsl* mutants are not fat

Immature and mature adult $dHsl^{63}$ and $dHsl^{59}$ mutants have a similar TAG content as the revertant control line $dhsl^{rev32}$ (Fig. S2.4A: $dHsl^{63}$ 1,57±0,02, $dHsl^{59}$ 1,70±0,25, $dHsl^{rev32}$ 1,60±0,09 μg TAG / μg protein in immature adult males; light grey and $dHsl^{63}$ 0,40±0,10, $dHsl^{59}$ 0,70±0,08, $dHsl^{rev32}$ 0,91±0,13 μg TAG/μg protein in mature adult males, in dark grey), indicating that *dHsl* is not essential for chronic organismal TAG storage control in *Drosophila*. In addition, the similarity of starvation survival time between $dHsl^{63}$, $dHsl^{59}$ mutants and the $dHsl^{rev32}$ control flies (Fig. S2.4 B,C) provides no evidence for a function of dHsl in starvation-induced TAG mobilization.

S2.6 Discussion

In silico analysis identified a putative *Drosophila* Hsl protein. dHsl shows high degree of conservation in catalytic relevant amino acids to mammalian Hsl homologues. This observation suggests a TAG lipase activity of dHsl. Initial analysis of flies that lack dHsl activity revealed that dHsl is not essential for the control of chronic TAG storage in *Drosophila*, consistent with the non-obese phenotype of Hsl knock-out mice (Okazaki et al., 2002; Osuga et al., 2000). However, further analyses that include the expression and

localization of dHsl in fat body cells as well as TAG mobilization upon dHsl overexpression will be necessary to establish the role of *dHsl* in TAG storage control in the fly.

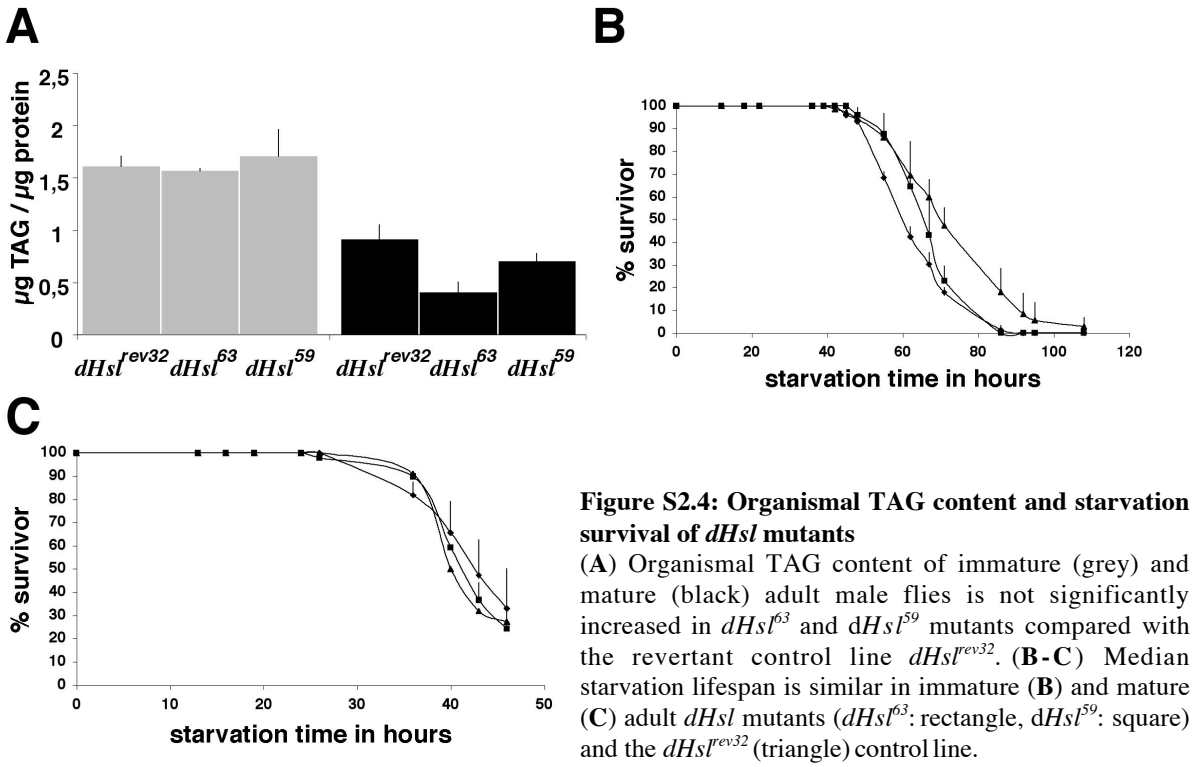

Figure S2.4: Organismal TAG content and starvation survival of *dHsl* mutants
(**A**) Organismal TAG content of immature (grey) and mature (black) adult male flies is not significantly increased in $dHsl^{63}$ and $dHsl^{59}$ mutants compared with the revertant control line $dHsl^{rev32}$. (**B-C**) Median starvation lifespan is similar in immature (**B**) and mature (**C**) adult *dHsl* mutants ($dHsl^{63}$: rectangle, $dHsl^{59}$: square) and the $dHsl^{rev32}$ (triangle) control line.

In contrast to the sterilility observed in male Hsl knock-out mice caused by oligospermia (Osuga et al., 2003), dHsl mutants are fertile and can be propagated as homozygous viable flies. However, unlike mammals, oligospermia in *Drosophila* does not result in complete sterility (Wakimoto et al., 2004). The isolation of several testis specific EST clones (Consortium 2003: AT08741, AT15816, AT27171, AT30201) suggests the expression of *dHsl* in the male germline. Future analysis of fecundity and testis morphology of *dHsl* mutant males will be necessary to address an evolutionary conserved function of Hsl during spermatogenesis.

In conclusion, the generation of a *dHsl* loss-of function mutation allows to further establish the evolutionary conservation of lipid storage droplet associated proteins, by analysing genetic interactions beween *dHsl* and mutants for *Drosophila* PAT domain proteins Lsd-1 and Lsd-2. In addition, genetic interaction between *bmm*, *dob* and *dHsl* can be used to address the degree and molecular basis for *Bmm*-independent lipolysis in the fly.

Supplement 3: Molecular characterization of the *Drosophila* PAT domain encoding gene *Lipid storage droplet-2* (*Lsd-2*)

Hydrolytic actions of TAG lipases in mammals are modulated at the lipid droplet surface by proteins of the PAT domain family, such as Perilipin (Greenberg et al., 1991). Perilipin is a lipid droplet-associated protein. It has dual function in the control of lipolysis. Under basal conditions, Perilipin acts as a barrier to Hsl and non-Hsl TAG lipases, thereby decreasing basal lipolysis and increasing organismal TAG storage (Brasaemle et al., 2000; Souza et al., 2002; Tansey et al., 2001). Upon lipolytic stimulation, Perilipin facilitates lipolysis a process mediated by TAG lipases and causes translocation of Hsl to the lipid droplet surface (Sztalryd et al., 2003). Perilipin-deficient mice are viable and fertile. However, they have a decreased amounts of organismal TAG and are resistant to diet-induced obesity. In addition, lack of Perilipin reverts the obesity of leptin receptor-deficient mice (Martinez-Botas et al., 2000; Tansey et al., 2001). Factors that mediate corresponding processes in invertebrates are unknown. In collaboration with Mathias Beller, I have characterized the function of the *Drosophila* gene *Lipid storage droplet-2* (*Lsd-2*) which encodes a PAT domain protein.

S3.1 The PAT domain protein family

The PAT domain was originally identified as a ~100 amino acid N-terminal sequence common to the mammalian proteins Perilipin, Adipocyte differentiation-related protein (ADRP, also called Adipophilin) and TIP47 (Fig. S3.1A) (Lu et al., 2001). Its function is unknown. Although its presence correlates with the ability of the mammalian proteins to localize to lipid droplets, it seems not required for the localization of the PAT domain proteins at that site (Garcia et al., 2003; McManaman et al., 2003; Targett-Adams et al., 2003). PAT domain containing proteins have been identified in a wide variety of species, including *Drosophila* and mammals, but not in the yeast *Saccharomyces cerevisiae* and the nematode *Caenorhabditis elegans* (Lu et al., 2001). Comparison of the two *Drosophila* PAT domain encoding genes *Lsd-1* and *Lsd-2*, with corresponding genes present in *Anopheles gambiae*, *Bombyx mori* and *Dictyostelium discoideum,* suggests that insect genomes code for only two PAT domain proteins (Fig. S3.1A). Based on sequence comparison, no homology can be assigned between specific mammalian and insect gene pairs. Thus, it was not obvious whether or not *Drosophila* PAT domain proteins are involved in lipid storage control and act in a Perilipin-like fashion. We therefore characterized the *Lsd-2* gene by gain-of-function and loss-of-function studies.

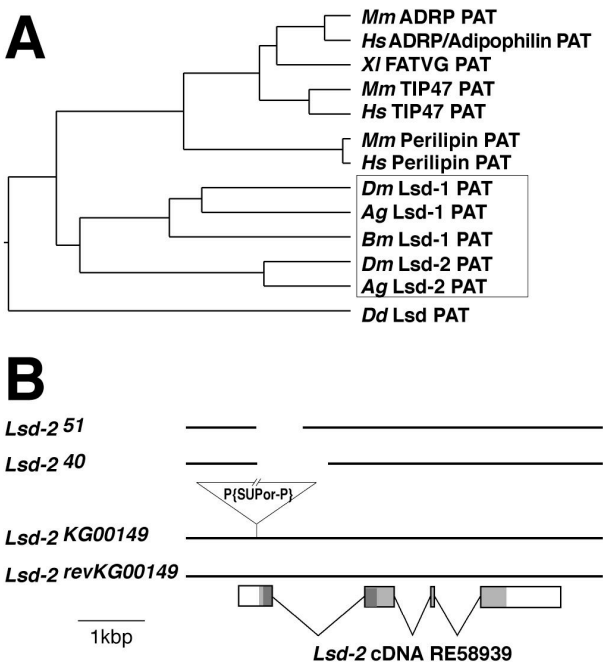

Figure S3.1: PAT domain protein family and molecular characteristics of the *Drosophila Lsd-2* gene. (**A**) Phylogenetic tree based on PAT domain amino acid sequences of selected vertebrate and invertebrate PAT domain encoding genes. Representatives of Lsd-1 and Lsd-2, the two PAT domain family members encoded by insect genomes, are contained in the box. Abbreviations: *Anopheles gambia* (*Ag*), *Bombyx mori* (*Bm*), *Dictyostelium discoideum* (*Dd*), *Drosophila melanogaster* (*Dm*), *Homo sapiens* (*Hs*), *Mus musculus* (*Mm*) and *Xenopus laevis* (*Xl*). (**B**) *Lsd-2* gene structure and gene locus of P-element integration mutant *Lsd-2*^{KG00149} and deletion mutants *Lsd-2*^{40} and *Lsd-2*^{51} compared to precise excision revertant *Lsd-2*^{revKG00149}. The *Lsd-2* ORF is indicated in light grey, and PAT domain localization is indicated in dark grey.

S3.2 Generation of *Lsd-2* mutants

The *Lsd-2* gene is located at cytogenetic map position 13 A8-9 on the *Drosophila* X-chromosome, adjacent to the *dob* gene (Fig. S3.1B, compare Fig. S1.1). Alignment of full-length *Lsd-2* cDNA (RE58939) (Rubin et al., 2000) with genomic sequence revealed that *Lsd-2* is encoded by four exons adding up to 2,2 kb in length. The 1,059 kb long *Lsd-2* ORF extends from exon 1 to exon 4.

To generate *Lsd-2* mutants a transposable P{SUPor-P}-element inserted in DNA corresponding to the 5´ untranslated leader region of the Lsd-2 transcript (*Lsd-2*^{KG00149}) (Roseman et al., 1995, Spradling et al., 1995) was used (Fig. S3.1B). Following a conventional P-element mobilization screen (Ashburner, 1989) two *Lsd-2* deletion mutants (*Lsd-2*^{51}, *Lsd-2*^{40}) as well as a "genetically matched" precise excision revertant (*Lsd-2*^{revKG00149}) were generated. Sequencing of the relevant part of the *Lsd-2* gene revealed the precise excision (*Lsd-2*^{revKG00149}) of the P-element, whereas the deletion mutants lack *Lsd-2* sequences from position –34 to +654 (*Lsd-2*^{51}) and –34 to +970 (*Lsd-2*^{40}) with respect to the predicted *Lsd-2* ATG start codon (Fig. S3.1B). The newly generated deficiencies only delete the first exon and partially the first intron of the *Lsd-2 gene*. In order to establish whether they express the protein, the expression of *Lsd-2* protein was examined by an antibody directed against bacterially produced *Lsd-2* protein (α-Lsd-2 antibody) in mutant flies, flies with the precise excision and wild-type flies. Western blot analysis with the α-Lsd-2 antibody revealed a doublet of bands with estimated molecular weights of 46 kDa and 44 kDa (Lsd-2H, Lsd-2L) in both wild-type and *Lsd-2*^{revKG00149} flies, respectively (Fig. S3.4A, for

technical details see Grönke et al., 2003). In contrast, no *Lsd-2* protein was detected in extracts from the *Lsd-2* mutants $Lsd\text{-}2^{51}$, $Lsd\text{-}2^{40}$ and the P-element line $Lsd\text{-}2^{KG00149}$. These results confirm the specificity of the α-Lsd-2 antibodies and indicate that these alleles are protein null mutants of the *Lsd-2* gene.

S3.3 Lsd-2 is expressed in the fat body of embryos and larvae

Mammalian Perilipin and ADRP were originally identified as genes that are highly expressed in adipose tissue (Greenberg et al., 1991; Jiang and Serrero, 1992). Perilipin expression is restricted to differentiated adipocytes and steroidogenic cells, whereas both ADRP and TIP47 have a broad tissue distribution (Brasaemle et al., 1997; Diaz and Pfeffer, 1998). In order to examine the spatial and temporal expression of *Lsd-2* in *Drosophila,* developmental Northern blot and RNA ISH for embryos and larval tissue were employed (Fig S.3.2).

Developmental Northern blot analysis detects a single *Lsd-2* transcript of 2,4 kb present during all stages of the *Drosophila* life cycle which is strongly enriched in early embryos (0-3 hours) (Fig. S3.2A). This enrichment reflects a maternal store of transcripts in early embryos which lasts until blastoderm stage (Fig. S3.2B-D). This pattern is consistent with a recent report showing that Lsd-2 is expressed in wild-type ovaries (Teixeira et al., 2003). Upon cellularization maternal *Lsd-2* transcripts are degraded, except in the pole cells, i.e. the germline precursor cells, where the transcript is present until midembryonic stages. During germ band retraction, *Lsd-2* is transiently expressed in the amnioserosa (Fig. S3.2F) and transcripts appear in the developing fat body (Fig. S3.2G). The fat body-expression of *Lsd-2* is sustained until late embryonic stages, where it is additionally expressed in parts of the midgut. While *Lsd-2* is only weakly expressed in first and second instar larvae (Fig. S3.2A), strong expression of *Lsd-2* is detected in the third instar larval fat body (Fig. S3.2H). In contrast to the embryo, *Lsd-2* expression is restricted to the fat body, since no expression was observed in third instar larval midgut, Malpighian tubules (Fig. S3.2I) or salivary glands (Fig. S3.2H). However, by GeneChip analysis, *Lsd-2* was found to be expressed in the larval wing disc (Butler et al., 2003), suggesting a function outside the fat storage tissue. In summary, postembryonic *Lsd-2* expression resembles the adipocyte-specific expression of Perilipin and is consistent with the proposal that *Lsd-2* is involved in organismal TAG storage control in *Drosophila.*

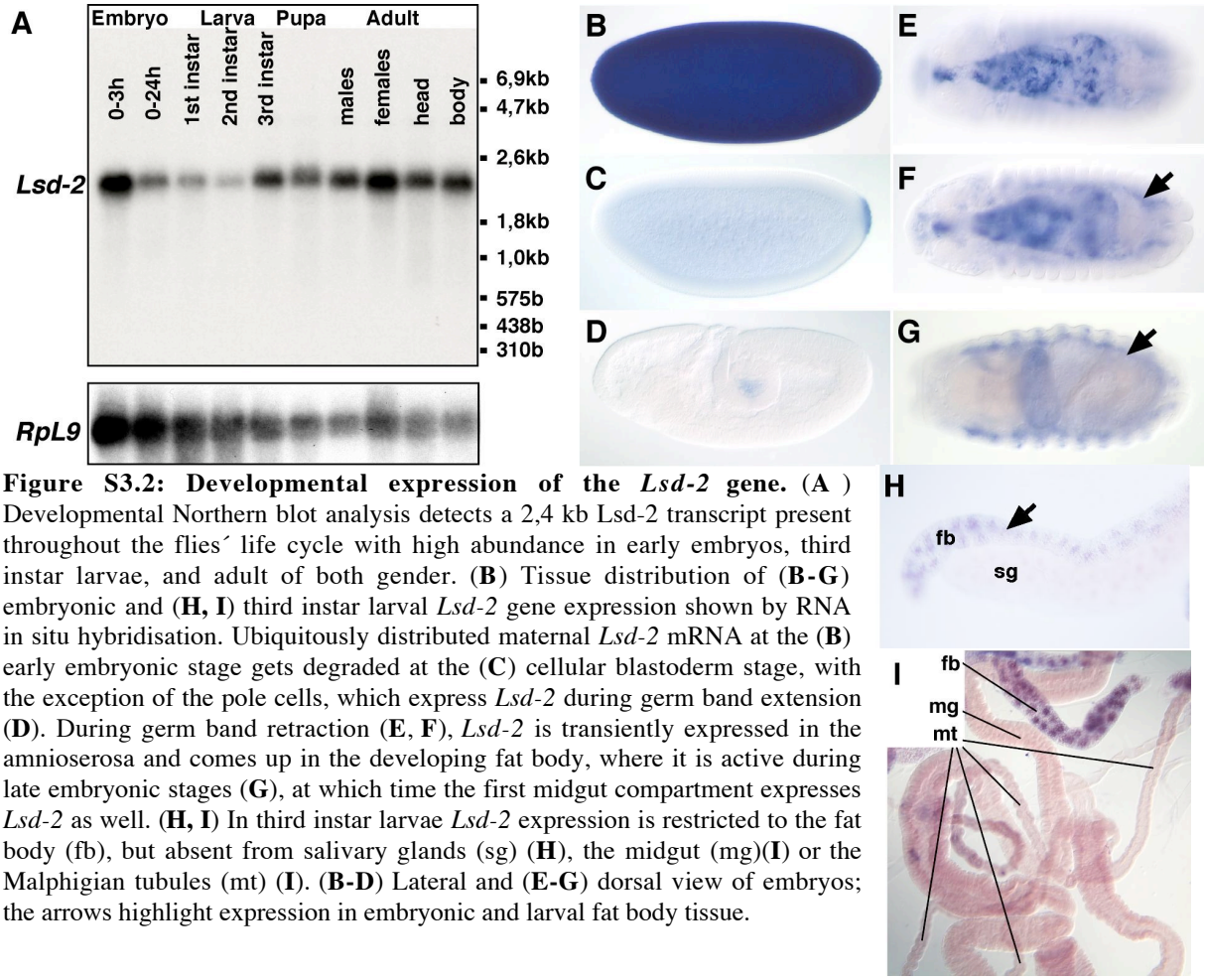

Figure S3.2: Developmental expression of the *Lsd-2* gene. (**A**) Developmental Northern blot analysis detects a 2,4 kb Lsd-2 transcript present throughout the flies´ life cycle with high abundance in early embryos, third instar larvae, and adult of both gender. (**B**) Tissue distribution of (**B-G**) embryonic and (**H, I**) third instar larval *Lsd-2* gene expression shown by RNA in situ hybridisation. Ubiquitously distributed maternal *Lsd-2* mRNA at the (**B**) early embryonic stage gets degraded at the (**C**) cellular blastoderm stage, with the exception of the pole cells, which express *Lsd-2* during germ band extension (**D**). During germ band retraction (**E**, **F**), *Lsd-2* is transiently expressed in the amnioserosa and comes up in the developing fat body, where it is active during late embryonic stages (**G**), at which time the first midgut compartment expresses *Lsd-2* as well. (**H, I**) In third instar larvae *Lsd-2* expression is restricted to the fat body (fb), but absent from salivary glands (sg) (**H**), the midgut (mg)(**I**) or the Malphigian tubules (mt) (**I**). (**B-D**) Lateral and (**E-G**) dorsal view of embryos; the arrows highlight expression in embryonic and larval fat body tissue.

S3.4 Intracellular localization of Lsd-2

To investigate the subcellular distribution of *Lsd-2* protein *in vivo*, an Lsd-2:EGFP fusion protein was expressed in fat body cells using the UAS/Gal4 system (Brand and Perrimon, 1993) in conjunction with a fat body-Gal4 driver (FB-Gal4). Fluorescent confocal microscopic analysis of *ex vivo* larval fat body cells reveals that Lsd-2:EGFP is associated with vesicular structures of various sizes (Fig. S3.3A). Purification of lipid droplets by density gradient fractionation (for technical details see Grönke et al., 2003) resulted in the detection of Lsd-2:EGFP fusion protein on the surface of isolated lipid droplets, which were identified by Nile Red staining (Fig. S3.3B).

In order to examine the localization of the endogenous Lsd-2 protein, density fractionated fat body homogenates from third instar larvae were analyzed by Western blot using the α-Lsd-2 antibody (Fig. S3.3C). Lsd-2 is strongly enriched in lipid droplet fractions and almost completely excluded from cytosolic fractions which were identified by the presence of the cytoplasmic protein eIF4A. Taken together, both ectopically expressed and endogenous Lsd-2 localizes specifically to the surface of lipid droplets. In combination with the

spatiotemporal expression patterns these results suggest that Lsd-2, like the mammalian PAT domain protein Perilipin and Bmm, is involved in TAG storage control on the surface of lipid droplets.

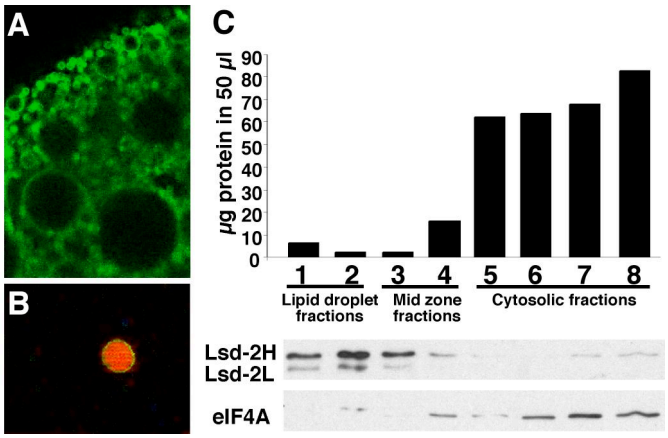

Figure S3.3: Lipid droplet association of Lsd-2 protein. (**A**) Confocal microscopic image of a third instar larval fat body cell expressing an Lsd-2:EGFP fusion protein showing association of the fusion protein with intracellular vesicles. (**B**) Epifluorescent microscopic image of an isolated lipid droplet after density gradient fractionation of larval fat body tissue described in (**A**). The Lsd-2:EGFP fusion protein is tightly associated with the lipid droplet surface. Nile red staining confirms the identity of the vesicle as a lipid storage droplet. (**C**) Western blot analysis of endogenous Lsd-2 intracellular localization in wild-type third instar larval fat body cell homogenates fractionated by density gradient centrifugation. The upper panel shows the protein concentration of density fractions. The lower panels show a strong enrichment of Lsd-2 in a lipid droplet and low-density midzone fractions detected by α-Lsd-2 antibody. Cytoplasmic fractions are identified by the presence of eIF4A. Note Lsd-2 is represented by Lsd-2H (46 kDa) and Lsd-2L (44kDa); protein loading is adjusted in Western blot samples. The weak signal in eIF4A lane 2 originates from incomplete stripping of the Lsd-2 signal.

S3.5 *Lsd-2* controls fat storage of adult *Drosophila*

Perilipin expression in preadipocyte tissue culture increases lipid storage by reducing the rate of TAG hydrolysis (Brasaemle et al., 2000). In order to test whether *Lsd-2* activity is capable of modulating TAG storage levels in a Perilipin-like fashion, *Lsd-2* was overexpressed in the fat body of adult flies using two fat body-Gal4 drivers, FB-Gal4 and Adh-Gal4, respectively, which differ in their expression level. Western blots with proteins extracted from immature adult male flies which were tested with the α-Lsd-2 antibodies show gradually increased levels of UAS-*Lsd-2* transgene-dependent Lsd-2 activity in the fat body (Fig. S3.4A). Flies moderately overexpressing Lsd-2 elevate organismal TAG storage by 28 % (Fig. S3.4A, FB-Gal4: 1,212±0,045 µg TAG/µg protein; lane 2), whereas strong overexpression causes a TAG storage increase by 48,5 % (Fig. S3.4A, Adh-Gal4: 1,402±0,089 µg TAG/µg protein; lane 3), as compared to control individuals bearing the non-induced UAS-*Lsd-2* transgene (Fig. S3.4A, 0,944±0,070 µg TAG/µg protein; lane 1). These data demonstrate that *Lsd-2* activity is sufficient to modulate organismal TAG storage in a dosage-dependent manner. To test whether Lsd-2 activity is also essential for TAG storage, the TAG content of *Lsd-2* mutant flies was examined. Compared to the genetically matched control *Lsd-2*^{revKG00149} (1,014±0,028 µg TAG/µg protein; lane 4), the organismal TAG content of immature adult male *Lsd-2*^{51} (0,663±0,067 µg TAG/µg protein; lane 5), *Lsd-2*^{40} (0,730±0,105 µg TAG/µg

protein; lane 6) and *Lsd-2*^{KG00149} (0,636±0,046 μg TAG/μg protein; lane 7) is reduced by 34,5%, 28% and 37,2%, respectively.

In order to unambiguously establish that the lack of *Lsd-2* activity in the fat body is responsible for the decreased TAG content, *Lsd-2* was expressed in the fat body of *Lsd-2* mutant flies using the UAS-*Lsd-2* transgene in conjunction with the FB-Gal4 driver. Expression of *Lsd-2* in the fat body completely reverted the lean phenotype of *Lsd-2* mutant flies (1,170±0,067 μg TAG/μg protein; lane 8), indicating that loss-of *Lsd-2* activity is the cause for the mutant phenotype. The TAG content of *Lsd-2* mutants is closely correlated to their survival time under starvation. While lean *Lsd-2* mutants have a reduced median lifespan under these conditions, flies which overexpress *Lsd-2* in the fat body and turn into fat flies, outlive control flies under starvation (Fig. S3.4B). However, in contrast to other fat mutants like *bmm* and *AKHR*, flies overexpressing *Lsd-2* are able to completely deplete their TAG stores under starvation (data not shown). In summary, these results indicate that *Lsd-2* activity can adjust TAG storage at an organismal level at times when food is accessible to ensure extended survival when food supply is limited.

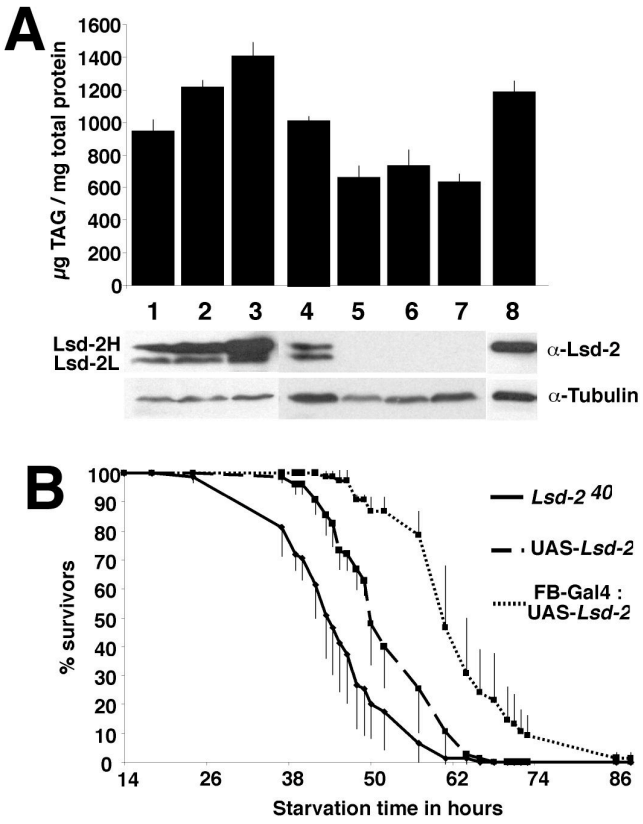

Figure S3.4: Correlation of *Lsd-2* protein amount, TAG content and survival time under starvation in male flies with *Lsd-2* gain-of-function and lack-of-function. (A) Organismal TAG content of flies correlated to their *Lsd-2* protein content shown by Western blot analysis with a-*Lsd-2* antibody (a-Tubulin was used for normalization). Lane 1-3 increasing TAG content and *Lsd-2* abundance of non-induced (lane 1), FB-Gal4-induced (lane 2) and Adh-Gal4-induced (lane 3) UAS-*Lsd-2* transgenic flies. Note: UAS-*Lsd-2* induction provides Lsd-2H only. Lane 4: normal TAG content of *Lsd-2*^{revKG00149} flies expressing endogenous *Lsd-2* levels. Lane 5-7: *Lsd-2* protein null mutants are lean (lane 5: *Lsd-2*^{51}, lane 6: *Lsd-2*^{40} and lane 7: *Lsd-2*^{KG00149}). Lane 8: reversion of *Lsd-2*^{KG00149} leanness by FB-Gal4:UAS-*Lsd-2* expression. (For details see text).

S3.6 Discussion

The fat storage tissue-specific expression as well as the localization to the lipid droplet surface of the *Drosophila* PAT domain-containing protein Lsd-2 resembles results obtained with the mammalian Lsd-2 homologue Perilipin. In addition, overexpression of Lsd-2 causes a dosage-dependent increase of TAG storage, whereas the lack of Lsd-2 results in lean flies. These findings again reminds one of the Perilipin gain-of function phenotype in preadipocyte tissue culture cells (Brasaemle et al., 2000) and the decreased organismal TAG content of Perilipin-deficient mice (Martinez-Botas et al., 2000; Tansey et al., 2001). Taken together these results suggest that Lsd-2 operates in a Perilipin-like manner by modulating the rate of lipolysis on the surface of lipid droplets. Perilipin fulfills two functions in the control of lipolysis. First, it acts as a barrier to protects TAG stores under non-stimulated conditions against TAG lipase-mediated hydrolysis (Brasaemle et al., 2000; Souza et al., 2002; Tansey et al., 2001). Secondly, upon lipolytic stimulation, Perilipin facilitates lipolysis and is essential for the translocation of Hsl to the lipid droplet surface (Sztalryd et al., 2003). Co-overexpression of Lsd-2 and the Bmm TAG lipase partially protects TAG storage against Bmm-mediated lipolysis (see Fig. 20), suggesting that Lsd-2 has a Perilipin-like barrier function. Whether Lsd-2 also facilitates lipolysis under lipolytically stimulated conditions and interacts with the *Drosophila* Hsl protein is, however, unknown.

Perilipin is a phosphoprotein (Egan et al., 1990) and phosphorylation mediated by protein kinase A (PKA) at selected PKA sites is necessary to support the translocation of Hsl to the lipid droplet surface (Sztalryd et al., 2003). Recently, it was shown that Lsd-2 is posttranslationally modified, likely by phosphorylation (Matthias Beller, personal communication). This observation suggests that Lsd-2 is involved in lipolysis under lipolytically stimulated conditions. The two Lsd-2 protein variants (Lsd-2H, Lsd-2L) detected in the Western blot analysis do probably not result from different phosphorylation or from degradation of the *Lsd-2* protein, since overexpression of the *Lsd-2* cDNA supports only the expression of the larger variant Lsd-2H. It is more likely that the two protein variants are caused by alternative splicing of *Lsd-2* exon 3, which codes for 17 amino acids corresponding to a molecular weight of 2 kDa. This assumption is consistent with the size difference between Lsd-2H (46 kDa) and Lsd-2L (44kDa). Alternative splicing has also been reported for the murine Perilipin gene (Greenberg et al., 1993; Lu et al., 2001). In adipocytes, the longer protein (Perilipin A) is the predominantly expressed form (Greenberg et al., 1993). Upon overexpression in CHO cells Perilipin A protects lipid droplets against lipolysis, whereas the shorter Perilipin variant (Perilipin B) does not have such an effect.

This finding suggests different functions of the two Perilipin variants (Tansey et al., 2002). Whether the two *Lsd-2* proteins in *Drosophila* have the same or different functions is currently unknown. The cloning of an *Lsd-2* cDNA lacking exon 3 and gain-of-function studies using this construct are necessary to address this question.

In contrast to flies that overexpress the Bmm TAG lipase, *Lsd-2* mutants have only a relative weak lean phenotype. The existence of a second PAT domain containing protein Lsd-1, suggests that it can partially substitute for Lsd-2 activity to sustain lipid storage in Lsd-2 mutants. Consistent with this proposal, immature *Lsd-2*, *Lsd-1* double mutants almost completely lack TAG stores (R. Kühnlein, personal communication). However, the function of Lsd-1 awaits a detailed analysis, since Lsd-1 single mutants have an increased rather than a decreased organismal TAG store. This can in part be explained by the upregulation of *Lsd-2* protein levels in these flies (R. Kühnlein, personal communication). The observation, that *Lsd-1* mRNA levels are downregulated upon food-deprivation suggest, however, a function of *Lsd-1* in the acute starvation response.

In summary, gain-of-function and loss-of function analyses demonstrate an essential function of the *Drosophila Lsd-2* protein in the control of organismal TAG storage at the level of lipid droplets and establish PAT domain containing proteins as evolutionary conserved mediators of TAG storage control.

Supplement 4: Linkage between circadian rhythm and energy homeostasis – an introduction

The adult *Drosophila* fly exhibits a discontinuous feeding behaviour where the uptake of food is limited to certain time periods of the day. Flies fed only during nighttime show significantly higher mortality rates compared to *ad libitum* or daytime fed controls (Oishi et al., 2004). These observations support the hypothesis that food uptake in *Drosophila* is mostly restricted to daytime. Although not experimentally shown, it is argued that the periods of food uptake correlate with periods of high locomotor activity which are observed mostly during daytime with two mayor peaks: the first after sunrise and the second late in the evening shortly before dawn. The rhythmicity of flies' locomotor activity is thought to be under the control of an endogenous oscillator, the circadian clock, and is used as read out system in the analysis of clock mutations.

The molecular core of the circadian clock consists of an autoregulatory feedback loop in which the protein products of the clock genes inhibit transcription of their own genes, resulting in rhythmic gene expression with a periodicity of about 24 hours (overview in Stanewsky 2003; Rippberger and Schibler 2001; Gachon et al., 2004). One intrinsic property of the circadian clock is, that the cycling persists even in the absence of external time cues. Since the period length is not exactly 24 h, it is synchronized (entrained) by the photoperiod (light/dark = L/D cycle) every day. Analysis of circadian clocks in various organisms revealed, that the basic principle of an autoregulatory feedback loop is evolutionary conserved and that most of essential *Drosophila* clock genes have orthologues in mammals (Gachon et al., 2004, Stanewsky, 2003).

The circadian rhythm of behavior (e.g. wheel-running activity in mice, locomotor activity in *Drosophila*) is controlled by specialized pacemaker regions within the brain, the suprachiasmatic nucleus (SCN) in the hypothalamus of mouse and human and the lateral head neurons in *Drosophila* (reviewed in Helfrich-Förster, 2004). Self-sustained circadian clocks are not restricted to central pacemaker neurons, but are working in most body cells also in peripheral tissues. In mammals the SCN contains the master circadian clock, which phase is directly light-entrained via neuronal connection with the retina. The SCN clock then synchronizes overt rhythms in physiology and behaviour likely by both synaptic transmission and humoral signals (Shibata and Tominaga 1991; Silver et al., 1996).

When food is available only for a limited period of time each day, rats increase their locomotor activity 2 to 4 hours before the onset of food availability. Such food anticipatory

behaviour induced by restricted feeding is also observed in birds and – outside the vertebrates – in insects like bees. It is often accompanied by increases in body temperature, gastrointestinal motility and activity of digestive enzymes (Mistlberger, 1994). Recently it was shown in mammals that restricted feeding can uncouple circadian oscillators in peripheral tissues from the central pacemaker in the SCN (Stokkan et al., 2001; Damiola et al., 2000). Feeding mice (i.e. nocturnal animals which normally forage only at night time) exclusively during the day completely inverses the phase of circadian oscillators in peripheral tissues (e.g. liver), but not in the SCN. These food-induced phase resetting indicates that mechanisms involved in energy homeostasis and circadian rhythm are closely linked in mammals. Restricted feeding is always associated with restricted fasting and it is currently not clear, which of the conditions is causative for the synchronization of peripheral clocks (Gachon et al., 2004). Additional evidence for a link between energy homeostasis and circadian rhythms comes from another recent observation that suggests that circadian oscillators can adapt their phase to the nutrient state (NAD^+/NADH-ratio) of the cell (Rutter et al., 2001). Although the *in vivo* relevance of this finding still has to be shown experimentally, it raises the possibility that food entrains the circadian clock by direct modulation of cellular redox state (Schibler et al., 2001).

In *Drosophila*, a link between energy homeostasis and circadian rhythm is by far not as well established as in the mammalian system. Privation of food during the day does not result in an increase of locomotor activity levels immediately before the time point of food availability. This suggests that food anticipatory behaviour is absent or at least not strong in flies (Oishi et al., 2004). In addition, nighttime-restricted feeding of flies does neither abolish the diurnal locomotor activity pattern nor does it affect the cycle of clock gene expression in peripheral tissues (Oishi et al., 2004). Thus, in peripheral organs of *Drosophila* restricted feeding is not a more potent Zeitgeber than the light-dark cycle (Oishi et al., 2004). In contrast to mammals, where only the clock of the SCN is entrainable by light, photoreceptive autonomous circadian oscillators of *Drosophila* are present throughout the body (Plautz et al., 1997), suggesting that also the clock of peripheral tissues is entrainable by light. Since experiments with restricted feeding in constant darkness (DD) conditions gave no conclusive results, because of the desynchronization of individual flies (Oishi et al., 2004), the question still remains if food-entrainable oscillators also exist in *Drosophila*.

Currently, there is only one *Drosophila* gene described, *takeout* (*to*), which could provide a molecular link between energy homeostasis and circadian rhythm in the fly (Sarov-Blat et

al., 2000). The *to* protein belongs to a family of lipophilic ligand binding proteins with unknown function, which is conserved within insects but not found in vertebrates. *to* mRNA undergoes daily cycling and is downregulated or undetectable in circadian clock mutants, suggesting it is a clock-regulated output gene (Sarov-Blat et al., 2000). In the adult fly *to* expression is found in tissues/organs that can be related to feeding and olfaction, including the crop, parts of the proventriculus, the antenna (Sarov-Blat et al., 2000) and the fat body (Dauwalder et al., 2002). *to* mRNA and protein levels are upregulated under starvation conditions. This starvation-induction is blocked in *Drosophila* clock mutants, indicating that the activation of *to* expression is dependent on the circadian clock (Sarov-Blat et al., 2000). Flies mutant for *to* have no obvious circadian locomotor activity defect when monitored under *ad libitum* fed conditions, but the mutants exhibit an aberrant starvation response by dying earlier than control flies (Sarov-Blat et al., 2000). Interestingly clock mutants per^{r01} and tim^{01} also were shown to die more rapidly under starvation (Sarov-Blat et al., 2000). However, the physiological cause of this starvation hypersensitivity is unknown. Taken together, although *to* could be a molecular link between circadian rhythm and energy homeostasis, the mechanisms how it participates in these linked activities is currently unknown.

To identify new genes that possibly link energy homeostasis and circadian rhythm, the 223 starvation responsive genes identified in this work by GeneChip analysis were compared to the 336 published circadianly cycling transcripts in adult *Drosophila* (McDonald & Rosbash 2000; Claridge-Chang et al., 2001; Lin et al., 2002; Ueda et al. 2002). From the 223 starvation responsive genes 26 were identified as cycling transcripts in at least one of the circadian cycling GeneChip analyses (Table S4.1).

Cycling genes are enriched in the starvation responsive gene set, since 12% (26 of 223) of starvation responsive genes cycle, whereas only 1-6% of the total *Drosophila* genes were found to do so (reviewed in Stanewsky, 2003). This at least two-fold enrichment of the starvation-responsive genes among the cycling genes suggests a link between circadian rhythm and energy homeostasis in *Drosophila*. However, none of the core clock genes is regulated under starvation, consistent with previous findings about Timeless and Period protein regulation under food-deprivation (Sarov-Blat et al., 2000). Sorting the 26 candidate genes in groups according to their predicted or known molecular function reveals that 20% are involved in carbohydrate metabolism, 11% in lipid metabolism and 40% have an

unknown function. One of the uncharacterized genes *Drosophila rhythmically expressed gene 2* (*Dreg-2*) was chosen for further analysis (supplement 5).

gene name / CG number	molecular function	biological process	reference
CG9886	carbohydrate kinase activity	carbohydrate metabolism	4
Sodh-1	Sorbitol dehydrogenase 1	carbohydrate metabolism	2,4
Pgm / CG5165	Phosphogluconate mutase	monosaccharide metabolism	4
CG1213	glucose transporter activity	carbohydrate metabolism; carbohydrate transport	3
CG8036	transketolase activity	pentose-phosphate shunt	4
CG1583	Phospholipase A2	lipid metabolism	3
CG8628	Acyl-CoA binding protein	cell acyl-CoA homeostasis; lipid transport	2
BcDNA:GH02901 / CG9009	long-chain-fatty-acid-CoA ligase activity	fatty acid metabolism	2,3,4
hgo / CG4779	homogentisate 1,2-dioxygenase	phenylalanine catabolism; tyrosine catabolism	2
CG11796	4-hydroxyphenylpyruvate dioxygenase activity	amino acid catabolism	1,2,4
Cyp6a20	electron transporter activity; oxidoreductase activity	steroid metabolism	2
Cyp6a17	electron transporter activity; oxidoreductase activity	steroid metabolism	4
Nmdmc	NAD-dependent methylenetetrahydrofolate dehydrogenase	10-formyltetrahydrofolate metabolism,	1
CG10237	retinal binding; tocopherol binding; carrier activity	coenzyme and prosthetic group metabolism; vitamin/cofactor transport	1,2
CG6409		GPI anchor biosynthesis	4
CG5958	retinal binding, alpha-tocopherol transport domain.	coenzyme and prosthetic group metabolism	4
CG3348	Chitin binding domain, Tachycitin,	unknown	2
CG11854	similar to *take out (to)*	unknown	2
CG7224	conserved small protein	unknown	4
CG17124	protein phosphatase inhibitor activity	unknown	3
fok / CG10746	fledgling of Klp38B	unknown	4
CG3767	Juvenile hormone-inducible protein 26 , abbreviated as Jhl-26	unknown	4
Dreg-2 / CG3200		unknown	1
CG1441	oxidoreductase activity	unknown	1,2,3,4
CG10513	similar to CG10514	unknown	2,3
CG10514	CHK (Choline kinase) smart domain	unknown	2

Table S4.1: Nutritionally and circadianly regulated genes. References: 1. Lin et al., 2002; 2. Claridge-Chang et al., 2001; 3. McDonald & Rosbash, 2000; 4. Ueda et al., 2002.

Not all previously known clock-controlled genes could be identified by the GeneChip approaches. For example, only one out of four clock-controlled genes which codes for a NAD-Kinase, that were identified by a genetic approach using a real-time luciferase reporter gene in combination with P-element mutagenesis was found in the GeneChip analyses (Stempfl et al., 2002; Claridge-Chang et al., 2001; Ueda et al., 2002). Additional, two clock controlled genes, *Dreg5* (Van Gelder and Krasnow, 1996) and *crg1* (Rouyer et al., 1997) were not identified by any of the puplished GeneChip studies, suggesting that not all rhythmically expressed genes can be identified by this approach. Therefore, the collection of starvation responsive genes was reevaluated to identify genes, whose orthologues in vertebrates have been linked to circadian rhythm. By this method the *Drosophila nocturnin* gene *CG31299* (formerly *CG4782* and *CG4796*) was identified and chosen for further analysis.

Supplement 4: Characterization of the *Drosophila nocturnin* gene

In vertebrates, *nocturnin* was first identified in the claw frog *Xenopus laevis*. It expresses a rhythmically cycling transcript, which reaches peak level in the early night and was therefore termed *nocturnin* for „night-factor“ (Green and Besharse, 1996). In the adult frog, *nocturnin* is expressed in photoreceptor cells of the retina. The frogs retina contains an endogenous circadian clock and expresses homologues of known clock genes (Cahill et al., 1991; Besharse and Iuvone, 1983). Like mRNA, Xenopus *nocturnin* protein, which localizes to the cytoplasm, exhibits rhythmic cycling (Baggs and Green, 2003). The rhythmic expression of *nocturnin* is conserved in *Xenopus* and mouse, where *nocturnin* is expressed at different levels in various tissues including the SCN, heart, kidney, liver and retina (Dupressoir et al., 1999; Wang et al., 2001). Recent *in vitro* studies revealed a deadenylase function of the *Xenopus* Nocturnin protein (see below), which together with the cycling expression in clock-containing cells led to the proposal that *nocturnin* could be involved in post-transcriptional regulation of the circadian clock or its output pathways (Baggs and Green, 2003). However, its *in vivo* function in vertebrates is unknown. In *Drosophila*, *nocturnin* was identified as a starvation-induced gene by comparative transcriptome analysis (see supplemental Fig. 1), suggesting that *nocturnin* is involved in the starvation response of the adult fly. The generation of *nocturnin* mutants presented in this work allows to disclose a potential *in vivo* function of the *Drosophila nocturnin* gene with respect to circadian rhythm and energy homeostasis.

S4.1 Nocturnin is an evolutionary conserved putative deadenylase

In *Drosophila,* three different Nocturnin proteins can be predicted based on cDNA sequences: two small proteins Nocturnin SG260 (UniProt:Q9VGS4 + exon 7) and Nocturnin SG259 (UniProt:Q8MTZ6) with a size of 447 (49,9kDa) and 450 (50,3 kDa) amino acids respectively and a long 642 (71,8 kDa) amino acid protein Nocturnin SG258 (UniProt:Q9VGS5 + exon 7) (Fig. S4.1A). The three putative *Drosophila* Nocturnin proteins share an evolutionary conserved carboxyterminal part but differ in their variable aminoterminal regions. The function of the 222 amino acid long aminoterminal part of Nocturnin SG258 is unknown and seems to be restricted to flies since no sequence homology to other proteins or known domains could be identified. Even within insects, it is not conserved. The corresponding sequences were found in the *Drosophila melanogaster* and the

Drosophila pseudoobscura genomes but not in the genomes of other insects such as *Anopheles gambiae* or *Apis melifera* (data not shown).

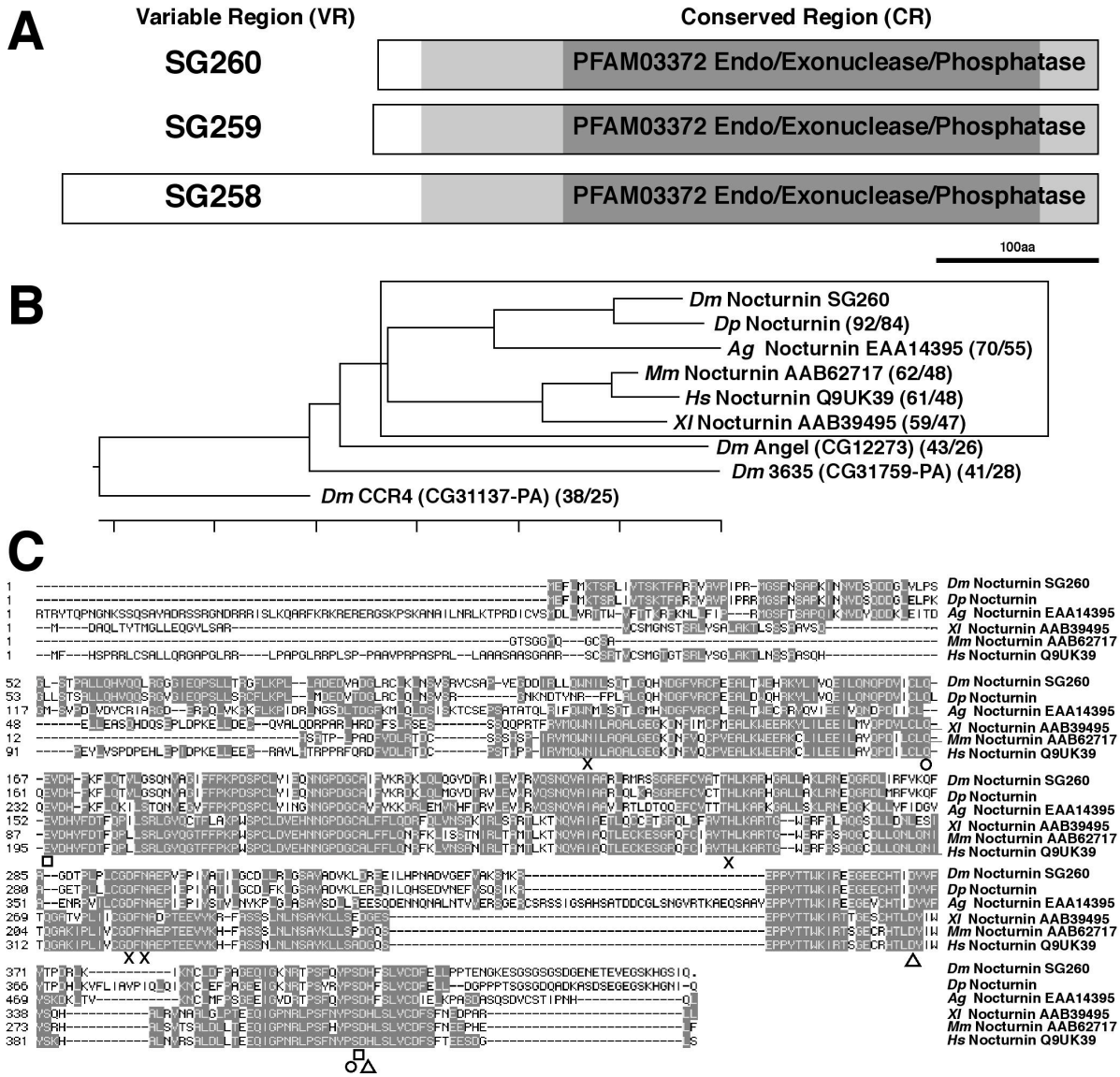

Figure S4.1: Nocturnin is an evolutionary conserved putative deadenylase. (**A**) Structure of *Drosophila* Nocturnin proteins. The three predicted Nocturnin proteins SG258 (642 aa), SG259 (450 aa) and SG260 (447aa) all possess a carboxyterminal Mg^{2+}-dependent endonuclease-like catalytic domain (PFAM03372), characteristic for yCCR4-related proteins but differ in their aminoterminus. The function of the 222 amino acid long aminoterminal part of Nocturnin SG258 is not know as it shows no homology to other proteins or protein domains. (**B**) Sequence similarity tree based on amino acid sequences of selected Nocturnin proteins from invertebrates and vertebrates (Nocturnin family boxed) and *Drosophila* orthologues of yCCR-related proteins CCR4, Angel, 3635. (**C**) Sequence alignment of the Nocturnin protein family (box in **3B**, conserved amino acids are shaded in grey). Amino acids involved in the catalytic function of Nocturnin protein are highly conserved among vertebrates and invertebrates. Important residues involved in the Mg^{2+}-dependent endonuclease are indicated as follows: **Δ** for catalytic residue, **o** for residues involved in orientation and stabilization of catalytic residues, **x** for phosphate binding and □ for Mg^{2+} binding residues (modified after Dupressoir et al., 2001).

Within the evolutionary conserved carboxyterminal region Nocturnin contains an Mg^{2+}-dependent endonuclease-like catalytic domain (PFAM03372), with sequence homology to

the yeast Carbon Catabolite Repressor 4 (yCCR4) protein (Fig. S4.1A). The yCCR4 protein was originally identified as a transcriptional coactivator and in addition, it was shown to be a catalytic subunit of the mayor yeast cytoplasmic deadenylase complex (Chen et al., 2002). *In silico* analysis led to the identification of additional yCCR4-like proteins which together form the yCCR4-related protein superfamily. It consists of 4 distinct protein families, which are the Nocturnin, 3653, Angel and CCR4 families (Dupressoir et al., 2001).

In *Drosophila,* single homologues of all four CCR4-related families have been identified. Phylogenetic tree analysis demonstrate that *Drosophila* Nocturnin is more closely related to Nocturnin proteins from *Xenopus*, mice or humans than to *Drosophila* orthologues of the yCCR4 related proteins Angel, Ccr4 and 3635 (Fig. S4.1B). This relationship suggests that *CG31299* encodes a *bona fide Drosophila* Nocturnin orthologue. Nothing is known about the function of the Angel or the 3635 proteins, but *Drosophila* CCR4 was recently found to be involved in general and regulated mRNA deadenylation. *CCR4* mutants are homozygous viable but show elongated bulk poly(A) mRNA and defects in Hsp70 mRNA deadenylation (Temme et al., 2004). Yeast and human CCR4 proteins display poly(A)-degrading nuclease activity *in vitro* and *Drosophila* CCR4 was copurified with deadenylase activity from Schneider cell extracts, indicating that the enzymatic deadenylation activity is conserved from yeast to *Drosophila* and humans (Temme et al., 2004). In addition, the *Xenopus* Nocturnin protein was shown to exhibit poly(A)-specific Mg^{2+}-dependent exonuclease activity *in vitro* (Baggs and Green 2003), suggesting that the deadenylase activity is conserved between all yCCR4-related protein families.

Sequence alignment of selected Nocturnin protein family members from invertebrates and vertebrates demonstrates the high conservation of amino acid residues involved in their catalytic function (Fig. S4.1C) (Dlakic, 2000; Dupressoir et al., 2001). In addition to amino acid residues of the catalytic center, residues important for Mg^{2+}- and phosphate binding as well as amino acid residues necessary for orientation and stabilization of catalytic residues are invariable between Nocturnin homologues from the different species (Fig. S4.1C). The high degree of conservation among essential catalytic residues suggests that the *Drosophila* Nocturnin protein, like the *Xenopus* homologue, exhibits deadenylase activity.

S4.2 Genomic organization of the *nocturnin* gene region

The *nocturnin* (*CG31299*) gene is located at the cytogenetic map position 86D7 on the right arm of the *Drosophila* third chromosome. To determine the exon/intron organization of the *nocturnin* gene, cDNAs were amplified from wild-type embryonic cDNA (0-22h),

sequenced and aligned to genomic (AE003690) and existing EST (GH03334, RE65127) sequences (for details see Material and Methods). This comparison showed that the *nocturnin* gene is encoded by 10 exons that give rise to at least three different *nocturnin* transcripts by alternative splicing and differential promoter use. I designated them *nocturnin SG258*, *nocturnin SG259* and *nocturnin SG260* (Fig. S4.2A). *nocturnin SG259*, which corresponds to the EST clone RE65127, starts at the putative *nocturnin* promoter 1 (P1) and contains 8 exons (exons 1, 3, 4, and 6-10) adding up to a length of 1,949 kb. The 1,860 kb long transcript *nocturnin SG260* represents an alternative splice form of *nocturnin SG259* and differs from it only in the absence of exon 4. *nocturnin SG258*, which corresponds to the cDNA GH03334, is transcribed from promoter 2 (P2). It contains 6 exons (exons 2, and 6-10) and has a length of 1,866 kb. The existence of exon 5 is still questionable, because it could only be found in cDNAs obtained from *curled* mutant alleles but not yet from wild-type (see S4.8). Exons 6-10 are shared between all identified *nocturnin* transcripts and represent the evolutionary conserved part of the *nocturnin* gene.

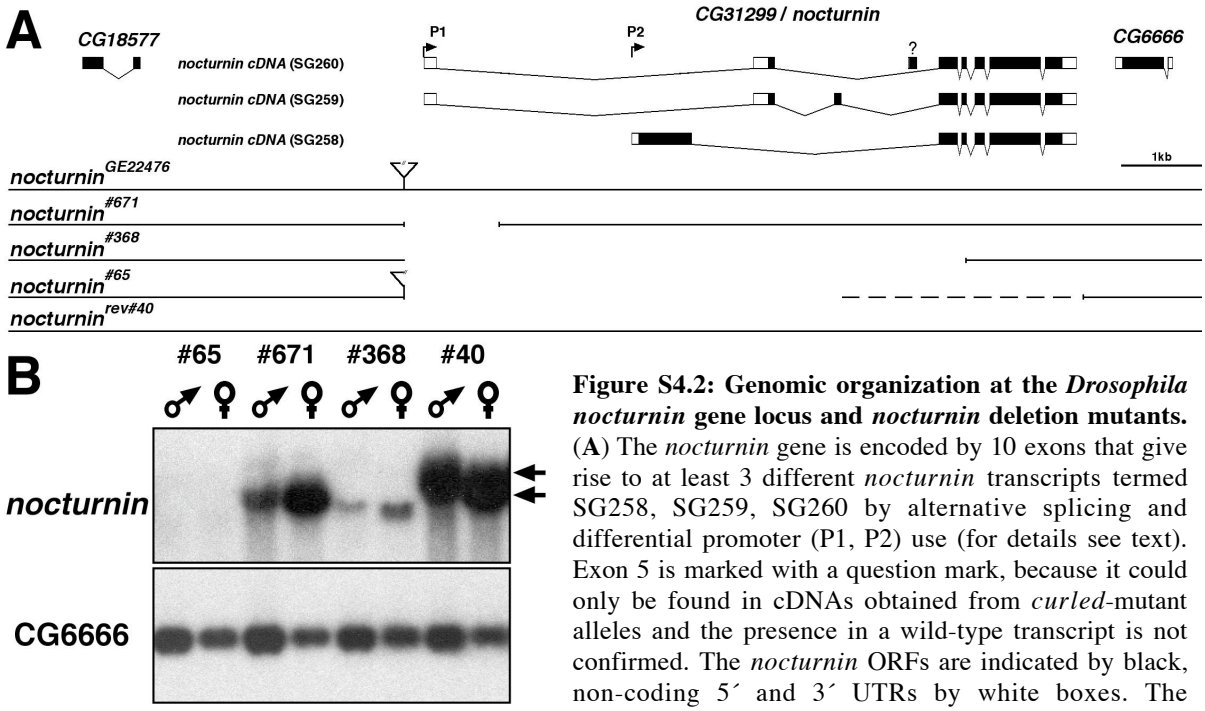

Figure S4.2: Genomic organization at the *Drosophila nocturnin* gene locus and *nocturnin* deletion mutants. (**A**) The *nocturnin* gene is encoded by 10 exons that give rise to at least 3 different *nocturnin* transcripts termed SG258, SG259, SG260 by alternative splicing and differential promoter (P1, P2) use (for details see text). Exon 5 is marked with a question mark, because it could only be found in cDNAs obtained from *curled*-mutant alleles and the presence in a wild-type transcript is not confirmed. The *nocturnin* ORFs are indicated by black, non-coding 5´ and 3´ UTRs by white boxes. The integration site of P-element GE22476 used to generate *nocturnin* deletion mutants in the 5´-region upstream of P1 is indicated by an inverted triangle. Below the gene locus organization of *nocturnin* deletion mutants is shown: *nocturnin*$^{\#671}$ belongs to class I events of small deletions, *nocturnin*$^{\#368}$ and *nocturnin*$^{\#65}$ fall into class II events of big deletions. The hatched line in *nocturnin*$^{\#65}$ indicates the genomic region in which the 3´-breakpoint is expected. *nocturnin*$^{rev\#40}$ is a precise excision revertant that serves as a genetically matched control (for details see text). (**B**) Northern blot analysis identifies *nocturnin*$^{\#65}$ as transcript null mutation. *nocturnin*$^{\#671}$ specifically lacks only the long *nocturnin* transcript (upper arrow), nocturnin$^{\#368}$ shows only a very weak band slightly shorter than the wild-type lower band, *nocturnin*$^{rev\#40}$ precise excision control shows two distinguishable *nocturnin* bands (arrows) as seen in wild-type (compare developmental Northern blot Fig. S4.3). Expression of the transcript of the immediate neighbour gene *CG6666* is not affected in *nocturnin* mutants.

S4.3 Generation of *nocturnin* mutants

Flies of the fly line *nocturnin*^{GE22476} carry an P{EP} insertion in the 5´ upstream region of the *nocturnin* gene at position –2,956 kb relative to the predicted ATG startcodon in exon 2 (Fig. S4.2A). To generate *nocturnin* mutant alleles, a conventional P-element mobilization scheme was employed using the *nocturnin*^{GE22476} allele (Ashburner, 1989). Deletions in the *nocturnin* genomic region caused by the imprecise mobilization of the GE22476 P-element were identified using a PCR-based screen and further characterized by means of PCR analysis and sequencing (for details see Material and Methods). Deletion mutants can be grouped in two classes: class I (11 cases) represent small deletions, leaving exon 2 unaffected; class II (2 cases) are large deletions including exon 2.

Deletion mutant *nocturnin*$^{\#671}$ is an example for a class I mutation (Fig. S4.2A). It lacks sequences from –2916 to –1729 relative to the predicted ATG startcodon in exon 2. This 1,187 kb deletion removes the putative promoter P1 as well as exon 1, but neither the P2 promoter nor exon 2. Therefore, it is likely to affect only transcripts starting at the P1 promoter. Class II deletion mutant *nocturnin*$^{\#368}$ lacks sequences from –2953 to +4119 relative to the putative ATG startcodon in exon 2 (Fig. S4.2A). In this 7,072 kb deletion, both the putative promoters and the predicted ATG startcodons were removed. The second class II deletion mutant, *nocturnin*$^{\#65}$, includes residual P-element sequences and could not be mapped at the sequence level. PCR analysis allowed, however, to map the 3´ breakpoint of the deletion between exon 4 and exon 10 (hatched line in Fig. S4.2A). Furthermore, Northern blot analysis suggests that the breakpoint is located 3´ of the *nocturnin*$^{\#368}$ breakpoint (see below). The allele *nocturnin*$^{\#40}$ is a precise excision of the P-element, that contains *nocturnin* wild-type sequence and serves as a "genetically matched" control.

The influence of the generated deletions on the expression of the *nocturnin* gene was examined by Northern blot analysis using a probe that is complementary to the shared 3´ part of the *nocturnin* gene. In adult *nocturnin*$^{rev\#40}$ flies two transcripts are detected (arrows in Fig. S4.2B) as observed with wild-type flies (compare Fig. S4.3A). In the class I mutant *nocturnin*$^{\#671}$, only the lower band is detected. This suggests that the longer band in wild-type flies corresponds to *nocturnin SG259* and *nocturnin SG260* starting at P1, whereas the shorter band corresponds to *nocturnin SG258* starting at P2. In the class II deletion mutant *nocturnin*$^{\#368}$, only a very weak band can be detected. It is also slightly shorter than any of the wild-type bands. The existence of residual transcript in *nocturnin*$^{\#368}$ mutants is surprising, because both putative promoter elements are deleted. Thus, it might be the result of a deletion-caused rearrangement of residual promoter elements driving expression of a

shortened *nocturnin* transcript at low levels. This transcript contains only a shortened ORF, which codes for the last 224 amino acids of the Nocturnin protein and lacks amino acids essential for the catalytic activity. Thus, *nocturnin*$^{\#368}$ is likely to be a loss-of-function allele, whereas *nocturnin*$^{\#65}$ is a transcript null mutation since it lacks detectable transcript expression as revealed by Northern blot analysis (Fig S4.2B). In order to test whether the generated deletions only affect the expression of the *nocturnin* gene and not also the expression of the neighbouring genes, I also examined the expression of the immediate neighbour gene *CG6666* in *nocturnin* deletion mutants using Northern blot analysis (Fig. S4.2B). No differences in *CG6666* expression were observed between *nocturnin* deletion mutants and the control *nocturnin*$^{rev\#40}$, indicating that the generated mutations are specific for the *nocturnin* gene.

S4.4 Expression analysis of the *nocturnin* gene

nocturnin is expressed during all stages of the *Drosophila* life cycle. Developmental Northern blot analysis detects two distinguishable *nocturnin* transcripts with estimated lengths of 1,8 kb and 2,0kb (Fig. S4.3A), whereby the shorter band corresponds to *nocturnin SG258* and the longer band to *nocturnin SG259* and *nocturnin SG260* (see above). In early embryos (0-3h) only *nocturnin SG258* is expressed suggesting a maternal contribution of this transcript. In later stages the longer transcripts *nocturnin SG259* and *nocturnin SG260* are the predominant mRNA species and are strongly expressed in third instar larvae and adult flies of both gender.

Whole-mount *in situ* hybridisation not discriminating between the different *nocturnin* transcripts, reveals a tissue specific expression of the *nocturnin* gene in the embryo and third instar larvae (S4.3B-E). In embryos (stage 16) *nocturnin* is heavily enriched in the salivary gland (sg), the proventriculus (pr) and the ring gland (rg) (Fig. S4.3B). In third instar larvae *nocturnin* expression is restricted to the proventriculus and the ring gland (Fig. S4.3C). *nocturnin* expression was not detected in third instar larval imaginal discs, brain, fat body or salivary glands (data not shown). No hybridisation signal was detected in *nocturnin*$^{\#65}$ mutant third instar larvae (Fig. S4.3D, E), which demonstrates the specificity of the *in situ* hybridisation signal. In conclusion, *nocturnin* is specifically expressed in the ring gland and the proventriculus. These sites of expression are consistent with a function of *nocturnin* in the regulation of energy homeostasis in the fly.

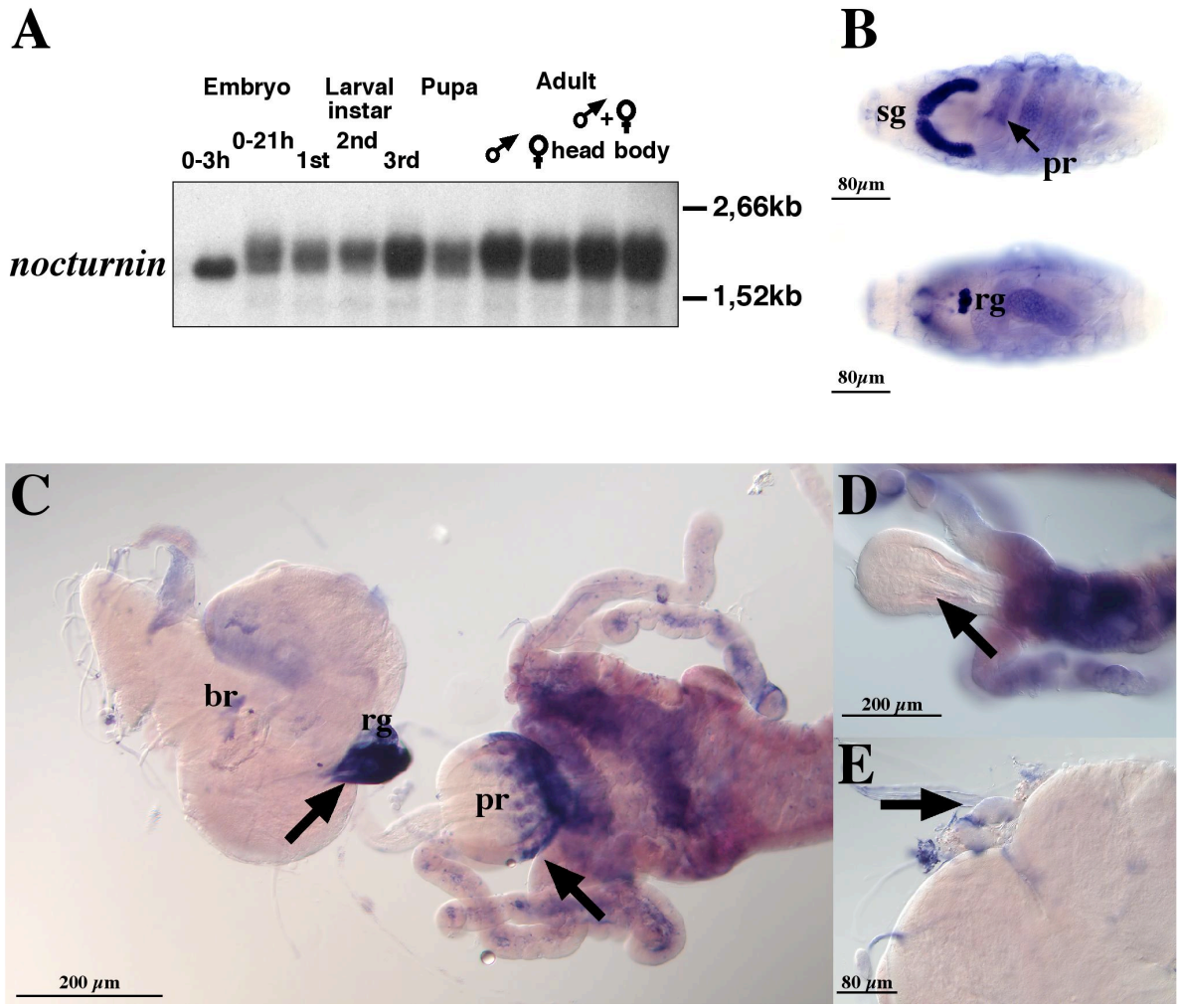

Figure S4.3: Developmental expression of the *nocturnin* gene. (**A**) Developmental Northern blot analysis detects two distinguishable *nocturnin* transcripts with estimated lengths of 1,8 kb and 2,0 kb present throughout the fly´s life cycle. (**B-C**) Tissue-specific expression of *nocturnin* transcripts in the embryo (**B**) and third instar larvae (**C**) shown by RNA *in situ* hybridisation directed against all *nocturnin* transcripts. (**B**) *nocturnin* is expressed in the embryonic salivary gland (sg), proventriculus (pr) and ring gland (rg). (**B**, dorsal view of embryos). (**C**) In third instar larvae *nocturnin* expression is restricted to the ring gland and the proventriculus. (**D, E**) no *nocturnin* hybridisation signal is detected in *nocturnin*$^{\#65}$ mutant third instar larvae proventriculus (**D**) or ring gland (**E**).

S4.5 Nutritional regulation of *nocturnin* transcription

nocturnin was initially identified in a GeneChip analysis comparing the transcriptome profile of starved and *ad libitum* fed adult flies as a gene upregulated under starvation conditions (supplement file 1). Quantitative Northern blot analysis confirms the starvation-induced increase of *nocturnin* mRNA (Fig. S4.4A). *nocturnin* expression is upregulated by 2,4-, 1,3- and 2,2- fold in flies starved for 6, 18 and 24 hours, respectively (Fig. S4.4B). However, in contrast to the GeneChip experiment, no upregulation was detected in the quantitative Northern blot after 12 hours of starvation. The starvation induction is specific for the adult stage, since no *nocturnin* induction could be observed in starved larvae (Zinke et al., 2002). Treatment of flies with paraquat, a free-radical generator inducing oxidative stress, does not

lead to an upregulation of *nocturnin* mRNA (Zou et al., 2000). Thus, the transcriptional regulation response to external cues is specific for starvation and not a general stress response.

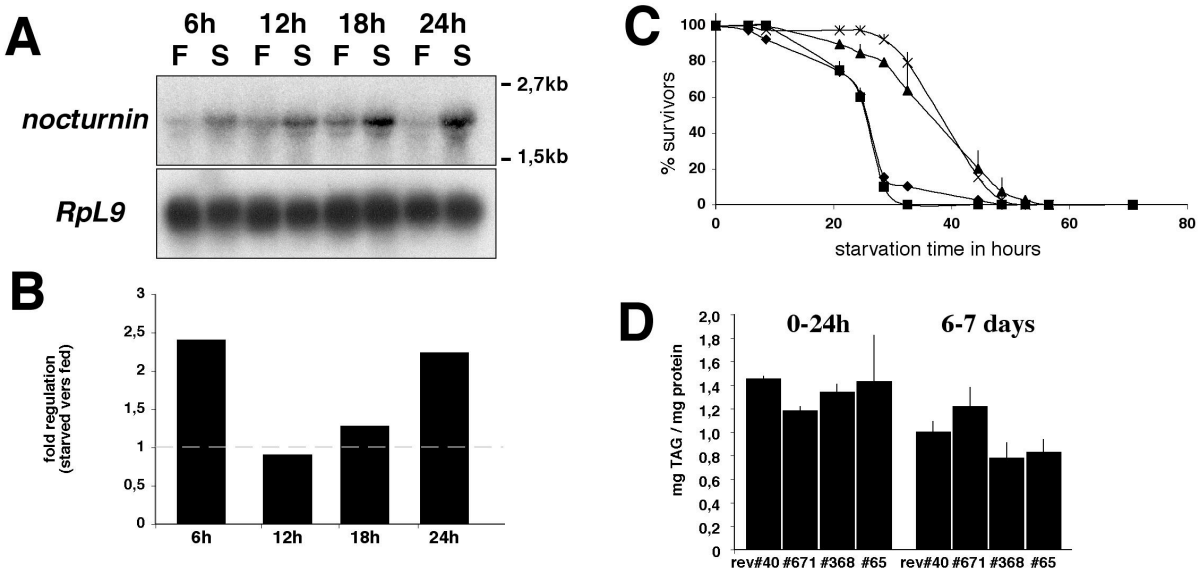

Figure S4.4: Nutritional regulation of *nocturnin* transcript, starvation survival time and Triacylglycerol content of *nocturnin* mutant flies. (**A-B**) Nutritional regulation of *nocturnin* gene expression. Quantitative Northern blot analysis confirms GeneChip data by detecting upregulation of *nocturnin* transcript abundance in flies starved (S) for 6, 18 and 24 hours compared to fed (F) controls. (**C, D**) Starvation monitoring and TAG content determination of *nocturnin* mutant flies *nocturnin*$^{\#65}$ (rhombus), *nocturnin*$^{\#368}$ (*nocturnin*$^{\#671}$ (x) compared to genetically matched control *nocturnin*$^{rev\#40}$ (Δ). (**C**) 6-7 days old adult male flies of *nocturnin* class II mutants' *nocturnin*$^{\#65}$ and *nocturnin*$^{\#368}$ are starvation hypersensitive with a reduction in median lifespan of 35 % compared to the control *nocturnin*$^{rev\#40}$. The starvation hypersensitivity phenotype of *nocturnin*$^{\#65}$ and *nocturnin*$^{\#368}$ mutants was also frequently observed in newly emerged as well as in females flies (data not shown). (**D**) Organismal TAG content is not significantly altered in immature (0-24h) as well as mature (6-7 days) adult male *nocturnin* mutant flies.

S4.6 *nocturnin* mutants are starvation sensitive but have a normal TAG content

The nutritional regulation of *nocturnin* expression suggests that its activity is involved in the starvation response of adult *Drosophila* flies. This proposal was tested by analysing the performance of *nocturnin* mutants under starvation. *nocturnin*$^{\#65}$ and *nocturnin*$^{\#368}$ mature adult males die more rapidly under starvation than *nocturnin*$^{rev\#40}$ control males, exhibiting a 35 % reduction in median lifespan (Fig. S4.4C). No decrease in survival time was observed in males of the hypomorphic *nocturnin*$^{\#671}$ allele. The starvation sensitivity phenotype of *nocturnin*$^{\#65}$ and *nocturnin*$^{\#368}$ mutants was also observed in some experiments with immature adults and female flies, but the result was not consistent in all experiments performed (data not shown).

Starvation survival time is often positively correlated with the TAG content of flies prior to starvation, which has been demonstrated for natural occuring TAG store variants (Harshman et al., 1999; Service et al., 1987) as well as for starvation responsive genes like *bmm* (2.2.10)

or *Lsd-1* (R. Kühnlein, personal communication). In contrast, *ad libitum* fed *nocturnin* deletion mutants have a similar TAG content as *nocturnin* wild-type flies (Fig. S4.4D). Immature (0-24h) and mature (6-7 days) adult male *nocturnin*$^{\#65}$ flies (1428±393/830±107) as well as mutant flies *nocturnin*$^{\#368}$ (1341±64/779±132) and *nocturnin*$^{\#671}$ (1180±35/1218±163) show a similar TAG content like the control *nocturnin*$^{\#rev40}$ (1451±22/999±9). These observation suggests that *nocturnin* is not involved in the chronic regulation of TAG storage in the fly.

S4.7 *nocturnin* mutants exhibit normal locomotor activity behaviour

Xenopus and mouse Nocturnin proteins are rhythmically expressed deadenylases present in clock containing cells (Baggs and Green, 2003; Green and Besharse, 1996; Wang et al., 2001; Barbot et al., 2002). Since deadenylation regulates mRNA decay and/or translational silencing, the authors speculate that vertebrate Nocturnin deadenylates clock-related transcripts and thus Nocturnin activity is likely to be involved in the post-transcriptional regulation of the circadian clock or its output pathways (Baggs and Green, 2003).

In *Drosophila*, locomotor activity is thought to be under the control of the circadian clock and is used as read out system in the analysis of clock mutations (Stanewsky, 2003). In order to examine whether *nocturnin* is involved in circadian rhythm control of *Drosophila*, the locomotor activity of *nocturnin*$^{\#65}$ mutants was compared to *nocturnin*$^{rev\#40}$ controls (Fig. S4.5A-D) (collaboration with Dr. Ralph Stanewsky, University Regensburg).

Ad libitum fed *nocturnin*$^{\#65}$ flies kept in 12 hour light, 12 hour dark (12h L/D) conditions exhibit locomotor activity patterns similar to that of *nocturnin*$^{rev\#40}$ control flies (compare Fig. S4.5 B-A). The pattern shows two mayor activity peaks, the first is found after lights-on and the second before the lights-off change. An intrinsic property of the circadian clock is that cycling of gene expression persists even in the absence of external time cues like the light on/off changes. Accordingly, locomotor activity of *nocturnin*$^{\#65}$ mutant flies is still rhythmic although with a lower amplitude, after seven days in constant darkness (Fig. S4.4B). Thus *nocturnin* function is not essential for normal locomotor activity behaviour of *Drosophila* flies kept under standard conditions such as *ad libitum* feeding, constant temperature (25°C) and constant humidity. Under starvation conditions *nocturnin*$^{rev\#40}$ flies display prolonged hyperactivity prior to death (Fig. S4.5C) as has been observed with wild-type flies (Lee and Park, 2004) probably reflecting food-seeking behaviour. *nocturnin*$^{\#65}$ mutant flies die earlier under starvation (Fig. S4.5D), but exhibit locomotor hyperactivity prior to death (Fig. S4.5C).

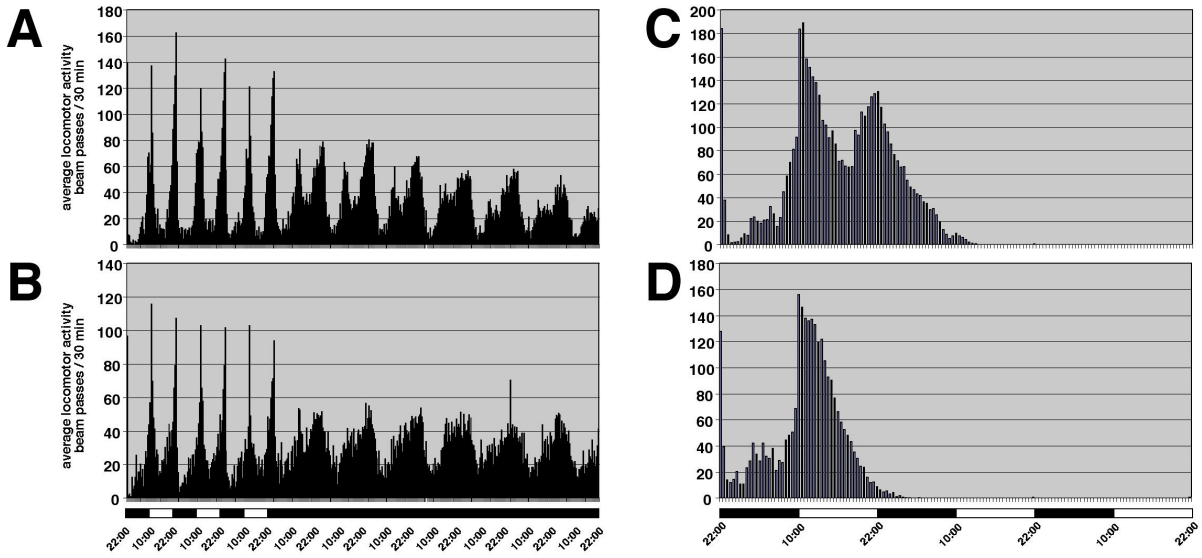

Figure S4.5: Locomotor activity of *nocturnin* mutants under *ad libitum* fed and starvation conditions. (**A**) Average locomotor activity of *ad libitum* fed *nocturnin*$^{\#40}$ males (n=27) compared to (**B**) *nocturnin*$^{\#65}$ mutant males (n=23). Flies were analyzed for the first three days under a 12h light, 12 h dark cycle (12h LD) and were then exposed to constant darkness for the remaining 7 days of the experiment (light phase indicated by bar below lower panel: open bars display lights-on time, filled bars display lights-off time). *nocturnin*$^{\#65}$ mutants show no obvious differences in circadian activity behaviour compared to the *nocturnin*$^{rev\#40}$ control. *nocturnin*$^{\#65}$ mutant exhibit a normal bimodal activity pattern with an activity peak in the early morning and late evening, which persists under constant darkness conditions although with lower amplitude. (**C**) Average locomotor activity of *nocturnin*$^{rev\#40}$ males under starvation (n=32) in comparison with (**D**) *nocturnin*$^{\#65}$ mutant flies (n=20). *nocturnin*$^{\#65}$ males die more rapidly under starvation, but show similar hyperactivity behaviour prior to death as the control.

In conclusion, there is no evidence that *nocturnin* activity participates in the circadian rhythm control of *Drosophila* at the level of locomotor activity. Consistent with this results, there is no evidence for a cycling of the *Drosophila nocturnin* mRNA as it has been shown for the vertebrate homologues (Green and Besharse, 1996; Wang et al., 2001; Barbot et al., 2002). Furthermore, *nocturnin* was not identified as a cycling transcript in any of the four genome-wide GeneChip approaches (McDonald & Rosbash 2000; Claridge-Chang et al., 2001, Lin et al., 2002; Ueda et al. 2002) and in a preliminary quantitative Northern blot analysis using the mRNA of total *Drosophila* males (data not shown). Taken together, these results argue against a function of *nocturnin* in the posttranscriptional regulation of the circadian clock in *Drosophila*.

S4.8 *nocturnin* is *curled*

The two class II deletion alleles *nocturnin*$^{\#65}$ and *nocturnin*$^{\#368}$ both exhibit a recessive wing phenotype, in which the wings are curved upwards. (Fig. S4.6D). This phenotype is specific for the two *nocturnin* null alleles. It was neither detected in any of the eleven class I deletion mutants, nor in flies of the remaining 687 P-element mobilization events that were

characterized in the screen. I therefore concluded that the phenotype is specifically linked to class II deletion events.

In *Drosophila*, only few mutants are known which show this wing phenotypes, including the widely used dominant marker gene *Curly* (*Cy*) and the recessive marker gene *curled* (*cu*). The molecular identity of neither *Cy* nor *cu* is currently known. *Cy* is located on the second chromosome, whereas *cu* is located on the third chromosome at cytogenetic map position 86D1-4 (Ashburner et al. 1981), a position close to the cytogenetic map position 86D7 annotated for the *nocturnin* gene. Based on the similar cytological locations, I asked whether *nocturnin* and *curled* are the same gene. To address this question, I performed genetic complementation experiments using two out of seven described *cu* alleles (Consortium, T.F., 2003); Individuals bearing the spontaneous mutation cu^{1} or the X-ray induced allele cu^{2} (Carpenter, 2004) were crossed against $nocturnin^{\#65}$ mutants.

Neither cu^{1} nor cu^{2} was able to complement the wing phenotype of $nocturnin^{\#65}$ mutants (data not shown). These results demonstrate that *cu* activity is affected in $nocturnin^{\#65}$ mutants. Formally however, the cytogenetic position of the *cu* gene 86D1-4 as defined by cytologically mapping the *Df(3R)M86D* (86D1;86D4) chromosome (Ashburner et al., 1981) differs from the position (86D7) where the *nocturnin* gene has been mapped. However, PCR analysis on $nocturnin^{\#65}$ / *Df(3R)M86D* flies shows that genomic sequences of the *nocturnin* gene are deleted in the deficiency *Df(3R)M86D* (Fig. S4.6B, for details see Material and Methods). Thus, the deficiency *Df(3R)M86D* uncovers the region of the *nocturnin* gene. It is, therefore, possible that *nocturnin* and *cu* mutations affect the same gene. In this case the mapping of the 3´ breakpoints of *Df(3R)M86D* or the annotation of *nocturnin* to map position 86D7 must be incorrect. In order to link the *nocturnin* and *cu* gene by molecular means, I compared the genomic DNA of cu^{2} and $nocturnin^{\#65}$ mutant flies with the DNA of wild-type. PCR analysis on the respective genomic DNA showed no obvious differences when compared to wild-type flies (Fig. S4.6B), suggesting that the overall genomic organization of *nocturnin* is not significantly altered in size in cu^{2} mutants flies. In order to compare possible mutant lesions at the sequence level *nocturnin* cDNAs were cloned from cu^{1} and cu^{2} alleles and sequenced. To exclude sequence alteration due to cloning artefacts, *nocturnin* cDNAs were isolated from two independent cu^{1} fly lines and, in case of cu^{2}, from differently sized cDNAs that were isolated from the same fly line (details see Material and Methods).

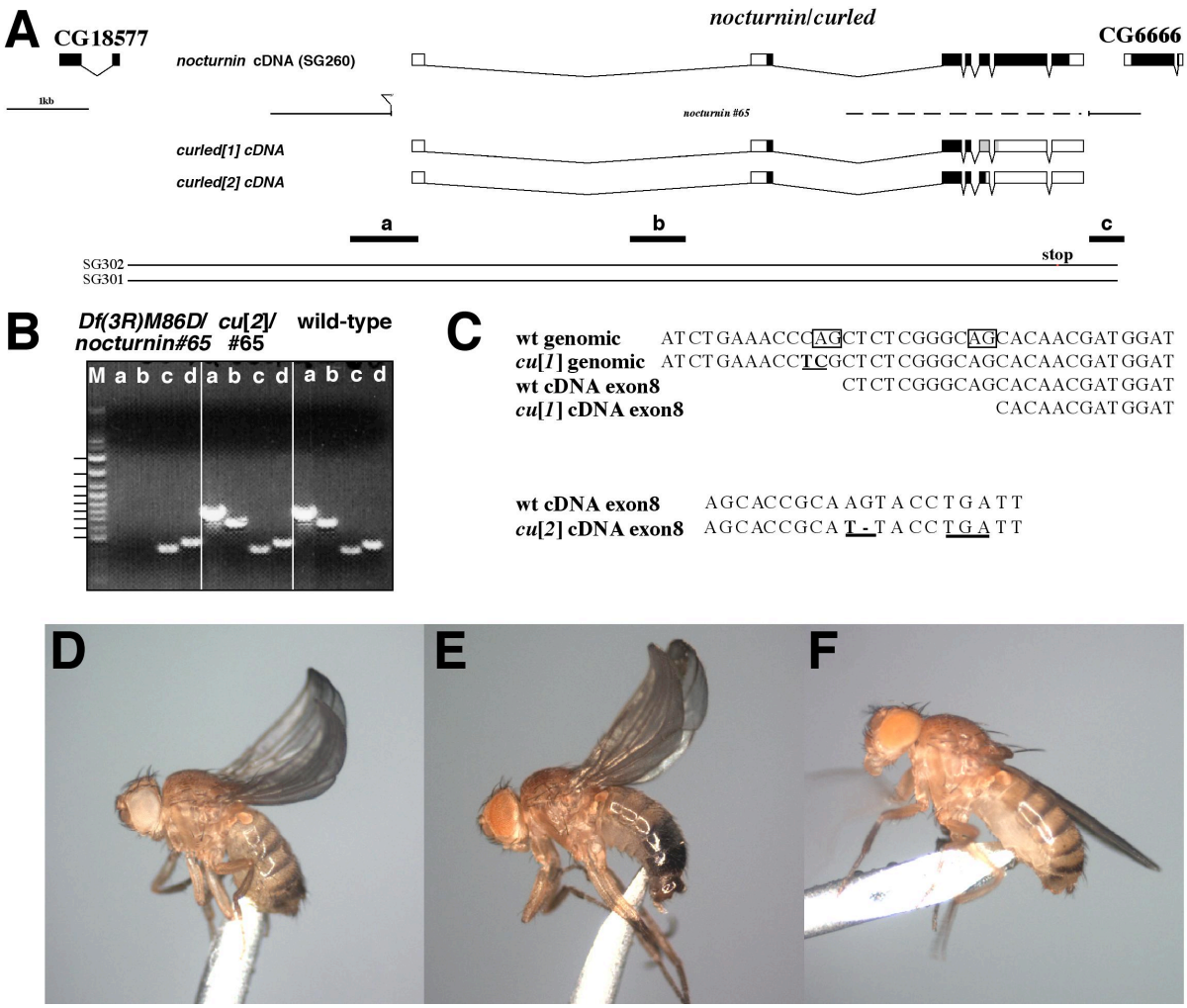

Figure S4.6: *nocturnin* is mutated in *curled*-mutant alleles. (**A**) *nocturnin* gene locus organization in wild-type, *nocturnin*$^{\#65}$ mutant and *cu*^{1} and *cu*^{2} alleles. *nocturnin* cDNAs amplified from *curled*^{1} and *curled*^{2} alleles carry frameshift mutations within exon 8 of the nocturnin gene, that lead to an introduction of a premature stop codon (for details see text and 4.6C). White boxes indicate non-coding 5´ and 3´ UTRs, black boxes the ORF and grey boxes out of frame sequence in the nocturnin ORF caused by frameshift mutations in *cu* alleles. Black boxes a, b, c correspond to the amplified genomic region used in the PCR experiment in (**B**). SG301 is the genomic rescue construct used to rescue the *cu* phenotype. SG302 is a mutated version of SG301, in where a stop codon is introduced to produce a nonfunctional Nocturnin protein, and serves as a negative control in the rescue experiment. (**B**) The *nocturnin* gene is deleted in the deficiency Df(3R)M86D as shown by the lack of amplification product of primer combination a and b (compare S4.6A). In the X-Ray induced *cu*^{2} allele no big deletions of *nocturnin* gene sequence could be observed but PCR analysis shows a wild-type-like pattern. Primer combination c amplifies on *nocturnin*$^{\#65}$ mutant DNA and serves as an internal control, as well as primer combination d that is directed against an unrelated gene locus (*bmm* gene). M in (**B**) is DNA size marker (**C**) Sequence alignment between wild-type and *cu* genomic DNA and cDNA. *cu*^{1} is a splice site mutation resulting in a 11 bp deletion of exon 8 5´ end and thereby introducing a premature stop codon in the *nocturnin* ORF. In *cu*^{1} the splice acceptor site consensus sequence of exon 8 (boxed in wild-type genomic sequence) is mutated from AG to CG (mutated sequence underlined in *cu* genomic sequence), which results in the use of the 11 bp downstream AG as a new splice acceptor site of exon 8. *cu*^{2} is a frameshift mutations where position 67, 68 of *nocturnin* exon 8 are mutated from AT to G, which leads to the introduction of a stop codon just 6 bp 3´of the mutation site (mutation and introduced stop codon underlined).(**D**) *cu* wing phenotype of a *nocturnin*$^{\#65}$ mutant fly (**E**). *nocturnin*$^{\#65}$ mutant flies that carry the mutated *nocturnin* genomic rescue construct SG302 have curled wings (**F**). Rescue of the curled wing phenotype of a *nocturnin*$^{\#65}$ mutant fly by one copy of the genomic rescue construct SG301.

In addition, only mutations detected in both independent cDNAs were considered. The corresponding genomic DNA from the mutants were amplified by PCR and sequenced as well. The results show that the sequence of the *nocturnin* gene is affected in both *cu* alleles (S4.6A, C). In cu^1, the splice acceptor site consensus sequence of exon 8 is mutated from AG to CG. This mutation causes the use of a 11 bp downstream AG as a new and mutant-specific splice acceptor site (Fig. S4.6C) resulting in an 11 bp deletion of the 5´ end of exon 8 which in turn introduces a premature stop codon in the *nocturnin* ORF. The corresponding translation product consists of only 177 amino acids or 211 amino acids, in case of the presence of exon 5 (see Material and Methods and Fig. S4.2A) of the normally 450 amino acids *nocturnin* wild-type protein.

In cu^2 mutant DNA a frameshift mutation in the *nocturnin* ORF was detected. It includes position 67 and 68 of *nocturnin* exon 8 which is altered from AT to G. This mutation leads to the introduction of a stop codon just 6 bp downstream of the mutation site (Fig. S4.6C). The resulting ORF encodes only the aminoterminal 150 amino acids (or 185 in case exon 5 is present, see above) of wild-type Nocturnin. Taken together, the two *cu* alleles, cu^1 and cu^2, exhibit mutation in the *nocturnin* gene. In both cases, the mutation cause a shortening of the *nocturnin* protein. The shortened proteins lack essential amino acids and therefore are likely to represent lack-of function alleles of the *nocturnin* gene.

To unambiguously demonstrate that the *cu* mutant wing phenotype is caused by the mutation of the *nocturnin* gene, I performed rescue experiments expressing a *nocturnin*-transgene in *nocturnin* mutant flies. Overexpression of *nocturnin* using various Gal4-drivers in combination with UAS-*nocturnin* constructs induces lethality in both wild-type as well as *nocturnin* mutant flies (data not shown), thus, a *nocturnin* transgene containing the DNA of the wild-type gene (genomic rescue: SG301, Fig. S4.6A and Material and Methods) was expressed. In addition, as a control for the rescue experiment, a mutated version of the genomic rescue construct (SG302) was generated in which at position 74 of exon 10 a stop codon was introduced. This mutation results in a shortened and non-functional *nocturnin* protein (Fig. S4.6A). $nocturnin^{\#65}$ mutant flies that carry the mutated *nocturnin* genomic DNA fragment SG302 develop the curled wing phenotype (Fig. S4.6E), whereas $nocturnin^{\#65}$ mutants carrying one copy of the DNA fragment SG301 have normal wing morphology (Fig. S4.6F). This observation establishes that lack of *nocturnin* activity is causative for the *cu* wing phenotype.

S4.9 Discussion

S4.9.1 *nocturnin* and circadian rhythm

In vertebrates, Nocturnin proteins are rhythmically expressed deadenylases present in cells that contain an endogenous circadian clock (Baggs and Green 2003; Green and Besharse, 1996; Wang et al., 2001; Barbot et al., 2002), suggesting that Nocturnin is involved in the post-transcriptional regulation of the circadian clock or its output pathways (Baggs and Green 2003). However, *in vivo* studies verifying this hypothesis are currently missing due to the lack of a *nocturnin* "knock-out" mouse-model. In *Drosophila* kept under standard conditions, the lack of *nocturnin* activity does not result in a locomotor activity phenotype. In addition, there is no evidence for a cycling of the *nocturnin* transcript. These findings argue against a function for *nocturnin* in the posttranscriptional regulation of the circadian clock in *Drosophila*. However, since analyses addressing the cycling of *nocturnin* mRNA used either whole animals or heads, it cannot be excluded that nocturnin cycles only in specific tissues or a few clock-pacemaker cells.

Interestingly, in mice the amplitude of *nocturnin* mRNA cycling is tissue specific. *nocturnin* mRNA cycles with very high amplitude in the liver between 30 and 150 fold depending on the mouse strain used (Barbot et al., 2002). Lower amplitudes between 2 and 5 fold were detected for the retina, heart, spleen and kidney, while no cycling was observed in the testis, brain and lung (Barbot et al., 2002). ISH experiments on mice brains suggest also low amplitude rhythmicity in the brain region, nevertheless this rhythmic expression is much weaker than the high amplitude detected in peripheral tissues (Dupressoir et al., 1999; Wang et al., 2001). Thus, in case of *Drosophila*, ISH or tissue specific quantitative RT-PCR analyses are necessary to examine whether a similar tissue-specific cycling also exists in adult *Drosophila* flies.

In addition to adult locomotor activity, pupal eclosion is another biological rhythm that depends on clock-gene expression (Stanewsky, 2003). Several clock-gene mutants specifically affecting eclosion rhythms without affecting adult locomotor activity behaviour have been isolated, e.g. *lark* (Stanewsky, 2003; Newby and Jackson, 1993). Since the eclosion behaviour of *nocturnin* mutant flies has not been analyzed, it cannot be excluded that *nocturnin* is involved in clock-dependent regulation of eclosion rhythms. Furthermore, *lark* RNA is expressed constitutively, but LARK protein expression is circadianly regulated (Jackson et al., 1998, Zhang et al., 2000). Thus, circadian cycling of gene activities is not necessarily linked to the cycling of the corresponding transcript but can be regulated

posttranscriptionally. The generation of Nocturnin antibodies will be necessary to address a possible circadian cycling of the Nocturnin protein. In conclusion, there is no evidence that *nocturnin* is involved in regulating circadian rhythms in *Drosophila*. Additional experiments are necessary to exclude such a function at the level of few cells and with respect to the protein, respectively..

S4.9.2 *nocturnin* and energy homeostasis

Ad libitum fed flies lacking *nocturnin* activity have a normal organismal TAG content, demonstrating that *nocturnin* is not essential for chronic regulation of TAG storage in *Drosophila*. However, *nocturnin* mRNA is upregulated under starvation and *nocturnin* mutants are starvation sensitive. Thus, *nocturnin* is involved in the acute starvation response. The correlation between TAG content and starvation survival time, demonstrated for fat mutants like *adp* (Häder et al., 2003) as well as for fly strains selected for increased starvation resistance (e.g. Harshman et al., 1999; Service et al., 1987), suggests that TAG is the most important energy resource and a mayor determinant of survival time under starvation.

Upon food deprivation, *nocturnin* mutants die earlier than expected from their prestarvation organismal TAG content. This finding suggests an improper TAG mobilization similar to flies lacking *Bmm* TAG lipase activity, a proposal that can be addressed by *post mortem* TAG content determination of starved *nocturnin* mutants. In addition, analysis of the glycogen content of *nocturnin* mutants will be required to address a possible role for *nocturnin* in carbohydrate metabolism. *nocturnin* is expressed in tissues that can be related to organismal energy storage control, including the ring gland as well as the proventriculus, a part of the foregut. The ring gland, which is subdivided in the prothoracic gland, the corpora allata and corpora cardiaca is the major endocrine tissue of *Drosophila* ands as such involved in the control of many physiological processes of the fly. Recently, it was shown that ablation of corpora cardiaca neurons expressing the adipokinetic hormone (AKH) results in larvae with reduced trehalose content and adult flies with an increased survival time under starvation conditions (Lee and Park, 2004). In addition, the corpora cardiaca cells were found to be crucial regulators of glucose homeostasis important for sensing the hemolymph sugar level (Kim and Rulifson, 2004). These observation argue for a direct link between the ring gland and the regulation of energy homeostasis. *Drosophila nocturnin* is expressed in all three parts of the ring gland, including the corpora cardiaca, the significance of this pattern awaits elucidation.

S4.9.3 *nocturnin* is *curled*

The *cu* phenotype itself is known for more than 80 years since its discovery by Thomas Morgan in 1923 (Bridges and Morgan, 1923). However, knowledge about the underlaying molecular mechanism has not much accumulated during this time. It was shown that the strength of the *cu* wing phenotype is dependent on environmental conditions. Good nutrition of larvae enhances the *cu* phenotype, as does high temperature during the last days of pupal development (Nozawa, 1956). In addition, it was shown, that flies reared on a riboflavin-deficient medium during their development show a weaker *cu* phenotype as compared to controls (Pavelka and Jindrak, 2001). How these environmental factors affect the characteristics of the *cu* phenotype is unclear.

Apart from *cu* there are only few mutants known that exhibit a curved wing phenotype, among them *Curl*, *Curl in Chromosome 3*, *curl*, *curled-X* and *Curly* (Consortium T.F., 2003). In an analysis of the imaginal wing disc development of *Curly* mutant pupae, no obvious abnormalities were detected until 45 h after pupae formation, a stage where wing formation is almost completed (stage P2d after Waddington, 1943). Based on this observation, the author speculates, that the curvature of the wing is produced by slight differences in the contraction of the upper and lower surface during the phase of drying out of the wing in the newly emerged fly (Waddington, 1943). To date, no comparable analysis of the imaginal wing disc development in *cu* mutant flies was done. Thus, it will be necessary to define the phenocritic stage of *cu* wild-type function for *Drosophila* wing formation.

In *Drosophila* very much information is available about the early wing disc development until pupation and many genes involved in wing pattern formation are described (overview in Ramirez-Weber and Kornberg, 2000; Klein, 2001). In contrast, almost nothing is known about the late stages of wing development. In particular events happening in the pupae or newly emerged fly. The cloning of the *nocturnin*/*curled* gene presented in this work is a first step towards the analysis of the molecular events underlying these late stages in *Drosophila* wing development. One important question is, for example, where and when *nocturnin*/*curled* is expressed and how it participates in the development of the *Drosophila* wing. It is interesting to note that *nocturnin*/*curled* expression could not be detected in third instar larval wing discs by ISH, a finding that is consistent with the undetected *nocturnin* expression by GeneChip experiments with third instar larval wing discs (Butler et al, 2003). However, it cannot be excluded that *nocturnin*/*curled* is expressed in the third instar larval wing disc at low levels which are undetectable with the described methods. Tissue specific

rescue experiments, using wing-disc-specific Gal4 driver lines in combination with UAS-nocturnin-EGFP constructs, as well as a more sensitive expression analysis, for example, with RT-PCR or the availability of Nocturnin antibodies that can be applied to pupal wing discs would help to answer the question whether *nocturnin*/*curled* has a cell-autonomous function in the wing.

Supplement 5: Characterization of the *Drosophila rhythmically expressed gene 2* (*Dreg-2*)

The *Drosophila* gene, termed *rhythmically expressed gene 2* (*Dreg-2*, *CG3200*), was originally identified as a circadianly cycling transcript expressed in heads and bodies of adult male flies (van Gelder et al., 1995). Furthermore, its rhythmic expression was recently confirmed by GeneChip analysis (Lin et al., 2002). *Dreg-2* mRNA exhibits a single peak of expression in the early morning and a single trough of expression at night. In wild-type flies the rhythmicity of *Dreg-2* expression is dependent on the light-dark cycle and feeding conditions (van Gelder et al., 1995). In this work, *Dreg-2* was identified as a starvation-induced gene in adult *Drosophila* flies (supplemental Fig. 1), suggesting that *Dreg-2* is involved in the adult starvation response. In order to examine the function of *Dreg-2* in the context of energy homeostasis and circadian rhythm, I initiated the characterization of the *Dreg-2* gene.

S5.1 Genomic organization at the *Dreg-2* gene locus

Dreg-2 is located at the cytogenetic map position 61 C6-7 on the left arm of the *Drosophila* third chromosome (Fig. S5.1). Alignment of cDNA (van Gelder et al., 1995), EST (GH02773, LP03758, RH60312, Rubin et al., 2000) and genomic sequences revealed, that *Dreg-2* is encoded by three exons (exon 1: 224 bp, exon 2: 89 bp, exon 3: 569 bp) spanning a total of 1,4 kb of genomic region.

Figure S5.1 Genomic organization of the *Dreg-2* locus and *Dreg-2* deletion mutants. Genomic organization at the *Dreg-2* locus (coding sequence shown as black, UTRs as white boxes) at cytogentic position 61 C6-7. The fly line *Dreg-2*^{GE23065} which carries a *P{EP}* transposable element in the 5´ promotor region of *Dreg-2* was used to generate the deletion mutant *Dreg-2*$^{\#70}$ (details see text S5.4).

The 882 bp long *Dreg-2* transcript contains a 783 bp long ORF. It encodes a Dreg-2 protein of 260 amino acids corresponding to a predicted molecular mass of 30,1 kDa.

S5.2 *Dreg-2* encodes an evolutionary conserved protein

A protein databases search (Protein-Protein Blast, NCBI) revealed that Dreg-2-related proteins are conserved from yeast to human (Fig. S5.2A). *Drosophila* encodes a second Dreg-2-like protein (CG15192), which has an orthologue in *Anopheles* as well. The existence of two Dreg-2 like genes appears to be restricted to insects, since mammalian genomes like mouse, rat and human or the genome of yeast and the nematode *Caenorhabditis elegans* contain only a single Dreg-2-like protein. Since the function of any Dreg-2-related protein is unknown, a domain database search was initiated using the SMART server (Schultz et al., 1998; Letunic et al., 2004). This search identified a haloacid dehalogenase-like hydrolase (Pfam00702) domain within Dreg-2 which covers the aminoterminal region of the protein from amino acid position 7 to 224 (Fig S5.1B).

Proteins containg this domain have been shown to exhibit L-2 haloacid dehalogenase, epoxide hydrolase and phosphatase activity (Hisano et al., 1996). Among the phosphatases enzymes with very different substrate specificities, for example, the yeast protein Dog1 have been characterized. Its activity catalyzes the dephosphorylation of 2-deoxyglucose-6-phosphate (Sanz et al., 1994). Moreover, the mammalian EPXH2 exhibits lipid phosphate phosphatase activity (Newman et al., 2002). The presence of a hydrolase domain suggests an enzymatic function for Dreg-2. However, a wide range of substrate specificities of the different haloacid dehalogenase-like hydrolases do not allow to assign the Dreg-2 to a specific function and thus, prevents a prediction of the physiological process *Dreg-2* is involved in.

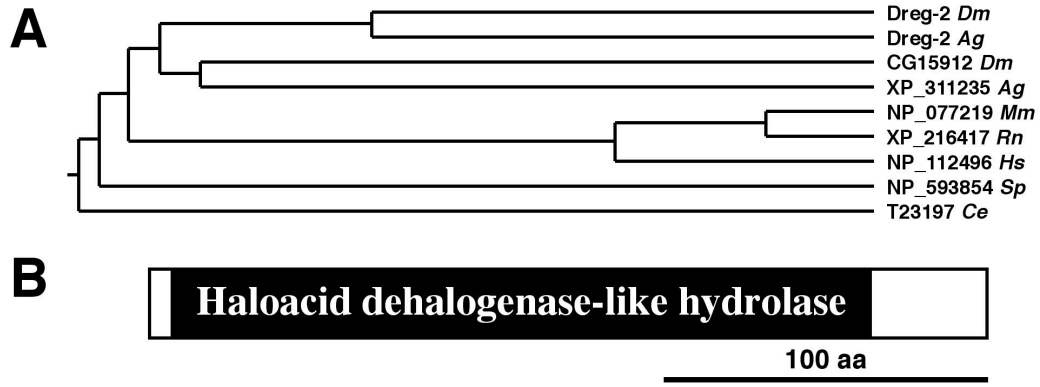

Figure S5.2 Dreg-2 is an evolutionary conserved protein. (**A**) Phylogenetic tree based on sequence alignment of Dreg-2-like proteins from *Drosophila melanogaster* (*Dm*), *Anopheles gambia* (*Ag*), *Mus musculus* (*Mm*), *Rattus norvegicus* (*Rn*), *Homo sapiens* (*Hs*), *Schizosaccharomyces pombe* (*Sp*) and *Caenorhabditis elegans* (*Ce*). (**B**) Structure of the Dreg-2 protein. From amino acid position 7 to 224 the Dreg-2 protein contains a haloacid dehalogenase-like hydrolase domain (Pfam00702).

S5.2 Developmental expression of *Dreg-2*

In order to further detail the expression analysis, the temporal and spatial transcription pattern of *Dreg-2* was analyzed by developmental Northern blot and ISH on embryos (Fig. S5.3).

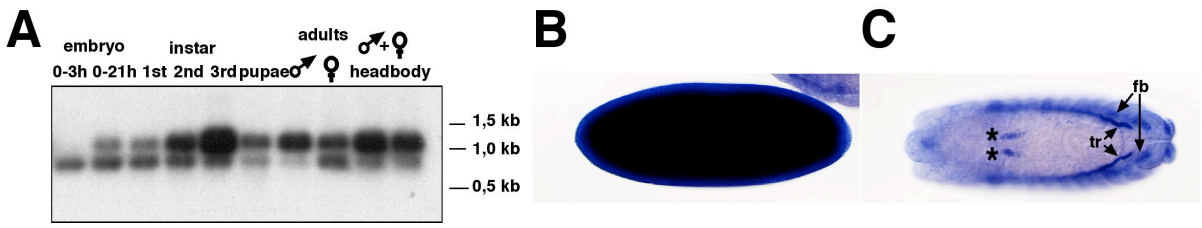

Figure S5.3 Developmental expression of *Dreg-2*. (A-C) The temporal and spatial expression pattern of *Dreg-2* was analyzed by developmental Northern blot and ISH. (**A**) Developmental Northern Blot analysis detects two *Dreg-2* transcripts with a size of 0,8 kb and 1,0 kb expressed in various ontogenetic stages of *Drosophila*. The 1,0 kb transcript is the predominant mRNA species in third instar larvae, pupae and adult stages, whereas in young embryos (0-3 hour) only the 0,8 kb transcript is present. (**B**) While *Dreg-2* mRNA is evenly distributed in young embryos, (**C**) in older embryos *Dreg-2* expression is restricted to specific tissues, including the fat body (fb) as well as non identified cluster of cells (asteriks in **C**). Note: only the lumen of the tracheal system (tr) is stained, indicating an unspecific hybridisation of the ISH probe.

Consistent with the results of van Gelder et al. in adult *Drosophila* males a single transcript of approximately 1 kb present in heads and bodies was detected in the Northern blot analysis (Fig. S5.2B) (van Gelder et al., 1995). In addition to the 1 kb mRNA, adult females express a shorter transcript of approximately 0,8 kb which is also detected in embryos, larvae and pupae (Fig. S5.2B). The molecular identity of the shorter transcript is currently unknown. While the 1 kb variant is the predominant *Dreg-2* mRNA species in later stages (third instar larvae to adult), in young embryos (0-3 hours) only the 0,8 kb mRNA is present. Thus, it is likely to represent the maternally expressed transcript, which is stored in the egg. The ubiquitous distribution of the transcript in early stage embryos (Fig. S5.2C) supports the view of the maternally transcribed *Dreg-2* mRNA. In older embryos, *Dreg-2* is expressed in the fat body (Fig. S5.2D). This site of expression is consistent with the argument that *Dreg-2* acts in organismal energy homeostasis.

S5.3 Nutritional regulation of *Dreg-2*

Dreg-2 was identified in a GeneChip approach as a gene which is upregulated under starvation conditions. *Dreg-2* transcript amounts increase in response to starvation by factor of 1,8 after 6 hours and stay upregulated after 12, 18 and 24 hours being 1,8, 1,8 and 2,4 fold, respectively, more active than the wild-type gene (Fig. S5.3A). Starvation-induction of *Dreg-2* was confirmed by Northern blot analysis (Fig. S5.3B). In addition, upregulation of *Dreg-2* expression is also observed in larvae starved for 4 and 12 hours resulting in 3,5 and

1,7 fold *Dreg-2* induction, respectively (Zinke et al., 2002). The upregulation is starvation-specific, since *Dreg-2* expression is not changed in larvae fed with 20% sucrose. The nutritional regulation as well as the expression in the fat body suggest *Dreg-2* to be involved in the control of energy homeostasis in *Drosophila*.

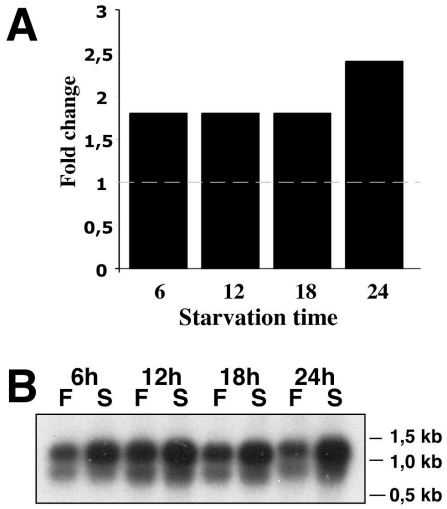

Figure S5.3 Nutritional regulation of *Dreg-2*. (**A**) Upregulation of Dreg-2 transcription detected by the GeneChip analysis in flies starved for 6, 12, 18 and 24 hours by factor 1,8, 1,8, 1,8 and 2,4. (**B**) Northern blot analysis comparing *Dreg-2* transcript abundance of starved (S) and *ad libitum* fed (F) male flies confirms starvation-induction of *Dreg-2* transcription.

S5.4 Generation of a *Dreg-2* mutant

In order to examine the *in vivo* function of *Dreg-2* in the context of energy homeostasis and circadian rhythm, *Dreg-2* mutant flies were generated by the imprecise excision of a *P{EP}* transposable element located 150 bp upstream of the *Dreg-2* transcription start site in the fly line *P{EP} Dreg-2*^{GE23064} (Fig. S5.1) following a conventional P-element mobilization scheme (Ashburner, 1989). A PCR based screening assay (details see Material and Methods) led to the identification of the mutant allele *Dreg-2*$^{\#70}$, which lacks the genomic wild-type DNA sequence from position 587355 to 589667 (Consortium, T.F., 2003; *D.mel*. chromosome 3L). Within this 2,319 kb DNA fragment 1,3 kb of the 5´-promotor region, exon 1, exon 2 and 143 bp of exon 3 of *Dreg-2* are deleted (Fig. S5.1). As a result, *Dreg-2*$^{\#70}$ mutant flies lack sequences encoding the aminoterminal half (130 amino acids) of the Dreg-2 protein. The remaining sequences encode an ORF containing the carboxyterminal 78 amino acids of *Dreg-2*, suggesting that *Dreg-2*$^{\#70}$ is either a strong hypomorph or even a lack-of-function allele of the *Dreg-2* gene. *Dreg-2*$^{\#70}$ mutant flies are homozygous viable and exhibit no obvious morphological. Thus, *Dreg-2* could act specifically in adult energy homeostasis and circadian rhythm of the fly.

S5.5 Physiological characterization of *Dreg-2* mutants

Dreg-2 mutants were examined for their ability to act in starvation conditions. Under starvation, immature and mature adult *Dreg-2*$^{\#70}$ mutant males survive as long as control flies (Fig. S5.3E, F). Consistently, fat body-specific overexpression of a UAS-*Dreg-2* transgene does not result in decreased organismal TAG content in immature or mature adult flies (Fig S5.3C). These observation argue against a function of *Dreg-2* in acute lipid mobilization. In

addition, preliminary results indicate that *Dreg-2*$^{\#70}$ mutant flies have normal organismal TAG content (data not shown). Thus, *Dreg-2* is not involved in the control of chronic TAG storage in *Drosophila*.

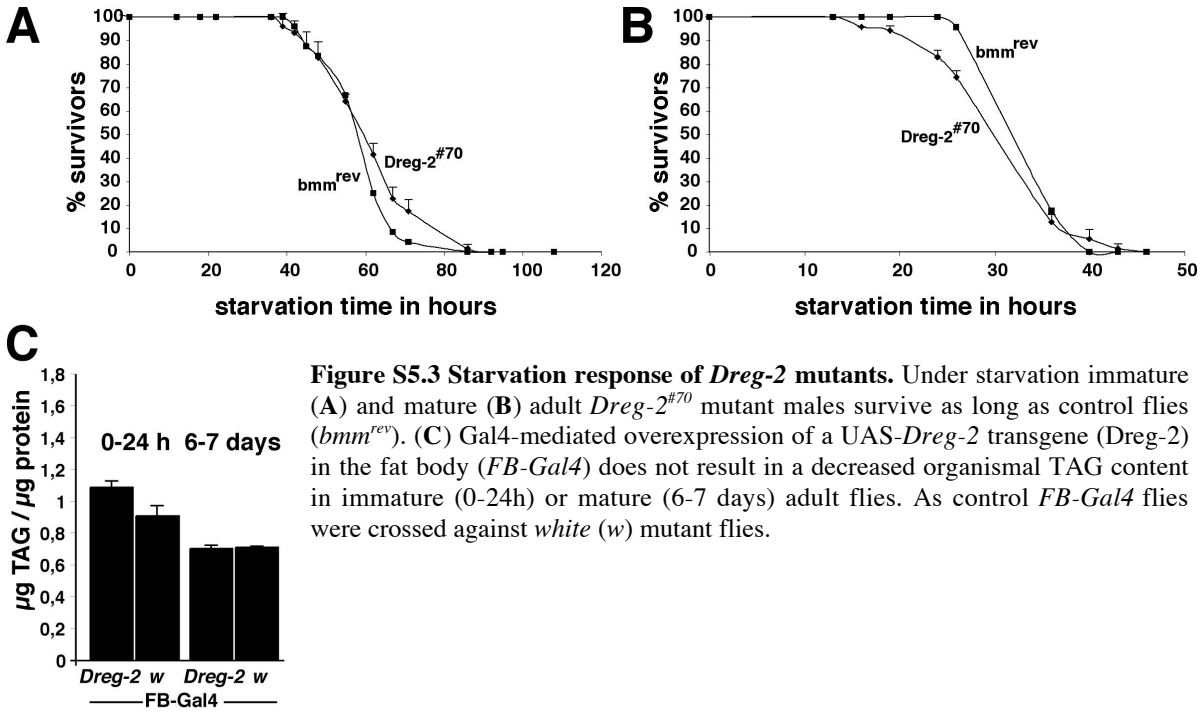

Figure S5.3 Starvation response of *Dreg-2* mutants. Under starvation immature (**A**) and mature (**B**) adult *Dreg-2*$^{\#70}$ mutant males survive as long as control flies (*bmm*^{rev}). (**C**) Gal4-mediated overexpression of a UAS-*Dreg-2* transgene (Dreg-2) in the fat body (*FB-Gal4*) does not result in a decreased organismal TAG content in immature (0-24h) or mature (6-7 days) adult flies. As control *FB-Gal4* flies were crossed against *white* (*w*) mutant flies.

To further test whether *Dreg-2* is involved in circadian rhythm control, I examined their locomotor activity (collaboration with Dr. Ralph Stanewsky). Mutations in circadianly cycling clock genes can completely disrupt the daily organization of locomotor activity behaviour in adult *Drosophila* flies (Stanewsky, 2003). *Dreg-2* mutant flies under standard conditions (*ad libitum* feeding, 25°C, 12h L/D) show a normal bimodal activity pattern with a morning peak around lights-on and an evening peak before lights-off (Fig. S5.4A). The locomotor activity of *Dreg-2* mutant flies is still rhythmic after seven days in constant darkness, indicating that *Dreg-2* function is not essential for locomotor activity behaviour of *Drosophila* flies. This conclusion is supported by the normal locomotor behaviour of starved *Dreg-2* mutants, which show the typical hyperactivity pattern prior to death (Fig. S5.4B).

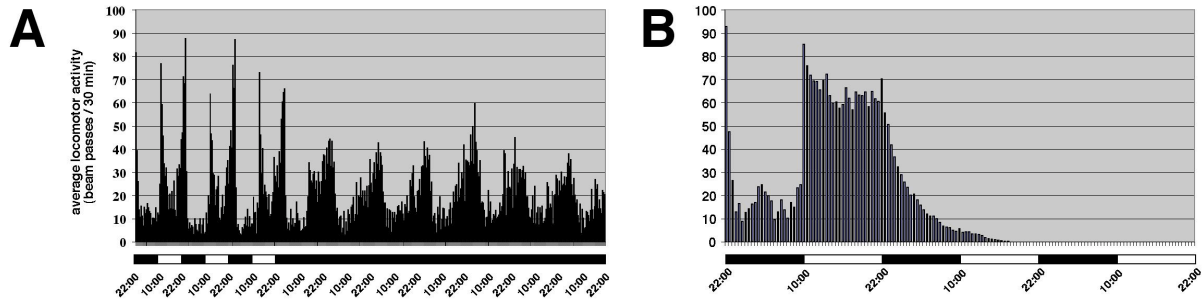

Figure S5.4 Locomotor activity behaviour of *Dreg-2* mutants. (**A**) Average locomotor activity of *Dreg-2*$^{\#70}$ mutant males (n=27) under standard conditions: 25°C, ad libitum feeding. For the first three days flies were analyzed under a 12h light, 12 h dark cycle (12h LD) and were subsequently submitted to constant darkness for the remaining 7 days of the experiment (light phase indicated by bar below lower pannel: open bars display time of ligths-on, filled bars display time of ligths-off). *Dreg-2*$^{\#70}$ mutant flies show a normal bimodal activity pattern with a morning peak around lights-on and an evening peak before lights-off, which persists under constant darkness conditions although with a lower amplitude. (**B**) Average locomotor activity of *Dreg-2*$^{\#70}$ mutants under starvation (n=32) reveals a normal starvation response with a typical hyperactivity behaviour prior to death.

S5.6 Discussion

The starvation-induced upregulation as well as the expression in the fat body suggest that *Dreg-2* is involved in the regulation of energy homeostasis in larvae and adult flies. However, overexpression in the fat body does not result in TAG mobilization. Furthermore, *Dreg-2* mutants have normal starvation survival time and organismal TAG content. Thus, *Dreg-2* is not essential for acute or chronic TAG storage control. Since *Dreg-2* mutants show normal activity behaviour under starvation conditions, the function of *Dreg-2* in the context of energy homeostasis remains unclear. The presence of a haloacid dehalogenase-like hydrolase domain (Pfam00702) suggests hydrolytic activity of the Dreg-2 protein. Other proteins containing this domain have been shown to be involved in carbohydrate metabolism, like the Dog1 phosphatase in yeast (Sanz et al., 1994), or detoxification processes, like the mammalian soluble epoxide hydrolase (sEH) (Newman et al., 2002; Cronin et al., 2003). Additional experiments, including the analysis of organismal glycogen content of *Dreg-2* mutant flies as well as *in vitro* hydrolase assays are necessary to identify the substrate specificity of the Dreg-2 hydrolase and to address the function of *Dreg-2* in starvation response.

Dreg-2 was identified as a circadianly cycling transcript in adult Drosophila males, however, the diurnal control of *Dreg-2* expression is complex and dependent on external cues like the light-dark cycle and feeding conditions (van Gelder et al., 1995). Our studies demonstrate, that *Dreg-2* activity is not essential for locomotor activity behaviour of adult *Drosophila* wild-type flies, indicating that *Dreg-2,* consistent with its circadian regulation, is not a core clock gene controlling behaviour. Given the nutritional regulation it appears likely that *Dreg-*

2 is involved in a physiological process related to energy homeostasis, which is circadianly regulated. However, in which process *Dreg-2* is involved remains unclear.

Dreg-2-like proteins are conserved from yeast to human suggesting an important role of these proteins. In contrast *Dreg-2*$^{\#70}$ mutant flies are homozygous viable and show no obvious morphological, circadian rhythm or energy homeostasis phenotype. A possible explanation for the lack of a phenotype could be that *Dreg-2*$^{\#70}$ is only a hypomorphic allele. Although this is not very likely, because *Dreg-2*$^{\#70}$ mutants lack a big part of the promotor region and in addition sequences coding for half of the protein, including highly conserved amino acids (data not shown), additional experiments are necessary, to verify the complete lack of *Dreg-2* function in these flies. In contrast to mammals or the nematode *C. elegans, Drosophila* contains two Dreg-2 like proteins suggesting that they might act redundantly. As the function of the Dreg-2-related protein CG15192 is not known, this possibility cannot be excluded. However, in contrast to *Dreg-2* CG15192 is not upregulated under starvation conditions (data not shown) and exhibits no circadian cycling (McDonald & Rosbash 2000; Claridge-Chang et al., 2001, Lin et al., 2002; Ueda et al. 2002) suggesting that it has a different function. In conclusion, although the nutritional regulation and the circadian cycling suggest *Dreg-2* to be involved in energy homeostasis and circadian rhythm control, initial analysis of *Dreg-2* mutant flies provides no evidence for such a function.

5 References

Abell, B. M., Holbrook, L. A., Abenes, M., Murphy, D. J., Hills, M. J. and Moloney, M. M. (1997). Role of the proline knot motif in oleosin endoplasmic reticulum topology and oil body targeting. *Plant Cell* **9**, 1481-93.

Allison, D. B., Kaprio, J., Korkeila, M., Koskenvuo, M., Neale, M. C. and Hayakawa, K. (1996). The heritability of body mass index among an international sample of monozygotic twins reared apart. *Int J Obes Relat Metab Disord* **20**, 501-6.

Andrews, D. L., Beames, B., Summers, M. D. and Park, W. D. (1988). Characterization of the lipid acyl hydrolase activity of the major potato (*Solanum tuberosum*) tuber protein, patatin, by cloning and abundant expression in a baculovirus vector. *Biochem J* **252**, 199-206.

Arquier, N., Bourouis, M., Colombani, J. and Leopold, P. (2005). *Drosophila* Lk6 Kinase Controls Phosphorylation of Eukaryotic Translation Initiation Factor 4E and Promotes Normal Growth and Development. *Curr Biol* **15**, 19-23.

Arrese, E. L., Canavoso, L. E., Jouni, Z. E., Pennington, J. E., Tsuchida, K. and Wells, M. A. (2001). Lipid storage and mobilization in insects: current status and future directions. *Insect Biochem Mol Biol* **31**, 7-17.

Arrese, E. L. and Wells, M. A. (1994). Purification and properties of a phosphorylatable triacylglycerol lipase from the fat body of an insect, *Manduca sexta*. *J Lipid Res* **35**, 1652-60.

Ashburner, M., Angel, P., Detwiler, C., Faithfull, J., Gubb, D., Harrington, G., Littlewood, T., Tsubota, S., Velissariou, V. and Walker, V. (1981). Report of New Mutants. *D. I. S.* **56**, 186--191.

Ashbuner, M. (1989). Drosophila- A Laboratory Manual. *Cold Spring Harbour Laboratory Press*.

Athenstaedt, K. and Daum, G. (2003). YMR313c/TGL3 encodes a novel triacylglycerol lipase located in lipid particles of *Saccharomyces cerevisiae*. *J Biol Chem* **278**, 23317-23.

Atkins, J. and Glynn, P. (2000). Membrane association of and critical residues in the catalytic domain of human neuropathy target esterase. *J Biol Chem* **275**, 24477-83.

Bachman, E. S., Dhillon, H., Zhang, C. Y., Cinti, S., Bianco, A. C., Kobilka, B. K. and Lowell, B. B. (2002). betaAR signaling required for diet-induced thermogenesis and obesity resistance. *Science* **297**, 843-5.

Baggs, J. E. and Green, C. B. (2003). Nocturnin, a deadenylase in *Xenopus laevis* retina: a mechanism for posttranscriptional control of circadian-related mRNA. *Curr Biol* **13**, 189-98.

Bajotto, G., Murakami, T., Nagasaki, M., Tamura, T., Tamura, N., Harris, R. A., Shimomura, Y. and Sato, Y. (2004). Downregulation of the skeletal muscle pyruvate dehydrogenase complex in the Otsuka Long-Evans Tokushima Fatty rat both before and after the onset of diabetes mellitus. *Life Sci* **75**, 2117-30.

Barbot, W., Wasowicz, M., Dupressoir, A., Versaux-Botteri, C. and Heidmann, T. (2002). A murine gene with circadian expression revealed by transposon insertion: self-sustained rhythmicity in the liver and the photoreceptors. *Biochim Biophys Acta* **1576**, 81-91.

Bate, Martinez, Arias (1993). The Development of *Drosophila melanogaster* Volume I. *Cold Spring Harbour Laboratory Press*.

Baulande, S., Lasnier, F., Lucas, M. and Pairault, J. (2001). Adiponutrin, a transmembrane protein corresponding to a novel dietary- and obesity-linked mRNA specifically expressed in the adipose lineage. *J Biol Chem* **276**, 33336-44.

Beenakkers, A. M., Van der Horst, D. J. and Van Marrewijk, W. J. (1985). Insect lipids and lipoproteins, and their role in physiological processes. *Prog Lipid Res* **24**, 19-67.

Besharse, J. C. and Iuvone, P. M. (1983). Circadian clock in *Xenopus* eye controlling retinal serotonin N-acetyltransferase. *Nature* **305**, 133-5.

Blanchette-Mackie, E. J., Dwyer, N. K., Barber, T., Coxey, R. A., Takeda, T., Rondinone, C. M., Theodorakis, J. L., Greenberg, A. S. and Londos, C. (1995). Perilipin is located on the surface layer of intracellular lipid droplets in adipocytes. *J Lipid Res* **36**, 1211-26.

Blom, N., Gammeltoft, S. and Brunak, S. (1999). Sequence and structure-based prediction of eukaryotic protein phosphorylation sites. *J Mol Biol* **294**, 1351-62.

Blüher, M., Michael, M. D., Peroni, O. D., Ueki, K., Carter, N., Kahn, B. B. and Kahn, C. R. (2002). Adipose tissue selective insulin receptor knockout protects against obesity and obesity-related glucose intolerance. *Dev Cell* **3**, 25-38.

Böhni, R., Riesgo-Escovar, J., Oldham, S., Brogiolo, W., Stocker, H., Andruss, B. F., Beckingham, K. and Hafen, E. (1999). Autonomous control of cell and organ size by CHICO, a *Drosophila* homolog of vertebrate IRS1-4. *Cell* **97**, 865--875.

Bradfield, J. Y., Lee, Y. H. and Keeley, L. L. (1991). Cytochrome P450 family 4 in a cockroach: molecular cloning and regulation by regulation by hypertrehalosemic hormone. *Proc Natl Acad Sci U S A* **88**, 4558-62.

Brand, A. H. and Perrimon, N. (1993). Targeted gene expression as a means of altering cell fates and generating dominant phenotypes. *Development* **118**, 401-15.

Brasaemle, D. L., Barber, T., Wolins, N. E., Serrero, G., Blanchette-Mackie, E. J. and Londos, C. (1997). Adipose differentiation-related protein is an ubiquitously expressed lipid storage droplet-associated protein. *J Lipid Res* **38**, 2249-63.

Brasaemle, D. L., Rubin, B., Harten, I. A., Gruia-Gray, J., Kimmel, A. R. and Londos, C. (2000). Perilipin A increases triacylglycerol storage by decreasing the rate of triacylglycerol hydrolysis. *J Biol Chem* **275**, 38486-93.

Brasaemle, D. L., Dolios, G., Shapiro, L. and Wang, R. (2004). Proteomic analysis of proteins associated with lipid droplets of basal and lipolytically stimulated 3T3-L1 adipocytes. *J Biol Chem* **279**, 46835-42.

Bridges, C. B. and Morgan, T. H. (1923). The third-chromosome group of mutant characters of *Drosophila melanogaster*. *Publs Carnegie Instn* **327**, 1--251.

Brockmann, G. A. and Bevova, M. R. (2002). Using mouse models to dissect the genetics of obesity. *Trends Genet* **18**, 367-76.

Brogiolo, W., Stocker, H., Ikeya, T., Rintelen, F., Fernandez, R. and Hafen, E. (2001). An evolutionarily conserved function of the *Drosophila* insulin receptor and insulin-like peptides in growth control. *Curr Biol* **11**, 213-21.

Brown, D. A. (2001). Lipid droplets: proteins floating on a pool of fat. *Curr Biol* **11**, R446-9.

Brunet, A., Bonni, A., Zigmond, M. J., Lin, M. Z., Juo, P., Hu, L. S., Anderson, M. J., Arden, K. C., Blenis, J. and Greenberg, M. E. (1999). Akt promotes cell survival by phosphorylating and inhibiting a Forkhead transcription factor. *Cell* **96**, 857-68.

Brüning, J. C., Gautam, D., Burks, D. J., Gillette, J., Schubert, M., Orban, P. C., Klein, R., Krone, W., Müller-Wieland, D. and Kahn, C. R. (2000). Role of brain insulin receptor in control of body weight and reproduction. *Science* **289**, 2122-5.

Buszczak, M., Lu, X., Segraves, W. A., Chang, T. Y. and Cooley, L. (2002). Mutations in the *midway* gene disrupt a *Drosophila* acyl coenzyme A: diacylglycerol acyltransferase. *Genetics* **160**, 1511-8.

Butler, M. J., Jacobsen, T. L., Cain, D. M., Jarman, M. G., Hubank, M., Whittle, J. R., Phillips, R. and Simcox, A. (2003). Discovery of genes with highly restricted expression patterns in the *Drosophila* wing disc using DNA oligonucleotide microarrays. *Development* **130**, 659-70.

Butterworth, F. M., Bodenstein, D. and King, R. C. (1965). Adipose Tissue of *Drosophila melanogaster*. I. An Experimental Study of Larval Fat Body. *J Exp Zool* **158**, 141-53.

Cahill, G. M., Grace, M. S. and Besharse, J. C. (1991). Rhythmic regulation of retinal melatonin: metabolic pathways, neurochemical mechanisms, and the ocular circadian clock. *Cell Mol Neurobiol* **11**, 529-60.

Canavoso, L. E., Frede, S. and Rubiolo, E. R. (2004). Metabolic pathways for dietary lipids in the midgut of hematophagous *Panstrongylus megistus* (Hemiptera: *Reduviidae*). *Insect Biochem Mol Biol* **34**, 845-54.

Carpenter, A. T. C. (2002.4.2). Personal communication to FlyBase available from http://flybase.bio.indiana.edu/.bin/fbpcq.html?FBrf0149628.

Celniker, S. E. and Rubin, G. M. (2003). The *Drosophila melanogaster* genome. *Annu Rev Genomics Hum Genet* **4**, 89-117.

Chen, J., Chiang, Y. C. and Denis, C. L. (2002). CCR4, a 3'-5' poly(A) RNA and ssDNA exonuclease, is the catalytic component of the cytoplasmic deadenylase. *Embo J* **21**, 1414-26.

Chen, H. C., Stone, S. J., Zhou, P., Buhman, K. K. and Farese, R. V., Jr. (2002). Dissociation of obesity and impaired glucose disposal in mice overexpressing acyl coenzyme a:diacylglycerol acyltransferase 1 in white adipose tissue. *Diabetes* **51**, 3189-95.

Chien, S., Reiter, L. T., Bier, E. and Gribskov, M. (2002). Homophila: human disease gene cognates in *Drosophila*. *Nucleic Acids Res* **30**, 149-51.

Chung, S. S., Ho, E. C., Lam, K. S. and Chung, S. K. (2003). Contribution of polyol pathway to diabetes-induced oxidative stress. *J Am Soc Nephrol* **14**, S233-6.

Clancy, D. J., Gems, D., Harshman, L. G., Oldham, S., Stocker, H., Hafen, E., Leevers, S. J. and Partridge, L. (2001). Extension of Life-Span by Loss of CHICO, a *Drosophila* Insulin Receptor Substrate Protein. *Science* **292**, 104-106.

Claridge-Chang, A., Wijnen, H., Naef, F., Boothroyd, C., Rajewsky, N. and Young, M. W. (2001). Circadian regulation of gene expression systems in the *Drosophila* head. *Neuron* **32**, 657-71.

Clement, K., Boutin, P. and Froguel, P. (2002). Genetics of obesity. *Am J Pharmacogenomics* **2**, 177-87.

Clifford, G. M., Londos, C., Kraemer, F. B., Vernon, R. G. and Yeaman, S. J. (2000). Translocation of hormone-sensitive lipase and perilipin upon lipolytic stimulation of rat adipocytes. *J Biol Chem* **275**, 5011-5.

Consortium, T. F. (2003). The FlyBase database of the *Drosophila* genome projects and community literature. *Nucleic Acids Res* **31**, 172-5.

Contreras, J. A., Karlsson, M., Osterlund, T., Laurell, H., Svensson, A. and Holm, C. (1996). Hormone-sensitive lipase is structurally related to acetylcholinesterase, bile salt-stimulated lipase, and several fungal lipases. Building of a three-dimensional model for the catalytic domain of hormone-sensitive lipase. *J Biol Chem* **271**, 31426-30.

Cronin, A., Mowbray, S., Durk, H., Homburg, S., Fleming, I., Fisslthaler, B., Oesch, F. and Arand, M. (2003). The N-terminal domain of mammalian soluble epoxide hydrolase is a phosphatase. *Proc Natl Acad Sci U S A* **100**, 1552-7.

Damiola, F., Le Minh, N., Preitner, N., Kornmann, B., Fleury-Olela, F. and Schibler, U. (2000). Restricted feeding uncouples circadian oscillators in peripheral tissues from the central pacemaker in the suprachiasmatic nucleus. *Genes Dev* **14**, 2950-61.

Dauwalder, B., Tsujimoto, S., Moss, J. and Mattox, W. (2002). The *Drosophila takeout* gene is regulated by the somatic sex-determination pathway and affects male courtship behavior. *Genes Dev* **16**, 2879-92.

Demerec, M. (1994). Biology of *Drosophila*. *Cold Spring Harbour Laboratory Press*.

Dhondt, S. G., Pierrette; Stelmach, Boguslawa A.; Legrand, Michel and Heitz, Thierry. (2000). Soluble phospholipase A2 activity is induced before oxylipin accumulation in tobacco mosaic virus-infected tobacco leaves and is contributed by patatin-like enzymes. *The Plant Journal* **23**, 431-440.

Diaz, E. and Pfeffer, S. R. (1998). TIP47: a cargo selection device for mannose 6-phosphate receptor trafficking. *Cell* **93**, 433-43.

Dlakic, M. (2000). Functionally unrelated signalling proteins contain a fold similar to Mg2+-dependent endonucleases. *Trends Biochem Sci* **25**, 272-3.

Doane, W. W. (1960). Developmental physiology of the mutant *female sterile (2) adipose* of *Drosophila melanogaster*.II. Effects of altered environment and residual genome on its expression. *J. exp. Zool.* **145**, 23--42.

Dupressoir, A., Barbot, W., Loireau, M. P. and Heidmann, T. (1999). Characterization of a mammalian gene related to the yeast CCR4 general transcription factor and revealed by transposon insertion. *J Biol Chem* **274**, 31068-75.

Dupressoir, A., Morel, A. P., Barbot, W., Loireau, M. P., Corbo, L. and Heidmann, T. (2001). Identification of four families of yCCR4- and Mg2+-dependent endonuclease-related proteins in higher eukaryotes, and characterization of orthologs of yCCR4 with a conserved leucine-rich repeat essential for hCAF1/hPOP2 binding. *BMC Genomics* **2**, 9.

Egan, J. J., Greenberg, A. S., Chang, M. K., Wek, S. A., Moos, M. C., Jr. and Londos, C. (1992). Mechanism of hormone-stimulated lipolysis in adipocytes: translocation of hormone-sensitive lipase to the lipid storage droplet. *Proc Natl Acad Sci U S A* **89**, 8537-41.

Enright, A. J., John, B., Gaul, U., Tuschl, T., Sander, C. and Marks, D. S. (2003). MicroRNA targets in *Drosophila*. *Genome Biol* **5**, R1.

Feigl, G., Gram, M. and Pongs, O. (1989). A member of the steroid hormone receptor gene family is expressed in the 20-OH-ecdysone inducible puff 75B in *Drosophila melanogaster*. *Nucleic Acids Res* **17**, 7167-78.

Flier, J. S. and Hollenberg, A. N. (1999). ADD-1 provides major new insight into the mechanism of insulin action. *Proc Natl Acad Sci U S A* **96**, 14191-2.

Flier, J. S. (2004). Obesity wars: molecular progress confronts an expanding epidemic. *Cell* **116**, 337-50.

Fortier, M., Wang, S. P., Mauriege, P., Semache, M., Mfuma, L., Li, H., Levy, E., Richard, D. and Mitchell, G. A. (2004). Hormone-sensitive lipase-independent adipocyte lipolysis during beta-adrenergic stimulation, fasting, and dietary fat loading. *Am J Physiol Endocrinol Metab* **287**, E282-8.

Fortini, M. E., Skupski, M. P., Boguski, M. S. and Hariharan, I. K. (2000). A survey of human disease gene counterparts in the Drosophila genome. *J Cell Biol* **150**, F23-30.

Fredrikson, G., Stralfors, P., Nilsson, N. O. and Belfrage, P. (1981). Hormone-sensitive lipase of rat adipose tissue. Purification and some properties. *J Biol Chem* **256**, 6311-20.

Friedman, J. M. (2004). Modern science versus the stigma of obesity. *Nat Med* **10**, 563-9.

Furuyama, T., Kitayama, K., Yamashita, H. and Mori, N. (2003). Forkhead transcription factor FOXO1 (FKHR)-dependent induction of PDK4 gene expression in skeletal muscle during energy deprivation. *Biochem J* **375**, 365-71.

Gachon, F., Nagoshi, E., Brown, S. A., Ripperger, J. and Schibler, U. (2004). The mammalian circadian timing system: from gene expression to physiology. *Chromosoma* **113**, 103-12.

Gäde, G. and Auerswald, L. (2003). Mode of action of neuropeptides from the adipokinetic hormone family. *Gen Comp Endocrinol* **132**, 10-20.

Gäde, G. and Beenakkers, A. M. (1977). Adipokinetic hormone-induced lipid mobilization and cyclic AMP accumulation in the fat body of *Locusta migratoria* during development. *Gen Comp Endocrinol* **32**, 481-7.

Garcia, A., Sekowski, A., Subramanian, V. and Brasaemle, D. L. (2003). The central domain is required to target and anchor Perilipin A to lipid droplets. *J Biol Chem* **278**, 625-35.

Garofalo, R. S. (2002). Genetic analysis of insulin signaling in *Drosophila*. *Trends Endocrinol Metab* **13**, 156-62.

Garton, A. J., Campbell, D. G., Cohen, P. and Yeaman, S. J. (1988). Primary structure of the site on bovine hormone-sensitive lipase phosphorylated by cyclic AMP-dependent protein kinase. *FEBS Lett* **229**, 68-72.

Glynn, P. (1999). Neuropathy target esterase. *Biochem J* **344 Pt 3**, 625-31.

Green, C. B. and Besharse, J. C. (1996). Identification of a novel vertebrate circadian clock-regulated gene encoding the protein nocturnin. *Proc Natl Acad Sci U S A* **93**, 14884-8.

Greenberg, A. S., Egan, J. J., Wek, S. A., Garty, N. B., Blanchette-Mackie, E. J. and Londos, C. (1991). Perilipin, a major hormonally regulated adipocyte-specific phosphoprotein associated with the periphery of lipid storage droplets. *J Biol Chem* **266**, 11341-6.

Greenberg, A. S., Egan, J. J., Wek, S. A., Moos, M. C., Jr., Londos, C. and Kimmel, A. R. (1993). Isolation of cDNAs for perilipins A and B: sequence and expression of lipid droplet-associated proteins of adipocytes. *Proc Natl Acad Sci U S A* **90**, 12035-9.

Greenberg, A. S., Shen, W. J., Muliro, K., Patel, S., Souza, S. C., Roth, R. A. and Kraemer, F. B. (2001). Stimulation of lipolysis and hormone-sensitive lipase via the extracellular signal-regulated kinase pathway. *J Biol Chem* **276**, 45456-61.

Grönke, S., Beller, M., Fellert, S., Ramakrishnan, H., Jäckle, H. and Kühnlein, R. P. (2003). Control of fat storage by a *Drosophila* PAT domain protein. *Curr Biol* **13**, 603-6.

Halaas, J. L., Gajiwala, K. S., Maffei, M., Cohen, S. L., Chait, B. T., Rabinowitz, D., Lallone, R. L., Burley, S. K. and Friedman, J. M. (1995). Weight-reducing effects of the plasma protein encoded by the obese gene. *Science* **269**, 543-6.

Häder, T., Müller, S., Aguilera, M., Eulenberg, K. G., Steuernagel, A., Ciossek, T., Kühnlein, R. P., Lemaire, L., Fritsch, R., Dohrmann, C. et al. (2003). Control of triglyceride storage by a WD40/TPR-domain protein. *EMBO Rep* **4**, 511-6.

Haemmerle, G., Zimmermann, R., Hayn, M., Theussl, C., Waeg, G., Wagner, E., Sattler, W., Magin, T. M., Wagner, E. F. and Zechner, R. (2002). Hormone-sensitive lipase deficiency in mice causes diglyceride accumulation in adipose tissue, muscle, and testis. *J Biol Chem* **277**, 4806-15.

Haemmerle, G., Zimmermann, R. and Zechner, R. (2003). Letting lipids go: hormone-sensitive lipase. *Curr Opin Lipidol* **14**, 289-97.

Harshman, L. G., Moore, K. M., Sty, M. A. and Magwire, M. M. (1999). Stress resistance and longevity in selected lines of *Drosophila melanogaster*. *Neurobiol. Aging* **20**, 521--529.

Haunerland, N. H. (1994). Fatty acid binding protein in locust and mammalian muscle. Comparison of structure, function and regulation. *Comp Biochem Physiol B Biochem Mol Biol* **109**, 199-208.

Helfrich-Förster, C. (2004). The circadian clock in the brain: a structural and functional comparison between mammals and insects. *J Comp Physiol A Neuroethol Sens Neural Behav Physiol* **190**, 601-13.

Helmert, U. and Strube, H. (2004). The development of obesity in Germany in the period from 1985 until 2000. *Gesundheitswesen* **66**, 409-15.

Henderson, D. S., Wiegand, U. K., Norman, D. G. and Glover, D. M. (2000). Mutual correction of faulty PCNA subunits in temperature-sensitive lethal *mus209* mutants of *Drosophila melanogaster*. *Genetics* **154**, 1721-33.

Hirschberg, H. J., Simons, J. W., Dekker, N. and Egmond, M. R. (2001). Cloning, expression, purification and characterization of patatin, a novel phospholipase A. *Eur J Biochem* **268**, 5037-44.

Hisano, T., Hata, Y., Fujii, T., Liu, J. Q., Kurihara, T., Esaki, N. and Soda, K. (1996). Crystallization and preliminary x-ray crystallographic studies of L-2-haloacid dehalogenase from *Pseudomonas sp*. YL. *Proteins* **24**, 520-2.

Holm, C. (2003). Molecular mechanisms regulating hormone-sensitive lipase and lipolysis. *Biochem Soc Trans* **31**, 1120-4.

Holm, C., Davis, R. C., Osterlund, T., Schotz, M. C. and Fredrikson, G. (1994). Identification of the active site serine of hormone-sensitive lipase by site-directed mutagenesis. *FEBS Lett* **344**, 234-8.

Holness, M. J. and Sugden, M. C. (2003). Regulation of pyruvate dehydrogenase complex activity by reversible phosphorylation. *Biochem Soc Trans* **31**, 1143-51.

Hope, R. G., Murphy, D. J. and McLauchlan, J. (2002). The domains required to direct core proteins of hepatitis C virus and GB virus-B to lipid droplets share common features with plant oleosin proteins. *J Biol Chem* **277**, 4261-70.

Hwangbo, D. S., Gersham, B., Tu, M. P., Palmer, M. and Tatar, M. (2004). *Drosophila dFOXO* controls lifespan and regulates insulin signalling in brain and fat body. *Nature* **429**, 562-6.

International Obesity Task Force [Online]. http://www.iotf.org [accessed January 2004].

Jenkins, C. M., Mancuso, D. J., Yan, W., Sims, H. F., Gibson, B. and Gross, R. W. (2004). Identification, cloning, expression, and purification of three novel human calcium-independent phospholipase A2 family members possessing triacylglycerol lipase and acylglycerol transacylase activities. *J Biol Chem*.

Jiang, H. P. and Serrero, G. (1992). Isolation and characterization of a full-length cDNA coding for an adipose differentiation-related protein. *Proc Natl Acad Sci U S A* **89**, 7856-60.

Kennedy, G. C. (1953). The role of depot fat in the hypothalamic control of food intake in the rat. *Proc R Soc Lond B Biol Sci* **140**, 578-96.

Kim, S. K. and Rulifson, E. J. (2004). Conserved mechanisms of glucose sensing and regulation by *Drosophila* corpora cardiaca cells. *Nature* **431**, 316-20.

Klein, T. (2001). Wing disc development in the fly: the early stages. *Curr Opin Genet Dev* **11**, 470-5.

Kraemer, F. B. and Shen, W. J. (2002). Hormone-sensitive lipase: control of intracellular tri-(di-)acylglycerol and cholesteryl ester hydrolysis. *J Lipid Res* **43**, 1585-94.

Kukulies, J. and Komnick, H. (1984). Lipid transport through the enterocytes of larval *Aeshna cyanea* (Insecta, Odonata). *Eur J Cell Biol* **34**, 118-29.

Lee, G. and Park, J. H. (2004). Hemolymph sugar homeostasis and starvation-induced hyperactivity affected by genetic manipulations of the *adipokinetic hormone*-encoding gene in *Drosophila melanogaster*. *Genetics* **167**, 311-23.

Lee, W. C., Salido, E. and Yen, P. H. (1994). Isolation of a new gene *GS2* (DXS1283E) from a CpG island between STS and KAL1 on Xp22.3. *Genomics* **22**, 372-6.

Leff, T. (2003). AMP-activated protein kinase regulates gene expression by direct phosphorylation of nuclear proteins. *Biochem Soc Trans* **31**, 224-7.

Lehner, C. F. (1999). The beauty of small flies. *Nat Cell Biol* **1**, E129-30.

Letunic, I., Copley, R. R., Schmidt, S., Ciccarelli, F. D., Doerks, T., Schultz, J., Ponting, C. P. and Bork, P. (2004). SMART 4.0: towards genomic data integration. *Nucleic Acids Res* **32 Database issue**, D142-4.

Lin, Y., Han, M., Shimada, B., Wang, L., Gibler, T. M., Amarakone, A., Awad, T. A., Stormo, G. D., Van Gelder, R. N. and Taghert, P. H. (2002). Influence of the period-dependent circadian clock on diurnal, circadian, and aperiodic gene expression in *Drosophila melanogaster*. *Proc Natl Acad Sci U S A* **99**, 9562-7.

Lipshutz, R. J., Fodor, S. P., Gingeras, T. R. and Lockhart, D. J. (1999). High density synthetic oligonucleotide arrays. *Nat Genet* **21**, 20-4.

Liscum, L. (2000). Niemann-Pick type C mutations cause lipid traffic jam. *Traffic* **1**, 218-25.

Liu, P., Ying, Y., Zhao, Y., Mundy, D. I., Zhu, M. and Anderson, R. G. (2004). Chinese hamster ovary K2 cell lipid droplets appear to be metabolic organelles involved in membrane traffic. *J Biol Chem* **279**, 3787-92.

Londos, C., Brasaemle, D. L., Schultz, C. J., Adler-Wailes, D. C., Levin, D. M., Kimmel, A. R. and Rondinone, C. M. (1999). On the control of lipolysis in adipocytes. *Ann N Y Acad Sci* **892**, 155-68.

Lu, X., Gruia-Gray, J., Copeland, N. G., Gilbert, D. J., Jenkins, N. A., Londos, C. and Kimmel, A. R. (2001). The murine *perilipin* gene: the lipid droplet-associated perilipins derive from tissue-specific, mRNA splice variants and define a gene family of ancient origin. *Mamm Genome* **12**, 741-9.

Martinez-Botas, J., Anderson, J. B., Tessier, D., Lapillonne, A., Chang, B. H., Quast, M. J., Gorenstein, D., Chen, K. H. and Chan, L. (2000). Absence of perilipin results in leanness and reverses obesity in Lepr(db/db) mice. *Nat Genet* **26**, 474-9.

May, C., Preisig-Müller, R., Hohne, M., Gnau, P. and Kindl, H. (1998). A phospholipase A2 is transiently synthesized during seed germination and localized to lipid bodies. *Biochim Biophys Acta* **1393**, 267-76.

McDonald, M. J. and Rosbash, M. (2001). Microarray analysis and organization of circadian gene expression in *Drosophila*. *Cell* **107**, 567-78.

McManaman, J. L., Zabaronick, W., Schaack, J. and Orlicky, D. J. (2003). Lipid droplet targeting domains of adipophilin. *J Lipid Res* **44**, 668-73.

McNeil, G. P., Zhang, X., Genova, G. and Jackson, F. R. (1998). A molecular rhythm mediating circadian clock output in *Drosophila*. *Neuron* **20**, 297-303.

Mildner, A. (2003). Funktionelle Charakterisierung des *Drosophila* Genes *brummer* und seiner humanen Homologen. *Diplomarbeit, Georg-August-Universität Göttingen*.

Miron, M., Lasko, P. and Sonenberg, N. (2003). Signaling from Akt to FRAP/TOR targets both 4E-BP and S6K in *Drosophila melanogaster*. *Mol Cell Biol* **23**, 9117-26.

Misra, S., Crosby, M. A., Mungall, C. J., Matthews, B. B., Campbell, K. S., Hradecky, P., Huang, Y., Kaminker, J. S., Millburn, G. H., Prochnik, S. E. et al. (2002). Annotation of the *Drosophila melanogaster* euchromatic genome: a systematic review. *Genome Biol* **3**, (12).

Mistlberger, R. E. (1994). Circadian food-anticipatory activity: formal models and physiological mechanisms. *Neurosci Biobehav Rev* **18**, 171-95.

Miura, S., Gan, J. W., Brzostowski, J., Parisi, M. J., Schultz, C. J., Londos, C., Oliver, B. and Kimmel, A. R. (2002). Functional conservation for lipid storage droplet association among Perilipin, ADRP, and TIP47 (PAT)-related proteins in mammals, *Drosophila*, and *Dictyostelium*. *J Biol Chem* **277**, 32253-7.

Moran, T. H. (2000). Cholecystokinin and satiety: current perspectives. *Nutrition* **16**, 858-65.

Mulder, H., Sorhede-Winzell, M., Contreras, J. A., Fex, M., Strom, K., Ploug, T., Galbo, H., Arner, P., Lundberg, C., Sundler, F. et al. (2003). Hormone-sensitive lipase null mice exhibit signs of impaired insulin sensitivity whereas insulin secretion is intact. *J Biol Chem* **278**, 36380-8.

Nakamura, N. and Fujimoto, T. (2003). Adipose differentiation-related protein has two independent domains for targeting to lipid droplets. *Biochem Biophys Res Commun* **306**, 333-8.

Naureckiene, S., Sleat, D. E., Lackland, H., Fensom, A., Vanier, M. T., Wattiaux, R., Jadot, M. and Lobel, P. (2000). Identification of HE1 as the second gene of Niemann-Pick C disease. *Science* **290**, 2298-301.

Newby, L. M. and Jackson, F. R. (1993). A new biological rhythm mutant of *Drosophila melanogaster* that identifies a gene with an essential embryonic function. *Genetics* **135**, 1077-90.

Newman, J. W., Morisseau, C., Harris, T. R. and Hammock, B. D. (2003). The soluble epoxide hydrolase encoded by EPXH2 is a bifunctional enzyme with novel lipid phosphate phosphatase activity. *Proc Natl Acad Sci U S A* **100**, 1558-63.

Nishio, Y., Isshiki, H., Kishimoto, T. and Akira, S. (1993). A nuclear factor for interleukin-6 expression (NF-IL6) and the glucocorticoid receptor synergistically activate transcription of the rat alpha 1-acid glycoprotein gene via direct protein-protein interaction. *Mol Cell Biol* **13**, 1854-62.

Noyes, B. E., Katz, F. N. and Schaffer, M. H. (1995). Identification and expression of the *Drosophila adipokinetic hormone* gene. *Mol Cell Endocrinol* **109**, 133-41.

Nozawa, K. (1956). The effects of the environmental conditions on *curled* expressivity and the interaction between two mimic genes, *curled* and *Curly*, in *Drosophila melanogaster*. *Jpn J. Genet.* **31**, 321--326.

O'Kane, C. J. (2003). Modelling human diseases in *Drosophila* and *Caenorhabditis*. *Semin Cell Dev Biol* **14**, 3-10.

Oishi, K., Shiota, M., Sakamoto, K., Kasamatsu, M. and Ishida, N. (2004). Feeding is not a more potent Zeitgeber than the light-dark cycle in *Drosophila*. *Neuroreport* **15**, 739-43.

Okazaki, H., Osuga, J., Tamura, Y., Yahagi, N., Tomita, S., Shionoiri, F., Iizuka, Y., Ohashi, K., Harada, K., Kimura, S. et al. (2002). Lipolysis in the absence of hormone-sensitive lipase: evidence for a common mechanism regulating distinct lipases. *Diabetes* **51**, 3368-75.

Oldham, S., Montagne, J., Radimerski, T., Thomas, G. and Hafen, E. (2000). Genetic and biochemical characterization of *dTOR*, the *Drosophila* homolog of the target of rapamycin. *Genes Dev* **14**, 2689-94.

Osterlund, T., Danielsson, B., Degerman, E., Contreras, J. A., Edgren, G., Davis, R. C., Schotz, M. C. and Holm, C. (1996). Domain-structure analysis of recombinant rat hormone-sensitive lipase. *Biochem J* **319 (Pt 2)**, 411-20.

Osuga, J., Ishibashi, S., Oka, T., Yagyu, H., Tozawa, R., Fujimoto, A., Shionoiri, F., Yahagi, N., Kraemer, F. B., Tsutsumi, O. et al. (2000). Targeted disruption of hormone-sensitive lipase results in male sterility and adipocyte hypertrophy, but not in obesity. *Proc Natl Acad Sci U S A* **97**, 787-92.

Pan, D., A.; and Hardie, D. Grahame. (2002). A homologue of AMP-activated protein kinase in *Drosophila melanogaster* is sensitive to AMP and is activated by ATP depletion. *Biochem J* **367**, 179-186.

Park, Y., Kim, Y. J. and Adams, M. E. (2002). Identification of G protein-coupled receptors for *Drosophila* PRXamide peptides, CCAP, corazonin, and AKH supports a theory of ligand-receptor coevolution. *Proc. Natl. Acad. Sci. USA* **99**, 11423--11428.

Patel, R., Soulages, J. L., Wells, M. A. and Arrese, E. L. (2004). cAMP-dependent protein kinase of *Manduca sexta* phosphorylates but does not activate the fat body triglyceride lipase. *Insect Biochem Mol Biol* **34**, 1269-79.

Pavelka, J. and Jindrak, L. (2001). Mechanism of the fluorescent light induced suppression of *Curly* phenotype in *Drosophila melanogaster*. *Bioelectromagnetics* **22**, 371-83.

Plautz, J. D., Kaneko, M., Hall, J. C. and Kay, S. A. (1997). Independent photoreceptive circadian clocks throughout *Drosophila*. *Science* **278**, 1632-5.

Ramirez-Weber, F. A. and Kornberg, T. B. (2000). Signaling reaches to new dimensions in *Drosophila* imaginal discs. *Cell* **103**, 189-92.

Reiling, J. H., Doepfner, K. T., Hafen, E. and Stocker, H. (2005). Diet-Dependent Effects of the *Drosophila* Mnk1/Mnk2 Homolog Lk6 on Growth via eIF4E. *Curr Biol* **15**, 24-30.

Ripperger, J. A. and Schibler, U. (2001). Circadian regulation of gene expression in animals. *Curr Opin Cell Biol* **13**, 357-62.

Rørth, P. (1996). A modular misexpression screen in *Drosophila* detecting tissue-specific phenotypes. *Proc Natl Acad Sci U S A* **93**, 12418-22.

Rørth, P. and Montell, D. J. (1992). *Drosophila* C/EBP: a tissue-specific DNA-binding protein required for embryonic development. *Genes Dev* **6**, 2299-311.

Roseman, R. R., Johnson, E. A., Rodesch, C. K., Bjerke, M., Nagoshi, R. N. and Geyer, P. K. (1995). A P element containing suppressor of hairy-wing binding regions has novel properties for mutagenesis in *Drosophila melanogaster*. *Genetics* **141**, 1061-74.

Ross, J., Jiang, H., Kanost, M. R. and Wang, Y. (2003). Serine proteases and their homologs in the *Drosophila melanogaster* genome: an initial analysis of sequence conservation and phylogenetic relationships. *Gene* **304**, 117-31.

Rouyer, F., Rachidi, M., Pikielny, C. and Rosbash, M. (1997). A new gene encoding a putative transcription factor regulated by the *Drosophila* circadian clock. *Embo J* **16**, 3944-54.

Rubin, G. M., Hong, L., Brokstein, P., Evans-Holm, M., Frise, E., Stapleton, M. and Harvey, D. A. (2000). A *Drosophila* complementary DNA resource. *Science* **287**, 2222-4.

Rulifson, E. J., Kim, S. K. and Nusse, R. (2002). Ablation of insulin-producing neurons in flies: growth and diabetic phenotypes. *Science* **296**, 1118-20.

Rutter, J., Reick, M., Wu, L. C. and McKnight, S. L. (2001). Regulation of clock and NPAS2 DNA binding by the redox state of NAD cofactors. *Science* **293**, 510-4.

Rydel, T. J., Williams, J. M., Krieger, E., Moshiri, F., Stallings, W. C., Brown, S. M., Pershing, J. C., Purcell, J. P. and Alibhai, M. F. (2003). The crystal structure, mutagenesis, and activity studies reveal that patatin is a lipid acyl hydrolase with a Ser-Asp catalytic dyad. *Biochemistry* **42**, 6696-708.

Saiki, R. K., Gelfand, D. H., Stoffel, S., Scharf, S. J., Higuchi, R., Horn, G. T., Mullis, K. B. and Erlich, H. A. (1988). Primer-directed enzymatic amplification of DNA with a thermostable DNA polymerase. *Science* **239**, 487-91.

Sambrook, J., Russell, D.W. (2001). Molecular Cloning A Laboratory Manual Vol. 1-3. *Cold Spring Harbour Laboratory Press*.

Sanz, P., Randez-Gil, F. and Prieto, J. A. (1994). Molecular characterization of a gene that confers 2-deoxyglucose resistance in yeast. *Yeast* **10**, 1195-202.

Sarov-Blat, L., So, W. V., Liu, L. and Rosbash, M. (2000). The *Drosophila takeout* gene is a novel molecular link between circadian rhythms and feeding behavior. *Cell* **101**, 647-56.

Sato, H., Frank, D. W., Hillard, C. J., Feix, J. B., Pankhaniya, R. R., Moriyama, K., Finck-Barbancon, V., Buchaklian, A., Lei, M., Long, R. M. et al. (2003). The mechanism of action of the *Pseudomonas aeruginosa*-encoded type III cytotoxin, ExoU. *Embo J* **22**, 2959-69.

Schibler, U., Ripperger, J. A. and Brown, S. A. (2001). Circadian rhythms. Chronobiology--reducing time. *Science* **293**, 437-8.

Schultz, J., Milpetz, F., Bork, P. and Ponting, C. P. (1998). SMART, a simple modular architecture research tool: identification of signaling domains. *Proc Natl Acad Sci U S A* **95**, 5857-64.

Service, P. M. (1987). Physiological Mechanisms of Increased Stress Resistance in *Drosophila-melanogaster* Selected For Postponed Senescence. *Physiological Zoology* **60**, 321-326.

Shibata, S. and Tominaga, K. (1991). [Brain neuronal mechanisms of circadian rhythms in mammalians]. *Yakugaku Zasshi* **111**, 270-83.

Shibui, A., Tsunoda, T., Seki, N., Suzuki, Y., Sugane, K. and Sugano, S. (1999). Isolation and chromosomal mapping of a novel human gene showing homology to Na+/PO4 cotransporter. *J Hum Genet* **44**, 190-2.

Silver, R., LeSauter, J., Tresco, P. A. and Lehman, M. N. (1996). A diffusible coupling signal from the transplanted suprachiasmatic nucleus controlling circadian locomotor rhythms. *Nature* **382**, 810-3.

Slavin, B. G. (1972). The cytophysiology of mammalian adipose cells. *Int Rev Cytol* **33**, 297-334.

Smith, R. M. and Jarett, L. (1980). Surface structure changes of rat adipocytes during lipolysis stimulated by various lipolytic agents. A scanning electron microscopic study. *J Cell Biol* **84**, 57-65.

Smith, S. J., Cases, S., Jensen, D. R., Chen, H. C., Sande, E., Tow, B., Sanan, D. A., Raber, J., Eckel, R. H. and Farese, R. V., Jr. (2000). Obesity resistance and multiple mechanisms of triglyceride synthesis in mice lacking Dgat. *Nat Genet* **25**, 87-90.

Soni, K. G., Lehner, R., Metalnikov, P., O'Donnell, P., Semache, M., Gao, W., Ashman, K., Pshezhetsky, A. V. and Mitchell, G. A. (2004). Carboxylesterase 3 (EC 3.1.1.1) is a major adipocyte lipase. *J Biol Chem* **279**, 40683-9.

Souza, S. C., Muliro, K. V., Liscum, L., Lien, P., Yamamoto, M. T., Schaffer, J. E., Dallal, G. E., Wang, X., Kraemer, F. B., Obin, M. et al. (2002). Modulation of hormone-sensitive lipase and protein kinase A-mediated lipolysis by perilipin A in an adenoviral reconstituted system. *J Biol Chem* **277**, 8267-72.

Speakman, J. R. (2004). Obesity: the integrated roles of environment and genetics. *J Nutr* **134**, 2090S-2105S.

Spiegelman, B. M. and Flier, J. S. (1996). Adipogenesis and obesity: rounding out the big picture. *Cell* **87**, 377-89.

Spradling, A. C. and Rubin, G. M. (1982). Transposition of cloned P elements into *Drosophila* germ line chromosomes. *Science* **218**, 341-7.

Spradling, A. C., Stern, D., Beaton, A., Rhem, E. J., Laverty, T., Mozden, N., Misra, S. and Rubin, G. M. (1999). The Berkeley *Drosophila* Genome Project gene disruption project: Single P-element insertions mutating 25% of vital *Drosophila* genes. *Genetics* **153**, 135-77.

Spradling, A. C., Stern, D. M., Kiss, I., Roote, J., Laverty, T. and Rubin, G. M. (1995). Gene disruptions using P transposable elements: an integral component of the *Drosophila* genome project. *Proc Natl Acad Sci U S A* **92**, 10824-30.

Stanewsky, R. (2003). Genetic analysis of the circadian system in *Drosophila melanogaster* and mammals. *J Neurobiol* **54**, 111-47.

Stark, A., Brennecke, J., Russell, R. B. and Cohen, S. M. (2003). Identification of *Drosophila* MicroRNA targets. *PLoS Biol* **1**, E60.

Staubli, F., Jorgensen, T. J. D., Cazzamali, G., Williamson, M., Lenz, C., Sondergaard, L., Roepstorff, P. and Grimmelikhuijzen, C. J. P. (2002). Molecular identification of the insect adipokinetic hormone receptors. *Proceedings of the National Academy of Sciences of the United States of America* **99**, 3446-3451.

Stempfl, T., Vogel, M., Szabo, G., Wulbeck, C., Liu, J., Hall, J. C. and Stanewsky, R. (2002). Identification of circadian-clock-regulated enhancers and genes of *Drosophila melanogaster* by transposon mobilization and luciferase reporting of cyclical gene expression. *Genetics* **160**, 571-93.

Stokkan, K. A., Yamazaki, S., Tei, H., Sakaki, Y. and Menaker, M. (2001). Entrainment of the circadian clock in the liver by feeding. *Science* **291**, 490-3.

Stralfors, P. and Belfrage, P. (1983). Phosphorylation of hormone-sensitive lipase by cyclic AMP-dependent protein kinase. *J Biol Chem* **258**, 15146-52.

Stralfors, P. and Honnor, R. C. (1989). Insulin-induced dephosphorylation of hormone-sensitive lipase. Correlation with lipolysis and cAMP-dependent protein kinase activity. *Eur J Biochem* **182**, 379-85.

Stryer. (2004). Biochemistry.

Sztalryd, C. and Kraemer, F. B. (1994). Regulation of hormone-sensitive lipase during fasting. *Am J Physiol* **266**, E179-85.

Sztalryd, C., Xu, G., Dorward, H., Tansey, J. T., Contreras, J. A., Kimmel, A. R. and Londos, C. (2003). Perilipin A is essential for the translocation of hormone-sensitive lipase during lipolytic activation. *J Cell Biol*.

Stunkard, A. J., Foch, T. T. and Hrubec, Z. (1986). A twin study of human obesity. *Jama* **256**, 51-4.

Stunkard, A. J., Harris, J. R., Pedersen, N. L. and McClearn, G. E. (1990). The body-mass index of twins who have been reared apart. *N Engl J Med* **322**, 1483-7.

Tansey, J. T., Huml, A. M., Vogt, R., Davis, K. E., Jones, J. M., Fraser, K. A., Brasaemle, D. L., Kimmel, A. R. and Londos, C. (2003). Functional studies on native and mutated forms of perilipins. A role in protein kinase A-mediated lipolysis of triacylglycerols. *J Biol Chem* **278**, 8401-6.

Tansey, J. T., Sztalryd, C., Gruia-Gray, J., Roush, D. L., Zee, J. V., Gavrilova, O., Reitman, M. L., Deng, C. X., Li, C., Kimmel, A. R. et al. (2001). Perilipin ablation results in a lean mouse with aberrant adipocyte lipolysis, enhanced leptin production, and resistance to diet-induced obesity. *Proc Natl Acad Sci U S A* **98**, 6494-9.

Targett-Adams, P., Chambers, D., Gledhill, S., Hope, R. G., Coy, J. F., Girod, A. and McLauchlan, J. (2003). Live cell analysis and targeting of the lipid droplet-binding adipocyte differentiation-related protein. *J Biol Chem* **278**, 15998-6007.

Tatar, M., Kopelman, A., Epstein, D., Tu, M. P., Yin, C. M. and Garofalo, R. S. (2001). A mutant *Drosophila* insulin receptor homolog that extends life-span and impairs neuroendocrine function. *Science* **292**, 107-10.

Tauchi-Sato, K., Ozeki, S., Houjou, T., Taguchi, R. and Fujimoto, T. (2002). The surface of lipid droplets is a phospholipid monolayer with a unique fatty acid composition. *J. Biol. Chem.*, M207712200.

Tautz, D. and Pfeifle, C. (1989). A non-radioactive in situ hybridization method for the localization of specific RNAs in Drosophila embryos reveals translational control of the segmentation gene hunchback. *Chromosoma* **98**, 81-5.

Teixeira, L., Rabouille, C., Rorth, P., Ephrussi, A. and Vanzo, N. F. (2003). *Drosophila* Perilipin/ADRP homologue Lsd2 regulates lipid metabolism. *Mech Dev* **120**, 1071-81.

Temme, C., Zaessinger, S., Meyer, S., Simonelig, M. and Wahle, E. (2004). A complex containing the CCR4 and CAF1 proteins is involved in mRNA deadenylation in *Drosophila*. *Embo J* **23**, 2862-71.

Theopold, U., Ekengren, S. and Hultmark, D. (1996). HLH106, a *Drosophila* transcription factor with similarity to the vertebrate sterol responsive element binding protein. *Proc Natl Acad Sci U S A* **93**, 1195-9.

Tornqvist, H. and Belfrage, P. (1981). Monoacylglycerol lipase from rat adipose tissue. *Methods Enzymol* **71 Pt C**, 646-52.

Tong, Q., Dalgin, G., Xu, H., Ting, C. N., Leiden, J. M. and Hotamisligil, G. S. (2000). Function of GATA transcription factors in preadipocyte-adipocyte transition. *Science* **290**, 134-8.

Tschape, J. A., Hammerschmied, C., Muhlig-Versen, M., Athenstaedt, K., Daum, G. and Kretzschmar, D. (2002). The neurodegeneration mutant *loechrig* interferes with cholesterol homeostasis and Appl processing. *Embo J* **21**, 6367-76.

Ueda, H. R., Matsumoto, A., Kawamura, M., Iino, M., Tanimura, T. and Hashimoto, S. (2002). Genome-wide transcriptional orchestration of circadian rhythms in *Drosophila*. *J Biol Chem* **277**, 14048-52.

Umlauf, E., Csaszar, E., Moertelmaier, M., Schuetz, G. J., Parton, R. G. and Prohaska, R. (2004). Association of stomatin with lipid bodies. *J Biol Chem* **279**, 23699-709.

Van der Horst, D. J., Van Marrewijk, W. J. and Diederen, J. H. (2001). Adipokinetic hormones of insect: release, signal transduction, and responses. *Int Rev Cytol* **211**, 179-240.

Van Gelder, R. N., Bae, H., Palazzolo, M. J. and Krasnow, M. A. (1995). Extent and character of circadian gene expression in *Drosophila melanogaster*: identification of twenty oscillating mRNAs in the fly head. *Curr Biol* **5**, 1424-36.

Van Gelder, R. N. and Krasnow, M. A. (1996). A novel circadianly expressed *Drosophila melanogaster* gene dependent on the *period* gene for its rhythmic expression. *Embo J* **15**, 1625-31.

van Tienhoven, M., Atkins, J., Li, Y. and Glynn, P. (2002). Human neuropathy target esterase catalyzes hydrolysis of membrane lipids. *J Biol Chem* **277**, 20942-8.

Villena, J. A., Roy, S., Sarkadi-Nagy, E., Kim, K. H. and Sul, H. S. (2004). Desnutrin, an adipocyte gene encoding a novel patatin domain-containing protein, is induced by fasting and glucocorticoids: ectopic expression of desnutrin increases triglyceride hydrolysis. *J Biol Chem* **279**, 47066-75.

Waddington, C. H. (1940). The genetic control of wing development in *Drosophila*. *J. Genet.* **41**, 75--139.

Wang, Y., Osterbur, D. L., Megaw, P. L., Tosini, G., Fukuhara, C., Green, C. B. and Besharse, J. C. (2001). Rhythmic expression of Nocturnin mRNA in multiple tissues of the mouse. *BMC Dev Biol* **1**, 9.

Welte, M. A., Gross, S. P., Postner, M., Block, S. M. and Wieschaus, E. F. (1998). Developmental regulation of vesicle transport in *Drosophila* embryos: forces and kinetics. *Cell* **92**, 547-57.

Wolfe, J., Akam, M. E. and Roberts, D. B. (1977). Biochemical and immunological studies on larval serum protein 1, the major haemolymph protein of *Drosophila melanogaster* third-instar larvae. *Eur J Biochem* **79**, 47-53.

Wolins, N. E. S., James R. Schoenfish, Marissa J. Tzekov, Anatoly Bensch, Kenneth G. Bickel, Perry E. (2003). Adipocyte protein S3-12 coats nascent lipid droplets. *J. Biol. Chem.* 278(39):37713-21.

Wu, P., Blair, P. V., Sato, J., Jaskiewicz, J., Popov, K. M. and Harris, R. A. (2000). Starvation increases the amount of pyruvate dehydrogenase kinase in several mammalian tissues. *Arch Biochem Biophys* **381**, 1-7.

Xu, P., Vernooy, S. Y., Guo, M. and Hay, B. A. (2003). The *Drosophila* microRNA Mir-14 suppresses cell death and is required for normal fat metabolism. *Curr Biol* **13**, 790-5.

Yandell, M., Bailey, A. M., Misra, S., Shu, S., Wiel, C., Evans-Holm, M., Celniker, S. E. and Rubin, G. M. (2005). A computational and experimental approach to validating annotations and gene predictions in the *Drosophila melanogaster* genome. *Proc Natl Acad Sci U S A* **102**, 1566-71.

Yeaman, S. J. (2004). Hormone-sensitive lipase--new roles for an old enzyme. *Biochem J* **379**, 11-22.

Zhang, Y., Proenca, R., Maffei, M., Barone, M., Leopold, L. and Friedman, J. M. (1994). Positional cloning of the mouse *obese* gene and its human homologue. *Nature* **372**, 425-32.

Zhang, H., Stallock, J. P., Ng, J. C., Reinhard, C. and Neufeld, T. P. (2000). Regulation of cellular growth by the *Drosophila* target of rapamycin dTOR. *Genes Dev* **14**, 2712-24.

Zhang, X., McNeil, G. P., Hilderbrand-Chae, M. J., Franklin, T. M., Schroeder, A. J. and Jackson, F. R. (2000). Circadian regulation of the lark RNA-binding protein within identifiable neurosecretory cells. *J Neurobiol* **45**, 14-29.

Ziegler, R. (1990). Biological effects of synthetic AKH in Manduca sexta and estimates of the amount of AKH in corpora cardiaca. *Arch Insect Biochem Physiol* **15**, 111-6.

Zimmermann, R., Strauss, J. G., Haemmerle, G., Schoiswohl, G., Birner-Gruenberger, R., Riederer, M., Lass, A., Neuberger, G., Eisenhaber, F., Hermetter, A. et al. (2004). Fat mobilization in adipose tissue is promoted by adipose triglyceride lipase. *Science* **306**, 1383-6.

Zinke, I., Schutz, C. S., Katzenberger, J. D., Bauer, M. and Pankratz, M. J. (2002). Nutrient control of gene expression in *Drosophila*: microarray analysis of starvation and sugar-dependent response. *Embo J* **21**, 6162-73.

Zou, S., Meadows, S., Sharp, L., Jan, L. Y. and Jan, Y. N. (2000). Genome-wide study of aging and oxidative stress response in *Drosophila melanogaster*. *Proc Natl Acad Sci U S A* **97**, 13726-31.

6 Summary

Energy homeostasis is a fundamental property of all organisms. It includes the ability to control storage and mobilization of fat, mainly triacylglycerols (TAG). A genome-wide comparative transcriptome analysis with *ad libitum* fed and starved adult *Drosophila* flies was performed. Nutritionally regulated genes were identified and a subset was functionally characterized.

The starvation-upregulated gene *brummer* (*bmm*) encodes a protein of the evolutionary conserved Bmm/Nutrin family of Patatin-like domain-containing lipases. Bmm has TAG lipase activity necessary for fat mobilization fueling *Drosophila* embryogenesis. In postembryonic stages, *bmm* is expressed in the fat body. Functional Bmm:EGFP protein localizes to the surface of lipid storage droplets via evolutionary conserved sequences. Chronic overexpression of *bmm* in the fat body depletes organismal TAG stores, whereas *bmm* loss-of-function causes obesity in the fly. The results indicate that *bmm* acts as an evolutionary conserved key regulator of organismal TAG storage control in *Drosophila*.

Mammalian genomes encode four Bmm/Nutrin TAG lipases. The only *bmm* paralogue in fly, *doppelgänger von brummer* (*dob*), is also upregulated under starvation conditions and exerts a Bmm-like TAG lipase activity *in vivo*. However, flies lacking both Bmm and Dob activities are able to mobilize their TAG storage during starvation conditions. Thus, additional TAG lipases are involved in starvation-induced TAG mobilization in flies. Therefore, the *Drosophila* mutant of the homologue of the Hormone sensitive lipase (dHsl), a key enzyme in mammalian lipolysis, was generated to further elucidate the lipolytic cascade in *Drosophila*.

At the lipid droplet surface, Bmm antagonizes the function of the *Drosophila* PAT domain protein Lsd-2. Fat body-specific overexpression of Lsd-2 results in excessive TAG accumulation, whereas *Lsd-2* loss-of-function mutants are lean. The lean phenotype of *Lsd-2* mutant flies is reminiscent of mice deficient for the mammalian Lsd-2 homologue Perilipin. These results suggest that Lsd-2 operates in a Perilipin-like manner by modulating the rate of lipolysis. The functional characterization of *bmm* and *Lsd-2* suggests that the surface of lipid droplets represents an evolutionary conserved intracellular compartment boundary involved in the control of lipolysis. This observation emphasizes the value of *Drosophila* as a model organism to be used for research in energy homeostasis and metabolic disease.

Energy homeostasis and circadian rhythm processes in mammals are closely linked, but factors mediating this link remain to be established. I found that circadianly cycling genes are also enriched among the starvation responsive genes. Therefore, I tested whether this feature exists in *Drosophila*. The results suggest that although the *Drosophila* genes *nocturnin* and *Drosophila rhythmically expressed gene 2* are involved in energy homeostasis and circadian rhythm, respectively, a functional link between energy homeostasis and circadian rhythm could not be established.

7 Lebenslauf

Sebastian Matthias Grönke

Geburtsdatum und-ort: 06.07.1974 in Diepholz

Eltern: Marion Grönke geb. Boesser und Gerhard Grönke

Nationalität: Deutsch

1980-1984	Grundschule, Eystrup
1984-1985	Orientierungsstufe, Hoya
1985-1993	Gymnasium, Nienburg
1993	Abitur, Gymnasium Hindenburg-Schule, Nienburg
1994-1995	Zivildienst, Lebenshilfe, Hoya
1995- 2001	Studium der Biologie an der Georg-August-Universität Göttingen
10/1997	Vordiplom
01/2000	Diplomprüfung (Entwicklungsbiologie, Zoologie, Biochemie)
02/2000- 01/2001	Diplomarbeit Max-Planck-Institut für biophysikalische Chemie, Abt. Molekulare Entwicklungsbiologie (Prof. Dr. H. Jäckle/ Dr. R. Kühnlein) Thema: Identifizierung und Charakterisierung eines Energiehomöostasefaktors der adulten Taufliege *Drosophila melanogaster*
seit 03/2001	Promotion Max-Planck-Institut für biophysikalische Chemie, Abt. Molekulare Entwicklungsbiologie (Prof. Dr. H. Jäckle/ Dr. R. Kühnlein), Göttingen

Veröffentlichungen außerhalb der Doktorarbeit:

Missirlis, F., Ulschmid, J. K., Hirosawa-Takamori, M., Grönke, S., Schäfer, U., Becker, K., Phillips, J. P., and Jäckle, H. (2002). Mitochondrial and cytoplasmic thioredoxin reductase variants encoded by a single *Drosophila* gene are both essential for viability. J Biol Chem *277*, 11521-11526.

Carrera, P., Moshkin, Y. M., Grönke, S., Sillje, H. H., Nigg, E. A., Jäckle, H., and Karch, F. (2003). Tousled-like kinase functions with the chromatin assembly pathway regulating nuclear divisions. Genes Dev *17*, 2578-2590.